Microbial yeast biosensors to monitor signal transmission and heterodimer formation for human G-protein-coupled receptors

Nakamura, Yasuyuki

(Degree)
博士（工学）

(Date of Degree)
2014-03-25

(Date of Publication)
2016-03-25

(Resource Type)
doctoral thesis

(Report Number)
甲第6090号

(URL)
https://hdl.handle.net/20.500.14094/D1006090

博 士 論 文

Microbial yeast biosensors to monitor signal transmission and heterodimer formation for human G-protein-coupled receptors

ヒト G タンパク質共役型受容体のシグナル伝達および ヘテロ二量体形成モニタリングのための酵母バイオセンサー

平成 26 年 1 月

神戸大学大学院工学研究科

中村　泰之

CONTENTS

INTRODUCTION

G-protein-coupled receptors (GPCRs) are physiologically important membrane proteins that sense signaling molecules such as hormones and neurotransmitters, and are the targets of several prescribed drugs. Recently, the process of heterodimerization among GPCRs has attracted attention because of its potential to generate the diversity in the regulatory machinery of signaling. Since the mechanism of GPCR signaling in yeast is similar to that in mammalian cells and various GPCRs have been successfully expressed in yeast *Saccharomyces cerevisiae*, the yeast is an attractive host organism for the study of human GPCRs. In this thesis, we developed microbial yeast biosensors to monitor signal transmission and heterodimer formation for human GPCRs. Because these biosensors permitted the facile detection of GPCR dimerizations as well as the convenient monitoring of the signal activation, it is applicable to the identification of obscured heterodimer partners and the screening of new agonistic and antagonistic peptides for target human GPCRs. Additionally, we integrated these two detection systems into a single yeast strain to enable the simultaneous detections of dimerization and signaling of human GPCRs. The constructed yeast biosensors will assist the elucidation of mechanisms and roles of GPCR dimerizations, and promote the discovery of new GPCR heterodimer pairs and lead peptides as potential therapeutic targets.

G-protein-coupled receptor

G-protein-coupled receptors (GPCRs) are located in the plasma membrane and transmit external signals into the cell. GPCRs constitute the largest family of membrane proteins and are involved in the majority of signal transduction. The common

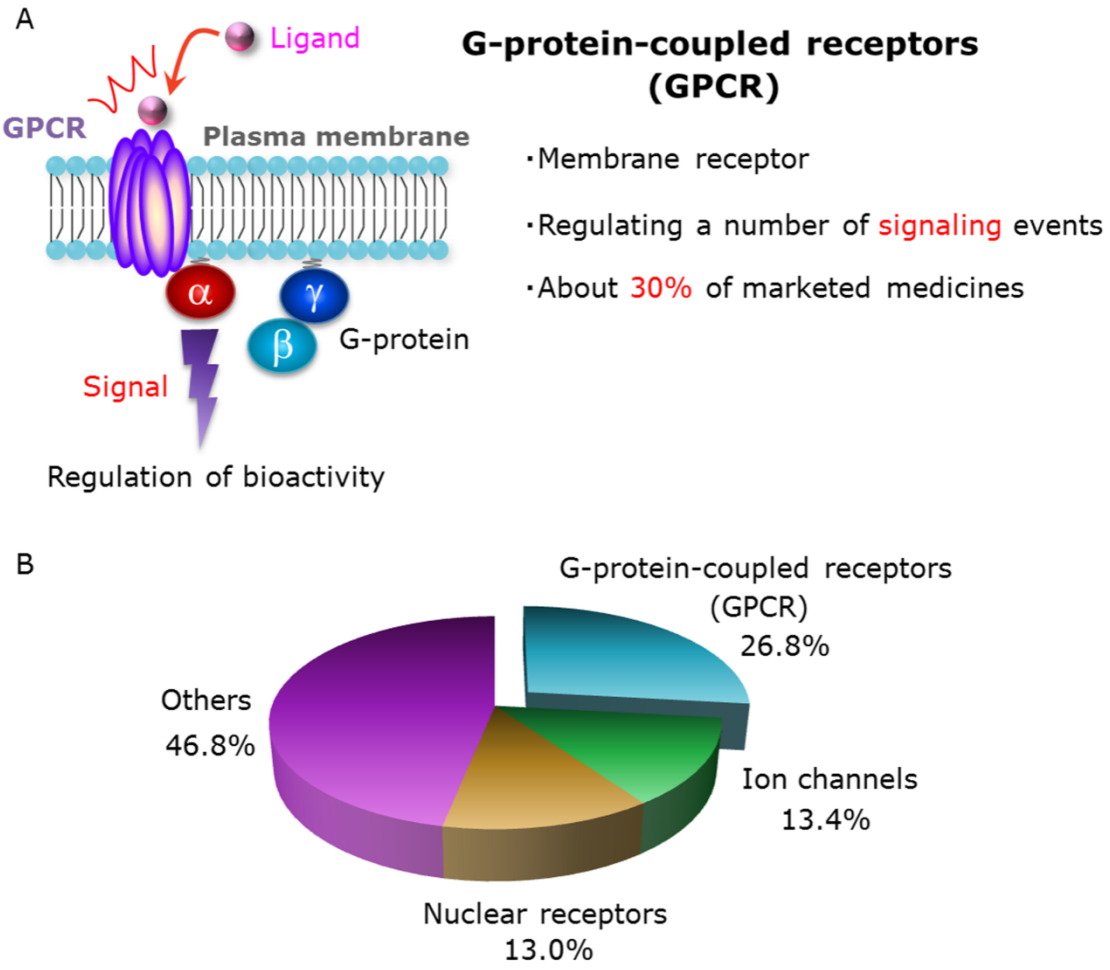

Fig. 1. (A) Characteristics of G-protein-coupled receptor. (B) Molecular targets of known drugs.

architecture of GPCRs has a seven transmembrane domain structure (Fredriksson et al., 2003; Takeda et al., 2002) that responds to a remarkable range of stimuli, including neurotransmitters, hormones, and ions (Lefkowitz and Shenoy, 2005). GPCRs transduce signals by activating heterotrimeric guanine nucleotide-binding proteins (G-proteins, Gilman, 1987) (**Figure 1**). GPCRs are the most important research target in biomolecular and medical sciences because they are the most common targets of therapeutic drugs (Gudermann et al., 1995; Heilker et al., 2009). Due to their excellent potential for drug discovery, GPCR targets represent up to 30% of the portfolio of many pharmaceutical companies (Klabunde and Hessler, 2002). Although the human genome contains 720–800 GPCRs (Siehler, 2008), it is still less than 50 GPCRs that are the targets of commercially available drugs (Eglen et al., 2007). Thus, GPCRs are attractive proteins not only for basic understandings of physiological and biological actions but also for commercial targets in medicinal and pharmaceutical area.

GPCR dimerization

Protein–protein interactions have fundamental roles in a variety of biological functions, and are of central importance for virtually every process in a living cell. It is now clear that GPCRs interact with a range of proteins, including other GPCRs (Bockaert et al., 2010; Ferré and Franco, 2010; Ritter and Hall, 2009). Identifying and elucidating the function of such interactions will significantly enhance our understanding of cellular control systems, with the promise of new and improved pharmaceuticals. Evidence suggests that oligomerization (dimerization, including homo-dimerization and hetero-dimerization) of GPCRs is important for their trafficking to and from the plasma membrane (Benkirane et al., 1997; Grosse et al., 1997; Jordan et

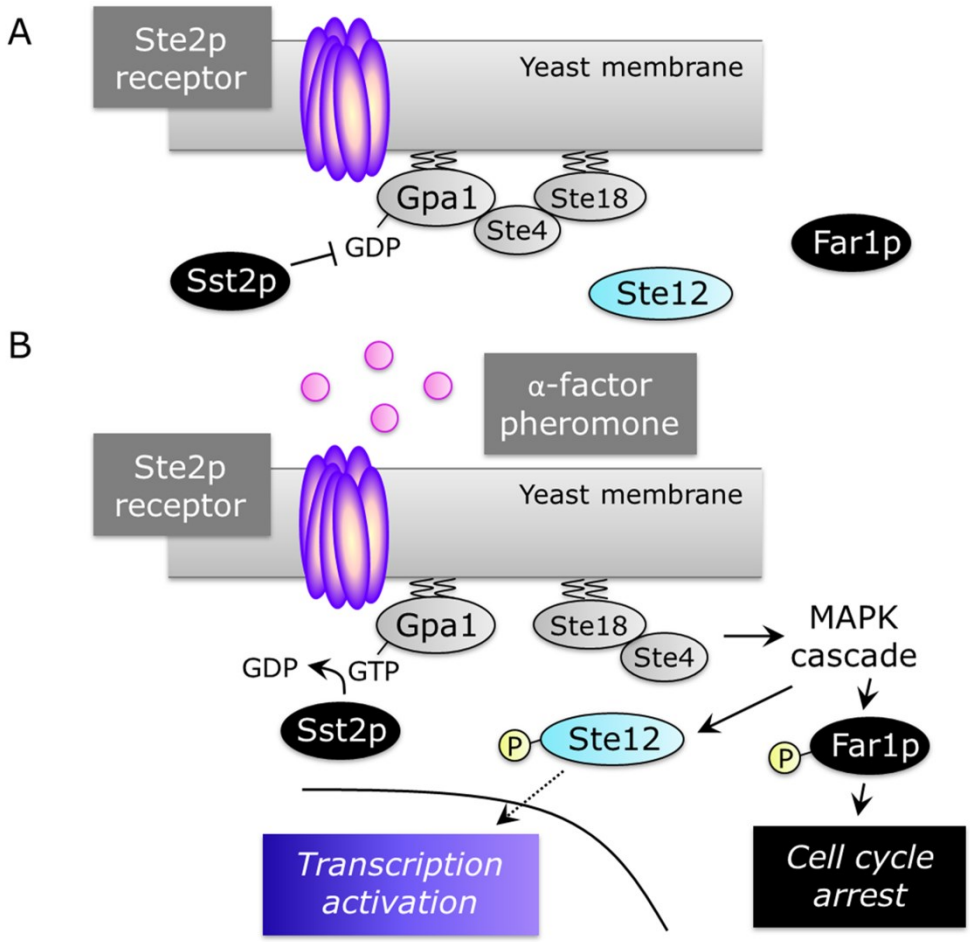

Fig. 2. Schematic illustration of the pheromone signaling pathway. (A) In the absence of α-factor, heterotrimeric G-protein is unable to activate the pheromone signaling pathway. (B) Binding of α-factor to Ste2p receptor activates the pheromone signaling pathway through heterotrimeric G-protein. Sequestered Ste4p–Ste18p complex from Gpa1p activates effectors and subsequent kinases that constitute the MAPK cascade, resulting in phosphorylation of Far1p and Ste12p. Phosphorylation of Far1p leads to cell cycle arrest. Phosphorylation of Ste12p induces global changes in transcription. Sst2p stimulates hydrolysis of GTP to GDP on Gpa1p, and helps to inactivate pheromone signaling.

al., 2001; Margeta-Mitrovic et al., 2000), for agonist binding activity (Jordan and Devi, 1999; Mijares et al., 2000; Potter et al., 1991), for signal transduction (AbdAlla et al., 2000; Hebert et al., 1996), and for down-regulation of receptor expression (Cvejic and Devi, 1997; Yesilaltay and Jenness, 2000).

Currently, the ascendancy of GPCRs as molecular targets has gradually decreased among newly developed Food and Drug Administration (FDA)-approved drugs (Drews, 2000; Overington et al., 2006), in part because conventional screening trials have been exhausted. Therefore, new screening trials, such as heterodimer-targeted ligand screening, are required for further drug discovery. Notably, dimerization has increased the potential diversity in regulation and modulation of GPCR signaling, and thus the specific evaluation of signaling properties among variously dimerized receptors will offer important implications for the development of new drugs as well as the understanding of signaling networks (Jordan and Devi, 1999).

Yeast *Saccharomyces cerevisiae*

The budding yeast *Saccharomyces cerevisiae* is one of the simplest unicellular eukaryotes, and is often used as a eukaryotic model organism for cellular and molecular biology (Lushchak, 2006; Schneiter, 2007; Sychrová, 2004; Wang and Dohlman, 2006; Winderickx et al., 2008). Yeast has several benefits, including the possession of eukaryotic secretory machinery, post-translational modifications, rapid cell growth, and well-established and versatile genetic techniques.

In addition, the *S. cerevisiae* is a useful microbial host organism for studying GPCRs as monomolecular models (Ishii et al., 2010; Minic et al., 2005). All eukaryotes conserve heterotrimeric G-proteins that comprise Gα-, Gβ- and Gγ-subunits.

Mammalian cells possess several types of G-proteins on the inner leaflets of plasma membranes. These G-proteins enable to regulate diverse physiological responses through coupling with a variety of transmembrane GPCRs (Hur and Kim, 2002). However, this diversity makes it difficult to identify which G-protein is responsible for controlling the specific signals (Ishii et al., 2010). Because haploid *S. cerevisiae* expresses one type of GPCR (either the **a**-cell specific pheromone receptor, Ste2p, or the α-cell specific pheromone receptor, Ste3p) and one type of heterotrimeric complex of G-proteins (yeast Gα, Gβ and Gγ; Gpa1p, Ste4p and Ste18p) (**Figure 2**), it can offer a simple way to transduce the signal promoted by the agonistic ligand (Fukuda et al., 2011). The heterotrimeric G-protein is divided into two key components from the perspective of structure and function. Gα (Gpa1p) is associated with the intracellular plasma membrane through the dual lipid modifications of myristoylation and palmitoylation in the N-terminus (Manahan et al., 2000), whereas the Gβγ dimer (the Ste4p–Ste18p complex) is also localized to the inner leaflet of the plasma membrane through the farnesylation and myristoylation in the C-terminus of Ste18p that forms a complex with Ste4p (Hirschman and Jenness, 1999; Manahan et al., 2000).

In the yeast haploid **a**-cell, the heterotrimeric G-proteins are closely associated with the intracellular domain of the Ste2p receptor, and the pheromone (α-factor; tridecapeptide)-bound receptor is conformationally changed and activates the G-proteins (Dosil et al., 2000). Gpa1p is thereby changed from an inactive GDP-bound state to an active GTP-bound state and dissociated Ste4p–Ste18p complex. Subsequently, the dissociated Ste4p–Ste18p complex binds to the following effectors through Ste4p, and then activates the mitogen-activated protein kinase (MAPK) cascade (Leberer et al., 1997: Leeuw et al., 1998). The Ste5p scaffold protein binds to the

kinases of the MAPK cascade composed of Ste11p, Ste7p and Fus3p, and brings them to the plasma membrane. The concentration of the bound kinases on the membrane possibly promotes amplification of the signal (Elion, 2001; Pryciak and Huntress, 1998). As a consequence, the activated pheromone signaling leads to the phosphorylation of Far1p and the transcription factor Ste12p. These phosphorylated proteins trigger cell cycle arrest in G1 (Chang and Herskowitz, 1990, 1992; McKinney and Cross, 1995) and global changes in transcription (Dolan et al., 1989; Song et al., 1991). *FIG1* gene expression is representative of the drastic changes in transcription in response to pheromone signaling (Muller et al., 2003). As a principal negative regulator, the Gpa1-specific GTPase-activating protein Sst2p, a member of the regulator of G-protein signaling family, is also involved in the pathway (Apanovitch et al., 1998; Dohlman et al., 1996).

Expression of heterologous GPCRs

Many heterologous GPCRs containing adrenergic, muscarinic, serotonin, neurotensin, somatostatin, olfactory and many other receptors have been successfully expressed in yeast, and the feasibility of yeast-based GPCR screening systems has been demonstrated (Brown et al., 2000; Erlenbach et al., 2001; King et al., 1990; Ladds et al., 2005; Leplatois et al., 2001; Li et al., 2007; Minic et al., 2005; Price et al., 1995). Yeast Gpa1p, which is equivalent to Gα, shares high homology, in part, with human $G\alpha_i$ classes, and a number of GPCRs of human and other species are able to interact with Gpa1p and activate pheromone signaling in yeast (Brown et al., 2000; Leplatois et al., 2001; Price et al., 1995). Many other human GPCRs can also function as yeast signaling modulators as a result of various genetic modifications, including chimeric Gpa1p

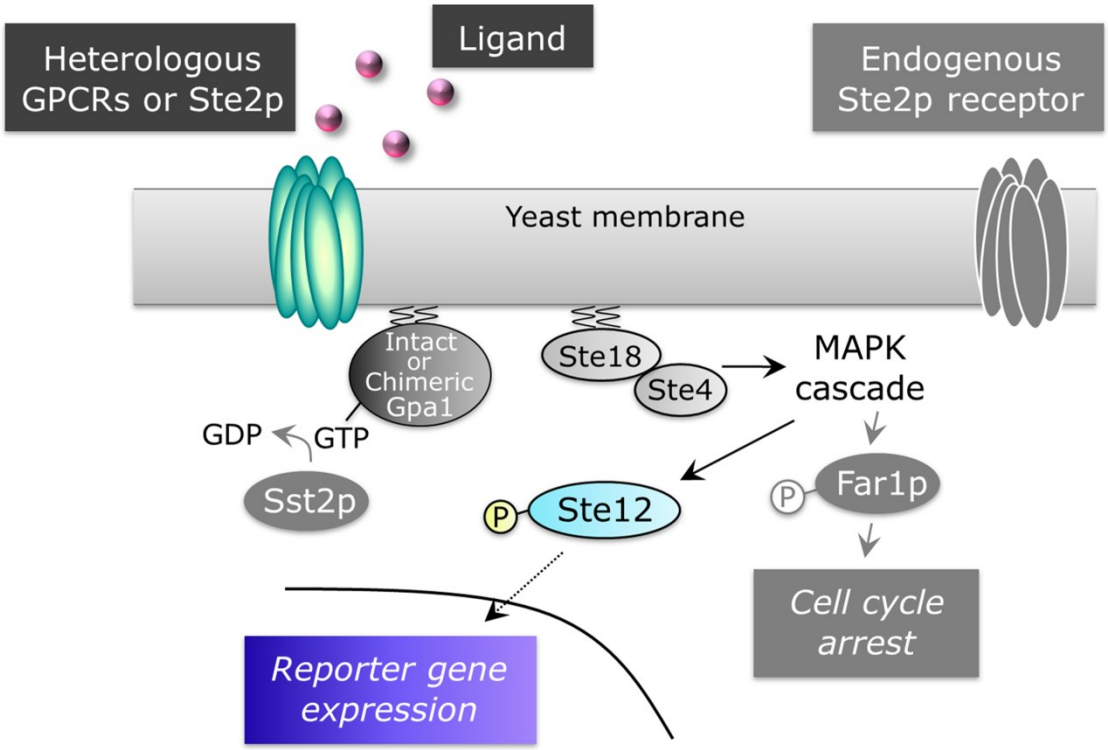

Fig. 3. Schematic illustration of typical genetic modifications enabling the pheromone signaling pathway to be used as a biosensor to represent activation of GPCRs. Intact or chimeric Gpa1p can transduce the signal from yeast endogenous Ste2p or heterologous GPCRs that are expressed on the yeast plasma membrane. Transcription machineries that are closely regulated by the phosphorylated transcription factor, Ste12p, are used to detect activation of pheromone signaling with various reporter genes. *FAR1*, *SST2* and *STE2* are often disrupted (shown in light gray) to prevent growth arrest, improve ligand sensitivity, and avoid competitive expression of yeast endogenous receptor.

systems (so-called 'transplants'), in which only five amino acids in the C-terminus of Gpa1p are substituted for those of human Gα subunits, such as the $G\alpha_{i/o}$, $G\alpha_s$ and $G\alpha_q$ families (**Figure 3**) (Erlenbach et al., 2001). Indeed, these transplants have allowed functional coupling of serotonin, muscarinic, purinergic and many other receptors to the yeast pheromone pathway (Brown et al., 2000; Erlenbach et al., 2001; Li et al., 2007; Pausch et al., 2004). Introduction of reporter genes, such as green fluorescent protein (*GFP*) (Iguchi et al., 2010; Togawa et al., 2010), β-galactosidase (*lacZ*) (Brown et al., 2000), luciferase (*luc*) (Fukutani et al., 2012) and growth selection marker (*HIS3*) (Manfredi et al., 1996) downstream of the pheromone signaling (G-protein signaling) pathway further facilitates the detection of the agonist-promoted signal.

If the expression of human GPCR on the plasma membrane of *ste2*Δ yeast **a**-cell permits coupling with yeast monopolistic G-proteins, the promoted signaling by the cognate ligand or analog agonist can be easily monitored with reporter gene assays (Fukuda et al., 2011; Ishii et al., 2010). The use of an established fluorescence-based reporter gene assay provides the most convenient measurement procedure: the cell culture is simply diluted into buffers and the fluorescence is read using fluorometric instruments (Ishii et al., 2012). A flow cytometer is an especially powerful tool for comparative quantification and quantitative screening (cell sorting) (Ishii et al., 2012).

Yeast two-hybrid system

Many methodologies for elucidating protein interactions have been developed during the past couple of decades. To investigate interactions inside cells under physiological conditions, especially, yeast would be a most typical organism, and various *in vivo* approaches are now available.

The yeast two-hybrid (Y2H) system, which was originally designed to detect protein–protein interactions *in vivo* by separation of a transcription factor into a DNA-binding domain and a transcription activation domain, is a typical representative of a yeast-based genetic approach (Fields and Song, 1989), and numerous improved Y2H systems have been developed to overcome its potential problems (Ishii et al., 2010). Despite significant progress in development of the Y2H systems, the analysis of interactions between membrane proteins remained a significant challenge because of the hydrophobic nature of these proteins (Thaminy et al., 2003). Recently, a modified two-hybrid approach, the split-ubiquitin membrane Y2H system witch can specifically apply to membrane proteins, has emerged as a powerful tool to protein–protein interaction in living cells (Stagljar et al., 1998).

Constituent of this thesis

In this study, we established the yeast-based approaches for elucidating the relationship between functions and structures of human GPCRs. For evaluating GPCR functions, we improved the system to monitor signal transmission for human GPCRs. For examining GPCR structures, we developed the system to monitor heterodimer formation among different types of human GPCRs. Finally, we combined these two systems into one yeast strain to simultaneously monitor the dimerization and the signaling. The findings of physiologically relevant GPCR dimers raise the prospect of developing new drugs against a wide range of diseases by focusing on the machinery of targeted dimers. This study is expected to provide a helpful tool for the elucidating of molecular biological functions of GPCR dimers and for the screening of GPCR dimer-specific agonistic ligands.

The contents in each part were described as below.

Part I: Microbial yeast biosensors to monitor signal transmission for human G-protein-coupled receptors

Yeast-based fluorescence reporter ligand detection system is useful for GPCR signaling assay since detection using a fluorescence reporter considerably simplifies the measurement procedure. However, the weak fluorescence generated from an agonist-induced cells expressing enhanced green fluorescent protein (EGFP) has limited the classes of GPCRs, which can be analyzed with this conventional detection system. In order to extend the ranges of applicable GPCRs, we constructed an improved fluorescence-based microbial yeast biosensor that can monitor the activation of human GPCR signaling responding to its agonist using tetrameric *Zoanthus* sp. green fluorescent protein (ZsGreen) as a reporter. In addition, we established a highly sensitive ligand detection system using yeast cell surface display technology that is applicable to peptide screening, and demonstrate that the display of various peptide analogs of neurotensin can activate signaling through the neurotensin receptor in yeast cells. Moreover, using the refined fluorescence biosensor, we successfully applied to antagonist characterization and site-directed mutagenesis analyses of human serotonin receptor. Furthermore we succeeded in the functional signal activation of mutated human angiotensin receptor in engineered yeast cells. This study showed that our strategy could apply to various human GPCRs by improving the sensitivity of detection system and modifying the human GPCRs.

Part II: Microbial yeast biosensors to monitor heterodimer formation for human G-protein-coupled receptors

Potentially immeasurable heterodimer combinations of human GPCRs result in a great deal of physiological diversity and provide a new opportunity for drug discovery. However, due to the existence of numerous combinations, the sets of GPCR dimers are almost entirely unknown and thus their dominant roles are still poorly understood. This study shows a mitogen-activated protein kinase (MAPK) signal-independent method specialized to screen candidate heterodimer partners for human GPCRs based on split-ubiquitin two-hybrid technology. By using the constructed method, we successfully identified new candidates as heterodimer partners for human GPCRs. In addition, since our system is independent from the activation of MAPK signal, it permits not only the identification of heterodimer partners, but also the monitoring of ligand-induced conformational changes. Finally, this study shows an advanced method to simultaneously analyze dimerization and ligand response of GPCRs using two yeast-based systems for split-ubiquitin two-hybrid assay and G-protein signaling assay. To monitor the specific profiling for functional consequences of dimerization linked to ligand-mediated signaling, we successfully demonstrated that the system was capable of simultaneously monitoring the dimerization and the signaling by human GPCRs.

References

AbdAlla S, Lother H, Quitterer U. 2000. AT1-receptor heterodimers show enhanced G-protein activation and altered receptor sequestration. Nature 407(6800):94–98.

Apanovitch DM, Slep KC, Sigler PB, Dohlman HG. 1998. Sst2 is a GTPase-activating protein for Gpa1: purification and characterization of a cognate RGS-Galpha protein pair in yeast. Biochemistry 37(14):4815–4822.

Benkirane M, Jin DY, Chun RF, Koup RA, Jeang KT. 1997. Mechanism of transdominant inhibition of CCR5-mediated HIV-1 infection by ccr5delta32. J Biol Chem 272(49):30603–30606.

Bockaert J, Perroy J, Bécamel C, Marin P, Fagni L. 2010. GPCR interacting proteins (GIPs) in the nervous system: Roles in physiology and pathologies. Annu Rev Pharmacol Toxicol 50:89–109.

Brown AJ, Dyos SL, Whiteway MS, White JH, Watson MA, Marzioch M, Clare JJ, Cousens DJ, Paddon C, Plumpton C et al. 2000. Functional coupling of mammalian receptors to the yeast mating pathway using novel yeast/mammalian G protein α-subunit chimeras. Yeast 16(1):11–22.

Chang F, Herskowitz I. 1990. Identification of a gene necessary for cell cycle arrest by a negative growth factor of yeast: FAR1 is an inhibitor of a G1 cyclin, CLN2. Cell 63(5):999–1011.

Chang F, Herskowitz I. 1992. Phosphorylation of FAR1 in response to alpha-factor: a possible requirement for cell-cycle arrest. Mol Biol Cell 3(4):445–450.

Cvejic S, Devi LA. 1997. Dimerization of the delta opioid receptor: Implication for a role in receptor internalization. J Biol Chem 272(43):26959–26964.

Dohlman HG, Song J, Ma D, Courchesne WE, Thorner J. 1996. Sst2, a negative

regulator of pheromone signaling in the yeast *Saccharomyces cerevisiae*: expression, localization, and genetic interaction and physical association with Gpa1 (the G-protein α subunit). Mol Cell Biol 16(9):5194–5209.

Dolan JW, Kirkman C, Fields S. 1989. The yeast STE12 protein binds to the DNA sequence mediating pheromone induction. Proc Natl Acad Sci USA 86(15):5703–5707.

Dosil M, Schandel KA, Gupta E, Jenness DD, Konopka JB. 2000. The C terminus of the *Saccharomyces cerevisiae* α-factor receptor contributes to the formation of preactivation complexes with its cognate G protein. Mol Cell Biol 20(14):5321–5329.

Drews J. 2000. Drug discovery: a historical perspective. Science 287(5460):1960–1964.

Eglen RM, Bosse R, Reisine T. 2007. Emerging concepts of guanine nucleotide-binding protein-coupled receptor (GPCR) function and implications for high throughput screening. Assay Drug Dev Technol 5(3):425–451.

Elion EA. 2001. The Ste5p scaffold. J Cell Sci 114:3967–3978.

Erlenbach I, Kostenis E, Schmidt C, Hamdan FF, Pausch MH, Wess J. 2001. Functional expression of M_1, M_3 and M_5 muscarinic acetylcholine receptors in yeast. J Neurochem 77(5):1327–1337.

Ferré S, Franco R. 2010. Oligomerization of G-protein-coupled receptors: A reality. Curr Opin Pharmacol 10(1):1–5.

Fredriksson R, Lagerström MC, Lundin L-G, Schiöth HB. 2003. The G-protein-coupled receptors in the human genome form five main families. Phylogenetic analysis, paralogon groups, and fingerprints. Mol Pharmacol 63:1256–1272.

Fields S, Song O. 1989. A novel genetic system to detect protein–protein interactions.

Nature 340(6230):245–246.

Fukuda N, Ishii J, Kaishima M, Kondo A. 2011. Amplification of agonist stimulation of human G-protein-coupled receptor signaling in yeast. Anal Biochem 417(2):182–187.

Fukutani Y, Ishii J, Noguchi K, Kondo A, Yohda M. 2012. An improved bioluminescence-based signaling assay for odor sensing with a yeast expressing a chimeric olfactory receptor. Biotechnol Bioeng 109(12):3143–3151.

Gilman AG. 1987. G proteins: Transducers of receptor-generated signals. Annu Rev Biochem 56:615–649.

Grosse R, Schöneberg T, Schultz G, Gudermann T. 1997. Inhibition of gonadotropin-releasing hormone receptor signaling by expression of a splice variant of the human receptor. Mol Endocrinol 11(9):1305–1318.

Gudermann T, Nurnberg B, Schultz G. 1995. Receptors and G proteins as primary components of transmembrane signal transduction. Part 1. G-protein-coupled receptors: Structure and function. J Mol Med (Berl) 73(2):51–63.

Hebert TE, Moffett S, Morello JP, Loisel TP, Bichet DG, Barret C, Bouvier M. 1996. A peptide derived from a beta2-adrenergic receptor transmembrane domain inhibits both receptor dimerization and activation. J Biol Chem 271(27):16384–16392.

Heilker R, Wolff M, Tautermann CS, Bieler M. 2009. G-protein-coupled receptor-focused drug discovery using a target class platform approach. Drug Discov Today 14:231–240.

Hirschman JE, Jenness DD. 1999. Dual lipid modification of the yeast Gγ subunit Ste18p determines membrane localization of Gβγ. Mol Cell Biol 19(11):7705–7711.

Hur EM, Kim KT. 2002. G protein-coupled receptor signalling and cross-talk: achieving rapidity and specificity. Cell Signal 14(5):397–405.

Iguchi Y, Ishii J, Nakayama H, Ishikura A, Izawa K, Tanaka T, Ogino C, Kondo A. 2010. Control of signalling properties of human somatostatin receptor subtype-5 by additional signal sequences on its amino-terminus in yeast. J Biochem 147(6): 875–884.

Ishii J, Fukuda N, Tanaka T, Ogino C, Kondo A. 2010. Protein–protein interactions and selection: yeast-based approaches that exploit guanine nucleotide-binding protein signaling. FEBS J 277(9):1982–1995.

Ishii J, Yoshimoto N, Tatematsu K, Kuroda S, Ogino C, Fukuda H, Kondo A. 2012. Cell wall trapping of autocrine peptides for human G-protein-coupled receptors on the yeast cell surface. PLoS One 7(5):e37136.

Jordan BA, Devi LA. 1999. G-protein-coupled receptor heterodimerization modulates receptor function. Nature 399(6737):697–700.

Jordan BA, Trapaidze N, Gomes I, Nivarthi R, Devi LA. 2001. Oligomerization of opioid receptors with beta 2-adrenergic receptors: A role in trafficking and mitogen-activated protein kinase activation. Proc Natl Acad Sci USA 98(1): 343–348.

King K, Dohlman HG, Thorner J, Caron MG, Lefkowitz RJ. 1990. Control of yeast mating signal transduction by a mammalian β_2-adrenergic receptor and Gs α subunit. Science 250(4977):121–123.

Klabunde T, Hessler G. 2002. Drug design strategies for targeting G-protein-coupled receptors. Chembiochem 3(10):928–944.

Ladds G, Goddard A, Davey J. 2005. Functional analysis of heterologous GPCR

signalling pathways in yeast. Trends Biotechnol 23(7):367–373.

Leberer E, Thomas DY, Whiteway M. 1997. Pheromone signalling and polarized morphogenesis in yeast. Curr Opin Genet Dev 7(1):59–66.

Leeuw T, Wu CL, Schrag JD, Whiteway M, Thomas DY, Leberer E. 1998. Interaction of a G-protein β-subunit with a conserved sequence in Ste20/PAK family protein kinases. Nature 391(6663):191–195.

Lefkowitz RJ, Shenoy SK. 2005. Transduction of receptor signals by beta-arrestins. Science 308(5721):512–517.

Leplatois P, Josse A, Guillemot M, Febvre M, Vita N, Ferrara P, Loison G. 2001. Neurotensin induces mating in *Saccharomyces cerevisiae* cells that express human neurotensin receptor type 1 in place of the endogenous pheromone receptor. Eur J Biochem 268(18):4860–4867.

Li B, Scarselli M, Knudsen CD, Kim SK, Jacobson KA, McMillin SM, Wess J. 2007. Rapid identification of functionally critical amino acids in a G protein-coupled receptor. Nat Methods 4(2):169–174.

Lushchak VI. 2006. Budding yeast *Saccharomyces cerevisiae* as a model to study oxidative modification of proteins in eukaryotes. Acta Biochim Pol 53(4):679–684.

Manahan CL, Patnana M, Blumer KJ, Linder ME. 2000. Dual lipid modification motifs in Gα and Gγ subunits are required for full activity of the pheromone response pathway in *Saccharomyces cerevisiae*. Mol Biol Cell 11(3):957–968.

Manfredi JP, Klein C, Herrero JJ, Byrd DR, Trueheart J, Wiesler WT, Fowlkes DM, Broach JR. 1996. Yeast α mating factor structure-activity relationship derived from genetically selected peptide agonists and antagonists of Ste2p. Mol Cell Biol 16(9):4700–4709.

Margeta-Mitrovic M, Jan YN, Jan LY. 2000. A trafficking checkpoint controls GABA(B) receptor heterodimerization. Neuron 27(1):97–106.

McKinney JD, Cross FR. 1995. FAR1 and the G1 phase specificity of cell cycle arrest by mating factor in *Saccharomyces cerevisiae*. Mol Cell Biol 15(5):2509–2516.

Mijares A, Lebesque D, Wallukat G, Hoebeke J. 2000. From agonist to antagonist: Fab fragments of an agonist-like monoclonal anti-beta(2)-adrenoceptor antibody behave as antagonists. Mol Pharmacol 58(2):373–379.

Minic J, Sautel M, Salesse R, Pajot-Augy E. 2005. Yeast system as a screening tool for pharmacological assessment of g protein coupled receptors. Curr Med Chem 12(8):961–969.

Muller EM, Mackin NA, Erdman SE, Cunningham KW. 2003. Fig1p facilitates Ca2+ influx and cell fusion during mating of *Saccharomyces cerevisiae*. J Biol Chem 278(40):38461–38469.

Overington JP, Al-Lazikani B, Hopkins AL. 2006. How many drug targets are there? Nat Rev Drug Discov 5(12):993–996.

Pausch MH, Lai M, Tseng E, Paulsen J, Bates B, Kwak S. 2004. Functional expression of human and mouse P2Y12 receptors in *Saccharomyces cerevisiae*. Biochem Biophys Res Commun 324(1):171–177.

Potter LT, Ballesteros LA, Bichajian LH, Ferrendelli CA, Fisher A, Hanchett HE, Zhang R. 1991. Evidence of paired M2 muscarinic receptors. Mol Pharmacol 39(2): 211–221.

Price LA, Kajkowski EM, Hadcock JR, Ozenberger BA, Pausch MH. 1995. Functional coupling of a mammalian somatostatin receptor to the yeast pheromone response pathway. Mol Cell Biol 15(11):6188–6195.

Pryciak PM, Huntress FA. 1998. Membrane recruitment of the kinase cascade scaffold protein Ste5 by the Gβγ complex underlies activation of the yeast pheromone response pathway. Genes Dev 12(17)2684–2697.

Ritter SL, Hall RA. 2009. Fine-tuning of GPCR activity by receptor-interacting proteins. Nat Rev Mol Cell Biol 10(12):819–830.

Schneiter R. 2007. Intracellular sterol transport in eukaryotes, a connection to mitochondrial function? Biochimie 89(2):255–259.

Siehler S. 2008. Cell-based assays in GPCR drug discovery. Biotechnol J 3(4):471–483.

Song D, Dolan JW, Yuan YL, Fields S. 1991. Pheromone-dependent phosphorylation of the yeast STE12 protein correlates with transcriptional activation. Genes Dev 5(5):741–750.

Stagljar I, Korostensky C, Johnsson N, te Heesen S. 1998. A genetic system based on split-ubiquitin for the analysis of interactions between membrane proteins *in vivo*. Proc Natl Acad Sci USA 95(9):5187–5192.

Sychrová H. 2004. Yeast as a model organism to study transport and homeostasis of alkali metal cations. Physiol Res 53:S91–S98.

Takeda S, Kadowaki S, Haga T, Takaesu H, Mitaku S. 2002. Identification of G protein-coupled receptor genes from the human genome sequence. FEBS Lett 520(1–3):97–101.

Togawa S, Ishii J, Ishikura A, Tanaka T, Ogino C, Kondo A. 2010. Importance of asparagine residues at positions 13 and 26 on the amino-terminal domain of human somatostatin receptor subtype-5 in signaling. J Biochem 147(6):867–873.

Wang Y, Dohlman HG. 2006. Regulation of G protein and mitogen-activated protein kinase signaling by ubiquitination: insights from model organisms. Circ Res

99(12):1305–1314.

Winderickx J, Delay C, De Vos A, Klinger H, Pellens K, Vanhelmont T, Van Leuven F, Zabrocki P. 2008. Protein folding diseases and neurodegeneration: lessons learned from yeast. Biochim Biophys Acta 1783(7):1381–1395.

Yesilaltay A, Jenness DD. 2000. Homo-oligomeric complexes of the yeast alpha-factor pheromone receptor are functional units of endocytosis. Mol Biol Cell 11(9): 2873–2884.

SYNOPSIS

Part I. Microbial yeast biosensors to monitor signal transmission for human G-protein-coupled receptors

Chapter 1

Bright fluorescence monitoring system utilizing *Zoanthus* sp. green fluorescent protein (*ZsGreen*) for human G-protein-coupled receptor signaling in microbial yeast cells

G-protein-coupled receptors (GPCR(s)) are currently the most important pharmaceutical targets for drug discovery because they regulate a wide variety of physiological processes. Consequently, simple and convenient detection systems for ligands which regulate the function of GPCR have attracted attention as powerful tools for new drug development. We previously developed a yeast-based fluorescence reporter ligand detection system using flow cytometry. However, using this conventional detection system, fluorescence from a cell expressing GFP and responding to a ligand is weak, making detection of these cells by fluorescence microscopy difficult. We here report improvements to the conventional yeast fluorescence reporter assay system resulting in the development of a new highly-sensitive fluorescence reporter assay system with extremely bright fluorescence and high signal-to-noise (S/N) ratio. This new system allowed the easy detection of GPCR signaling in yeast using fluorescence microscopy. Somatostatin receptor and neurotensin receptor (implicated in Alzheimer's disease and Parkinson's disease, respectively) were chosen as human GPCR(s). The facile detection of binding to these receptors by cognate peptide ligands

was demonstrated. In addition, we established a highly sensitive ligand detection system using yeast cell surface display technology that is applicable to peptide screening, and demonstrate that the display of various peptide analogs of neurotensin can activate signaling through the neurotensin receptor in yeast cells. Our system could be useful for identifying lead peptides with agonistic activity towards targeted human GPCR(s).

Chapter 2

Applications of microbial signaling biosensor using *Zoanthus* sp. green fluorescent protein for antagonist characterization and site-directed mutagenesis of human serotonin 1A receptor

The neurotransmitter serotonin (5-HT) regulates a wide spectrum of human physiology through the 5-HT receptor family. As the signaling mediator, 5-HT_{1A} receptor (HTR1A) that is the most widely studied subtype is a significant molecular target in medicinal and therapeutic fields. Yeast-based fluorescence reporter system is useful for GPCR assay since detection using a fluorescence reporter considerably simplifies the measurement procedure. However, previously reported systems using enhanced green fluorescent protein (*EGFP*) as the reporter gene still showed low signal-to-noise (S/N) ratio, making it difficult to apply to antagonist characterization and mutagenesis approaches. In this study, we employed a highly-potent fluorescence reporter (ZsGreen) and Gα-engineered yeast strain for making a refined yeast-based GPCR biosensor. Using the refined fluorescence biosensor, we successfully applied to antagonist characterization and site-directed mutagenesis analyses of human HTR1A receptor. The HTR1A antagonist, pindolol, was detected to specifically inhibit the agonist-induced activating HTR1A. In mutagenesis experiments, not only previously

reported mutants, but also the role of the highly conserved DRY motif in activation of HTR1A was investigated. Since our system provided rapid and facile assays for antagonist characterization and site-directed mutagenesis of HTR1A, our system has a potential for the effective tool towards human GPCR analyses.

Chapter 3

Yeast-based biosensing for functional Asn295-mutated human angiotensin II type 1 receptor signal activation

Angiotensin II (Ang II) type 1 receptor (AGTR1) is a G-protein-coupled receptor (GPCR). Its natural ligand, Ang II, is an important effector molecule controlling blood pressure and volume in the cardiovascular system, and is consequently involved in various diseases such as hypertension and heart failure. Thus, the signaling mediator, AGTR1, is a significant molecular target in medicinal and therapeutic fields. Yeast is a useful organism for sensing GPCR signaling because it provides a simplified version of the complicated machinery used by mammalian cells for signal transduction. Although yeast cells can successfully transmit a signal through a variety of human GPCRs expressed in the cell membrane, there have been no reports of the functional activation of AGTR1-mediated signaling in yeast cells. In the present study, we introduced a single mutation into human AGTR1 and used yeast-human chimeric Gα to exert the functional activation of AGTR1 in yeast cells. The engineered yeast cells expressing AGTR1 mutated at Asn295 and the chimeric Gα successfully transmitted the signal inside the yeast cells in response to Ang II peptide added to the assay medium. Further, we demonstrated that the autocrined Ang II peptide and its analog (Ang III peptide), produced and secreted by the engineered yeast cells, could by themselves promote

AGTR1-mediated signaling. This means that screening for agonistic peptides with various sequences from a self-produced genetic library would be a viable strategy. Thus, the constructed yeast biosensor, integrating an Asn295-mutated AGTR1 receptor, will be valuable in the design of drugs to treat AGTR1-related diseases.

Part II. Microbial yeast biosensors to monitor heterodimer formation for human G-protein-coupled receptors

Chapter 1

Rapid, facile detection of heterodimer partners for target human G-protein-coupled receptors using a modified split-ubiquitin membrane yeast two-hybrid system

Potentially immeasurable heterodimer combinations of human G-protein-coupled receptors (GPCRs) result in a great deal of physiological diversity and provide a new opportunity for drug discovery. However, due to the existence of numerous combinations, the sets of GPCR dimers are almost entirely unknown and thus their dominant roles are still poorly understood. Thus, the identification of GPCR dimer pairs has been a major challenge. Here, we established a specialized method to screen potential heterodimer partners of human GPCRs based on the split-ubiquitin membrane yeast two-hybrid system. We demonstrate that the mitogen-activated protein kinase (MAPK) signal-independent method can detect ligand-induced conformational changes and rapidly identify heterodimer partners for target GPCRs. Our data present the abilities to apply for the intermolecular mapping of interactions among GPCRs and to uncover potential GPCR targets for the development of new therapeutic agents.

Chapter 2

Simultaneous method for analyzing dimerization and signaling of G-protein-coupled receptor in yeast by dual-color reporter system

Understanding the role of G-protein-coupled receptor (GPCR) dimerization in cellular function has now become a major research focus. The potentially large functional and physiological diversity of dimerization among GPCRs is expected to provide opportunities for novel drug discovery. However, there is currently a lack of cell-based assays capable of specific profiling for the functional consequences of dimerization linked to ligand-mediated signaling. Here we present an advanced method to simultaneously analyze the dimerization and ligand response of GPCRs using two yeast-based systems for split-ubiquitin two-hybrid assay and G-protein signaling assay. To permit simultaneous detection, we established a two-color (dual-color) fluorescence reporter gene assay using enhanced green fluorescent protein (EGFP) and a far-red derivative of the tetrameric fluorescent protein DsRed-Express2 (E2-Crimson). In the present study, we tested our method first by analyzing dimerization and ligand-mediated signaling by the yeast endogenous pheromone receptor (Ste2p). Second, we showed that the system facilitated mutational analysis of domains involved in dimerization and signaling by Ste2p. Third, we successfully demonstrated that the system could simultaneously monitor homo- and hetero-dimerization and somatostatin-induced signaling in the test case of the human SSTR5 somatostatin receptor. Our strategy is expected to provide a useful tool for the elucidation of molecular biological functions of GPCR dimers and for the screening of GPCR dimer-specific agonistic ligands.

Part I

Microbial yeast biosensors to monitor signal transmission for human G-protein-coupled receptors

Chapter 1: Bright fluorescence monitoring system utilizing *Zoanthus* sp. green fluorescent protein (*ZsGreen*) for human G-protein-coupled receptor signaling in microbial yeast cells

Introduction

G-protein-coupled receptors (GPCRs) represent the largest family of transmembrane receptors and regulate a number of signaling events (Fredriksson et al., 2003; Rasmussen et al., 2007). In humans, these receptors are activated by a large variety of stimuli ranging from small molecules to larger hormones. The stimulation of GPCRs has been reported to engage a broad range of physiological responses, such as blood pressure regulation, smooth muscle contraction, neurotransmission, and cell proliferation (Cotton and Claing, 2009). Their key roles in cell signaling have made GPCRs frequent pharmaceutical and therapeutic targets for drug discovery (Gudermann et al., 1995). GPCRs are cell surface transmembrane receptors that transduce signals via heterotrimeric guanine nucleotide binding proteins (G-proteins) comprising Gα-, Gβ- and Gγ-subunits in all eukaryotes (Ishii et al., 2010).

The eukaryotic unicellular yeast, *Saccharomyces cerevisiae*, is a typical host cell used to study heterologous GPCRs at the molecular level (Iguchi et al., 2010; Togawa et al., 2010). Compared with mammalian cell lines, *S. cerevisiae* provides a simple and predictive way for studying GPCR signaling because it expresses only one kind of G-protein (Li et al., 2007). A variety of human GPCRs are known to transduce signals in yeast cells through the endogenous yeast Gα-subunit (Gpa1p) or a yeast–human chimeric G-protein (Fukuda et al., 2011; Ishii et al., 2012a). Furthermore, *S. cerevisiae*

is used for not only fundamental studies of signaling, but also for research into ligand screening and receptor mutagenesis due to its rapid cell growth and amenability to genetic manipulation compared with other eukaryotes (Evans et al., 2009; Klein et al., 1998; Ladds et al., 2005; Li et al., 2007).

Yeast cell-surface display technology is a powerful platform that enables proteins expressed in yeast to be tethered onto the cell surface (Gai and Wittrup, 2007; Kondo and Ueda, 2004; Pepper et al., 2008; Shibasaki et al., 2009; Ueda and Tanaka, 2000). This is accomplished by the use of "anchor" proteins that naturally localize on the cell surface in yeast cells. Typically, the gene encoding the target protein is fused to the anchor protein together with a secretion signal sequence at the N-terminus. This enables both the secretion of the fusion protein and tethers the protein firmly to the cell surface. Two typical anchor proteins are the C-terminal domains of truncated α-agglutinin (Sag1p; a manno-protein involved in sexual adhesion), and truncated Flo1p (a lectin-like cell-wall protein involved in flocculation) containing the glycosyl-phosphatidylinositol (GPI) anchor attachment signal sequence. Both proteins are used to fuse the target protein at their N-terminus (Murai et al., 1997; Sato et al., 2002). To date, yeast cell-surface display technology has been adopted for a broad range of applications including enzymatic catalysis, immune adsorption, and protein engineering (Feldhaus et al., 2003; Murai et al., 1997; Nakamura et al., 2001; Sato et al., 2002).

Yeast cell-surface display of low molecular peptides on the cell surface forms the basis of several ligand assay systems (Hara et al., 2012; Ishii et al., 2012b). Expressing a peptide ligand fused to an anchor protein together with a cognate GPCR in a single yeast cell can lead to a series of biological processes within the cell that include

expression of peptide ligands, binding to a receptor, signal transmission, and trapping of peptides on the cell wall (Ishii et al., 2012b). In principle, because the tethered peptides are unable to diffuse out of the expression cell, they do not interfere or interact with neighboring cells. This technique forms the basis of the Cell Wall Trapping of Autocrine Peptides (CWTrAP) system. In CWTrAP, transformation of a plasmid library allows the display of various peptides in the engineered yeast with a signal-responsive reporter gene. This allows the facile production of a yeast cell library expressing different candidate peptides and the concurrent screening of target peptides.

Three reporter genes, *HIS3* (auxotrophy), *lacZ* (colorimetry), and *luc* (luminometry), are often used to detect the activation of GPCR signaling in yeast cells (Fukutani et al., 2012; Klein et al., 1998; Li et al., 2007). These reporter genes offer comprehensive screening, comparative quantification, and extremely high detection sensitivity, respectively. In contrast, the green fluorescent protein (*GFP*) reporter gene provides the most simple procedure for the preparation of measurement samples, by merely washing the cells (Fukuda et al., 2011; Iguchi et al., 2010; Ishii et al., 2012a, 2012b; Togawa et al., 2010). The most common detection methods for GFP are fluorescence microscopy and flow cytometry (FCM). The detection sensitivity and throughput of FCM are high, enabling comparative quantification (Boder and Wittrup, 1997; Fukuda et al., 2007), population analysis (Medico et al., 2001), and quantitative cell sorting (Aharoni et al., 2006; Stoeckius et al., 2009). However, not all researchers have access to expensive FCM equipment.

On the other hand, fluorescence microscopes are comparatively common and inexpensive, are simple to operate, and allow cell visualization. However, unlike other reporter gene assay systems, fluorescence microscopy cannot amplify the fluorescence

signal by prolonging the reaction time between the enzyme and the substrate (Ishii et al., 2014). This make it difficult to capture fluorescence images of cells responding to the ligand using conventional yeast GPCR assay systems, even when enhanced green fluorescent protein (*EGFP*) reporter gene is expressed. There is therefore need to improve the fluorescence reporter system in yeast GPCR assays.

We here report a highly-sensitive fluorescence reporter system applicable to both the yeast-based GPCR assay and CWTrAP technology. By using the tetrameric *Zoanthus* sp. green fluorescent protein (*ZsGreen*), extremely high sensitivity (high signal-to-noise (S/N) ratio) and bright fluorescence were attained, allowing easy observation using fluorescence microscopy. First, we employed human somatostatin receptor subtype-5 (hSSTR5), used previously, to demonstrate the dramatic improvement in the sensitivity and brightness by comparing with a conventional yeast-based fluorescence reporter system. The usefulness of this approach was exhibited with yeast cell-surface display technology. Second, we validated the applicability of this methodology using human somatostatin receptor subtype-2 (hSSTR2) and human neurotensin receptor subtype-1 (hNTSR1) and demonstrated sufficient brightness to permit verification of trapped peptide ligands on the yeast cell wall. Third, we demonstrated that the display of various peptidic neurotensin analogs can activate hNTSR1-mediated signaling in yeast cells.

Materials and Methods

Media. Synthetic dextrose (SD) medium contained 6.7 g/L yeast nitrogen base without amino acids (YNB) (BD-Diagnostic Systems, Sparks, MD, USA) and 20 g/L glucose. For SDM71 media, SD medium was adjusted to pH 7.1 with 200 mM MOPSO buffer (Nacalai Tesque, Kyoto, Japan). YPD medium contained 10 g/L yeast extract (Nacalai Tesque), 20 g/L peptone (BD-Diagnostic Systems) and 20 g/L glucose. As appropriate, SD medium was supplemented with amino acids or nucleotides (20 mg/L histidine, 60 mg/L leucine, 20 mg/L methionine, or 20 mg/L uracil). For solid medium, agar was added at 20 g/L.

Plasmids. All plasmids used in this study are summarized in **Table 1**. All oligonucleotides used for the plasmid constructions are listed in **Table 2**. Plasmid maps are presented in **Figure 1**.

The plasmid used for expression of *Zoanthus* sp. green fluorescent protein (ZsGreen) was constructed as follows. A DNA fragment encoding the *ZsGreen* gene was PCR-amplified from pZsGreen (Takara Bio, Shiga, Japan) using the oligonucleotides o1 and o2, digested with *Nhe*I+*Eco*RI, and inserted into the same sites between the *PGK1* promoter (P_{PGK1}) and the *PGK1* terminator (T_{PGK1}) on pGK416 (Ishii et al., 2009), yielding the plasmid pGK416-ZsGreen.

Table 1. Yeast strains and plasmids used in this study.

Strain or plasmid	Description	Reference
Strain		
BY4741	*MAT**a** his3Δ1 leu2Δ0 met15Δ0 ura3Δ0*	Brachmann et al. (1998)
IMFD-70	BY4741 *sst2Δ::AUR1-C ste2Δ::LEU2 fig1Δ::EGFP his3Δ::*P_{FIG1}*-EGFP far1Δ*	Togawa et al. (2010)
IMFD-72	IMFD-70 *gpa1Δ::Gi3tp*	Ishii et al. (2012a)
IMFD-70Zs	BY4741 *sst2Δ::AUR1-C ste2Δ::LEU2 fig1Δ::EGFP his3Δ::*P_{FIG1}*-ZsGreen far1Δ*	This study
IMFD-72Zs	IMFD-70Zs *gpa1Δ::Gi3tp*	This study
IMFD-70ZsD	BY4741 *sst2Δ::AUR1-C ste2Δ::LEU2 fig1Δ::ZsGreen his3Δ::*P_{FIG1}*-ZsGreen far1Δ*	This study
IMFD-72ZsD	IMFD-70ZsD *gpa1Δ::Gi3tp*	This study
Plasmid		
pGK416	Yeast expression vector containing *PGK1* promoter, *CEN/ARS* origin and *URA3* marker	Ishii et al. (2009)
pGK416-ZsGreen	*ZsGreen* in pGK416	This study
pGK416-EGFP	*EGFP* in pGK416	Ishii et al. (2009)
pBlueScript II KS(+)	Cloning vector	Agilent Technologies
pBlue-FIG1p-URA3	P_{FIG1}*(300 bp)-URA3* in pBlueScript II KS(+)	This study
pBlue-FIG1pt-ZsGreen	P_{FIG1}*(300 bp)-URA3-ZsGreen-*T_{FIG1}*(200 bp)* in pBlue-FIG1p-URA3	This study
pBlue-HIS3t-URA3	T_{HIS3}*(300 bp)-URA3* in pBlueScript II KS(+)	This study
pBlue-HIS3t-FIG1p-ZsGreen	T_{HIS3}*(300 bp)-URA3-*P_{FIG1}*(450 bp)-ZsGreen* in pBlue-HIS3t-URA3	This study
pBlue-HIS3pt-FIG1pt-ZsGreen	T_{HIS3}*(300 bp)-URA3-*P_{FIG1}*(450 bp)-ZsGreen-*T_{FIG1}*(300 bp)-*P_{HIS3}*(200 bp)* in pBlue-HIS3t-FIG1p-ZsGreen	This study
pGK421	Yeast expression vector containing *PGK1* promoter, *2μ* origin and *MET15* marker	Togawa et al. (2010)
pGK421-SSTR5	*hSSTR5* in pGK421	Ishii et al. (2012a)
pGK421-SSTR2	*hSSTR2* in pGK421	Ishii et al. (2014)
pGK421-NTSR1	*hNTSR1* in pGK421	Ishii et al. (2014)
pGK426-S1442	*SST–Flag–Flo42* in pGK426	Ishii et al. (2012b)
pGK426-alpha42	*α-factor–Flag–Flo42* in pGK426	Ishii et al. (2012b)
pGK426-NTS42	*NTS–Flag–Flo42* in pGK426	This study
pGK426-NTS(8-13)42	$NTS_{8\text{-}13}$*–Flag–Flo42* in pGK426	This study
pGK426-NMN42	*NMN–Flag–Flo42* in pGK426	This study

Table 2. List of oligonucleotides.

o#	Name	Sequence
o1	NheI_ZsGreen_fw	5'-TTTTGCTAGCATGGCTCAGTCAAAGCACGG
o2	EcoRI_ZsGreen_rv	5'-TTTTGAATTCTCAGGGCAATGCAGATCCGG
o3	SacII_dFIG1up_fw	5'-GGGGCCGCGGTACAAAAATTATAACATTTT
o4	XbaI_dFIG1up_rv	5'-CCCCTCTAGATTTTTTTTTTTTTTTTTGT
o5	XbaI_URA3_fw	5'-CCCCTCTAGATTTTTGTTCTTTTTTTGA
o6	EcoRI_hr40-URA3_rv	5'-CCCCGAATTCTTTTTTTTTTTTTTTTTGTTTGTTTGTTTGTTTGTTTACGGGTAA TAACTGATATAATT
o7	EcoRI_ZsGreen_fw	5'-TTTTGAATTCATGGCTCAGTCAAAGCACGG
o8	XhoI_ZsGreen_rv	5'-TTTTCTCGAGTCAGGGCAATGCAGATCCGG
o9	XhoI_dFIG1dn_fw	5'-GGGGCTCGAGTTTTATCCTCAAATAAACAT
o10	KpnI_dFIG1dn_rv	5'-CCCCGGTACCAACAGACGGTAATGATTAGA
o11	SacII_dHIS3dn_fw	5'-AAAACCGCGGTATGAAATGCTTTTCTTGTT
o12	XbaI_dHIS3dn_rv	5'-GGGGTCTAGATGACACCGATTATTTAAAGC
o13	BamHI_hr40-URA3_rv	5'-CCCCGGATCCTGACACCGATTATTTAAAGCTGCAGCATACGATATATATAGGGT AATAACTGATATAATT
o14	BamHI_PFIG1_fw	5'-AAAAGGATCCATCACCCTGCATTGCCTCTT
o15	EcoRI_PFIG1_rv	5'-CCCCGAATTCTTTTTTTTTTTTTTTTTGTTTGTTTGTTT
o16	ClaI_ZsGreen_rv	5'-TTTTATCGATTCAGGGCAATGCAGATCCGG
o17	ClaI_TFIG1_fw	5'-GGGGATCGATTTTTATCCTCAAATAAACAT
o18	SalI_TFIG1_rv	5'-CCCCGTCGACATAACATTAGTATTTATAAA
o19	SalI_dHIS3up_fw	5'-AAAAGTCGACCTTTGCCTTCGTTTATCTTG
o20	KpnI_dHIS3up_rv	5'-AAAAGGTACCTCTTGGCCTCCTCTAGTACA
o21	NheI_SSTR2_fw	5'-TTTTGCTAGCATGGACATGGCGGATGAGCC
o22	BglII_SSTR2_rv	5'-CCCCAGATCTTCAGATACTGGTTTGGAGGT
o23	NheI_NTSR1_fw	5'-AAAAGCTAGCATGCGCCTCAACAGCTCCGC
o24	BglII_NTSR1_rv	5'-CCCCAGATCTCTAGTACAGCGTCTCGCGGG
o25	NheI_SS_fw	5'-GGGGGCTAGCATGAGATTTCCTTCAATTTT
o26	NTS_SS_rv	5'-ATTCTCATACAGCTGTCTTTTATCCAAAGA
o27	SalI_NTS_rv	5'-AAAAGTCGACGAGTATGTAGGGTCTTCTGGGTTTATTCTCATACAGCTG
o28	SalI_NTS(8-13)_rv	5'-GGGGGTCGACGAGTATGTAGGGTCTTCTTCTTTTATCCAAAGATACCC
o29	SalI_NMN_rv	5'-GGGGGTCGACCAGAATATAAGGAATTTTTCTTTTATCCAAAGATACCC

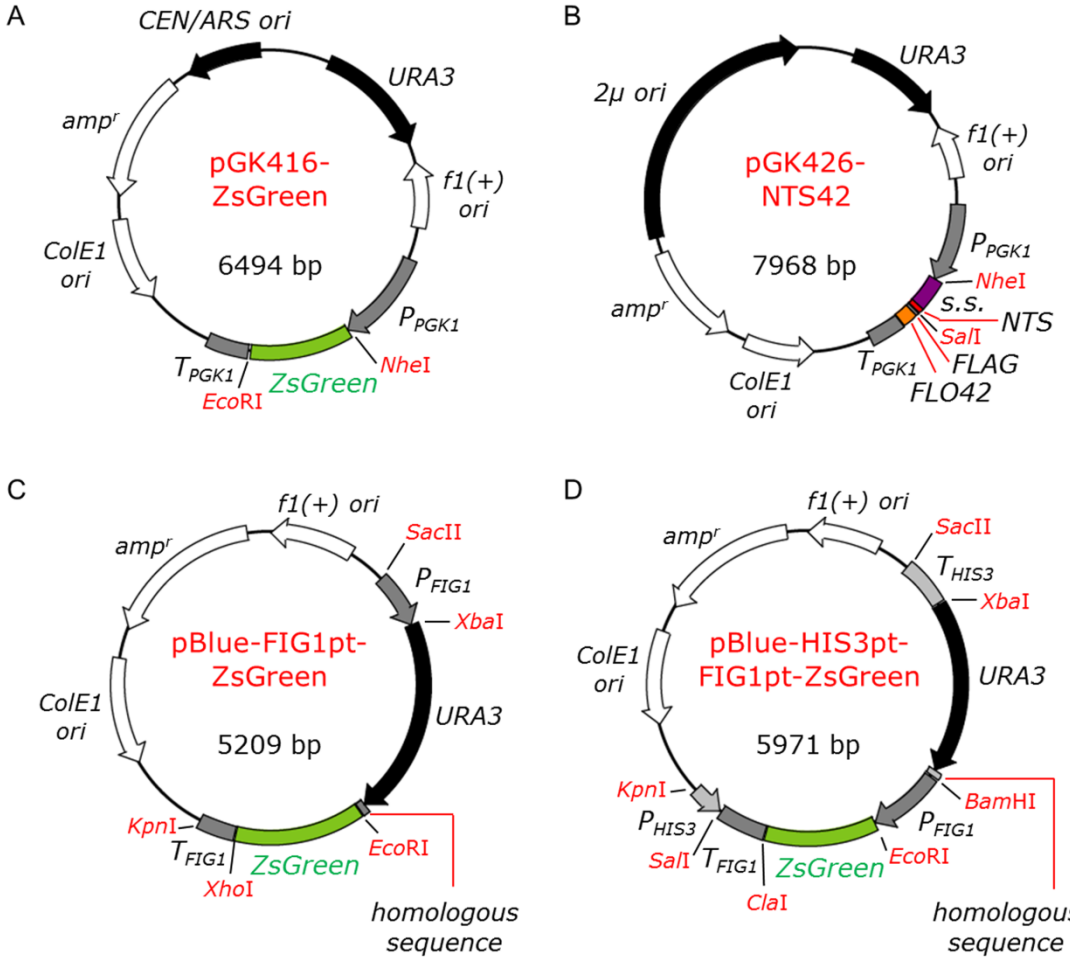

Fig. 1. Plasmids used in this study. (A) Single-copy plasmid pGK416-ZsGreen (B) Multi-copy plasmid pGK426-NTS42 (C) Integration plasmid pBlue-FIG1pt-ZsGreen (D) Integration plasmid pBlue-HIS3pt-FIG1pt-ZsGreen.

To express the *ZsGreen* gene under the control of the pheromone-responsive *FIG1* promoter (Iguchi et al., 2010; Nakamura et al., 2014; Togawa et al., 2010), the *ZsGreen* gene was inserted into a plasmid that integrated into the yeast chromosome at a position upstream of the *FIG1* gene. Plasmid construction was as follows. A DNA fragment containing the homologous sequence at the *FIG1* promoter (upstream of *FIG1* gene; 300 bp) was PCR-amplified from BY4741 (Brachmann et al., 1998) genomic DNA using oligonucleotides o3 and o4. A DNA fragment containing the *URA3* selectable marker (along with 40 nucleotides from the 3' side of the *FIG1* promoter at the 3' end) was PCR-amplified from pRS426 (American Type Culture Collection, Manassas, VA) using oligonucleotides o5 and o6. The amplified fragments were digested with *Sac*II+*Xba*I and *Xba*I+*Eco*RI (respectively) and ligated together into *Sac*II, *Eco*RI-cleaved pBlueScript II KS(+) vector (Agilent Technologies, Santa Clara, CA, USA). The resultant plasmid was named pBlue-FIG1p-URA3. A DNA fragment containing the *ZsGreen* gene was PCR-amplified from pZsGreen using oligonucleotides o7 and o8. A DNA fragment containing the homologous sequence of the *FIG1* terminator (downstream of *FIG1* gene; 200 bp) was PCR-amplified from BY4741 genomic DNA using oligonucleotides o9 and o10. The amplified fragments were digested with *Eco*RI+*Xho*I and *Xho*I+*Kpn*I (respectively) and ligated together into *Eco*RI, *Kpn*I-cleaved pBlue-FIG1p-URA3. The resultant plasmid was named pBlue-FIG1pt-ZsGreen.

The plasmid used for substituting P_{FIG1}-*ZsGreen*-T_{FIG1} for P_{FIG1}-*EGFP*-T_{FIG1} at the *HIS3* gene locus on the yeast chromosome was constructed as follows. A DNA fragment containing the homologous sequence of the *HIS3* terminator (downstream of *HIS3* gene; 300 bp) was PCR-amplified from BY4741 genomic DNA using oligonucleotides o11

and o12. A DNA fragment containing the *URA3* selectable marker (with 40 nucleotides from the 5' side of the *HIS3* terminator at the 3' end) was PCR-amplified from pRS426 (American Type Culture Collection, Manassas, VA) using oligonucleotides o5 and o13. The amplified fragments were digested with *Sac*II+*Xba*I and *Xba*I+*Bam*HI (respectively) and ligated together into *Sac*II, *Bam*HI-cleaved pBlueScript II KS(+) vector (Agilent Technologies, Santa Clara, CA, USA). The resultant plasmid was named pBlue-HIS3t-URA3. A DNA fragment containing the *FIG1* promoter (upstream of *FIG1* gene; 450 bp) was PCR-amplified from BY4741 genomic DNA using oligonucleotides o14 and o15. A DNA fragment containing the *ZsGreen* gene was PCR-amplified from pZsGreen using oligonucleotides o7 and o16. The amplified fragments were digested with *Bam*HI+*Eco*RI and *Eco*RI+*Cla*I (respectively) and ligated together into *Bam*HI, *Cla*I-cleaved pBlue-HIS3t-URA3. The resultant plasmid was named pBlue-HIS3t-FIG1p-ZsGreen. A DNA fragment containing the *FIG1* terminator (downstream of *FIG1* gene; 300 bp) was PCR-amplified from BY4741 genomic DNA using oligonucleotides o17 and o18. A DNA fragment containing the homologous sequence of the *HIS3* promoter (upstream of *HIS3* gene; 200 bp) was PCR-amplified from BY4741 genomic DNA using oligonucleotides o19 and o20. The amplified fragments were digested with *Cla*I+*Sal*I and *Sal*I+*Kpn*I (respectively) and ligated together into *Cla*I, *Sal*I-cleaved pBlue-HIS3t-FIG1p-ZsGreen. The resultant plasmid was named pBlue-HIS3pt-FIG1pt-ZsGreen.

The plasmids used for expression of membrane-tethered peptides, in which the pre, pro α-factor leader region gene (containing secretion signal sequence, s.s.), peptide gene and *FLO42* anchor gene with *FLAG* at the N-terminus are encoded, were constructed as follows. A DNA fragment containing s.s. of α-factor with a partial NTS sequence for

overlapping PCR was PCR-amplified from pGK426-S1442 (Ishii et al., 2012b) using oligonucleotides o25 and o26. The amplified fragment was then used as the template for overlapping PCR with the oligonucleotides o25 and o27. The *s.s.-NTS* was digested with *Nhe*I+*Sal*I and ligated into similarly digested pGK426-tgFLO42 (Ishii et al., 2012b), resulting in the plasmid pGK426-NTS42. A DNA fragment containing s.s. of α-factor and the C-terminal portion of NTS ($NTS_{8–13}$) was PCR-amplified from pGK426-NTS42 using oligonucleotides o25 and o28. The *s.s.-*$NTS_{8–13}$ was digested with *Nhe*I+*Sal*I and ligated into similarly digested pGK426-tgFLO42 (Ishii et al., 2012b), resulting in the plasmid pGK426-NTS(8-13)42. A DNA fragment containing s.s. of α-factor and neuromedin N (NMN) was PCR-amplified from pGK426-NTS42 using oligonucleotides o25 and o29. The *s.s.-NMN* was digested with *Nhe*I+*Sal*I and ligated into similarly digested pGK426-tgFLO42 (Ishii et al., 2012b), resulting in the plasmid pGK426-NMN42.

Yeast Strains. Yeast strains used in this study were generated from BY4741 (Brachmann et al., 1998) as a parental backbone strain and are listed in **Table 1**. Transformation with linear DNA fragments was performed using the lithium acetate method (Gietz et al., 1992). To eliminate the *URA3* selectable marker in each transformation step, we followed previous procedures (Iguchi et al., 2010; Togawa et al., 2010) modified to incorporate the marker recycling method (Akada et al., 2006).

The strains expressing *Zoanthus* sp. green fluorescence protein (ZsGreen) were generated as follows. The DNA fragment obtained by digesting pBlue-HIS3pt-FIG1pt-ZsGreen with *Sac*II and *Kpn*I was transformed into IMFD-70 (Togawa et al., 2010) and IMFD-72 (Ishii et al., 2012a). After confirming the correct

integration, the *URA3* marker was "popped-out" by homologous recombination using counter-selection with 5-fluoroorotic acid (5-FOA, Fluorochem, Derbyshire, UK). The resultant strains were designated as IMFD-70Zs and IMFD-72Zs, respectively. The DNA fragment obtained by digesting pBlue-FIG1pt-ZsGreen with *Sac*II and *Kpn*I was transformed into IMFD-70Zs and IMFD-72Zs. After confirming correct integration, the *URA3* marker was "popped-out" by counter-selection with 5-FOA. The constructed strains were designated as IMFD-70ZsD and IMFD-72ZsD, respectively.

Fluorescence Microscopy Imaging. The cultured cells were washed and suspended in distilled water. The cell suspensions were observed using a BZ-9000 fluorescence microscope (Keyence, Osaka, Japan). Green fluorescence images were acquired with a 470/40 band-pass filter for excitation and a 535/50 band-pass filter for emission. Digital image intensities of green fluorescence were carried out, from four experiments each, with the ImageJ software (freely downloadable from the ImageJ website, http://rsbweb.nih.gov/ij/) and expressed as Integrated Density (IntDen) or its percent.

Flow Cytometry Analysis. Flow cytometry measurements of green fluorescence followed previous procedures (Iguchi et al., 2010; Togawa et al., 2010). In brief, GFP was detected using a BD FACSCanto II flow cytometer equipped with a 488-nm blue laser (Becton, Dickinson and Company, Franklin Lakes, NJ, USA); the data were analyzed using BD FACSDiva software (v5.0; Becton, Dickinson and Company). The GFP fluorescence signal was collected through a 530/30 nm band-pass filter and the GFP-A mean of 10,000 cells was defined as 'green fluorescence intensity'.

Comparison Assay of Constitutively-expressed Two Green Fluorescence Proteins (ZsGreen and EGFP). Yeast transformants were grown in SD medium (supplemented as needed) at 30 °C overnight, and the cells then were inoculated into 5 mL of the respective fresh SD medium to give an initial optical density of 0.03 at 600 nm (OD_{600} = 0.03). The cells were incubated at 30 °C on a rotary shaker at 150 rpm for up to 18 h. After incubation, the yeast cells were observed using a fluorescence microscope, and then were diluted with 1 mL of sheath fluid and fluorescence was analyzed by flow cytometry.

GPCR Signaling Assay with Exogenously Added Ligands. GPCR signaling assays with exogenously added ligands basically followed previous procedures (Iguchi et al., 2010; Togawa et al., 2010). In brief, to assay signal activation from human GPCRs, yeast strains harboring the pGK421-based plasmids were grown in SD medium (supplemented as needed) at 30 °C overnight, then the cells then were inoculated into 5 mL of the respective fresh SD medium to give an initial OD_{600} = 0.03. The cells were incubated at 30 °C on a rotary shaker at 150 rpm for up to 18 h and harvested, washed, and resuspended in water to give an OD_{600} = 10. The suspensions were added (at 10 μL/well; to give an OD_{600} = 1) to the wells of 96-well cluster dishes containing fresh SDM71 medium (80 μL/well) supplemented (10 μL/well) with 10 μM of either somatostatin (SST) or neurotensin (NTS) (Calbiochem, Darmstadt, Germany) or distilled water (no SST (NTS), control). The plates were incubated at 30 °C with shaking (150 rpm) for 4 h, then the yeast cells were observed using a fluorescence microscope, diluted with 1 mL of sheath fluid, and fluorescence was analyzed by flow cytometry.

GPCR Signaling Assay using Membrane-tethered Peptide Ligands. GPCR signaling assays using membrane-tethered peptide ligands basically followed a previous procedure (Ishii et al., 2012b) with some modifications. In brief, to assay signal activation from human GPCRs, yeast strains harboring the pGK421-based GPCR expression plasmids and pGK426-based peptide display plasmids were grown in SD medium (supplemented as needed) at 30 °C overnight, then the cells then were inoculated into 5 mL of the respective fresh SDM71 medium to give an initial OD_{600} = 0.1. The cells were incubated at 30 °C on a rotary shaker at 150 rpm, then the yeast cells were observed using a fluorescence microscope, diluted with 1 ml of sheath fluid, and fluorescence was analyzed by flow cytometry.

Data Analysis. Data were analyzed using KaleidaGraph4.0. Statistical significance of the differences between more than two groups was calculated by one-way ANOVA, followed by Tukey's post test. Z' factor, a commonly used parameter reflecting the robustness and the quality of assays, was determined as follows: Z' factor = $1 - 3(SD_{positive\ control} + SD_{negative\ control})/ (mean_{positive\ control} - mean_{negative\ control})$, where "SD" represents standard deviation of multiple replicates of an assay (Zhang et al., 1999).

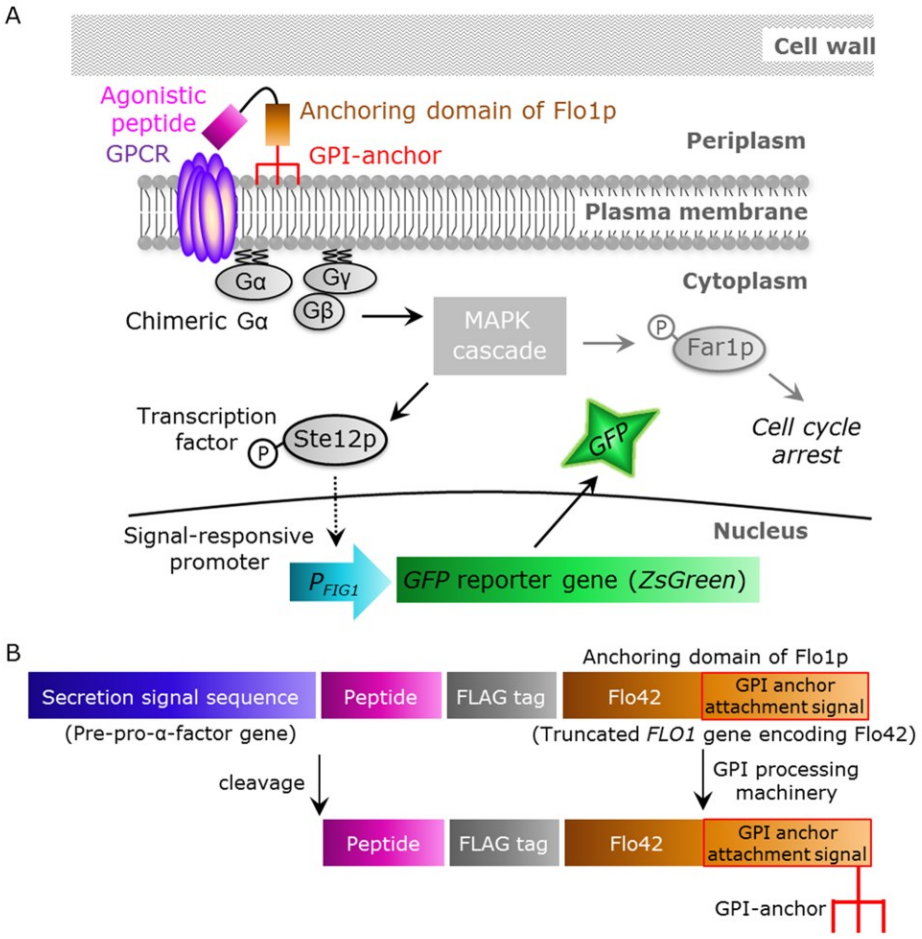

Fig. 2. Schematic illustration of signal activation of human GPCRs by membrane-tethered peptide ligands. (***A***) Overview of this study. The membrane-tethered peptide activates human GPCR, which is heterologously produced in yeast, thereby activating the chimeric Gα proteins. This promotes the mitogen-activated protein kinase (MAPK) cascade and transcription factor Ste12p. Phosphorylated Ste12p induces transcription of the GFP reporter gene by binding to a pheromone response element in the *FIG1* promoter. (***B***) Functional domains encoded by the membrane-tethered peptide plasmids. After processing by the secretory pathway, the signal sequence and glycosyl-phosphatidylinositol (GPI) targeting sequence are cleaved and the peptide sequence, which contains a free N-terminus, is tethered on the plasma membrane by GPI covalently linked to the C-terminus.

Results and Discussion

General strategy

The aim of this study was to establish a detection method for signals from human GPCRs induced by peptide ligands displayed on the yeast cell surface, thereby permitting observation by fluorescence microscopy. To tether agonistic peptides on the yeast cell membrane, a secretion signal sequence was fused to the N-terminus of the peptide, and a fusion of Flag tag and the C-terminal 42 amino acids of Flo1p (Flo42; anchor protein with GPI anchor attachment signal sequence) was fused to the C-terminus of the peptide (Ishii et al., 2012b). An outline of this strategy is shown in **Figure 2A** and **B**. Briefly, the yeast cells synthesize the candidate peptides fused with a secretion signal sequence and an anchoring motif. The membrane-anchored cognate agonistic peptides are capable of binding to the cell surface-expressed GPCRs and of transducing the signal into the cell. The GPI-anchored peptides are then cleaved from the plasma membrane by phosphatidylinositol-specific phospholipase C (PI-PLC) and tethered on the cell wall (Kondo and Ueda, 2004; Shibasaki et al., 2009).

To detect the activation of human GPCRs in yeast, the following gene modifications were implemented. The *sst2*Δ allele is deficient in the yeast principal negative regulator of G-protein signaling (RGS). This deletion therefore results in hypersensitivity for the agonistic stimulus (Ishii et al., 2006, 2010) and improves sensitivity towards low concentrations of ligand. The *far1*Δ allele is deficient in yeast G1-cyclin-dependent kinase inhibitor; this inhibitor induces G1 cell cycle arrest in response to signaling (Elion et al., 1993; Ishii et al., 2010). The *FAR1*-deficient strain can therefore grow and plasmid recovery occurs even in signal-activated states (Ishii et al., 2008). The *ste2*Δ allele is deficient in the yeast single GPCR, thereby allowing

expression of human GPCRs in *STE2*-disrupted strains without competitive receptor expression (Iguchi et al., 2010; Ishii et al., 2010; Nakamura et al., 2013; Togawa et al., 2010).

To detect signal activation, green fluorescence protein (GFP) reporter was integrated into the yeast genome. The expression of GFP is controlled by the signal responsive *FIG1* promoter. Therefore, stimulation by agonistic peptides results in the generation of a green fluorescence signal (Iguchi et al., 2010; Nakamura et al., 2014; Togawa et al., 2010). However, since the signal provided by the conventional detection system integrating an *EGFP* gene as the reporter is too weak to use for fluorescence microscopy, we explored a brighter fluorescent protein.

Comparison of two green fluorescence proteins (*ZsGreen* and *EGFP*) as reporter genes

To obtain the bright fluorescence required for easy observation by microscopy, we explored a recently described tetrameric *Zoanthus* sp. green fluorescent protein (ZsGreen) (brightness, 39,130 (quantum yield, 0.91; molar extinction coefficient, 43,000); excitation maximum, 493 nm; emission maximum, 505 nm) (Matz et al., 1999) as an alternative to EGFP (brightness, 16,100 (quantum yield, 0.70; molar extinction coefficient, 23,000); excitation maximum, 484 nm; emission maximum, 510 nm).

The performance (transcription, translation, folding and stability) of *ZsGreen* as a reporter gene in yeast was tested by comparing the fluorescence of yeast cells expressing either ZsGreen or EGFP using fluorescence microscopy and flow cytometry. Single-copy autonomous replicating plasmids, pGK416-ZsGreen and pGK416-EGFP, were constructed to express each green fluorescent protein constitutively under the

control of the *PGK1* promoter. Yeast BY4741 wild-type strains harboring these plasmids or mock vector were generated and their green fluorescence was evaluated.

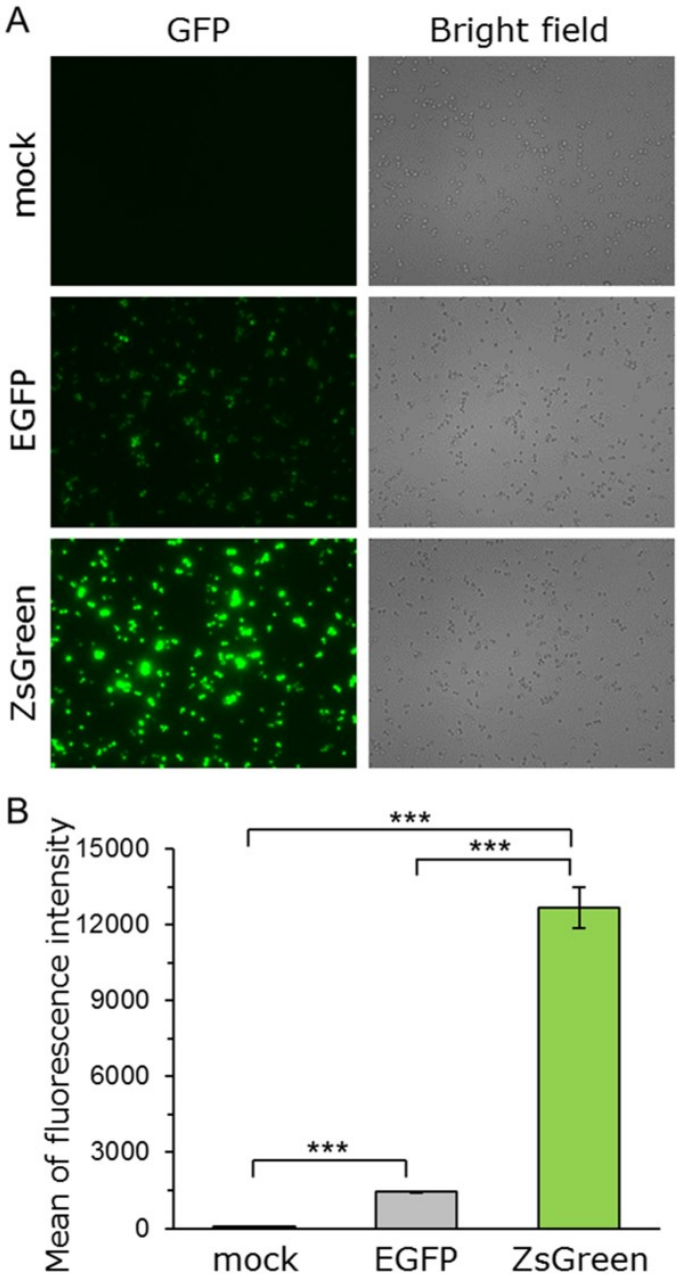

Fig. 3. Comparison of green fluorescence proteins (ZsGreen and EGFP). Yeast strain BY4741 was transformed with pGK416-ZsGreen, pGK416-EGFP or pGK416 (empty vector). All transformants were grown in SD selective medium for 18 h. (***A***) Visualization of the green fluorescence (ZsGreen and EGFP). Cells were examined using the 40× objective lens of a fluorescence microscope. Exposure time was 1 s. The left photographs are fluorescence micrographs, and the right photographs are bright-field micrographs. (***B***) The mean GFP fluorescence of 10,000 cells was measured by flow cytometry. Error bars represent the standard deviation from three separate runs ($n = 3$); ***, $p < 0.001$, by one-way ANOVA, Tukey's post test.

Using fluorescence microscopy, the cells expressing ZsGreen showed clearly brighter fluorescence than those expressing EGFP (**Figure 3A**). To compare the fluorescence intensity of these cells quantitatively, the average green fluorescence intensity per cell was measured by flow cytometry. The cells expressing ZsGreen exhibited a greater than 8.6-fold increase in fluorescence intensity compared with those expressing EGFP (**Figure 3B**). This is likely due to better protein features of ZsGreen than EGFP, including expression, translation and fluorescence property. In other cells (medaka melanoma cells, Chinese hamster ovary (CHO) cell line), the cells expressing ZsGreen also emitted brighter green fluorescence than those expressing EGFP, although there was a difference in GFP expression vector (promoter) (Hasegawa et al., 2009; Wan et al., 2012). Taken together, these results indicated that ZsGreen performs better than EGFP as a reporter in yeast.

Demonstration of improved signal activation detection using human somatostatin receptor subtype-5 (hSSTR5)

Somatostatin (SST), a cyclic neuropeptide which is a growth hormone release-inhibiting factor, is a natural ligand of somatostatin receptors. Five subtypes of somatostatin receptors have been identified (SSTR1–SSTR5) (Raynor et al., 1993a, b). These receptors are important therapeutic targets for acromegaly, Cushing's disease and Alzheimer's disease (Ben-Shlomo and Melmed, 2008; Lamberts et al., 1994; Saito et al., 2005).

The human SSTR5 receptor is known to transduce signals in yeast cells through the endogenous yeast Gα-subunit (Gpa1p). A yeast–human chimeric G-protein, in which the carboxyl-terminal 5 amino acid residues of Gpa1p (KIGII) are replaced with the

equivalent residues from human $G\alpha_{i3}$ (ECGLY) (Gpa1/$G\alpha_{i3}$ transplant, G_{i3}tp), has been shown to improve signal transmission via $G\alpha_i$-specific SSTR5 in yeast (Brown et al., 2000; Iguchi et al., 2010; Ishii et al., 2014).

The IMFD-70 (Gpa1p) and IMFD-72 (G_{i3}tp) strains were selected as the parental yeast strains as they contain two sets of P_{FIG1}-*EGFP*-T_{FIG1} cassettes (P_{FIG1}, *FIG1* promoter; T_{FIG1}, *FIG1* terminator) integrated into the genome (**Table 1**). One or both sets of P_{FIG1}-*EGFP*-T_{FIG1} cassettes were replaced with P_{FIG1}-*ZsGreen*-T_{FIG1} cassettes to generate IMFD-70Zs and IMFD-72Zs (single substitutions), and IMFD-70ZsD and IMFD-72ZsD (double substitutions) (**Table 1**). To evaluate the activity of *ZsGreen* as a reporter gene for detecting the signal from human GPCRs, we quantified the induction of green fluorescence responding to exogenously-added SST binding in hSSTR5-expressing yeast cells. Yeast IMFD-70, IMFD-72, IMFD-70Zs, IMFD-72Zs, IMFD-70ZsD and IMFD-72ZsD strains harboring pGK421-SSTR5 or mock vector were generated and examined using a signaling assay. As shown in **Figure 4A**, all yeast cells harboring the mock vector showed no fluorescence. In the case of yeast cells harboring pGK421-SSTR5, the addition of agonist to yeast strains IMFD-70 and IMFD-72 induced 3.9- and 5.6-fold higher fluorescence; however, the fluorescence was too weak to allow observation with a fluorescence microscope (**Figure 4A** and **B**). In contrast, strains IMFD-70Zs and IMFD-72Zs displayed a 33- and 65-fold increase, and strains IMFD-70ZsD and IMFD-72ZsD displayed a 83- and 104-fold increase in fluorescence intensity in response to agonist stimulation (**Figure 4A**). Using fluorescence microscopy, both the hSSTR5-expressing IMFD-70ZsD and IMFD-72ZsD exhibited changes in green fluorescence and morphology (Yu et al., 2008) in response to the SST-induced signal (**Figure 4B** and **C**).

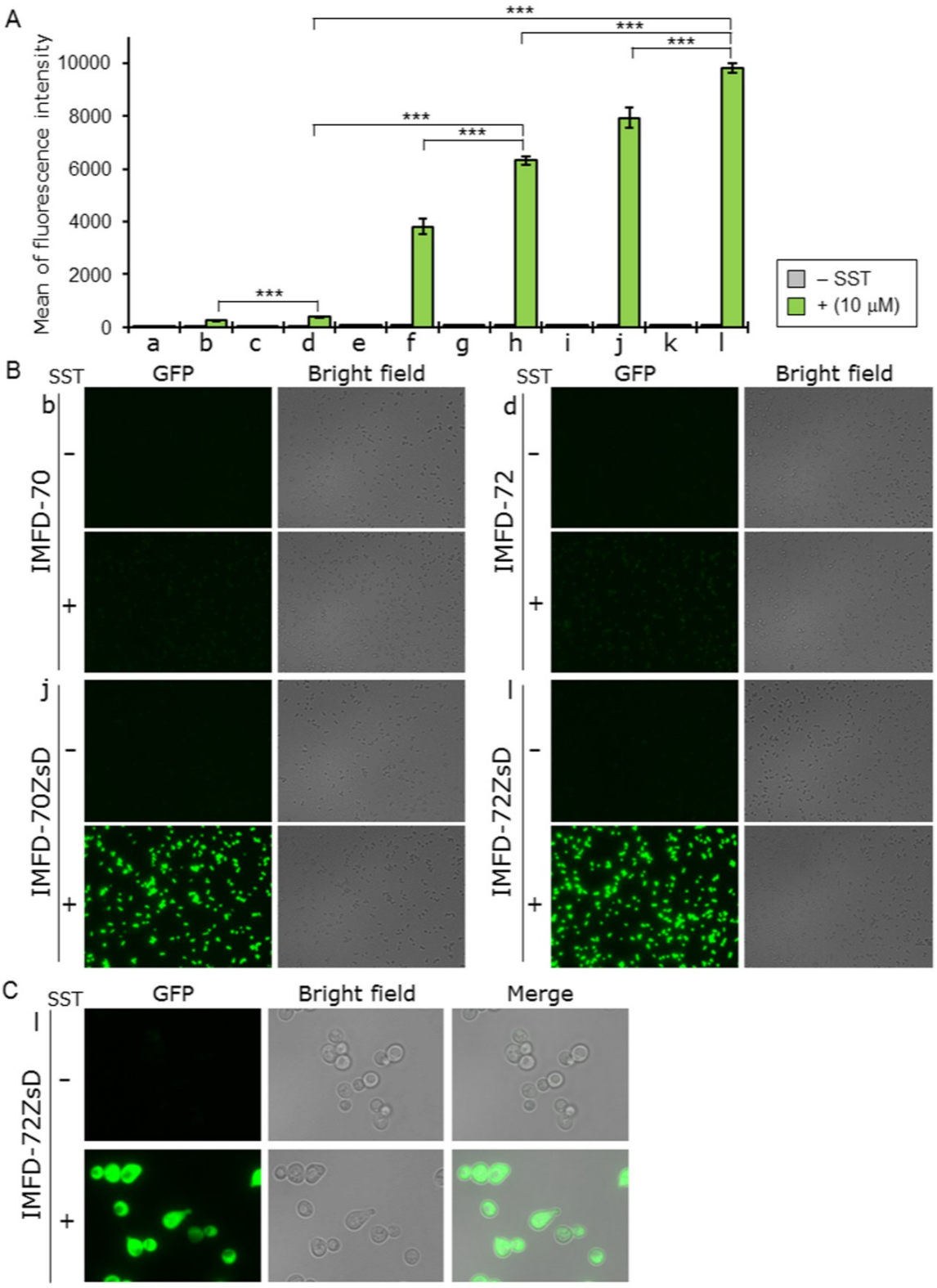
A
Mean of fluorescence intensity
10000
8000
6000
4000
2000
0
***
***
***
***
***
a b c d e f g h i j k l
– SST
+ (10 μM)
B
SST
GFP
Bright field
b
IMFD-70
d
IMFD-72
j
IMFD-70ZsD
l
IMFD-72ZsD
C
SST
GFP
Bright field
Merge
IMFD-72ZsD

Fig. 4. Activation of human somatostatin receptor subtype-5 (hSSTR5) produced in yeast by exogenously-added somatostatin. Yeast strains IMFD-70 (a, b); IMFD-72 (c, d); IMFD-70Zs (e, f); IMFD-72Zs (g, h); IMFD-70ZsD (i, j) and IMFD-72ZsD (k, l) were transformed with either pGK421 (empty vector) (a, c, e, g, i, k) or pGK421-SSTR5 (b, d, f, h, j, l). All transformants were grown in SD selective medium for 18 h. The cells then were incubated for another 4 h in pH-adjusted SD selective medium with or without 10 μM somatostatin (SST, 14 aa peptide). (***A***) The GFP fluorescence of 10,000 cells was measured by flow cytometry. Mean values of the green fluorescence signal of 10,000 cells. Error bars represent the standard deviation from three separate runs ($n = 3$); ***, $p < 0.001$, by one-way ANOVA, Tukey's post test. (***B,*** ***C***) Visualization of the green fluorescence. (***B***) Cells were examined using the 40× objective lens of a fluorescence microscope. Exposure time was 1 s. The left photographs are fluorescence micrographs, and the right photographs are bright-field micrographs. (***C***) Cells were examined using the 100× objective lens of a fluorescence microscope. Exposure time was 0.2 s.

Next, we examined whether this system is applicable to yeast cell-surface display technology in addition to observation by fluorescence microscopy. The hSSTR5 expression plasmid (pGK421-SSTR5) and peptide expression plasmids (pGK426-S1442 or pGK426-alpha42) were co-expressed in IMFD-72 and IMFD-72ZsD strains (**Table 1**). As shown in **Figure 5A**, the control strains harboring hSSTR5 and the yeast Ste2p receptor agonist, α-factor (α-factor–Flag–Flo42) as the control peptide, did not induce *GFP* reporter gene expression. In contrast, the yeast strains concomitantly expressing hSSTR5 and SST–Flag–Flo42 induced both *EGFP* and *ZsGreen* reporter gene expression. However, since EGFP fluorescence in IMFD-72 was weak, fluorescence microscopy could not distinctly differentiate between the strains displaying control (α-factor) and target (SST) peptides (**Figure 5B**), whereas IMFD-72ZsD strain using ZsGreen as a reporter clearly showed brighter green fluorescence and morphology change in response to the SST-induced signal (**Figure 5B** and **C**). These results indicated that our system provides dramatically improved sensitivity and brightness compared with a conventional yeast-based fluorescence reporter system.

Activation of human somatostatin receptor subtype-2 (hSSTR2)

To validate the applicability of this system for human somatostatin receptor subtype-2 (hSSTR2), the activation of hSSTR2 by exogenously-added SST was quantified. Yeast IMFD-70, IMFD-72, IMFD-70ZsD and IMFD-72ZsD strains harboring pGK421-SSTR2 were generated and studied using the signaling assay. As shown in **Figure 6A**, whereas the addition of agonist to yeast strains IMFD-70 and IMFD-72 induced a 3.0- and 4.6-fold higher fluorescence, agonist stimulation of strains IMFD-70ZsD and IMFD-72ZsD induced a 36- and 81-fold drastic increase in the

fluorescence intensity. Using fluorescence microscopy, the hSSTR2-expressing IMFD-72ZsD clearly exhibited changes in green fluorescence and morphology in response to the SST-induced signal (**Figure 6B** and **C**).

Next, to investigate the activation of hSSTR2 by membrane-tethered somatostatin, an hSSTR2 expression plasmid (pGK421-SSTR2) and peptide expression plasmids (pGK426-S1442 or pGK426-alpha42) were co-expressed in the IMFD-72ZsD strain (**Table 1**). As expected, the average fluorescence of the yeast strain concomitantly expressing hSSTR2 and SST–Flag–Flo42 increased with increasing incubation time, exhibiting a greater than 169-fold increase in fluorescence intensity compared with the yeast strain possessing hSSTR2 and α-factor–Flag–Flo42 after 12 h cultivation (**Figure 7A**). Using a fluorescence microscope, the yeast strain concomitantly expressing hSSTR2 and SST–Flag–Flo42 clearly showed a brighter green fluorescence change in response to the SST-induced signal (**Figure 7B**). These results indicated that our system is applicable to use with yeast cell-surface display technology.

Activation of human neurotensin receptor subtype-1 (hNTSR1)

Neurotensin (NTS) is a 13-amino-acid peptide found in the nervous system and in peripheral tissues (Carraway and Leeman, 1973; White et al., 2012). NTS shows a wide range of biological activities and has important roles in Parkinson's disease and the pathogenesis of schizophrenia, the modulation of dopamine neurotransmission, hypothermia, antinociception, and in promoting the growth of cancer cells (Bissette et al., 1976; Carraway and Plona, 2006; Griebel and Holsboer, 2012; Kitabgi, 2002; Schimpff et al., 2001). Three neurotensin receptors have been identified. NTSR1 (Tanaka et al., 1990) and NTSR2 (Chalon et al., 1996) belong to the class A GPCR

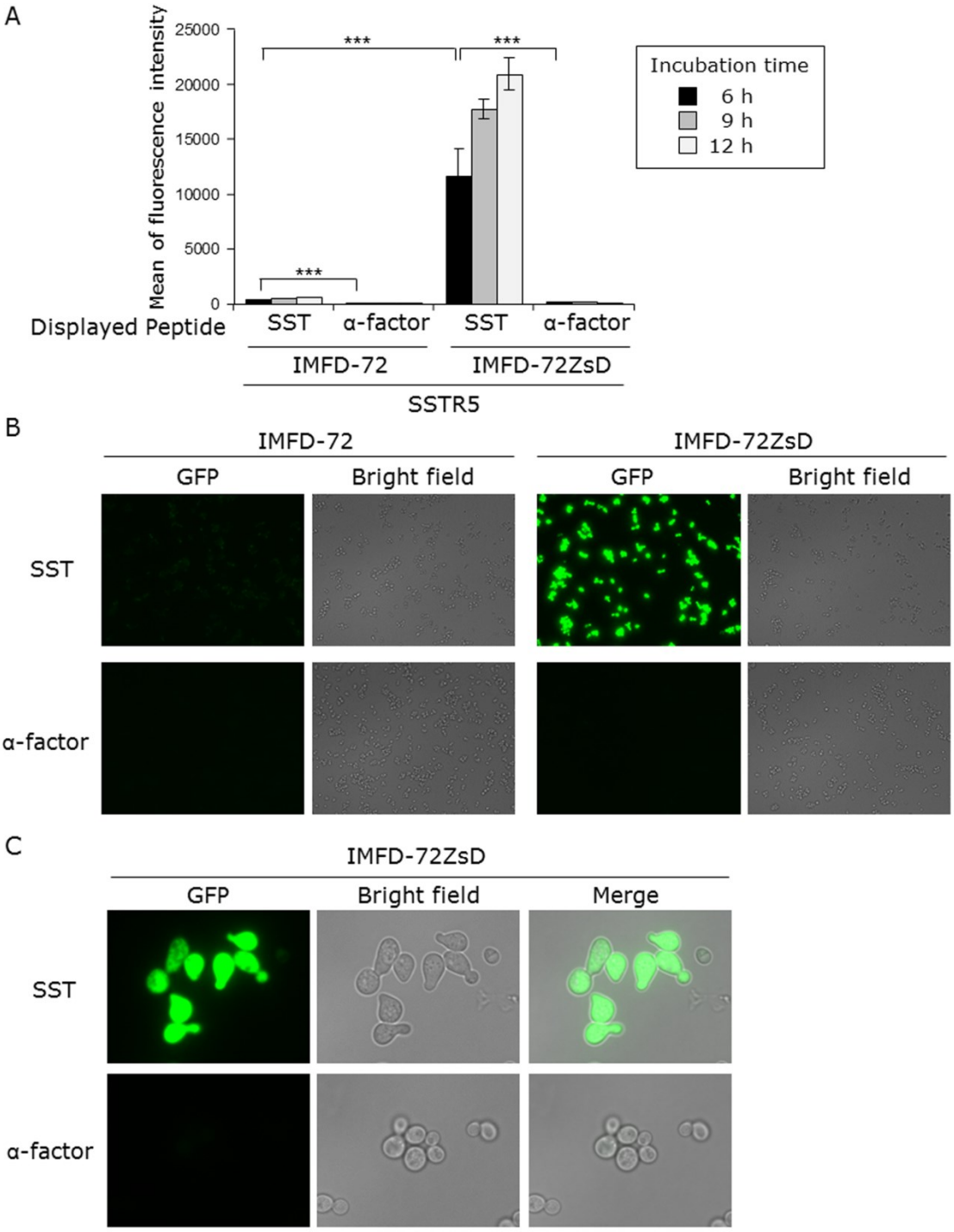
A
Mean of fluorescence intensity
25000
20000
15000
10000
5000
0
***
***
***
Incubation time
6 h
9 h
12 h
Displayed Peptide
SST
α-factor
SST
α-factor
IMFD-72
IMFD-72ZsD
SSTR5
B
IMFD-72
IMFD-72ZsD
GFP
Bright field
GFP
Bright field
SST
α-factor
C
IMFD-72ZsD
GFP
Bright field
Merge
SST
α-factor

Fig. 5. Activation of human somatostatin receptor subtype-5 (hSSTR5) by membrane-tethered somatostatin. Yeast strains IMFD-72 and IMFD-72ZsD, which coexpress pGK421-SSTR5 and either pGK426-S1442 (SST) or pGK426-alpha42 (α-factor), were incubated in pH-adjusted SD selective medium. (***A***) The GFP fluorescence of 10,000 cells was measured by flow cytometry. Mean values of the green fluorescence signal of 10,000 cells. Error bars represent the standard deviations ($n = 3$); ***, $p < 0.001$, by one-way ANOVA, Tukey's post test. (***B, C***) Fluorescence microscopy analysis of cells incubated for 9 h. (***B***) Cells were examined using the 40× objective lens of a fluorescence microscope. Exposure time was 0.67 s. The left photographs are fluorescence micrographs, and the right photographs are bright-field micrographs. (***C***) Cells were examined using the 100× objective lens of a fluorescence microscope. Exposure time was 0.14 s.

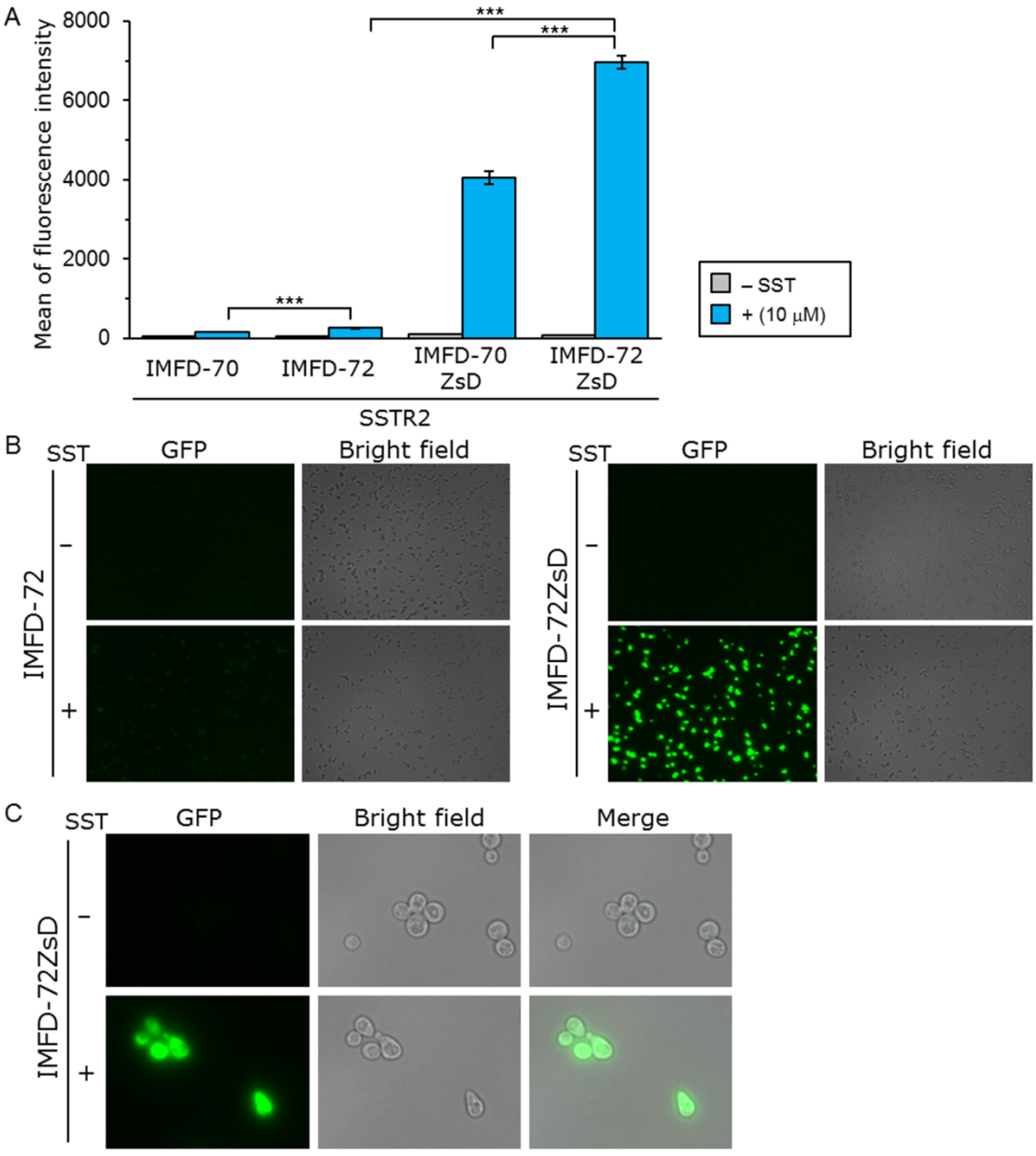
A
Mean of fluorescence intensity
8000
6000
4000
2000
0
***
***
***
IMFD-70
IMFD-72
IMFD-70 ZsD
IMFD-72 ZsD
SSTR2
– SST
+ (10 μM)
B
SST
GFP
Bright field
IMFD-72
IMFD-72ZsD
–
+
C
SST
GFP
Bright field
Merge
IMFD-72ZsD
–
+

Fig. 6. Activation of human somatostatin receptor subtype-2 (hSSTR2) by exogenously-added somatostatin. Yeast strains IMFD-70, IMFD-72, IMFD-70ZsD and IMFD-72ZsD were transformed with pGK421-SSTR2. All transformants were grown in SD selective medium for 18 h. The cells then were incubated for another 4 h in pH-adjusted SD selective medium with or without 10 μM somatostatin (SST, 14 aa peptide). (***A***) The GFP fluorescence of 10,000 cells was measured by flow cytometry. Mean values of the green fluorescence signal of 10,000 cells. Error bars represent the standard deviations ($n = 3$); ***, $p < 0.001$, by one-way ANOVA, Tukey's post test. (***B,*** ***C***) Visualization of the green fluorescence. (***B***) Cells were examined using the 40× objective lens of a fluorescence microscope. Exposure time was 1 s. The left photographs are fluorescence micrographs, and the right photographs are bright-field micrographs. (***C***) Cells were examined using the 100× objective lens of a fluorescence microscope. Exposure time was 0.33 s.

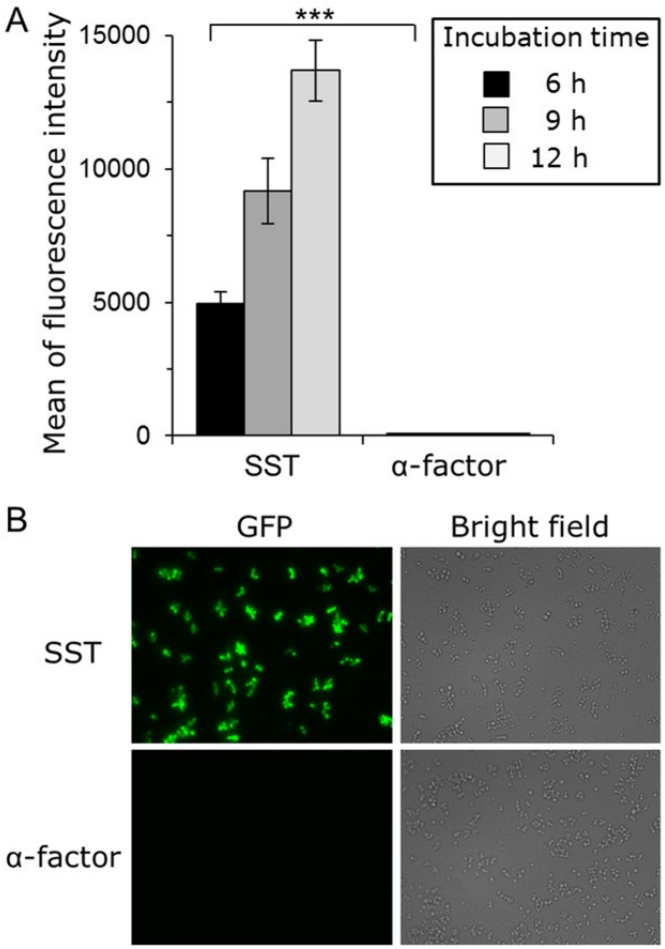

Fig. 7. Activation of human somatostatin receptor subtype-2 (hSSTR2) by membrane-tethered somatostatin. Yeast strain IMFD-72ZsD which coexpresses pGK421-SSTR2 and either pGK426-S1442 (SST) or pGK426-alpha42 (α-factor) was incubated in pH-adjusted SD selective medium. (***A***) The GFP fluorescence of 10,000 cells was measured by flow cytometry. Mean values of the green fluorescence signal of 10,000 cells. Error bars represent the standard deviations (n = 3); ***, $p < 0.001$, by one-way ANOVA, Tukey's post test. (***B***) Fluorescence microscopy analysis of the cells incubated for 9 h. Cells were examined using the 40× objective lens of a fluorescence microscope. Exposure time was 0.25 s. The left photographs are fluorescence micrographs, and the right photographs are bright-field micrographs.

family, whereas NTSR3 (also called SORT1) is a member of the sortilin family and contains a single transmembrane domain (Mazella, 2001). The crystal structure of the complex of NTSR1 and a partial NTS peptide was recently solved (White et al., 2012). Although many structures of the complex of GPCR and agonist or antagonist had been reported, this was the first report of the structure of NTSR1 bound with peptide hormone (White et al., 2012). Thus, attention was attracted to the study of NTSR1-mediated signaling in order to understand the GPCR-ligand binding modes.

Yeast IMFD-70, IMFD-72, IMFD-70ZsD and IMFD-72ZsD strains harboring pGK421-NTSR1 were generated for study using the signaling assay. As shown in **Figure 8A**, addition of agonist to yeast strains IMFD-70 and IMFD-72 resulted in only 1.3- and 2.3-fold higher fluorescence than in the absence of agonist, whereas strains IMFD-70ZsD and IMFD-72ZsD displayed a 7.9- and 45-fold increase in fluorescence intensity in response to agonist stimulation. Using fluorescence microscopy, the hNTSR1-expressing IMFD-72ZsD clearly exhibited changes in green fluorescence and morphology in response to the NTS-induced signal (**Figure 8B** and **C**). Similar to the results with hSSTR2, the IMFD-72ZsD strain harboring pGK421-NTSR1 exhibited a much higher average GFP intensity (S/N ratio) following stimulation by NTS compared with the IMFD-70ZsD strain harboring pGK421-NTSR1 (**Figure 8A**). These results indicated that the yeast–human chimeric G-protein subunit (G_{i3}tp) significantly improved hNTSR1-mediated signal transmission in yeast cells (Ishii et al., 2014).

To test whether the fluorescence microscopy approach is applicable for quantitative analysis, the yeast strain IMFD-72ZsD harboring pGK421-NTSR1 was used for observing green fluorescence images responding to several NTS concentrations. As shown in **Figure 9A**, the cells displayed the several distinct orders of brightness in

ZsGreen fluorescence. Then, using the green fluorescence images, digital image analysis with ImageJ was conducted. The digital intensities of green fluorescence varied in a NTS-dependent manner, indicating that the digital image analysis with fluorescence microscopy is available for the quantitative comparison of the signaling levels (**Figure 9B**).

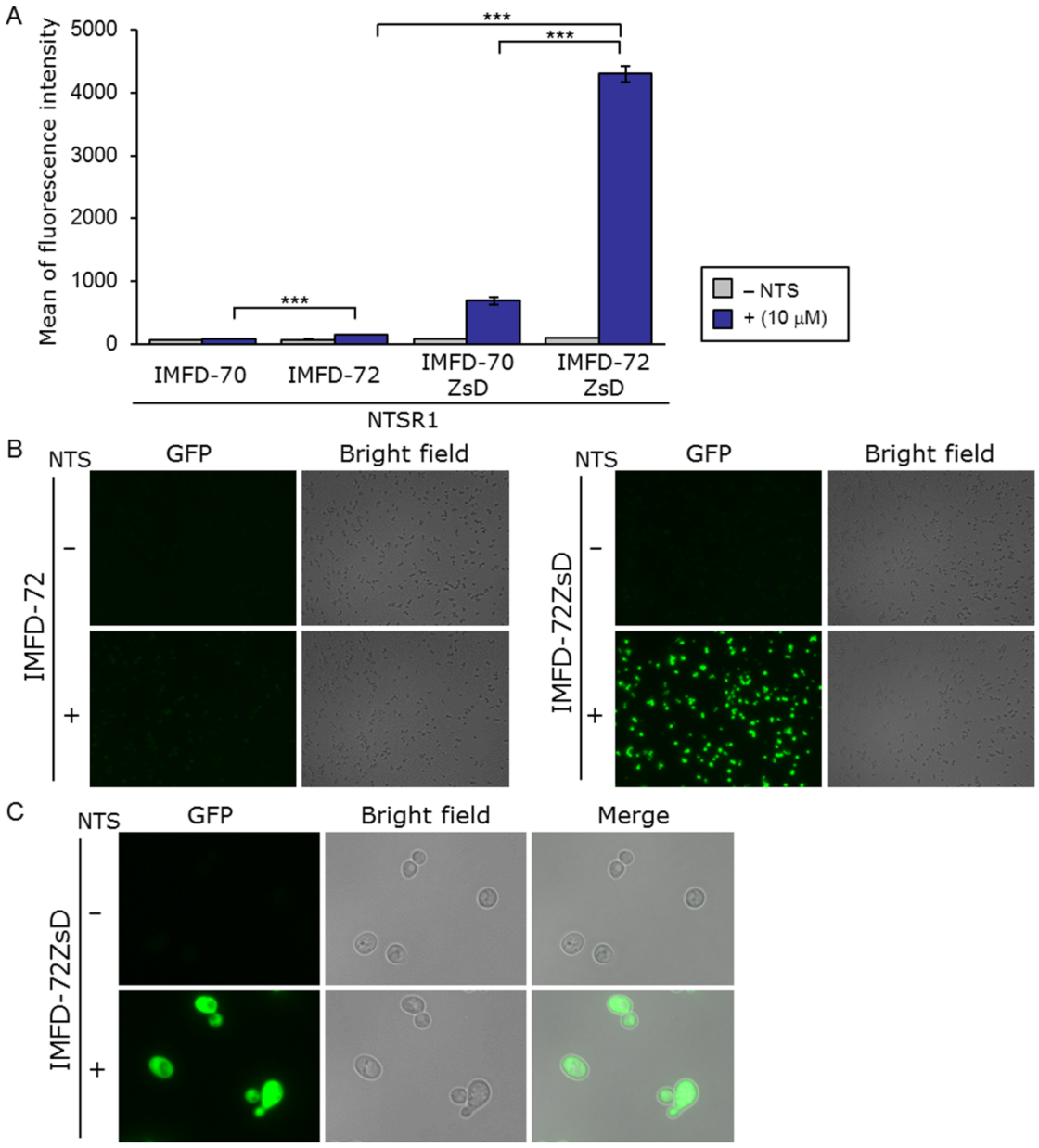

Fig. 8. Activation of human neurotensin receptor subtype-1 (hNTSR1) produced in yeast following exogenously-added neurotensin. Yeast strains IMFD-70, IMFD-72, IMFD-70ZsD and IMFD-72ZsD were transformed with pGK421-NTSR1. All transformants were grown in SD selective medium for 18 h. The cells then were incubated for another 4 h in pH-adjusted SD selective medium with or without 10 μM neurotensin (NTS, 13 aa peptide). (***A***) The GFP fluorescence of 10,000 cells was measured by flow cytometry. Mean values of the green fluorescence signal of 10,000 cells. Error bars represent the standard deviation from three separate runs ($n = 3$); ***, $p < 0.001$, by one-way ANOVA, Tukey's post test. (***B, C***) Visualization of the green fluorescence. (***B***) Cells were examined using the 40× objective lens of a fluorescence microscope. Exposure time was 1 s. The left photographs are fluorescence micrographs, and the right photographs are bright-field micrographs. (***C***) Cells were examined using the 100× objective lens of a fluorescence microscope. Exposure time was 0.5 s.

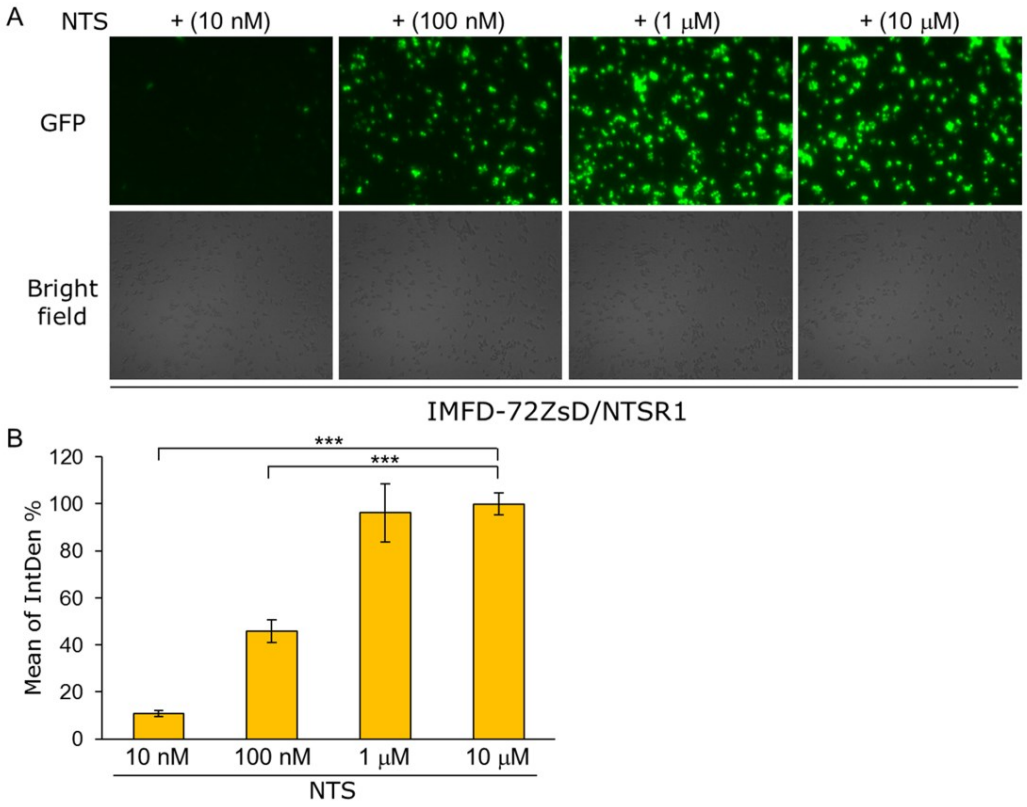

Fig. 9. Quantitative digital image analysis of ZsGreen fluorescence using fluorescence microscopy and ImageJ software. Yeast strain IMFD-72ZsD was transformed with pGK421-NTSR1. The transformant was grown in SD selective medium for 18 h. The cells then were incubated for another 4 h in pH-adjusted SD selective medium with neurotensin (NTS, 13 aa peptide) at several concentrations. (***A***) Visualization of the green fluorescence. Cells were examined using the 40× objective lens of a fluorescence microscope. Exposure time was 1 s. The upper photographs are fluorescence micrographs, and the lower photographs are bright-field micrographs. (***B***) The GFP fluorescence of 100 cells was measured as integrated density (IntDen, ImageJ software). Mean values of the green fluorescence signal of 100 cells. IntDen % was represented by relative IntDen normalized with the values of maximal effects of NTS-specific dose-responses. Error bars represent the standard deviation from four separate runs ($n = 4$); ***, $p < 0.001$, by one-way ANOVA, Tukey's post test.

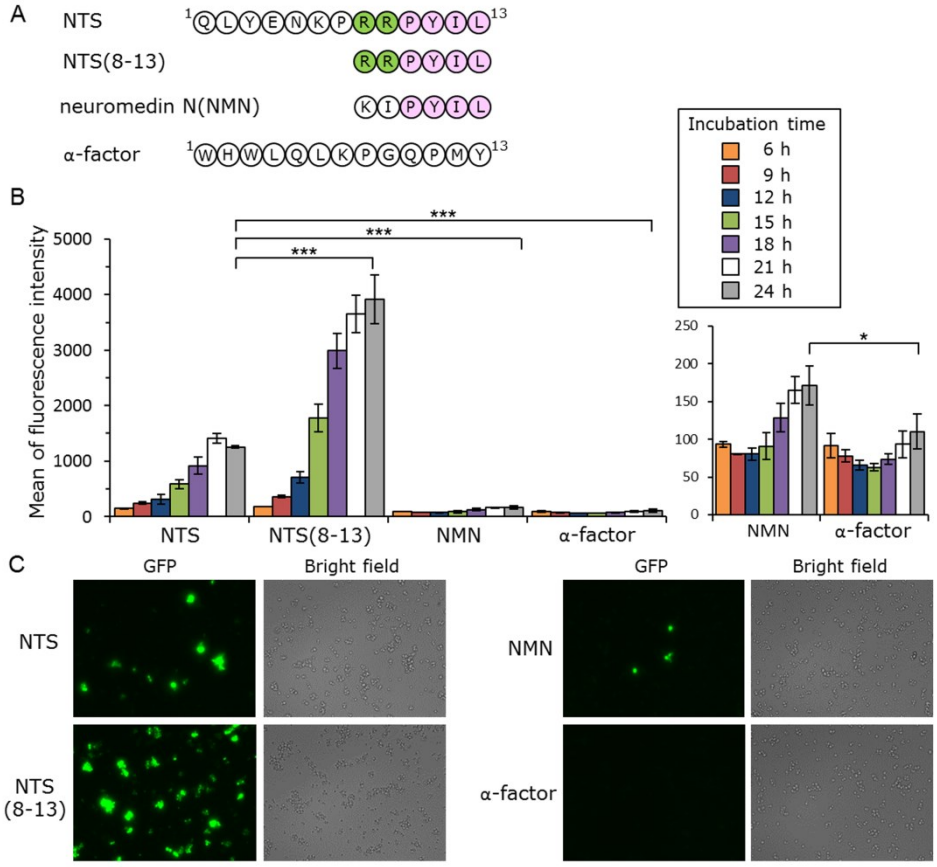

Fig. 10. Activation of human neurotensin receptor subtype-1 (hNTSR1) by membrane-tethered neurotensin. (***A***) Amino acid sequences of membrane-tethered peptides. (***B, C***) Yeast strain IMFD-72ZsD, which coexpresses pGK421-NTSR1 and either pGK426-NTS42 (NTS), pGK426-NTS(8-13)42 (NTS(8-13)), pGK426-NMN42 (NMN) or pGK426-alpha42 (α-factor), was incubated in pH-adjusted SD selective medium. (***B***) The GFP fluorescence of 10,000 cells was measured by flow cytometry. Mean values of the green fluorescence signal of 10,000 cells. Error bars represent the standard deviations (n = 3); *, $p < 0.05$, and ***, $p < 0.001$, by one-way ANOVA, Tukey's post test. (***C***) Fluorescence microscopy analysis of the cells incubated for 24 h. Cells were examined using the 40× objective lens of a fluorescence microscope. Exposure time was 0.67 s. The left photographs are fluorescence micrographs, and the right photographs are bright-field micrographs.

Activation of hNTSR1 by displaying neurotensin analogue peptides on the yeast cell surface

Finally, several neurotensin sequence analogues were employed to demonstrate that the display of various peptidic neurotensin analogs could also activate hNTSR1-mediated signaling in yeast cells (**Figure 10A**). Neurotensin-(8-13) ($NTS_{8–13}$), a pharmacophore of neurotensin, has higher potency and efficacy than full-length NTS (Barroso et al., 2000; White et al., 2012). Studies on the structure-activity relationship of neurotensin verified that positive charges at positions 8 and 9 are important but not prerequisite for its bioactivity (Granier et al., 1982). There is charge complementarity between $NTS_{8–13}$ and its binding pocket: the positively-charged arginine side chains of $NTS_{8–13}$ are adjacent to the electronegative rim of the binding site, and the C terminus of $NTS_{8–13}$ is predicted to form a salt bridge with R327 (White et al., 2012). A neurotensin-like peptide, neuromedin N (NMN), has high homology with the C-terminal sequence of neurotensin and is encoded by the same gene as neurotensin (Kislauskis et al., 1988; Minamino et al., 1984). Although the amino acid sequence of NMN (KIPYIL) is similar to that of $NTS_{8–13}$ (RRPYIL) (**Figure 10A**), NMN shows very weak biological activity (Minamino et al., 1984).

An hNTSR1 expression plasmid (pGK421-NTSR1) and peptide expression plasmids (pGK426-NTS42, pGK426-NTS(8-13)42, pGK426-NMN42 or pGK426-alpha42) were co-expressed in IMFD-72ZsD strain (**Table 1**). As shown in **Figure 10B**, the average fluorescence of the yeast strain concomitantly expressing hNTSR1 and NTS–Flag–Flo42 increased with increasing incubation time, exhibiting a greater than 11-fold increase in fluorescence intensity compared with the strain possessing hNTSR1 and α-factor–Flag–Flo42 after 24 h cultivation. The

membrane-tethered $NTS_{8–13}$ and NMN also induced ZsGreen fluorescence, exhibiting a greater than 35- and 1.5-fold increase in fluorescence intensity compared with α-factor after 24 h cultivation ($NTS_{8–13}$ > NTS > NMN > α-factor) (**Figure 10B**). Fluorescence microscopy demonstrated that the observed differences in fluorescence brightness arose from differences in the membrane-tethered neurotensin sequence (**Figure 10C**) and showed that the display of various peptidic neurotensin analogs can activate hNTSR1-mediated signaling in yeast cells. To confirm the value of this assay, a small scale screening was carried out with membrane-tethered NTS as a positive control and membrane-tethered α-factor as a negative control, respectively (**Figure 11**). The Z' factor that reflects both the assay signal dynamic range and the data variation associated with the measured signal (Zhang et al., 1999) was calculated to assess the assay quality. The value yielded upward of 0.5 (Z' factor = 0.57), showing the robustness and suitability for screening of the assay. It is expected that this technology will be applicable to the identification of peptide ligand pharmacophores, and for screening random or combinatorial peptide libraries for functional activation of GPCRs. The methodology presented in this study could be useful for the discovery of novel peptide ligands of human GPCRs.

In conclusion, we have established a fluorescence microscopy-based microbial yeast biosensor to detect human GPCR signaling that is applicable to CWTrAP technology and exhibits extremely bright fluorescence and high signal-to-noise (S/N) ratio. The biosensor employs a new highly-potent fluorescence reporter (ZsGreen) and Gα-engineered yeast strain. This system permitted the quick and easy visual distinction of cells responding to the agonist using fluorescence microscopy, thereby allowing

facile detection of agonistic ligands of human GPCRs. Since our system is applicable to not only hSSTR5 but also hSSTR2 and hNTSR1, this system can likely be extended to other human GPCRs, which comprise one of the most important types of drug targets being pursued today. Application of this method will allow the identification of lead peptides from combinatorial peptide libraries to provide starting points for drug screening.

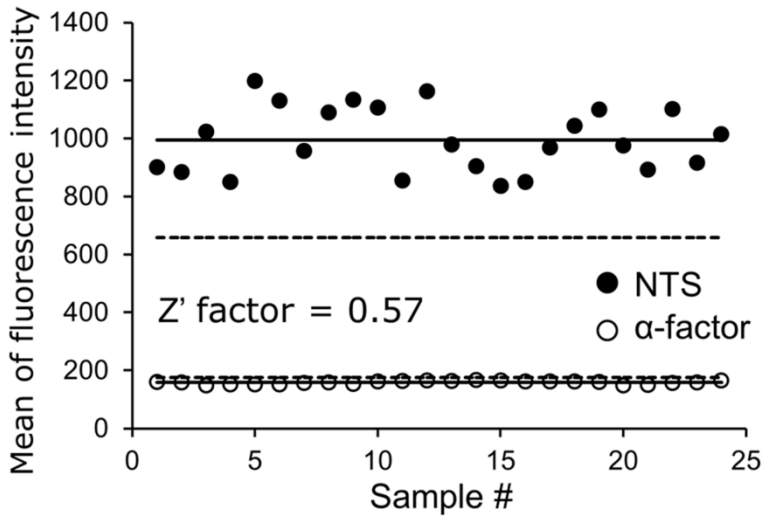

Fig. 11. Determination of the Z' factor. Yeast strain IMFD-72ZsD, which coexpresses pGK421-NTSR1 and either pGK426-NTS42 (NTS, positive control) or pGK426-alpha42 (α-factor, negative control), was incubated in pH-adjusted SD selective medium for 24 h. The GFP fluorescence of 10,000 cells was measured by flow cytometry. Mean values of the green fluorescence signal of 10,000 cells. The solid lines represent the mean value for the positive control and the negative control (996 and 160 respectively). The dashed lines marks the 3 standard deviation cut off for both the positive and negative control (standard deviation of 112 and 5.6 respectively). Z' factor > 0.5 indicates assays robust and suitable for screening.

References

Akada R, Kitagawa T, Kaneko S, Toyonaga D, Ito S, et al. (2006) PCR-mediated seamless gene deletion and marker recycling in Saccharomyces cerevisiae. Yeast 23: 399–405.

Aharoni A, Thieme K, Chiu CP, Buchini S, Lairson LL, et al. (2006) High-throughput screening methodology for the directed evolution of glycosyltransferases. Nat Methods 3: 609–614.

Barroso S, Richard F, Nicolas-Ethève D, Reversat JL, Bernassau JM, et al. (2000) Identification of residues involved in neurotensin binding and modeling of the agonist binding site in neurotensin receptor 1. J Biol Chem 275: 328–336.

Ben-Shlomo A, Melmed S (2008) Somatostatin agonists for treatment of acromegaly. Mol Cell Endocrinol 286: 192–198.

Bissette G, Nemeroff CB, Loosen PT, Prange AJ Jr, Lipton MA (1976) Hypothermia and intolerance to cold induced by intracisternal administration of the hypothalamic peptide neurotensin. Nature 262: 607–609.

Boder ET, Wittrup KD (1997) Yeast surface display for screening combinatorial polypeptide libraries. Nat Biotechnol 15: 553–557.

Brachmann CB, Davies A, Cost GJ, Caputo E, Li J, et al. (1998) Designer deletion strains derived from Saccharomyces cerevisiae S288C: a useful set of strains and plasmids for PCR-mediated gene disruption and other applications. Yeast 14: 115–132.

Brown AJ, Dyos SL, Whiteway MS, White JH, Watson MA, et al. (2000) Functional coupling of mammalian receptors to the yeast mating pathway using novel yeast/mammalian G protein alpha-subunit chimeras. Yeast 16: 11–22.

Carraway R, Leeman SE (1973) The isolation of a new hypotensive peptide, neurotensin, from bovine hypothalami. J Biol Chem 248: 6854–6861.

Carraway RE, Plona AM (2006) Involvement of neurotensin in cancer growth: evidence, mechanisms and development of diagnostic tools. Peptides 27: 2445–2460.

Chalon P, Vita N, Kaghad M, Guillemot M, Bonnin J, et al. (1996) Molecular cloning of a levocabastine-sensitive neurotensin binding site. FEBS Lett 386: 91–94.

Cotton M, Claing A (2009) G protein-coupled receptors stimulation and the control of cell migration. Cell Signal 21: 1045–1053.

Elion EA, Satterberg B, Kranz JE (1993) FUS3 phosphorylates multiple components of the mating signal transduction cascade: evidence for STE12 and FAR1. Mol Biol Cell 4: 495–510.

Evans BJ, Wang Z, Broach JR, Oishi S, Fujii N, et al. (2009) Expression of CXCR4, a G-protein-coupled receptor for CXCL12 in yeast identification of new-generation inverse agonists. Methods Enzymol 460: 399–412.

Feldhaus MJ, Siegel RW, Opresko LK, Coleman JR, Feldhaus JM, et al. (2003) Flow-cytometric isolation of human antibodies from a nonimmune Saccharomyces cerevisiae surface display library. Nat Biotechnol 21: 163–170.

Fredriksson R, Lagerström MC, Lundin LG, Schiöth HB (2003) The G-protein-coupled receptors in the human genome form five main families. Phylogenetic analysis, paralogon groups, and fingerprints. Mol Pharmacol 63: 1256–1272.

Fukuda N, Ishii J, Shibasaki S, Ueda M, Fukuda H, et al. (2007) High-efficiency recovery of target cells using improved yeast display system for detection of protein–protein interactions. Appl Microbiol Biotechnol 76: 151–158.

Fukuda N, Ishii J, Kaishima M, Kondo A (2011) Amplification of agonist stimulation of

human G-protein-coupled receptor signaling in yeast. Anal Biochem 417: 182–187.

Fukutani Y, Nakamura T, Yorozu M, Ishii J, Kondo A, et al. (2012) The N-terminal replacement of an olfactory receptor for the development of a yeast-based biomimetic odor sensor. Biotechnol Bioeng 109: 205–212.

Gai SA, Wittrup KD (2007) Yeast surface display for protein engineering and characterization. Curr Opin Struct Biol 17: 467–473.

Gietz D, St Jean A, Woods RA, Schiestl RH (1992) Improved method for high efficiency transformation of intact yeast cells. Nucleic Acids Res 20: 1425.

Granier C, van Rietschoten J, Kitabgi P, Poustis C, Freychet P (1982) Synthesis and characterization of neurotensin analogues for structure/activity relationship studies. Acetyl-neurotensin-(8--13) is the shortest analogue with full binding and pharmacological activities. Eur J Biochem 124: 117–124.

Griebel G, Holsboer F (2012) Neuropeptide receptor ligands as drugs for psychiatric diseases: the end of the beginning? Nat Rev Drug Discov 11: 462–478.

Gudermann T, Nürnberg B, Schultz G. (1995) Receptors and G proteins as primary components of transmembrane signal transduction. Part 1. G-protein-coupled receptors: structure and function. J Mol Med 73: 51–63.

Hara K, Ono T, Kuroda K, Ueda M (2012) Membrane-displayed peptide ligand activates the pheromone response pathway in Saccharomyces cerevisiae. J Biochem 151: 551–557.

Hasegawa S, Maruyama K, Takenaka H, Furukawa T, Saga T (2009) A medaka model of cancer allowing direct observation of transplanted tumor cells in vivo at a cellular-level resolution. Proc Natl Acad Sci USA 106: 13832–13837.

Iguchi Y, Ishii J, Nakayama H, Ishikura A, Izawa K, et al. (2010) Control of signalling

properties of human somatostatin receptor subtype-5 by additional signal sequences on its amino-terminus in yeast. J Biochem 147: 875–884.

Ishii J, Matsumura S, Kimura S, Tatematsu K, Kuroda S, et al. (2006) Quantitative and dynamic analyses of G protein-coupled receptor signaling in yeast using Fus1, enhanced green fluorescence protein (EGFP), and His3 fusion protein. Biotechnol Prog 22: 954–960.

Ishii J, Tanaka T, Matsumura S, Tatematsu K, Kuroda S, et al. (2008) Yeast-based fluorescence reporter assay of G protein-coupled receptor signalling for flow cytometric screening: FAR1-disruption recovers loss of episomal plasmid caused by signalling in yeast. J Biochem 143: 667–674.

Ishii J, Izawa K, Matsumura S, Wakamura K, Tanino T, et al. (2009) A simple and immediate method for simultaneously evaluating expression level and plasmid maintenance in yeast. J Biochem 145: 701–708.

Ishii J, Fukuda N, Tanaka T, Ogino C, Kondo A (2010) Protein–protein interactions and selection: yeast-based approaches that exploit guanine nucleotide-binding protein signaling. FEBS J 277: 1982–1995.

Ishii J, Moriguchi M, Hara KY, Shibasaki S, Fukuda H, et al. (2012a) Improved identification of agonist-mediated Gα(i)-specific human G-protein-coupled receptor signaling in yeast cells by flow cytometry. Anal Biochem 426: 129–133.

Ishii J, Yoshimoto N, Tatematsu K, Kuroda S, Ogino C, et al. (2012b) Cell wall trapping of autocrine peptides for human G-protein-coupled receptors on the yeast cell surface. PLoS One 7: e37136.

Ishii J, Oda A, Togawa S, Fukao A, Fujiwara T, et al. (2014) Microbial fluorescence sensing for human neurotensin receptor type 1 using Gα-engineered yeast cells.

Anal Biochem. 446: 37–43.

Kislauskis E, Bullock B, McNeil S, Dobner PR (1988) The rat gene encoding neurotensin and neuromedin N. Structure, tissue-specific expression, and evolution of exon sequences. J Biol Chem 263: 4963–4968.

Kitabgi P (2002) Targeting neurotensin receptors with agonists and antagonists for therapeutic purposes. Curr Opin Drug Discov Devel 5: 764–776.

Klein C, Paul JI, Sauvé K, Schmidt MM, Arcangeli L, et al. (1998) Identification of surrogate agonists for the human FPRL-1 receptor by autocrine selection in yeast. Nat Biotechnol 16: 1334–1337.

Kondo A, Ueda M (2004) Yeast cell-surface display-applications of molecular display. Appl Microbiol Biotechnol 64: 28–40.

Ladds G, Goddard A, Davey J (2005) Functional analysis of heterologous GPCR signaling pathways in yeast. Trends Biotechnol 23: 367–373.

Lamberts SW, de Herder WW, Krenning EP, Reubi JC (1994) A role of (labeled) somatostatin analogs in the differential diagnosis and treatment of Cushing's syndrome. J Clin Endocrinol Metab 78: 17–19.

Li B, Scarselli M, Knudsen CD, Kim SK, Jacobson KA, et al. (2007) Rapid identification of functionally critical amino acids in a G protein-coupled receptor. Nat Methods 4: 169–174.

Matz MV, Fradkov AF, Labas YA, Savitsky AP, Zaraisky AG, et al. (1999) Fluorescent proteins from nonbioluminescent Anthozoa species. Nat Biotechnol 17: 969–973.

Mazella J (2001) Sortilin/neurotensin receptor-3: a new tool to investigate neurotensin signaling and cellular trafficking? Cell Signal 13: 1–6.

Medico E, Gambarotta G, Gentile A, Comoglio PM, Soriano P (2001) A gene trap

vector system for identifying transcriptionally responsive genes. Nat Biotechnol 19: 579–582.

Minamino N, Kangawa K, Matsuo H (1984) Neuromedin N: a novel neurotensin-like peptide identified in porcine spinal cord. Biochem Biophys Res Commun 122: 542–549.

Murai T, Ueda M, Atomi H, Shibasaki Y, Kamasawa N, et al. (1997) Genetic immobilization of cellulase on the cell surface of Saccharomyces cerevisiae. Appl Microbiol Biotechnol 48: 499–503.

Nakamura Y, Shibasaki S, Ueda M, Tanaka A, Fukuda H, et al. (2001) Development of novel whole-cell immunoadsorbents by yeast surface display of the IgG-binding domain. Appl Microbiol Biotechnol 57: 500–505.

Nakamura Y, Ishii J, Kondo A (2013) Rapid, facile detection of heterodimer partners for target human G-protein-coupled receptors using a modified split-ubiquitin membrane yeast two-hybrid system. PLoS One 8: e66793.

Nakamura Y, Takemoto N, Ishii J, Kondo A (2014) Simultaneous method for analyzing dimerization and signaling of G-protein-coupled receptor in yeast by dual-color reporter system. Biotechnol Bioeng 111: 586–596.

Pepper LR, Cho YK, Boder ET, Shusta EV (2008) A decade of yeast surface display technology: where are we now? Comb Chem High Throughput Screen 11: 127–134.

Rasmussen SG, Choi HJ, Rosenbaum DM, Kobilka TS, Thian FS, et al. (2007) Crystal structure of the human beta2 adrenergic G-protein-coupled receptor. Nature 450: 383–387.

Raynor K, Murphy WA, Coy DH, Taylor JE, Moreau JP, et al. (1993a) Cloned

somatostatin receptors: identification of subtype-selective peptides and demonstration of high affinity binding of linear peptides. Mol Pharmacol 43: 838–844.

Raynor K, O'Carroll AM, Kong H, Yasuda K, Mahan LC, et al. (1993b) Characterization of cloned somatostatin receptors SSTR4 and SSTR5. Mol Pharmacol 44: 385–392.

Saito T, Iwata N, Tsubuki S, Takaki Y, Takano J, et al. (2005) Somatostatin regulates brain amyloid beta peptide Abeta42 through modulation of proteolytic degradation. Nat Med 11: 434–439.

Sato N, Matsumoto T, Ueda M, Tanaka A, Fukuda H, et al. (2002) Long anchor using Flo1 protein enhances reactivity of cell surface-displayed glucoamylase to polymer substrates. Appl Microbiol Biotechnol 60: 469–474.

Schimpff RM, Avard C, Fénelon G, Lhiaubet AM, Tennezé L, et al. (2001) Increased plasma neurotensin concentrations in patients with Parkinson's disease. J Neurol Neurosurg Psychiatry 70: 784–786.

Shibasaki S, Maeda H, Ueda M (2009) Molecular display technology using yeast-arming technology. Anal Sci 25: 41–49.

Stoeckius M, Maaskola J, Colombo T, Rahn HP, Friedländer MR, et al. (2009) Large-scale sorting of C. elegans embryos reveals the dynamics of small RNA expression. Nat Methods 6: 745–751.

Tanaka K, Masu M, Nakanishi S (1990) Structure and functional expression of the cloned rat neurotensin receptor. Neuron 4: 847–854.

Togawa S, Ishii J, Ishikura A, Tanaka T, Ogino C, et al. (2010) Importance of asparagine residues at positions 13 and 26 on the amino-terminal domain of human

somatostatin receptor subtype-5 in signalling. J Biochem 147: 867–873.

Ueda M, Tanaka A (2000) Genetic immobilization of proteins on the yeast cell surface. Biotechnol Adv 18: 121–140.

Wan CK, Shaikh SB, Green CR, Nicholson LF (2012) Comparison of bidirectional and bicistronic inducible systems for coexpression of connexin genes and fluorescent reporters. Anal Biochem 431: 90–95.

White JF, Noinaj N, Shibata Y, Love J, Kloss B, et al. (2012) Structure of the agonist-bound neurotensin receptor. Nature 490: 508–513.

Yu L, Qi M, Sheff MA, Elion EA (2008) Counteractive control of polarized morphogenesis during mating by mitogen-activated protein kinase Fus3 and G1 cyclin-dependent kinase. Mol Biol Cell 19: 1739–1752.

Zhang JH, Chung TD, Oldenburg KR (1999) A simple statistical parameter for use in evaluation and validation of high throughput screening assays. J Biomol Screen 4: 67–73.

Chapter 2: Applications of microbial signaling sensor using *Zoanthus* sp. green fluorescent protein for antagonist characterization and site-directed mutagenesis of human serotonin 1A receptor

Introduction

The neuromodulator serotonin [5-hydroxytryptamine (5-HT)] is essential for diverse functions at nearly every organ system in the human body (Berger et al., 2009; Roth et al., 2004; Wacker et al., 2013). The activity of 5-HT is mediated through activation of members of a large family of 5-HT receptor proteins that can be grouped into seven subfamilies (5-HT_{1-7}) on the basis of sequence homology and signaling mechanisms (Kroeze et al., 2002). In all 13 members, except for the 5-HT_3 receptor, which is a ligand-gated ion channel, the other 12 members are heterotrimeric guanine nucleotide binding protein (G-protein) coupled receptors (GPCRs). GPCRs belong to a large and diverse family of integral membrane proteins that participate in the regulation of many cellular processes and, therefore, represent key targets for pharmacological treatment. The serotonergic system is a target of many prescribed drugs, including atypical antipsychotics, antimigraine medications, anxiolytics, and antidepressants (Berger et al., 2009).

In addition, 5-HT is known to act as a growth factor on several types of non-tumoral cells (Nemecek et al., 1986; Sibella-Arguelles, 2001; Takuwa et al., 1989), and it was also related to oncogenes (Julius et al., 1989). Depending on the tumor type, either 5-HT_2 (Launay et al., 1996) or 5-HT_1 receptor antagonist have been found to inhibit the 5-HT-induced increase in tumor growth (Seuwen and Pouysségur, 1990).

Among subtype 1 receptors, 5-HT_{1A} receptor (HTR1A) is the most widely studied subtype. HTR1A is also involved in the proliferation of human tumor cells (Cattaneo et al., 1993, 1995; Ishizuka et al., 1992; Launay et al., 1996; Rajamannan et al., 2001). Previously, HTR1A antagonists and serotonin-uptake inhibitors were reported to inhibit the growth of tumor cell lines (Abdul et al., 1994, 1995; Dizeyi et al., 2004). Thus, simple and convenient detection systems for not only HTR1A agonists but also antagonists have a potential for the powerful tool towards new drug development.

The eukaryotic unicellular yeast *Saccharomyces cerevisiae* is a useful microbial host organism for studying GPCRs as monomolecular models (Ishii et al., 2010; Minic et al., 2005). Because of their uncompetitive and monopolistic G-protein signaling pathway, yeast can be used to simplify the complicated signaling pathways of higher eukaryotic cells (Iguchi et al., 2010; Togawa et al., 2010). A variety of human GPCRs are known to transduce signals in yeast cells through the endogenous yeast Gα-subunit (Gpa1p) or a yeast-human chimeric G-protein (Fukuda et al., 2011; Ishii et al., 2014). The yeast cells have successfully expressed many types of human GPCRs and have been adeptly used for various applications such as ligand screening and receptor mutagenesis using enzymatic and growth reporter genes (Klco et al., 2006; Minic et al., 2005; Scarselli et al., 2007). It was recently reported that the use of an established fluorescence-based reporter gene assay provides the most convenient measurement procedure: the cell culture is simply diluted into buffers and the fluorescence is read using fluorometric instruments (Ishii et al., 2012a, b). A flow cytometer is an especially powerful tool for comparative quantification and quantitative screening (cell sorting) (Ishii et al., 2012a, b). In addition, mutagenesis approaches can be implemented to obtain human GPCR structural information. Unfortunately, however, previously

reported systems using enhanced green fluorescent protein (*EGFP*) as reporter gene resulted in low signal-to-noise (S/N) ratio, making it difficult to apply to antagonist characterization and mutagenesis approaches.

In this study, we generated an engineered yeast strain, which can transduce the HTR1A-specific signal in response to its agonist by using the brighter fluorescent reporter (*ZsGreen*) gene. Using the generated yeast strain, we successfully performed not only antagonist characterization but also site-directed mutagenesis for human HTR1A receptor. This biosensor specifically responded to HTR1A antagonist, pindolol, inhibiting the agonist-induced activating HTR1A. In mutagenesis experiments, several mutants were analyzed to confirm the validity of the biosensor and the role of the highly conserved DRY motif in activation of HTR1A was investigated.

Materials and Methods

Plasmid constructions

All plasmids used in this study are listed in **Table 1**. All primers used for plasmid construction are listed in **Table 2**.

A DNA fragment encoding the human *HTR1A* gene was PCR-amplified from pPR3-HTR1A (Nakamura et al., 2013a) using the primers #1 and #2, digested with *Nhe*I+*Bgl*II, and inserted into the same sites between the *PGK1* promoter (P_{PGK1}) and the *PGK1* terminator (T_{PGK1}) on pGK421 (Togawa et al., 2010), yielding the plasmid pGK421-HTR1A.

The plasmids for expressing mutated HTR1A proteins were constructed as follows. To introduce point mutations, gene fragments encoding the upstream and downstream parts of mutated HTR1A were respectively PCR-amplified from pGK421-HTR1A using

primers #1 + #3 and #4 + #2 (for D82N); #1 + #5 and #6 + #2 (for D116N); #1 + #7 and #8 + #2 (for C109A); #1 + #9 and #10 + #2 (for C187A); #1 + #11 and #12 + #2 (for S199A); #1 + #13 and #14 + #2 (for T200A); #1 + #15 and #16 + #2 (for N386V); #1 + #17 and #18 + #2 (for D133A); #1 + #19 and #20 + #2 (for R134A); #1 + #21 and #22 + #2 (for Y135A). These amplified fragments then were used as the templates for overlap PCR with primers #1 and #2. The resulting linear mutated *HTR1A* fragments were digested with *Nhe*I+*Bgl*II and ligated into similarly digested pGK421, resulting in plasmids designated pGK421-HTR1A-D82N, -D116N, -C109A, -C187A, -S199A, -T200A, -N386V, -D133A, -R134A, or -Y135A, respectively.

Yeast strains and media

All yeast strains used in this study are listed in **Table 1**. Transformation with plasmids was performed using the lithium acetate method (Gietz et al., 1992).

Synthetic dextrose (SD) medium contained 6.7 g/L yeast nitrogen base without amino acids (YNB) (BD-Diagnostic Systems, Sparks, MD, USA) and 20 g/L glucose. For SDM71 media, SD medium was adjusted to pH 7.1 with 200 mM 3-(*N*-morpholino)-2-hydroxypropanesulfonic acid (MOPSO) (Nacalai Tesque, Kyoto, Japan). YPD medium contained 10 g/L yeast extract (Nacalai Tesque), 20 g/L peptone (BD-Diagnostic Systems) and 20 g/L glucose. Amino acids and nucleotides (20 mg/L histidine, 60 mg/L leucine, or 20 mg/L uracil) were supplemented into SD media to lack the relevant auxotrophic components. For solid medium, agar was added at 20 g/L.

HTR1A signaling assay

HTR1A signaling assays basically followed previous procedures (Nakamura et al.,

2013b, 2014) except changes in the ligand. In brief, to assay signal activation from human HTR1A, the yeast strains transformed with the wild-type or mutated HTR1A expression plasmids were grown in SD medium (supplemented as needed) at 30 °C overnight, and the cells then were inoculated into 5 mL of the respective fresh SD medium to give an initial optical density of 0.03 at 600 nm (OD_{600} = 0.03). The cells were incubated at 30 °C on a rotary shaker at 150 rpm for up to 18 h and harvested, washed, and resuspended in water to yield an OD_{600} = 10. The resulting yeast cell suspensions were added (at 10 μL/well; to give an OD_{600} = 1) to the wells of 96-well cluster dishes containing fresh SDM71 medium (80 μL/well) supplemented with 10-times concentrated 5-HT (Nacalai Tesque) (10 μL/well) at various concentrations or distilled water (without 5-HT; control). The plates were incubated at 30 °C with shaking (150 rpm) for 4 h. After incubation, the samples containing the yeast cells were diluted with 1 mL of sheath fluid, and fluorescence was analyzed by flow cytometer. Half maximal effective concentrations (EC_{50}) values were determined using KaleidaGraph4.0 Fits to a dosersplgst model.

Flow cytometry analysis

Flow cytometry measurements of green fluorescence followed previous procedures (Ishii et al., 2012b). In brief, fluorescent cells were detected using a BD FACSCanto II flow cytometer equipped with a 488-nm blue laser (Becton, Dickinson and Company, Franklin Lakes, NJ, USA); the data were analyzed using BD FACSDiva software (v5.0; Becton, Dickinson and Company). The GFP fluorescence signal was collected through a 530/30 nm band-pass filter and the GFP-A mean of 10,000 cells was defined as ‘green fluorescent intensity’.

Table 1. Yeast strains and plasmids used in this study.

Strain or plasmid	Specific features	Source
Strain		
BY4741	*MAT***a** *his3Δ1 leu2Δ0 met15Δ0 ura3Δ0*	Brachmann et al. (1998)
IMFD-70	BY4741 *sst2Δ::AUR1-C ste2Δ::LEU2 fig1Δ::EGFP his3Δ::*P_{FIG1}*-EGFP far1Δ*	Togawa et al. (2010)
IMFD-72	BY4741 *sst2Δ::AUR1-C ste2Δ::LEU2 fig1Δ::EGFP his3Δ::*P_{FIG1}*-EGFP far1Δ gpa1Δ::*G_{i3}*tp*	Ishii et al. (2012a)
IMFD-70ZsD	BY4741 *sst2Δ::AUR1-C ste2Δ::LEU2 fig1Δ::ZsGreen his3Δ::*P_{FIG1}*-ZsGreen far1Δ*	Nakamura et al. (2013b)
IMFD-72ZsD	BY4741 *sst2Δ::AUR1-C ste2Δ::LEU2 fig1Δ::ZsGreen his3Δ::*P_{FIG1}*-ZsGreen far1Δ gpa1Δ::*G_{i3}*tp*	Nakamura et al. (2013b)
Plasmid		
pGK421	Yeast expression vector containing *PGK1* promoter, *PGK1* terminator, 2μ origin and *MET15* marker	Togawa et al. (2010)
pGK421-HTR1A	Human HTR1A receptor expression in pGK421	This study
pGK421-HTR1A-D82N	Human HTR1A receptor (D82N) mutant expression in pGK421	This study
pGK421-HTR1A-D116N	Human HTR1A receptor (D116N) mutant expression in pGK421	This study
pGK421-HTR1A-C109A	Human HTR1A receptor (C109A) mutant expression in pGK421	This study
pGK421-HTR1A-C187A	Human HTR1A receptor (C187A) mutant expression in pGK421	This study
pGK421-HTR1A-S199A	Human HTR1A receptor (S199A) mutant expression in pGK421	This study
pGK421-HTR1A-T200A	Human HTR1A receptor (T200A) mutant expression in pGK421	This study
pGK421-HTR1A-N386V	Human HTR1A receptor (N386V) mutant expression in pGK421	This study
pGK421-HTR1A-D133A	Human HTR1A receptor (D133A) mutant expression in pGK421	This study
pGK421-HTR1A-R134A	Human HTR1A receptor (R134A) mutant expression in pGK421	This study
pGK421-HTR1A-Y135A	Human HTR1A receptor (Y135A) mutant expression in pGK421	This study

Table 2. List of primers.

	Name	Sequence
#1	NheI_HTR1A_fw	5'-AAAAGCTAGCATGGATGTGCTCAGCCCTGG
#2	BglII_HTR1A_rv	5'-TTTTAGATCTTCACTGGCGGCAGAACTTAC
#3	HTR1A-D82N_rv	5'-CGACACCATGAGGT**T**GGTGACCGCCAAAGA
#4	HTR1A-D82N_fw	5'-TCTTTGGCGGTCACC**A**ACCTCATGGTGTCG
#5	HTR1A-D116N_rv	5'-GCAGCACAGCACGT**T**GAGGGCGATGAACAG
#6	HTR1A-D116N_fw	5'-CTGTTCATCGCCCTC**A**ACGTGCTGTGCTGC
#7	HTR1A-C109A_rv	5'-GATGAACAGGTCG**GC**GGTTACCTGGCCCAG
#8	HTR1A-C109A_fw	5'-CTGGGCCAGGTAACC**GC**CGACCTGTTCATC
#9	HTR1A-C187A_rv	5'-CTTGCTAATGGTG**GC**TGCGTCGGGGTCCGA
#10	HTR1A-C187A_fw	5'-TCGGACCCCGACGCA**GC**CACCATTAGCAAG
#11	HTR1A-S199A_rv	5'-AGCTCCAAAGGTGG**C**ATAGATAGTGTAGCC
#12	HTR1A-S199A_fw	5'-GGCTACACTATCTAT**G**CCACCTTTGGAGCT
#13	HTR1A-T200A_rv	5'-GAAAGCTCCAAAGG**C**GGAATAGATAGTGTA
#14	HTR1A-T200A_fw	5'-TACACTATCTATTCC**G**CCTTTGGAGCTTTC
#15	HTR1A-N386V_rv	5'-GTAGCCCAGCCAA**AC**GATTATGGCGCCCAA
#16	HTR1A-N386V_fw	5'-TTGGGCGCCATAATC**GT**TTGGCTGGGCTAC
#17	HTR1A-D133A_rv	5'-GGCCCAGTACCTG**G**CCAGCGCGATGGCGCA
#18	HTR1A-D133A_fw	5'-TGCGCCATCGCGCTGG**C**CAGGTACTGGGCC
#19	HTR1A-R134A_rv	5'-GATGGCCCAGTAC**GC**GTCCAGCGCGATGGC
#20	HTR1A-R134A_fw	5'-GCCATCGCGCTGGAC**GC**GTACTGGGCCATC
#21	HTR1A-Y135A_rv	5'-CGTGATGGCCCAG**GC**CCTGTCCAGCGCGAT
#22	HTR1A-Y135A_fw	5'-ATCGCGCTGGACAGG**GC**CTGGGCCATCACG

Antagonist inhibition assay

To assay antagonist inhibition of signal activation from human HTR1A, the yeast strains transformed with the wild-type or mutated HTR1A expression plasmids were grown in SD medium (supplemented as needed) at 30 °C overnight, and the cells then were inoculated into 5 mL of the respective fresh SD medium to give an initial optical density of 0.03 at 600 nm (OD_{600} = 0.03). The cells were incubated at 30 °C on a rotary shaker at 150 rpm for up to 18 h and harvested, washed, and resuspended in water to yield an OD_{600} = 10. The resulting yeast cell suspensions were added (at 10 μL/well; to give an OD_{600} = 1) to the wells of 96-well cluster dishes containing fresh SDM71 medium with 100 μM or 1 mM 5-HT (80 μL/well) supplemented with 10-times concentrated pindolol (Tocris Bioscience, Bristol, United Kingdom) (10 μL/well) at various concentrations or distilled water (without pindolol; control). The plates were incubated at 30 °C with shaking (150 rpm) for 4 h. After incubation, the samples containing the yeast cells were diluted with 1 mL of sheath fluid, and fluorescence was analyzed by flow cytometer.

Results and Discussion

Comparing the reporting sensitivity between the ZsGreen and the EGFP systems

The aim of this study was to conduct antagonist characterization and site-directed mutagenesis analyses of human HTR1A receptor using yeast-based biosensor. To monitor the signal activation of human HTR1A receptor, previously engineered yeast cells in which the *GFP* reporter genes have been integrated into the genomes were used as the host strains (Nakamura et al., 2013b). In the engineered strains, the tetrameric *Zoanthus* sp. green fluorescent protein (ZsGreen), whose fluorescence is brighter than enhanced green fluorescent protein (EGFP), is used as the GFP reporter. The expression of ZsGreen is controlled by the signal responsive *FIG1* promoter. Therefore, the signaling activation by agonist stimulus results in the generation of a green fluorescence signal (Nakamura et al., 2013b).

In addition, all engineered yeast strains have the *ste2*Δ, *sst2*Δ, and *far1*Δ alleles that are deficient in the yeast single GPCR, the yeast principal negative regulator of G-protein signaling (RGS), and the yeast G1-cyclin-dependent kinase inhibitor; this inhibitor induces G1 arrest in response to signaling, respectively (Fukuda et al., 2011; Iguchi et al., 2010; Ishii et al., 2012b; Togawa et al., 2010). These deletions respectively allow expression of human GPCRs without competitive receptor expression (Iguchi et al., 2010; Ishii et al., 2010; Togawa et al., 2010), hypersensitive agonist stimulation even in the low ligand concentrations (Ishii et al., 2006), and vital growth in association with the plasmid retention under signal-activated states (Ishii et al., 2008).

The human HTR1A receptor is known to transduce signals in yeast cells through the endogenous yeast Gα-subunit (Gpa1p). A yeast-human chimeric G-protein, in which the carboxyl-terminal 5 amino acid residues of Gpa1p (KIGII) are replaced with the

equivalent residues from human $G\alpha_{i3}$ (ECGLY) (Gpa1/$G\alpha_{i3}$ transplant, G_{i3}tp), has been shown to improve signal transmission via $G\alpha_i$-specific HTR1A in yeast (Brown et al., 2000). Therefore, the effects of the performance of reporter gene and the yeast-human chimeric G-protein in engineered yeast cells were tested by comparing the fluorescence of yeast cells expressing either ZsGreen or EGFP as a reporter and either the endogenous yeast G-protein (Gpa1p) or the yeast-human chimeric G-protein (G_{i3}tp), when human HTR1A receptor was expressed in yeast cells. The human HTR1A receptor was expressed via a multicopy episomal plasmid under the control of constitutive *PGK1* promoter (pGK421-HTR1A) (**Table 1**). Yeast IMFD-70 (EGFP, Gpa1p), IMFD-72 (EGFP, G_{i3}tp), IMFD-70ZsD (ZsGreen, Gpa1p) and IMFD-72ZsD (ZsGreen, G_{i3}tp) strains (**Table 1**) harboring pGK421-HTR1A were generated and the signaling assays were performed. As shown in **Figure 1**, in all yeast cells, the addition of 5-HT resulted in a dose-dependent increase in fluorescence intensity. The half-maximal effective concentration (EC_{50}) values were 32 μM (IMFD-70), 18 μM (IMFD-72), 24 μM (IMFD-70ZsD) and 12 μM (IMFD-72ZsD), respectively. These results suggested that the affinity or sensitivity of HTR1A for 5-HT was increased by yeast-human chimeric Gα (G_{i3}tp). The addition of agonist to yeast strains IMFD-70 and IMFD-72 were modest response and induced only 1.2- and 1.4-fold higher maximum fluorescence (**Figure 2**). In contrast, strains IMFD-70ZsD and IMFD-72ZsD displayed a 2.3- and 4.0-fold increase in maximum fluorescence intensity in response to agonist stimulation (**Figure 1**). Because IMFD-72ZsD strain provided the highest fluorescence and signal-to-noise (S/N) ratio, further studies were conducted using the yeast strain IMFD-72ZsD.

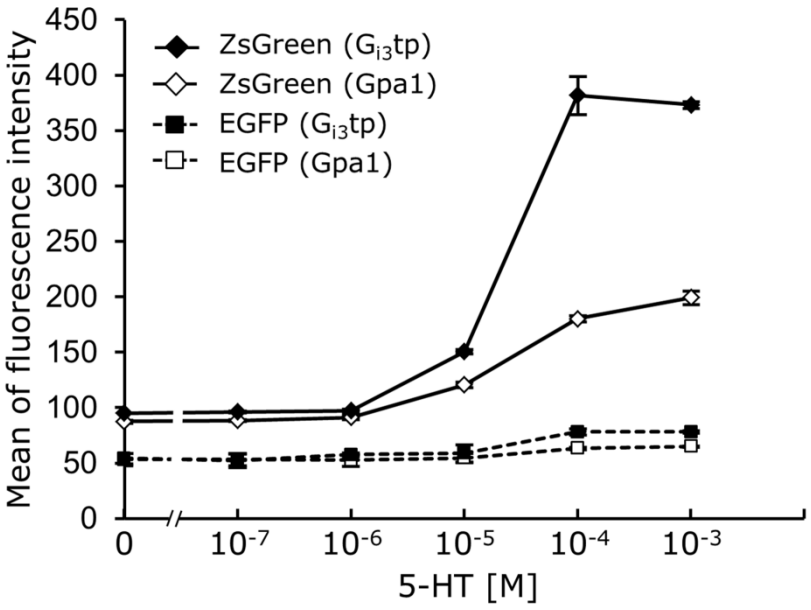

Fig. 1. Dose–response curves for 5-HT-specific HTR1A signaling activities of recombinant yeast cells. Yeast strains IMFD-70 (EGFP (Gpa1)), IMFD-72 (EGFP (G_{i3}tp)), IMFD-70ZsD (ZsGreen (Gpa1)) and IMFD-72ZsD (ZsGreen (G_{i3}tp)) were transformed with pGK421-HTR1A. All transformants were grown in SD selective medium for 18 h. The cells then were incubated for another 4 h in pH-adjusted SD selective medium with 5-HT at various concentrations. The GFP fluorescence of 10,000 cells was measured by flow cytometry. Each data point is presented as the mean ± standard deviation of separate runs (n = 3 each).

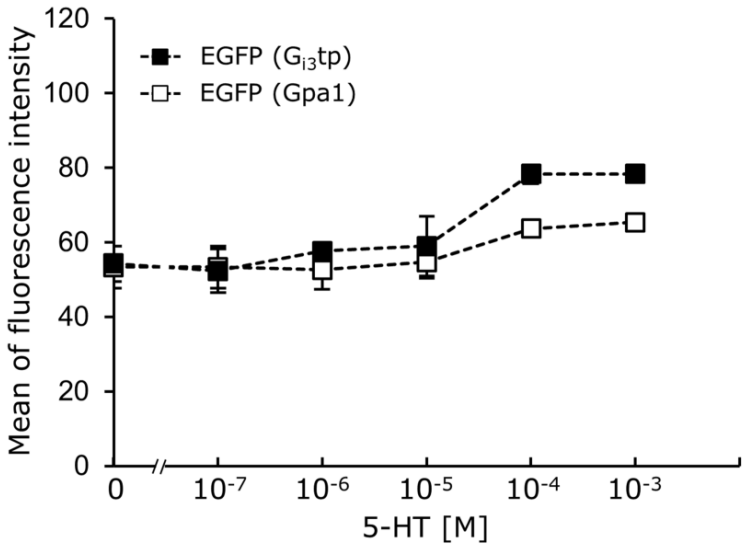

Fig. 2. Dose–response curves for 5-HT-specific HTR1A signaling activities of recombinant yeast cells. Yeast strains IMFD-70 (EGFP (Gpa1)) and IMFD-72 (EGFP (G_{i3}tp)) were transformed with pGK421-HTR1A. All transformants were grown in SD selective medium for 18 h. The cells then were incubated for another 4 h in pH-adjusted SD selective medium with 5-HT at various concentrations. The GFP fluorescence of 10,000 cells was measured by flow cytometry. Each data point is presented as the mean ± standard deviation of separate runs (n = 3 each).

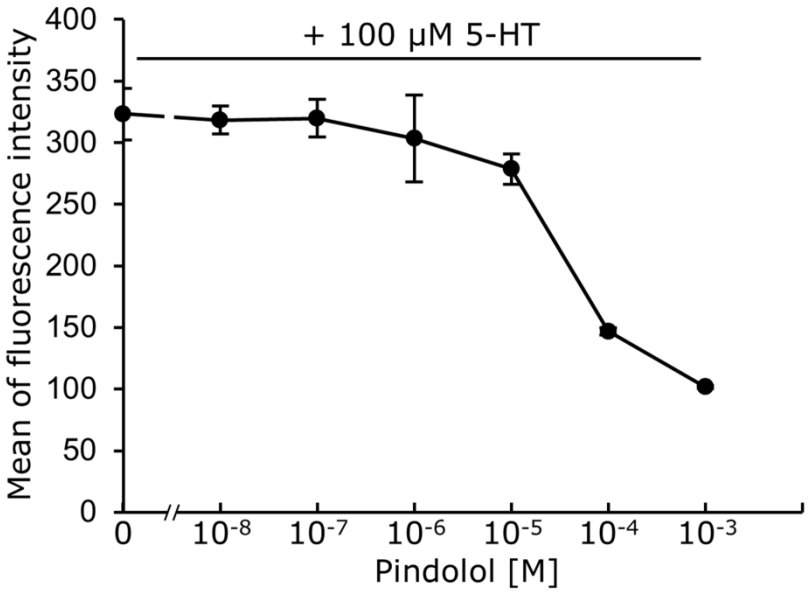

Fig. 3. Inhibition of 5-HT (100 µM)-mediated functional responses of HTR1A by pindolol. The dose–response relationship to pindolol was determined by recombinant yeast strain IMFD-72ZsD (ZsGreen (G_{i3}tp)) transformed with pGK421-HTR1A. The transformants were grown in SD selective medium for 18 h. The cells then were incubated for another 4 h in pH-adjusted SD selective medium with 5-HT (100 µM) and pindolol at various concentrations. The GFP fluorescence of 10,000 cells was measured by flow cytometry. Each data point is presented as the mean ± standard deviation of separate runs (n = 3 each).

Antagonist inhibition of 5-HT induced activating HTR1A

To measure antagonist inhibition of the agonist-induced activating HTR1A, the fluorescence responses to various concentrations of HTR1A antagonist, pindolol were examined. Yeast IMFD-72ZsD strain harboring pGK421-HTR1A was generated and examined using an antagonist inhibition assay. The cells were incubated in media containing 100 μM 5-HT and various concentrations of pindolol, and the resulting expression levels of the *ZsGreen* reporter gene were measured by flow cytometry. **Figure 3** shows that the cells exhibited suppressed fluorescence depending on the concentration of pindolol and reached almost basal level at a concentration of 100 μM pindolol. This indicated that pindolol exhibited a dose-dependent inhibition of the agonist-induced activating HTR1A. In addition, the cells were incubated in media containing 1 mM 5-HT and various concentrations of pindolol. The cells exhibited suppressed fluorescence depending on the concentration of pindolol and reached almost basal level at a concentration of 1 mM pindolol (**Figure 4**). These results indicated that our system was applicable for evaluating antagonist inhibition of the agonist-induced activating HTR1A.

Site-directed mutagenesis analysis of HTR1A

To evaluate the site-directed mutagenesis analysis of HTR1A, the fluorescence responses of yeast strains expressing several mutants of HTR1A were examined. We constructed 10 of plasmids for expressing mutants of HTR1A. The positions of the residues of HTR1A selected as targets for site-directed mutagenesis are shown in **Figure 5**.

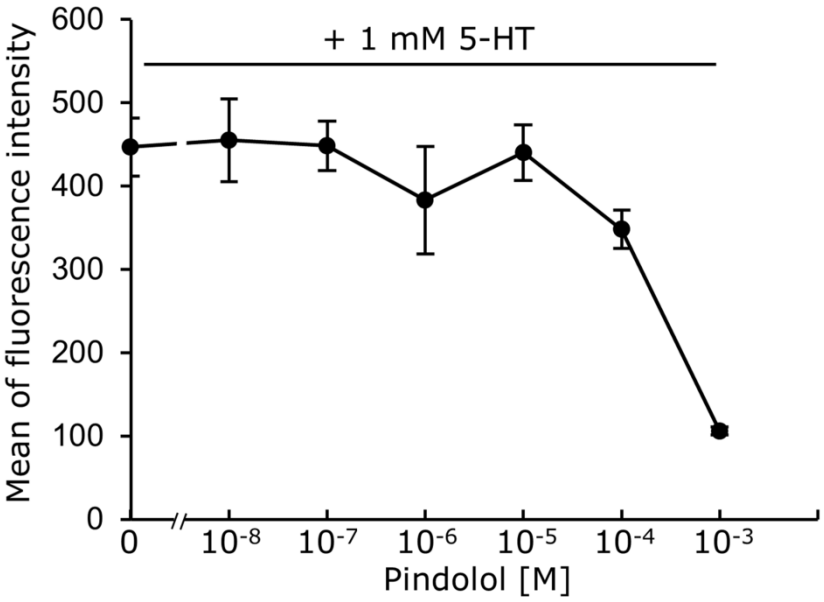

Fig. 4. Inhibition of 5-HT (1 mM)-mediated functional responses of HTR1A by pindolol. The dose–response relationship to pindolol was determined by recombinant yeast strain IMFD-72ZsD (ZsGreen (G_{i3}tp)) transformed with pGK421-HTR1A. The transformants were grown in SD selective medium for 18 h. The cells then were incubated for another 4 h in pH-adjusted SD selective medium with 5-HT (1 mM) and pindolol at various concentrations. The GFP fluorescence of 10,000 cells was measured by flow cytometry. Each data point is presented as the mean ± standard deviation of separate runs (n = 3 each).

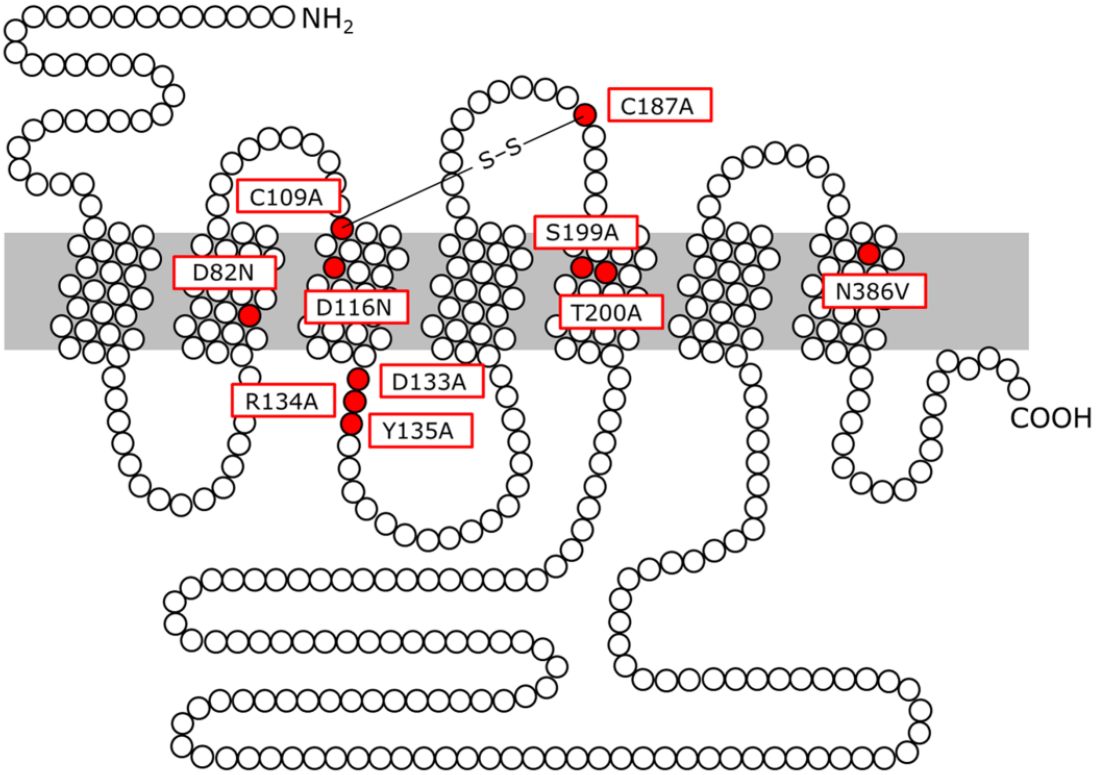

Fig. 5. Schematic illustration of the human HTR1A showing the positions of the mutations. Each circle represents an amino acid residue. The positions of amino acids mutated in this study are indicated as red circles.

Primarily, the previously reported mutants (D82N, D116N, C109A, C187A, S199A, T200A and N386V) were used for the site-directed mutagenesis. Yeast IMFD-72ZsD strains harboring pGK421-HTR1A-D82N or -D116N were generated and studied using the signaling assay. As shown in **Figure 6A** and **B**, the D82N and D116N mutants completely and significantly lost the ability to respond to 5-HT-specific signaling, respectively. This result is consistent with the previous report in which the substitutions D82N and D116N resulted in a 60–100 fold decreased affinity for 5-HT (Ho et al., 1992). Subsequently, the yeast strains IMFD-72ZsD expressing the C109A or C187A mutants exhibited abolish HTR1A function (**Figure 6C** and **D**). The mutation of C109A or C187A was crucial for the signaling stimulated from 5-HT, suggesting that disulfide-bridge between Cys109 and Cys187 was critical for the affinity to 5-HT or the activation of receptor (Pucadyil et al., 2005). Other many GPCRs also form disulfide-bridge within cysteine residues between the first extracellular loop and the second extracellular loop (Klco et al., 2006). Next, yeast IMFD-72ZsD strains harboring pGK421-HTR1A-S199A or -T200A were generated and studied using the signaling assay. As shown in **Figure 7A** and **B**, the yeast strains expressing S199A or T200A displayed both 2.9-fold increase in maximum fluorescence intensity in response to agonist stimulation and the EC_{50} values were 54 μM (S199A) and 257 μM (T200A), respectively. This result is also consistent with the previous report in which a significant reduction of agonist binding and the activation of receptor (Ho et al., 1992). Additionally, the mutant N386V which displayed a lower affinity for pindolol without any effect on the affinity for other ligands had been reported. Yeast IMFD-72ZsD strain harboring pGK421-HTR1A-N386V was generated and studied using the signaling assay. As shown in **Figure 7C** and **D**, although the yeast strain expressing N386V displayed

only 1.3-fold increase in maximum fluorescence intensity in response to agonist stimulation, the EC_{50} values was 24 μM. This result indicated that the N386V affected not the affinity for 5-HT but the receptor activity or signaling. In addition, the cells were incubated in media containing 100 μM 5-HT and various concentrations of pindolol. As shown in **Figure 3** and **8**, while the yeast strain expressing WT or S199A displayed that fluorescence intensity started to decrease at a concentration of 100 μM pindolol, the yeast strain expressing N386V displayed that fluorescence intensity started to decrease at a concentration of 1 mM pindolol. This result indicated that the N386V mutant displayed a lower affinity for pindolol according to the previous report.

Finally, the previously no reported mutants (D133A, R134A and Y135A) were used for the site-directed mutagenesis. We selected the DRY motif as targets for the mutants. The DRY motif present in the second intracellular loop is considered to be the switch that activates G-proteins upon agonist binding to the receptor. This DRY motif is highly conserved amino acid sequence motif in many GPCRs (Rovati et al., 2007; Savarese and Fraser, 1992), but the role of the DRY motif in HTR1A activation is not known. Yeast IMFD-72ZsD strains harboring pGK421-HTR1A-D133A, -R134A or -Y135A were generated and studied using the signaling assay. As shown in **Figure 9**, the D133A and Y135A mutants significantly lost the ability to respond to 5-HT-specific signaling and the R134A mutant completely lost the ability to respond to 5-HT-specific signaling. These results suggested that the central arginine of the DRY motif seems to be more directly involved in receptor activation.

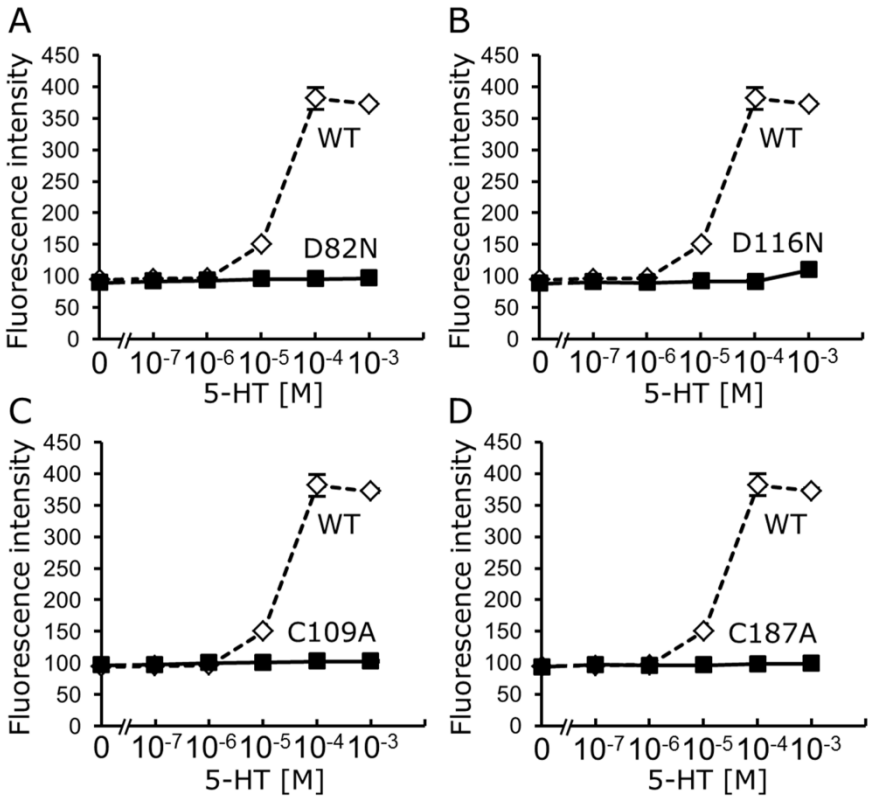

Fig. 6. Ligand response of wild-type (WT) and mutant HTR1A receptors (D82N, D116N, C109A, C187A). The dose–response relationship to 5-HT was determined by recombinant yeast strain IMFD-72ZsD (ZsGreen (G_{i3}tp)) expressing WT HTR1A receptor (open diamond ◊) or its mutants (filled square ■). Dose–response curves are shown for (A) D82N mutants, (B) D116N mutants, (C) C109A mutants, and (D) C187A mutants, respectively. The transformants were grown in SD selective medium for 18 h. The cells then were incubated for another 4 h in pH-adjusted SD selective medium with 5-HT at various concentrations. The GFP fluorescence of 10,000 cells was measured by flow cytometry. Each data point is presented as the mean ± standard deviation of separate runs (n = 3 each).

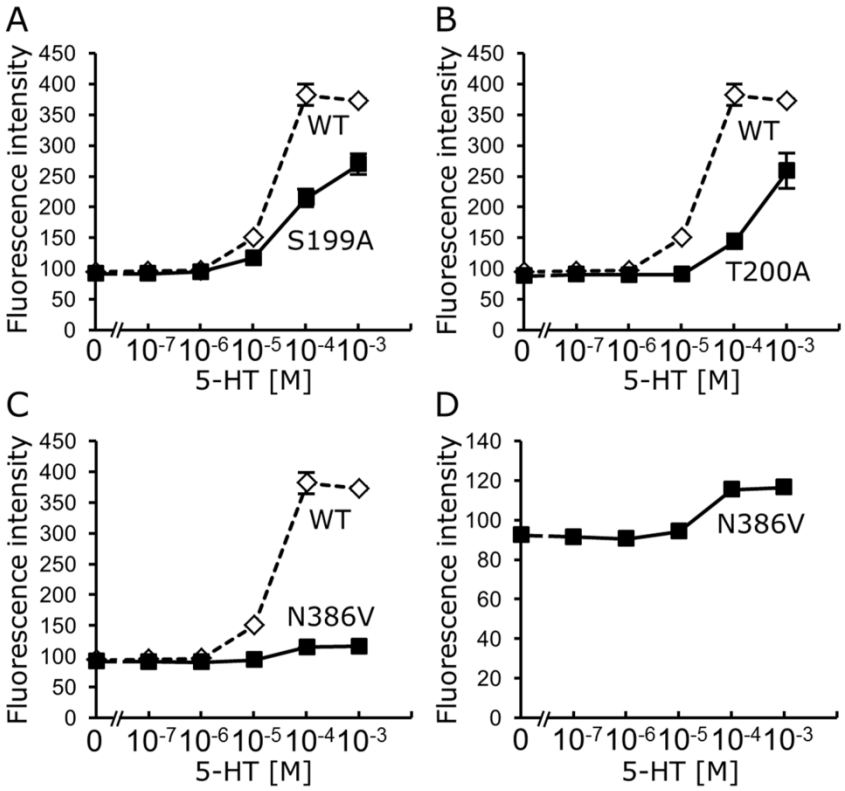

Fig. 7. Ligand response of wild-type (WT) and mutant HTR1A receptors (S199A, T200A, N386V). The dose–response relationship to 5-HT was determined by recombinant yeast strain IMFD-72ZsD (ZsGreen (G_{i3}tp)) expressing WT HTR1A receptor (open diamond ◊) or its mutants (filled square ■). Dose–response curves are shown for (A) S199A mutants, (B) T200A mutants, and (C, D) N386V mutants, respectively. The transformants were grown in SD selective medium for 18 h. The cells then were incubated for another 4 h in pH-adjusted SD selective medium with 5-HT at various concentrations. The GFP fluorescence of 10,000 cells was measured by flow cytometry. Each data point is presented as the mean ± standard deviation of separate runs (n = 3 each).

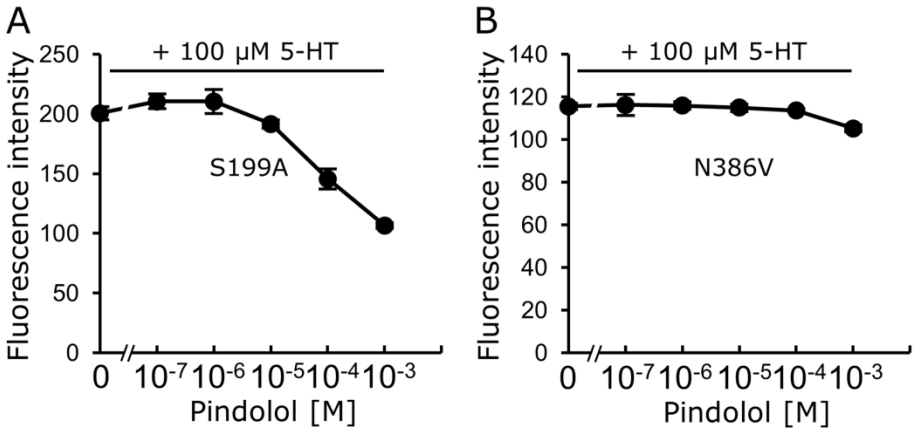

Fig. 8. Inhibition of 5-HT (100 μM)-mediated functional responses by pindolol in mutant HTR1A receptors. The dose–response relationship to pindolol was determined by recombinant yeast strain IMFD-72ZsD (ZsGreen (G_{i3}tp)) expressing HTR1A mutants. Dose–response curves are shown for (A) S199A mutants, and (B) N386V mutants, respectively. The transformants were grown in SD selective medium for 18 h. The cells then were incubated for another 4 h in pH-adjusted SD selective medium with 5-HT (100 μM) and pindolol at various concentrations. The GFP fluorescence of 10,000 cells was measured by flow cytometry. Each data point is presented as the mean ± standard deviation of separate runs (n = 3 each).

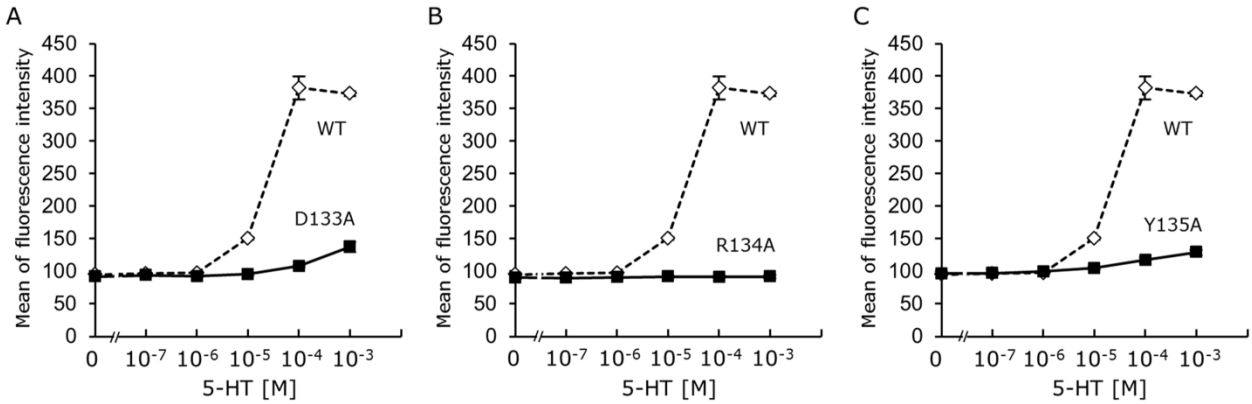

Fig. 9. Ligand response of wild-type (WT) and mutant HTR1A receptors (D133A, R134A, Y135A). The dose–response relationship to 5-HT was determined by recombinant yeast strain IMFD-72ZsD (ZsGreen (G_{i3}tp)) expressing WT HTR1A receptor (open diamond ◊) or its mutants (filled square ■). Dose–response curves are shown for (A) D133A mutants, (B) R134A mutants, and (C) Y135A mutants, respectively. The transformants were grown in SD selective medium for 18 h. The cells then were incubated for another 4 h in pH-adjusted SD selective medium with 5-HT at various concentrations. The GFP fluorescence of 10,000 cells was measured by flow cytometry. Each data point is presented as the mean ± standard deviation of separate runs (n = 3 each).

Conclusion

In this study, we successfully conducted antagonist characterization and site-directed mutagenesis analyses of human HTR1A receptor using yeast-based biosensor. The biosensor employs a highly-potent fluorescence reporter (ZsGreen) and Gα-engineered yeast strain. This biosensor specifically responded to HTR1A antagonist, pindolol, inhibiting the agonist-induced activating HTR1A. In mutagenesis experiments, several mutants were analyzed to confirm the validity of the biosensor and the role of the highly conserved DRY motif in activation of HTR1A was investigated. This yeast-based system using a fluorescent reporter gene will be available for other human GPCRs and be beneficial for the simplification of experimental procedures in a GPCR signaling study.

References

Abdul M, Anezinis PE, Logothetis CJ, Hoosein NM. 1994. Growth inhibition of human prostatic carcinoma cell lines by serotonin antagonists. Anticancer Res 14(3A): 1215–1220.

Abdul M, Logothetis CJ, Hoosein NM. 1995. Growth-inhibitory effects of serotonin uptake inhibitors on human prostate carcinoma cell lines. J Urol 154(1):247–250.

Berger M, Gray JA, Roth BL. 2009. The expanded biology of serotonin. Annu Rev Med 60:355–366.

Brachmann CB, Davies A, Cost GJ, Caputo E, Li J, Hieter P, Boeke JD. 1998. Designer deletion strains derived from *Saccharomyces cerevisiae* S288C: a useful set of strains and plasmids for PCR-mediated gene disruption and other applications. Yeast 14(2):115–132.

Brown AJ, Dyos SL, Whiteway MS, White JH, Watson MA, Marzioch M, Clare JJ, Cousens DJ, Paddon C, Plumpton C, Romanos MA, Dowell SJ. 2000. Functional coupling of mammalian receptors to the yeast mating pathway using novel yeast/mammalian G protein α-subunit chimeras. Yeast 16(1):11–22.

Cattaneo MG, Codignola A, Vicentini LM, Clementi F, Sher E. 1993. Nicotine stimulates a serotonergic autocrine loop in human small-cell lung carcinoma. Cancer Res 53(22):5566–5568.

Cattaneo MG, Fesce R, Vicentini LM. 1995. Mitogenic effect of serotonin in human small cell lung carcinoma cells via both 5-HT1A and 5-HT1D receptors. Eur J Pharmacol 291(2):209–211.

Dizeyi N, Bjartell A, Nilsson E, Hansson J, Gadaleanu V, Cross N, Abrahamsson PA. 2004. Expression of serotonin receptors and role of serotonin in human prostate cancer tissue and cell lines. Prostate 59(3):328–336.

Fukuda N, Ishii J, Kaishima M, Kondo A. 2011. Amplification of agonist stimulation of human G-protein-coupled receptor signaling in yeast. Anal Biochem 417(2):182–187.

Gietz D, St Jean A, Woods RA, Schiestl RH. 1992. Improved method for high efficiency transformation of intact yeast cells. Nucleic Acids Res 20(6):1425.

Iguchi Y, Ishii J, Nakayama H, Ishikura A, Izawa K, Tanaka T, Ogino C, Kondo A. 2010. Control of signalling properties of human somatostatin receptor subtype-5 by additional signal sequences on its amino-terminus in yeast. J Biochem 147(6):875–884.

Ishii J, Fukuda N, Tanaka T, Ogino C, Kondo A. 2010. Protein–protein interactions and selection: yeast-based approaches that exploit guanine nucleotide-binding protein signaling. FEBS J 277(9):1982–1995.

Ishii J, Moriguchi M, Hara KY, Shibasaki S, Fukuda H, Kondo A. 2012a. Improved identification of agonist-mediated Gα(i)-specific human G-protein-coupled receptor signaling in yeast cells by flow cytometry. Anal Biochem 426(2):129–133.

Ishii J, Yoshimoto N, Tatematsu K, Kuroda S, Ogino C, Fukuda H, Kondo A. 2012b. Cell wall trapping of autocrine peptides for human G-protein-coupled receptors on the yeast cell surface. PLoS One 7(5):e37136.

Ishii J, Oda A, Togawa S, Fukao A, Fujiwara T, Ogino C, Kondo A. 2014. Microbial fluorescence sensing for human neurotensin receptor type 1 using Gα-engineered

yeast cells. Anal Biochem 446:37–43.

Ishizuka J, Beauchamp RD, Townsend CM Jr, Greeley GH Jr, Thompson JC. 1992. Receptor-mediated autocrine growth-stimulatory effect of 5-hydroxytryptamine on cultured human pancreatic carcinoid cells. J Cell Physiol 150(1):1–7.

Julius D, Livelli TJ, Jessell TM, Axel R. 1989. Ectopic expression of the serotonin 1c receptor and the triggering of malignant transformation. Science 244(4908):1057–1062.

Klco JM, Nikiforovich GV, Baranski TJ. 2006. Genetic analysis of the first and third extracellular loops of the C5a receptor reveals an essential WXFG motif in the first loop. J Biol Chem 281(17):12010–12019.

Kroeze WK, Kristiansen K, Roth BL. 2002. Molecular biology of serotonin receptors structure and function at the molecular level. Curr Top Med Chem 2(6):507–528.

Launay JM, Birraux G, Bondoux D, Callebert J, Choi DS, Loric S, Maroteaux L. 1996. Ras involvement in signal transduction by the serotonin 5-HT2B receptor. J Biol Chem 271(6):3141–3147.

Minic J, Sautel M, Salesse R, Pajot-Augy E. 2005. Yeast system as a screening tool for pharmacological assessment of G protein coupled receptors. Curr Med Chem 12(8):961–969.

Nakamura Y, Ishii J, Kondo A. 2013a. Rapid, facile detection of heterodimer partners for target human G-protein-coupled receptors using a modified split-ubiquitin membrane yeast two-hybrid system. PLoS One 8(6):e66793.

Nakamura Y, Ishii J, Kondo A. 2013b. Bright fluorescence monitoring system utilizing *Zoanthus* sp. green fluorescent protein (*ZsGreen*) for human G-protein-coupled receptor signaling in microbial yeast cells. PLoS One 8(12):e82237.

Nakamura Y, Takemoto N, Ishii J, Kondo A. 2014. Simultaneous method for analyzing dimerization and signaling of G-protein-coupled receptor in yeast by dual-color reporter system. Biotechnol Bioeng 111(3):586–596.

Nemecek GM, Coughlin SR, Handley DA, Moskowitz MA. 1986. Stimulation of aortic smooth muscle cell mitogenesis by serotonin. Proc Natl Acad Sci U S A 83(3):674–678.

Rajamannan NM, Caplice N, Anthikad F, Sebo TJ, Orszulak TA, Edwards WD, Tajik J, Schwartz RS. 2001. Cell proliferation in carcinoid valve disease: a mechanism for serotonin effects. J Heart Valve Dis 10(6):827–831.

Roth BL, Sheffler DJ, Kroeze WK. 2004. Magic shotguns versus magic bullets: selectively non-selective drugs for mood disorders and schizophrenia. Nat Rev Drug Discov 3(4):353–359.

Rovati GE, Capra V, Neubig RR. 2007. The highly conserved DRY motif of class A G protein-coupled receptors: beyond the ground state. Mol Pharmacol 71(4):959–964.

Savarese TM, Fraser CM. 1992. In vitro mutagenesis and the search for structure-function relationships among G protein-coupled receptors. Biochem J 283(Pt 1):1–19.

Scarselli M, Li B, Kim SK, Wess J. 2007. Multiple residues in the second extracellular loop are critical for M3 muscarinic acetylcholine receptor activation. J Biol Chem 282(10):7385–7396.

Seuwen K, Pouysségur J. 1990. Serotonin as a growth factor. Biochem Pharmacol

39(6):985–990.

Sibella-Argüelles C. 2001. The proliferation of human T lymphoblastic cells induced by 5-HT1B receptors activation is regulated by 5-HT-moduline. C R Acad Sci III. 324(4):365–372.

Takuwa N, Ganz M, Takuwa Y, Sterzel RB, Rasmussen H. 1989. Studies of the mitogenic effect of serotonin in rat renal mesangial cells. Am J Physiol 257:431–439.

Togawa S, Ishii J, Ishikura A, Tanaka T, Ogino C, Kondo A. 2010. Importance of asparagine residues at positions 13 and 26 on the amino-terminal domain of human somatostatin receptor subtype-5 in signaling. J Biochem 147(6):867–873.

Wacker D, Wang C, Katritch V, Han GW, Huang XP, Vardy E, McCorvy JD, Jiang Y, Chu M, Siu FY, Liu W, Xu HE, Cherezov V, Roth BL, Stevens RC. 2013. Structural features for functional selectivity at serotonin receptors. Science 340(6132):615–619.

Chapter 3: Construction of a yeast-based signaling biosensor for human angiotensin II type 1 receptor via functional coupling between Asn295-mutated receptor and Gpa1/G_{i3} chimeric Gα

Introduction

Angiotensin II (Ang II) is a naturally occurring, linear octapeptide that exhibits several extremely potent biological activities, including reversible blood pressure elevation and smooth muscle contraction (Printz et al., 1972). While Ang II binds to two major subtypes of Ang II receptors, Ang II type 1 receptor (AGTR1) and Ang II type 2 receptor (AGTR2), the most noted physiological and pathophysiological actions are mainly invoked through AGTR1. Both AGTR1 and AGTR2 are heterotrimeric guanine nucleotide binding protein (G-protein) coupled receptors (GPCRs), which is a large and diverse family of integral membrane proteins. GPCRs participate in the regulation of many cellular processes and, therefore, represent key targets for pharmacological treatment. Ang II regulates the cardiovascular response through AGTR1 (Griendling et al., 1996; Mehta and Griendling, 2007) and is involved in a wide range of diseases such as hypertension, atherosclerosis, heart failure, and diabetes (Chien, 1999; Dzau and Lopez-Ilasaca, 2005; MacLellan and Schneider, 1998; McKinsey and Olson, 1999; Sadoshima and Izumo, 1997). Consequently, AGTR1 is a significant molecular target in various research fields, including medicine, therapeutics, and pharmaceutics.

All eukaryotes conserve heterotrimer G-proteins that comprise Gα-, Gβ-, and Gγ-subunits on the inner leaflets of plasma membranes. Mammalian cells possess several types of G-proteins that enable the control of diverse physiological responses

mediated by interactions with a variety of transmembrane GPCRs (Hur and Kim, 2002). However, this diversity makes it difficult to identify which G-protein-GPCR pair is responsible for specific signals (Ishii et al., 2010). Because haploid *Saccharomyces cerevisiae* expresses one type of GPCR (either the **a**-cell specific pheromone receptor, Ste2p, or the α-cell specific pheromone receptor, Ste3p) and one type of heterotrimeric complex of G-proteins (Gpa1p, Ste4p, and Ste18p, which encode yeast Gα, Gβ, and Gγ, respectively), it can offer a simple way to transduce the signal promoted by the agonistic ligand (Fukuda et al., 2011). Moreover, *S. cerevisiae* provides several advantages, including the possession of eukaryotic secretory machinery, post-translational modifications, rapid cell growth, and well-established and versatile genetic techniques (Ishii et al., 2010). The introduction of several kinds of reporter genes such as green fluorescent protein (*GFP*) (Iguchi et al., 2010; Togawa et al., 2010), β-galactosidase (*lacZ*) (Brown et al., 2000), luciferase (*luc*) (Fukutani et al., 2012), and growth selection marker (*HIS3*) (Manfredi et al., 1996) downstream of the pheromone signaling (G-protein signaling) pathway further facilitates the detection of the agonist-promoted signal. Thus, the eukaryotic unicellular yeast *S. cerevisiae* is a useful microbial host organism for studying GPCRs as monomolecular models (Ishii et al., 2010; Minic et al., 2005).

If expression of human GPCR on the plasma membrane of *ste2*Δ yeast **a**-cells permits coupling with yeast monopolistic G-proteins, the promoted signal in response to the cognate ligand or analog agonist can be easily monitored with reporter gene assays (Fukuda et al., 2011; Ishii et al., 2010). The use of an established fluorescence-based reporter gene assay provides the most convenient measurement procedure: the cell culture is simply diluted into buffers and the fluorescence is read using fluorometric

instruments (Ishii et al., 2012a, b). A flow cytometer is an especially powerful tool for comparative quantification and quantitative screening (cell sorting) (Ishii et al., 2012a, b). Signaling assays using fluorescent reporter genes have to date been applied to several GPCRs, including yeast endogenous Ste2p (Ishii et al., 2006), murine olfactory receptor (OR226) (Fukutani et al., 2012), human somatostatin receptors (SSTR5 and SSTR2) (Iguchi et al., 2010; Nakamura et al., 2013b; Togawa et al., 2010), and human neurotensin receptor (NTSR1) (Ishii et al., 2014; Nakamura et al., 2013b). However, there have been no reports regarding the functional activation of AGTR1-mediated signaling in yeast cells. Since AGTR1 is a peptidic ligand-responsive GPCR, functional expression of AGTR1 in yeast cells could be applied to screening Ang II analogs or entirely new peptidic backbones that work as agonists or antagonists.

In this study, we succeeded in functional signal activation of human AGTR1 in engineered yeast cells. AGTR1-mediated signaling in response to its agonists was easily monitored using a fluorescence reporter assay. To allow functional activation of AGTR1 in yeast cells, we introduced a single Ala or Ser mutation at Asn295 in AGTR1 and used yeast-human chimeric Gα in place of the intrinsic yeast protein, Gpa1p. In addition, we demonstrated that the autocrined Ang II peptide and its analog (Ang III peptide) produced and secreted by the engineered yeast cells could by themselves promote AGTR1-mediated signaling.

Materials and Methods

Plasmid construction

All plasmids used in this study are listed in **Table 1**. All primers used for plasmid construction are listed in **Table 2**. Plasmid maps are presented in **Figure 1**.

A DNA fragment encoding the human *AGTR1* gene was PCR-amplified from pPR3-AGTR1 (Nakamura et al., 2013a) using the primers #1 and #2, digested with *Nhe*I+*Bgl*II, and inserted into the same sites between the *PGK1* promoter (P_{PGK1}) and the *PGK1* terminator (T_{PGK1}) on pGK421 (Togawa et al., 2010), yielding the plasmid pGK421-AGTR1.

The plasmids for expressing mutated AGTR1 proteins were constructed as follows. To introduce point mutations, gene fragments encoding the upstream and downstream parts of mutated AGTR1 were respectively PCR-amplified from pGK421-AGTR1 using primers #1 + #3 and #4 + #2 (for N111G); #1 + #5 and #6 + #2 (for N111A); #1 + #7 and #8 + #2 (for N111S); #1 + #9 and #10 + #2 (for N295A); #1 + #11 and #12 + #2 (for N295S); #1 + #13 and #14 + #2 (for L305Q). These amplified fragments then were used as the templates for overlap PCR with primers #1 and #2. The resulting linear mutated *AGTR1* fragments were digested with *Nhe*I+*Bgl*II and ligated into similarly digested pGK421, resulting in plasmids designated pGK421-AGTR1-N111G, -N111A, -N111S, -N295A, -N295S, or -L305Q, respectively.

To secret the peptidic ligands, the plasmids expressing the fusions of secretion signal sequence (s.s.; containing pre, pro α-factor leader region) and mature regions of several peptidic ligands were constructed as follows. A DNA fragment encoding the fusion between s.s. of α-factor and angiotensin II (AGII) was PCR-amplified from pGK426-S1442 (Ishii et al., 2012a) using primers #15 and #16. The *s.s.-AGII* fragment

was digested with *Nhe*I+*Sal*I and ligated into similarly digested pGK426 (Ishii et al., 2009), resulting in the plasmid pGK426-ssAGII. A DNA fragment encoding the fusion between s.s. of α-factor and angiotensin III (AGIII) was PCR-amplified from pGK426-ssAGII using primers #15 and #17. The *s.s.-AGIII* fragment was digested with *Nhe*I+*Sal*I and ligated into similarly digested pGK426, resulting in the plasmid pGK426-ssAGIII. A DNA fragment encoding the fusion between s.s. of α-factor and angiotensin IV (AGIV) was PCR-amplified from pGK426-ssAGII using primers #15 and #18. The *s.s.-AGIV* fragment was digested with *Nhe*I+*Sal*I and ligated into similarly digested pGK426, resulting in the plasmid pGK426-ssAGIV.

Yeast transformation and media

All yeast strains used in this study are listed in **Table 1**. Transformation with plasmids was performed using the lithium acetate method (Gietz et al., 1992).

Synthetic dextrose (SD) medium contained 6.7 g/L yeast nitrogen base without amino acids (YNB) (BD-Diagnostic Systems, Sparks, MD, USA) and 20 g/L glucose. For SDM71 media, SD medium was adjusted to pH 7.1 with 200 mM 3-(*N*-morpholino)-2-hydroxypropanesulfonic acid (MOPSO) (Nacalai Tesque, Kyoto, Japan). YPD medium contained 10 g/L yeast extract (Nacalai Tesque), 20 g/L peptone (BD-Diagnostic Systems) and 20 g/L glucose. Amino acids and nucleotides (20 mg/L histidine, 60 mg/L leucine, or 20 mg/L uracil) were supplemented into SD media to lack the relevant auxotrophic components. For solid medium, agar was added at 20 g/L.

Table 1. Yeast strains and plasmids used in this study.

Strain or plasmid	Specific features	Source
Strain		
BY4741	*MAT***a** *his3Δ1 leu2Δ0 met15Δ0 ura3Δ0*	Brachmann et al. (1998)
IMFD-70ZsD	BY4741 *sst2*Δ::*AUR1-C ste2*Δ::*LEU2 fig1*Δ::*ZsGreen his3*Δ::P_{FIG1}-*ZsGreen far1*Δ	Nakamura et al. (2013b)
IMFD-72ZsD	BY4741 *sst2*Δ::*AUR1-C ste2*Δ::*LEU2 fig1*Δ::*ZsGreen his3*Δ::P_{FIG1}-*ZsGreen far1*Δ *gpa1*Δ::G_{i3}*tp*	Nakamura et al. (2013b)
Plasmid		
pGK421	Yeast expression vector containing *PGK1* promoter, *PGK1* terminator, 2μ origin and *MET15* marker	Togawa et al. (2010)
pGK421-AGTR1	Human AGTR1 receptor expression in pGK421	This study
pGK421-AGTR1-N111G	Human AGTR1 receptor (N111G) mutant expression in pGK421	This study
pGK421-AGTR1-N111A	Human AGTR1 receptor (N111A) mutant expression in pGK421	This study
pGK421-AGTR1-N111S	Human AGTR1 receptor (N111S) mutant expression in pGK421	This study
pGK421-AGTR1-N295A	Human AGTR1 receptor (N295A) mutant expression in pGK421	This study
pGK421-AGTR1-N295S	Human AGTR1 receptor (N295S) mutant expression in pGK421	This study
pGK421-AGTR1-L305Q	Human AGTR1 receptor (L305Q) mutant expression in pGK421	This study
pGK426	Yeast expression vector containing *PGK1* promoter, *PGK1* terminator, 2μ origin and *URA3* marker	Ishii et al. (2009)
pGK426-ssAGII	Ang II secretory expression in pGK426	This study
pGK426-ssAGIII	Ang III secretory expression in pGK426	This study
pGK426-ssAGIV	Ang IV secretory expression in pGK426	This study

Table 2. List of primers.

	Name	Sequence
#1	NheI_AGTR1_fw	5'-GGGGGCTAGCATGATTCTCAACTCTTCTAC
#2	BglII_AGTR1_rv	5'-GGGGAGATCTTCACTCAACCTCAAAACATG
#3	AGTR1-N111G_rv	5'-ACTAGCGTACAGG**CC**GAAACTGACGCTGGC
#4	AGTR1-N111G_fw	5'-GCCAGCGTCAGTTTC**GG**CCTGTACGCTAGT
#5	AGTR1-N111A_rv	5'-ACTAGCGTACAGG**GC**GAAACTGACGCTGGC
#6	AGTR1-N111A_fw	5'-GCCAGCGTCAGTTTC**GC**CCTGTACGCTAGT
#7	AGTR1-N111S_rv	5'-ACTAGCGTACAGG**GA**GAAACTGACGCTGGC
#8	AGTR1-N111S_fw	5'-GCCAGCGTCAGTTTC**TC**CCTGTACGCTAGT
#9	AGTR1-N295A_rv	5'-AGGATTCAGGCAA**GC**GTTAAAATAAGCTAT
#10	AGTR1-N295A_fw	5'-ATAGCTTATTTTAAC**GC**TTGCCTGAATCCT
#11	AGTR1-N295S_rv	5'-AGGATTCAGGCAA**C**TGTTAAAATAAGCTAT
#12	AGTR1-N295S_fw	5'-ATAGCTTATTTTAACA**G**TTGCCTGAATCCT
#13	AGTR1-L305Q_rv	5'-AAATTTTTTCCCC**T**GAAAGCCATAAAAAAG
#14	AGTR1-L305Q_fw	5'-CTTTTTTATGGCTTTC**A**GGGGAAAAAATTT
#15	NheI_SS_fw	5'-GGGGGCTAGCATGAGATTTCCTTCAATTTT
#16	SalI_AGII-SS_rv	5'-AAAAGTCGACTTAGAAGGGGTGTATGTACAC CCGGTCTCTTTTATCCAAAGATACCC
#17	SalI_AGIII-SS_rv	5'-AAAAGTCGACTTAGAAGGGGTGTATGTACAC CCGTCTTTTATCCAAAGATACCC
#18	SalI_AGIV-SS_rv	5'-AAAAGTCGACTTAGAAGGGGTGTATGTACAC TCTTTTATCCAAAGATACCC

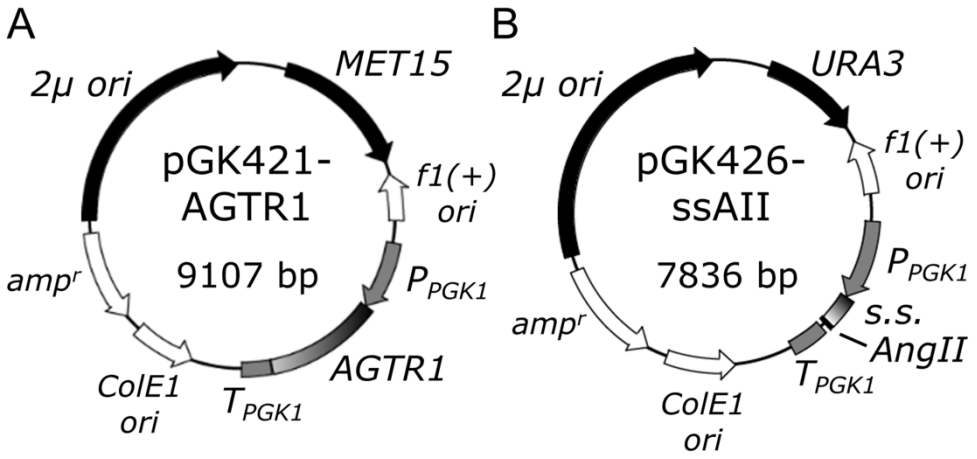

Fig. 1. Plasmids used in this study. (A) Multi-copy plasmid pGK421-AGTR1 (B) Multi-copy plasmid pGK426-ssAII.

AGTR1 signaling assay

AGTR1 signaling assays basically followed previously described procedures (Nakamura et al., 2013b, 2014) except for changes in the ligands. In brief, to assay signal activation from human AGTR1, the yeast strains transformed with the wild-type or mutated AGTR1 expression plasmids were grown in SD medium (supplemented as needed) at 30 °C overnight, then the cells were inoculated into 5 mL of the respective fresh SD medium to give an initial optical density of 0.03 at 600 nm (OD_{600} = 0.03). The cells were incubated at 30 °C on a rotary shaker at 150 rpm for up to 18 h, then harvested, washed, and resuspended in water to yield an OD_{600} = 10. The resulting yeast cell suspensions were added (at 10 μL/well; OD_{600} = 1) to the wells of 96-well cluster dishes containing fresh SDM71 medium (80 μL/well) supplemented with 10-times concentrated Ang II (Calbiochem, Darmstadt, Germany) (10 μL/well) at various concentrations or with distilled water (without Ang II; control). The plates were incubated at 30 °C with shaking (150 rpm) for 4 h. After incubation, the samples containing the yeast cells were observed using a fluorescence microscope or diluted with 1 mL of sheath fluid, then fluorescence was analyzed by flow cytometry. Half maximal effective concentration (EC_{50}) values were determined using KaleidaGraph4.0 Fits to a dosersplgst model.

Flow cytometry analysis

Flow cytometry measurements of green fluorescence followed a previously described procedure (Iguchi et al., 2010; Togawa et al., 2010). In brief, fluorescent cells were detected using a BD FACSCanto II flow cytometer equipped with a 488-nm blue laser (Becton, Dickinson and Company, Franklin Lakes, NJ, USA); the data were

analyzed using BD FACSDiva software (v5.0; Becton, Dickinson and Company). The GFP fluorescence signal was collected through a 530/30 nm band-pass filter; a GFP-A mean of 10,000 cells was defined as 'green fluorescent intensity'.

Fluorescence microscopy imaging

The cultured cells were washed and suspended in distilled water, and observed using a BZ-9000 fluorescence microscope (Keyence, Osaka, Japan). Green fluorescence images were acquired with a 470/40 band-pass filter for excitation and a 535/50 band-pass filter for emission.

AGTR1 signaling assay using secretory expression system of peptide ligands

AGTR1 signaling assays using a secretory expression system for the peptide ligands basically followed a previously reported procedure (Nakamura et al., 2013b) with some modifications. In brief, to assay signal activation from human AGTR1, yeast strains harboring pGK421-AGTR1-N295A or -N295S receptor expression plasmids and pGK426-based peptide expression plasmids were grown in SD medium (supplemented as needed) at 30 °C overnight, then the cells were inoculated into 5 mL of the respective fresh SDM71 medium to give an initial OD_{600} = 0.1. The cells were incubated at 30 °C on a rotary shaker at 150 rpm for 9 h. The yeast cells were observed using a fluorescence microscope, or diluted with 1 ml of sheath fluid and fluorescence was analyzed by flow cytometry.

Results and Discussion

Mutated AGTR1 is capable of coupling to the yeast signal transduction pathway

To monitor the signal activation of human AGTR1 receptor, previously engineered yeast cells in which the *GFP* reporter genes have been integrated into the genome were used as the host strains (Nakamura et al., 2013b). In the engineered strains, the tetrameric *Zoanthus* sp. green fluorescent protein (ZsGreen), the fluorescence of which is brighter than enhanced green fluorescent protein (EGFP), was used as the GFP reporter. The expression of ZsGreen is controlled by the signal responsive *FIG1* promoter. Therefore, signaling activation by agonist stimulus results in the generation of a green fluorescence signal (Nakamura et al., 2013b).

In addition, all engineered yeast strains have the *ste2*Δ, *sst2*Δ, and *far1*Δ alleles that are deficient in the yeast single GPCR, the yeast principal negative regulator of G-protein signaling (RGS), and the yeast G1-cyclin-dependent kinase inhibitor, an inhibitor that induces G1 cell cycle arrest in response to signaling (Fukuda et al., 2011; Iguchi et al., 2010; Ishii et al., 2012b; Togawa et al., 2010). These deletions respectively allow expression of human GPCRs without competitive receptor expression (Iguchi et al., 2010; Ishii et al., 2010; Togawa et al., 2010), hypersensitive agonist stimulation even at low ligand concentrations (Ishii et al., 2006), and growth in association with plasmid retention under signal-activated states (Ishii et al., 2008).

Since there have been no reports of functional activation of AGTR1-mediated signaling in yeast cells, we constructed multicopy episomal plasmids for expressing wild-type and six mutants of AGTR1 receptor under the control of the constitutive *PGK1* promoter (**Figure 2**, **Table 1**). The selected six AGTR1 mutants have increased affinities and potencies for Ang II, although they present the constitutive activations of

signaling in mammalian cells (Balmforth et al., 1997; Feng et al., 1998, 2005; Groblewski et al., 1997; Noda et al., 1996). Yeast IMFD-70ZsD strain, which specifically possesses intrinsic Gα (Gpa1p) (**Table 1**), was used to transform AGTR1 and its mutant expression plasmids, and then AGTR1 signaling assays were carried out. As shown in **Figure 3A**, none of the IMFD-70ZsD yeast cells expressing wild-type AGTR1 or its mutants showed green fluorescence, even in the presence of 1 mM Ang II. This result indicated that wild-type and mutant AGTR1 cannot transduce signals in yeast cells through the endogenous yeast Gα-subunit (Gpa1p).

A yeast-human chimeric Gα-subunit, in which the carboxyl-terminal 5 amino acid residues of Gpa1p (KIGII) are replaced with the equivalent residues from human $G\alpha_{i3}$ (ECGLY) (Gpa1/$G\alpha_{i3}$ transplant, G_{i3}tp), has been shown to improve signal transmission via several GPCRs expressed in yeast cells (Brown et al., 2000; Ishii et al., 2014; Nakamura et al., 2013b). Therefore, yeast IMFD-72ZsD strains, which specifically possess the chimeric Gα (G_{i3}tp) (**Table 1**), were used to transform AGTR1 and its mutant expression plasmids, and then AGTR1 signaling assays were performed. As shown in **Figure 3B**, the yeast strains expressing wild-type, and Asn111 and Leu305 mutants, of AGTR1 receptor showed no fluorescence. In contrast, the yeast strains expressing Asn295 mutants (N295A and N295S) displayed a 48-fold increase in fluorescence intensity in response to agonistic Ang II stimulation (**Figure 3B**). Microscope images of green fluorescence visually displayed clear differences in brightness in response to the Ang II-induced signal (**Figure 4** and **5**). These results indicated that the mutation of AGTR1 at Asn295 to either an alanine or serine residue permits functional coupling with yeast-human chimeric G-protein (G_{i3}tp) and enables signal transmission in the engineered yeast cells.

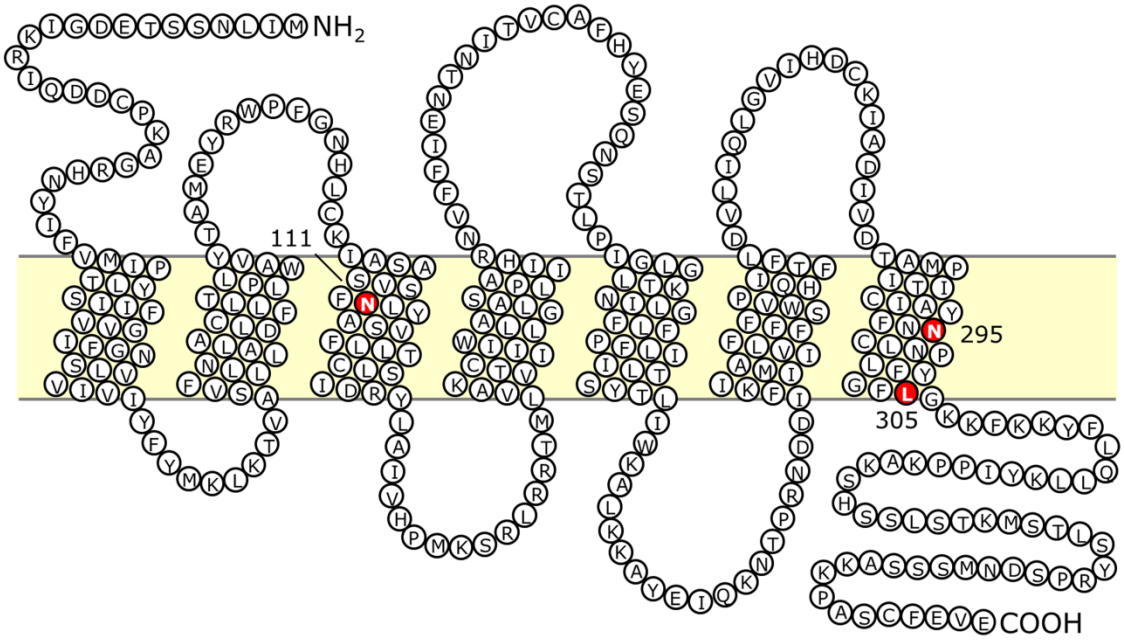

Fig. 2. Schematic illustration of the human AGTR1 showing the positions of the mutations. Each circle represents an amino acid residue. The positions of amino acids mutated in this study are indicated as red circles.

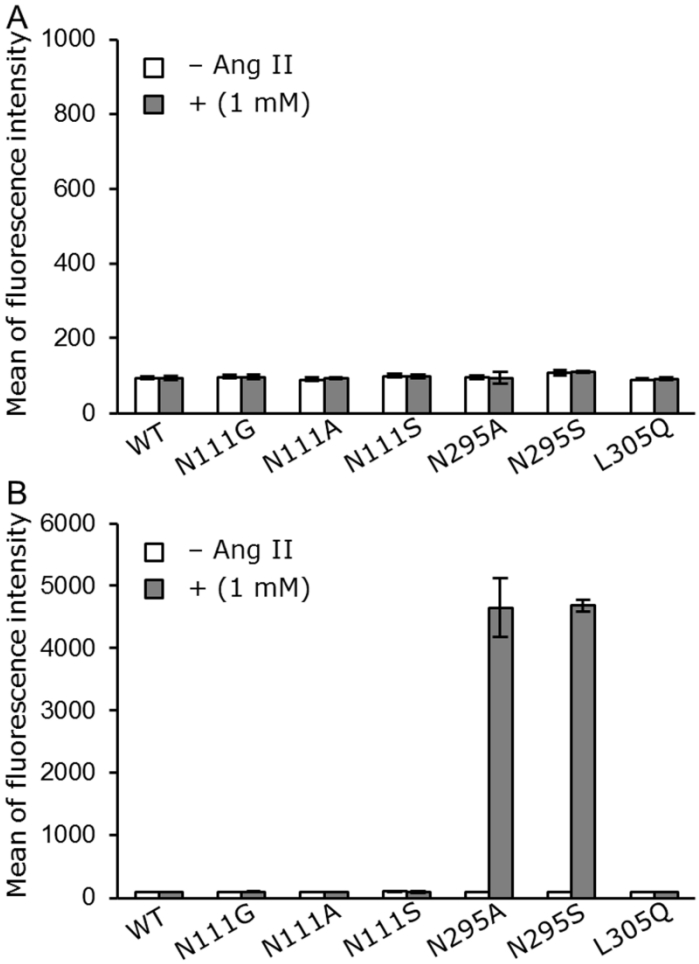

Fig. 3. Activation of human AGTR1 produced in yeast following exogenously-added angiotensin II. Yeast strains IMFD-70ZsD (Gpa1p) (A) and IMFD-72ZsD (G_{i3}tp) (B) were transformed with pGK421-AGTR1-based plasmids (WT AGTR1 or its mutants). All transformants were grown in SD selective medium for 18 h. The cells then were incubated for another 4 h in pH-adjusted SD selective medium with or without 1 mM angiotensin II (Ang II, 8 aa peptide). The GFP fluorescence of 10,000 cells was measured by flow cytometry. Mean values of the green fluorescence signal of 10,000 cells. Error bars represent the standard deviation from three separate runs (n = 3).

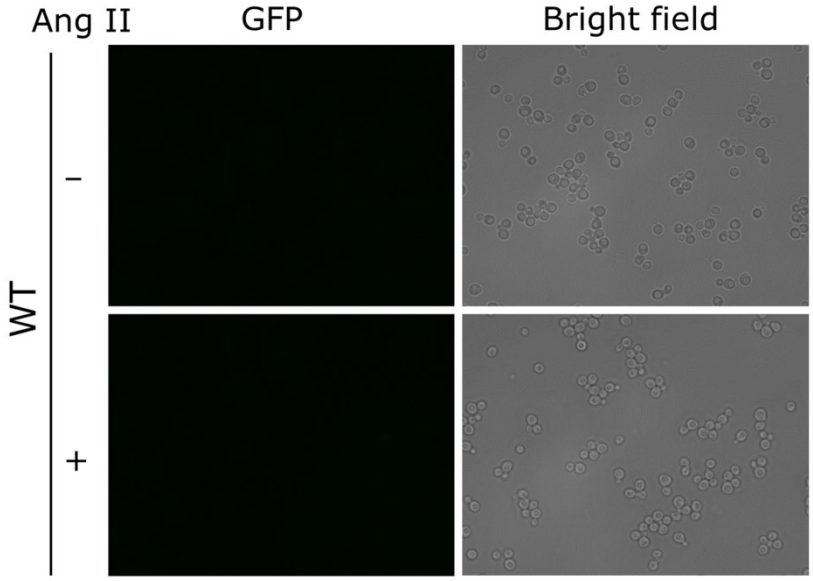

Fig. 4. Visualization of activated human AGTR1 produced in yeast following exogenously-added angiotensin II. Yeast strain IMFD-72ZsD was transformed with pGK421-AGTR1 (WT). The transformant was grown in SD selective medium for 18 h. The cells then were incubated for another 4 h in pH-adjusted SD selective medium with or without 1 mM angiotensin II (Ang II, 8 aa peptide). Cells were examined using the 100× objective lens of a fluorescence microscope. Exposure time was 0.5 s. The left photographs are fluorescence micrographs, and the right photographs are bright-field micrographs.

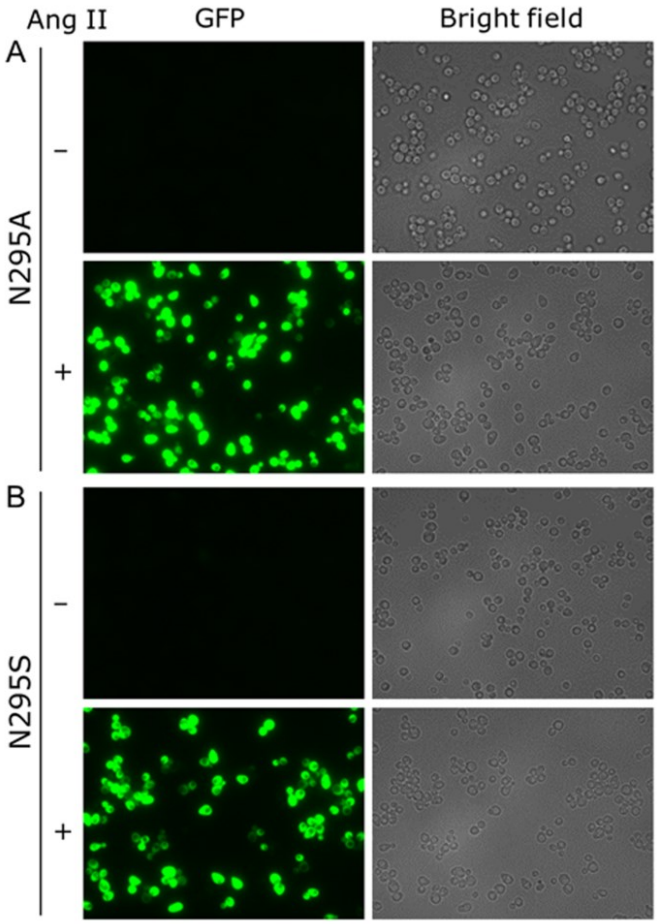

Fig. 5. Visualization of activated human AGTR1 produced in yeast following exogenously-added angiotensin II. Yeast strain IMFD-72ZsD was transformed with pGK421-AGTR1-N295A (A) or pGK421-AGTR1-N295S (B). All transformants were grown in SD selective medium for 18 h. The cells then were incubated for another 4 h in pH-adjusted SD selective medium with or without 1 mM angiotensin II (Ang II, 8 aa peptide). Cells were examined using the 100× objective lens of a fluorescence microscope. Exposure time was 0.5 s. The left photographs are fluorescence micrographs, and the right photographs are bright-field micrographs.

Dose-dependency of Asn295-mutated AGTR1 signaling for Ang II in Gα-engineered yeast cells

To investigate the dose-dependency of AGTR1 receptors with an Asn295 mutation, yeast IMFD-72ZsD strains harboring pGK421-AGTR1-N295A or -N295S were used in signaling assays. **Figure 6** shows the dose-response curve for the pharmacological efficacy of ligand-specific signaling of Asn295-mutated AGTR1 in yeast cells that express yeast-human chimeric G_{i3}tp (IMFD-72ZsD). Changing the Ang II concentration allowed confirmation of dose-dependent increases in fluorescence intensity in both cell types (**Figure 6**). The half-maximal effective concentration (EC_{50}) values were 368 μM (N295A) and 402 μM (N295S). These results suggested that the affinity or sensitivity of the N295A mutant for Ang II was higher than that of the N295S mutant. Previous reports revealed that Asn295 located in the seventh transmembrane helix is in spatial proximity to Asn111 in the third transmembrane helix, raising the possibility of an interaction between these two residues (Balmforth et al., 1997). Since this interaction is disrupted by the mutation of Asn295 to either an alanine or serine residue, its loss is likely responsible for the observed changes in ligand binding or receptor activation, thereby allowing AGTR1 to "relax" into its active conformation (Balmforth et al., 1997).

Activation of Asn295-mutated AGTR1 by secretory expressed angiotensin peptides

Finally, several Ang II peptidic analogs that differ in affinity or activity towards AGTR1 were employed to test whether the secretory expression system of various peptides could also permit the functional signaling activation of Asn295-mutated AGTR1 in yeast cells (**Figure 7A**). Ang III is a heptapeptide that has 40% of the pressor

activity of Ang II (Salhan et al., 2012). Ang IV is a hexapeptide that, like Ang III, has decreased activity compared to Ang II (Wright et al., 2008). Yeast cells were engineered to synthesize and secret these peptidic Ang II analogs by fusing with a secretion signal sequence.

The human Asn295-mutated AGTR1 expression plasmids (pGK421-AGTR1-N295A or -N295S) and peptide expression plasmids (pGK426-ssAGII, -ssAGIII, -ssAGIV or pGK426 (mock)) were co-transformed into the IMFD-72ZsD strain (**Table 1**). As shown in **Figure 7B**, the yeast strains concomitantly expressing AGTR1 (N295A and N295S) and secretory Ang II exhibited a greater than 94- and 91-fold increase in fluorescence intensity compared with the mock strain after 9 h cultivation. The secretory expressed Ang III also induced ZsGreen fluorescence, exhibiting a greater than 36- and 45-fold increase in fluorescence intensity compared with mock after 9 h cultivation (N295A and N295S, respectively) (**Figure 7B**). Although the strain secreting Ang IV showed no green fluorescence after 9 h cultivation (**Figure 7B**), it exhibited a greater than 1.5- and 2.4-fold increase in fluorescence intensity compared with mock after 18 h cultivation (N295A and N295S, respectively) (**Figure 8**). Microscope images of green fluorescence visually displayed clear differences in brightness arising from the distinct sequences of the secretory expressed angiotensin peptides (**Figure 9** and **10**). These results demonstrated that the secretory expression system could screen the peptidic angiotensin analogs, which can activate AGTR1-mediated signaling in yeast cells. Furthermore, the fluorescence intensity was clearly correlated with the agonistic activity of the ligands. Thus, it is expected that this yeast biosensor, integrating an Asn295-mutated AGTR1 receptor, will be useful for screening angiotensin agonists from peptidic libraries and for identifying their

pharmacophores. The methodology presented in this study could also be useful for other human GPCRs.

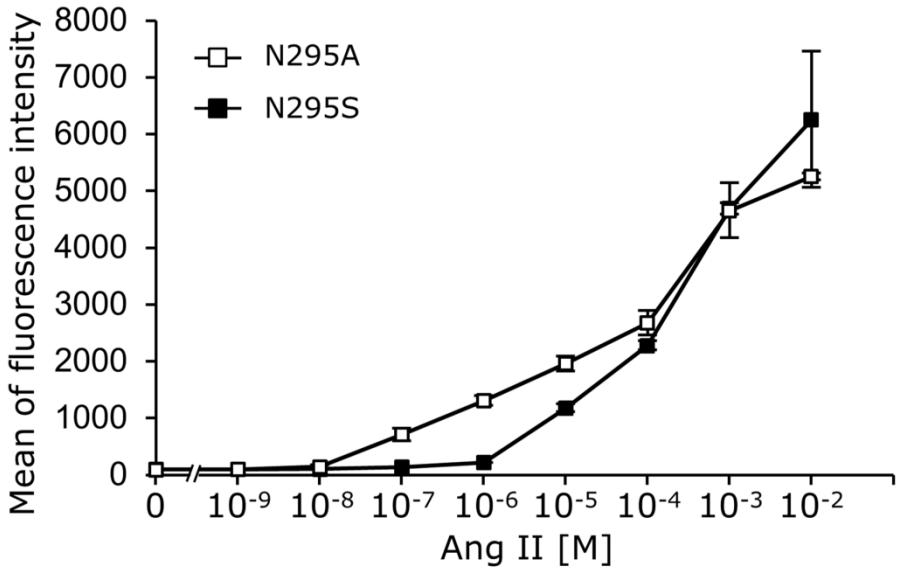

Fig. 6. Dose–response curves for angiotensin II-specific AGTR1 signaling activities of recombinant yeast cells. Yeast strain IMFD-72ZsD was transformed with pGK421-AGTR1-N295A or pGK421-AGTR1-N295S. All transformants were grown in SD selective medium for 18 h. The cells then were incubated for another 4 h in pH-adjusted SD selective medium with Ang II at various concentrations. The GFP fluorescence of 10,000 cells was measured by flow cytometry. Each data point is presented as the mean ± standard deviation of separate runs (n = 3 each).

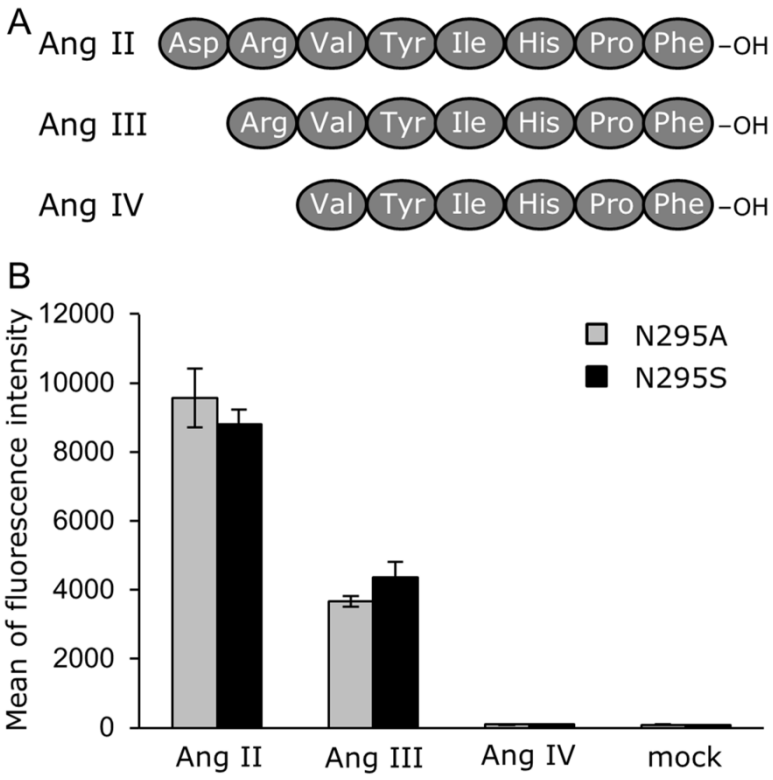

Fig. 7. Activation of human AGTR1 by secretory expressed angiotensin II. (A) Amino acid sequences of secretory expressed peptides. (B) Yeast strain IMFD-72ZsD, which coexpresses either pGK421-AGTR1-N295A or -N295S, and either pGK426-ssAGII (Ang II), pGK426-ssAGIII (Ang III), pGK426-ssAGIV (Ang IV) or pGK426 (mock), was incubated in pH-adjusted SD selective medium for 9 h. The GFP fluorescence of 10,000 cells was measured by flow cytometry. Mean values of the green fluorescence signal of 10,000 cells. Error bars represent the standard deviations (n = 3).

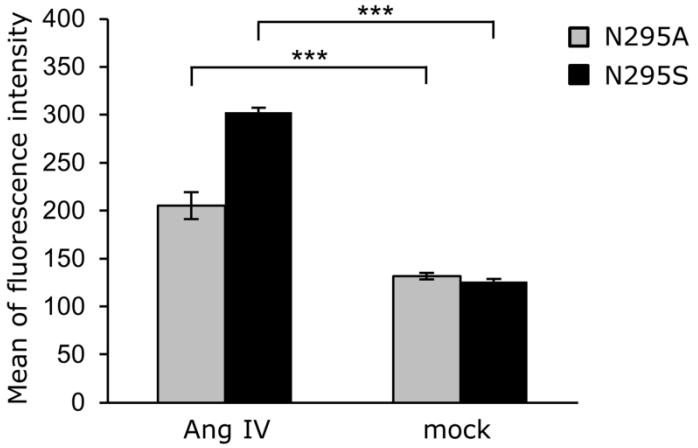

Fig. 8. Activation of human AGTR1 by secretory expressed angiotensin IV. Yeast strain IMFD-72ZsD, which coexpresses either pGK421-AGTR1-N295A or -N295S, and either pGK426-ssAGIV (Ang IV) or pGK426 (mock), was incubated in pH-adjusted SD selective medium for 18 h. The GFP fluorescence of 10,000 cells was measured by flow cytometry. Mean values of the green fluorescence signal of 10,000 cells. Error bars represent the standard deviations (n = 3). Statistical significance was assessed by the t-test (***, $p < 0.001$).

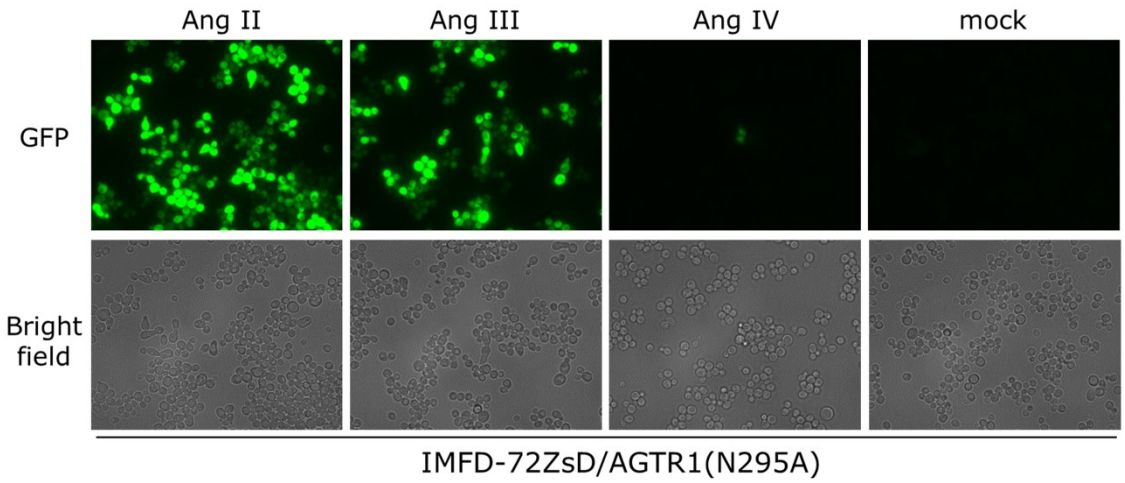

Fig. 9. Visualization of activated human AGTR1 (N295A) by secretory expressed angiotensin II. Yeast strain IMFD-72ZsD, which coexpresses pGK421-AGTR1-N295A and either pGK426-ssAGII (Ang II), pGK426-ssAGIII (Ang III), pGK426-ssAGIV (Ang IV) or pGK426 (mock), was incubated in pH-adjusted SD selective medium for 9 h. Cells were examined using the 100× objective lens of a fluorescence microscope. Exposure time was 0.33 s. The upper photographs are fluorescence micrographs, and the lower photographs are bright-field micrographs.

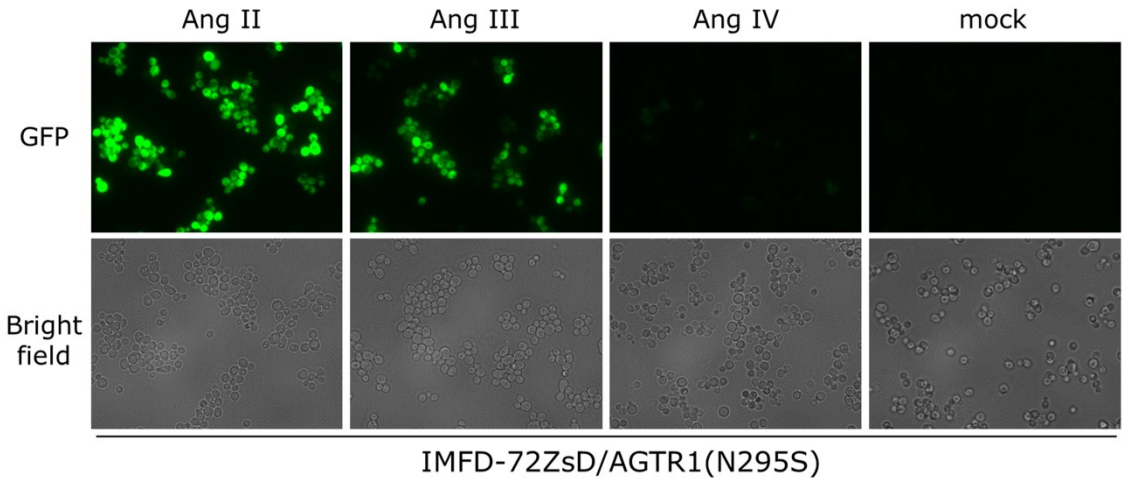

Fig. 10. Visualization of activated human AGTR1 (N295S) by secretory expressed angiotensin II. Yeast strain IMFD-72ZsD, which coexpresses pGK421-AGTR1-N295S and either pGK426-ssAGII (Ang II), pGK426-ssAGIII (Ang III), pGK426-ssAGIV (Ang IV) or pGK426 (mock), was incubated in pH-adjusted SD selective medium for 9 h. Cells were examined using the 100× objective lens of a fluorescence microscope. Exposure time was 0.33 s. The upper photographs are fluorescence micrographs, and the lower photographs are bright-field micrographs.

Conclusion

In this study, we established a fluorescence-based yeast biosensor based on an Asn295-mutated AGTR1 receptor. To exert the functional activation of AGTR1 in yeast cells, we introduced a single Ala or Ser mutation at Asn295 in AGTR1 and used yeast-human chimeric Gα. In addition, we demonstrated that the autocrined Ang II peptide and its analog (Ang III peptide) produced and secreted by the engineered yeast cells by themselves also could promote AGTR1-mediated signaling. Since our system is applicable to AGTR1, this system can likely be extended to other human GPCRs, which comprise one of the most important families of drug targets being pursued today. Consequently, the proposed system has the potential to be an effective tool for screening angiotensin agonists from peptidic libraries and to identify their pharmacophores. This work thus opens up a way for generating new devices in various pharmaceutical research areas.

References

Balmforth AJ, Lee AJ, Warburton P, Donnelly D, Ball SG. 1997. The conformational change responsible for AT1 receptor activation is dependent upon two juxtaposed asparagine residues on transmembrane helices III and VII. J Biol Chem 272(7):4245–4251.

Brachmann CB, Davies A, Cost GJ, Caputo E, Li J, Hieter P, Boeke JD. 1998. Designer deletion strains derived from *Saccharomyces cerevisiae* S288C: a useful set of strains and plasmids for PCR-mediated gene disruption and other applications. Yeast 14(2):115–132.

Brown AJ, Dyos SL, Whiteway MS, White JH, Watson MA, Marzioch M, Clare JJ, Cousens DJ, Paddon C, Plumpton C, Romanos MA, Dowell SJ. 2000. Functional coupling of mammalian receptors to the yeast mating pathway using novel yeast/mammalian G protein α-subunit chimeras. Yeast 16(1):11–22.

Chien KR. 1999. Stress pathways and heart failure. Cell 98(5):555–558.

Dzau VJ, Lopez-Ilasaca M. 2005. Searching for transcriptional regulators of Ang II-induced vascular pathology. J Clin Invest 115(9):2319–2322.

Feng YH, Miura S, Husain A, Karnik SS. 1998. Mechanism of constitutive activation of the AT1 receptor: influence of the size of the agonist switch binding residue Asn(111). Biochemistry 37(45):15791–15798.

Feng YH, Zhou L, Qiu R, Zeng R. 2005. Single mutations at Asn295 and Leu305 in the cytoplasmic half of transmembrane α-helix domain 7 of the AT1 receptor induce promiscuous agonist specificity for angiotensin II fragments: a pseudo-constitutive activity. Mol Pharmacol 68(2):347–355.

Fukuda N, Ishii J, Kaishima M, Kondo A. 2011. Amplification of agonist stimulation of

human G-protein-coupled receptor signaling in yeast. Anal Biochem 417(2):182–187.

Fukutani Y, Ishii J, Noguchi K, Kondo A, Yohda M. 2012. An improved bioluminescence-based signaling assay for odor sensing with a yeast expressing a chimeric olfactory receptor. Biotechnol Bioeng 109(12):3143–3151.

Gietz D, St Jean A, Woods RA, Schiestl RH. 1992. Improved method for high efficiency transformation of intact yeast cells. Nucleic Acids Res 20(6):1425.

Griendling KK, Lassègue B, Alexander RW. 1996. Angiotensin receptors and their therapeutic implications. Annu Rev Pharmacol Toxicol 36:281–306.

Groblewski T, Maigret B, Larguier R, Lombard C, Bonnafous JC, Marie J. 1997. Mutation of Asn111 in the third transmembrane domain of the AT1A angiotensin II receptor induces its constitutive activation. J Biol Chem 272(3):1822–1826.

Hur EM, Kim KT. 2002. G protein-coupled receptor signalling and cross-talk: achieving rapidity and specificity. Cell Signal 14(5):397–405.

Iguchi Y, Ishii J, Nakayama H, Ishikura A, Izawa K, Tanaka T, Ogino C, Kondo A. 2010. Control of signalling properties of human somatostatin receptor subtype-5 by additional signal sequences on its amino-terminus in yeast. J Biochem 147(6):875–884.

Ishii J, Matsumura S, Kimura S, Tatematsu K, Kuroda S, Fukuda H, Kondo A. 2006. Quantitative and dynamic analyses of G protein-coupled receptor signaling in yeast using Fus1, enhanced green fluorescence protein (EGFP), and His3 fusion protein. Biotechnol Prog 22(4):954–960.

Ishii J, Tanaka T, Matsumura S, Tatematsu K, Kuroda S, Ogino C, Fukuda H, Kondo A. 2008. Yeast-based fluorescence reporter assay of G protein-coupled receptor

signalling for flow cytometric screening: FAR1-disruption recovers loss of episomal plasmid caused by signalling in yeast. J Biochem 143(5):667–674.

Ishii J, Izawa K, Matsumura S, Wakamura K, Tanino T, Tanaka T, Ogino C, Fukuda H, Kondo A. 2009. A simple and immediate method for simultaneously evaluating expression level and plasmid maintenance in yeast. J Biochem 145(6):701–708.

Ishii J, Fukuda N, Tanaka T, Ogino C, Kondo A. 2010. Protein–protein interactions and selection: yeast-based approaches that exploit guanine nucleotide-binding protein signaling. FEBS J 277(9):1982–1995.

Ishii J, Yoshimoto N, Tatematsu K, Kuroda S, Ogino C, Fukuda H, Kondo A. 2012a. Cell wall trapping of autocrine peptides for human G-protein-coupled receptors on the yeast cell surface. PLoS One 7(5):e37136.

Ishii J, Moriguchi M, Hara KY, Shibasaki S, Fukuda H, Kondo A. 2012b. Improved identification of agonist-mediated Gα(i)-specific human G-protein-coupled receptor signaling in yeast cells by flow cytometry. Anal Biochem 426(2):129–133.

Ishii J, Oda A, Togawa S, Fukao A, Fujiwara T, Ogino C, Kondo A. 2014. Microbial fluorescence sensing for human neurotensin receptor type 1 using Gα-engineered yeast cells. Anal Biochem 446:37–43.

MacLellan WR, Schneider MD. 1998. Success in failure: modeling cardiac decompensation in transgenic mice. Circulation 97(15):1433–1435.

Manfredi JP, Klein C, Herrero JJ, Byrd DR, Trueheart J, Wiesler WT, Fowlkes DM, Broach JR. 1996. Yeast α mating factor structure-activity relationship derived from genetically selected peptide agonists and antagonists of Ste2p. Mol Cell Biol 16(9):4700–4709.

McKinsey TA, Olson EN. 1999. Cardiac hypertrophy: sorting out the circuitry. Curr

Opin Genet Dev 9(3):267–274.

Mehta PK, Griendling KK. 2007. Angiotensin II cell signaling: physiological and pathological effects in the cardiovascular system. Am J Physiol Cell Physiol 292(1):C82–97.

Minic J, Sautel M, Salesse R, Pajot-Augy E. 2005. Yeast system as a screening tool for pharmacological assessment of G protein coupled receptors. Curr Med Chem 12(8):961–969.

Nakamura Y, Ishii J, Kondo A. 2013a. Rapid, facile detection of heterodimer partners for target human G-protein-coupled receptors using a modified split-ubiquitin membrane yeast two-hybrid system. PLoS One 8(6):e66793.

Nakamura Y, Ishii J, Kondo A. 2013b. Bright fluorescence monitoring system utilizing *Zoanthus* sp. green fluorescent protein (*ZsGreen*) for human G-protein-coupled receptor signaling in microbial yeast cells. PLoS One 8(12):e82237.

Nakamura Y, Takemoto N, Ishii J, Kondo A. 2014. Simultaneous method for analyzing dimerization and signaling of G-protein-coupled receptor in yeast by dual-color reporter system. Biotechnol Bioeng 111(3):586–596.

Noda K, Feng YH, Liu XP, Saad Y, Husain A, Karnik SS. 1996. The active state of the AT1 angiotensin receptor is generated by angiotensin II induction. Biochemistry 35(51): 16435–16442.

Printz MP, Némethy G, Bleich H. 1972. Proposed models for angiotensin II in aqueous solution and conclusions about receptor topography. Nat New Biol 237(74):135–140.

Sadoshima J, Izumo S. 1997. The cellular and molecular response of cardiac myocytes to mechanical stress. Annu Rev Physiol 59:551–571.

Salhan D, Sagar A, Kumar D, Rattanavich R, Rai P, Maheshwari S, Adabala M, Husain M, Ding G, Malhotra A, Chander PN, Singhal PC. 2012. HIV-associated nephropathy: role of AT2R. Cell Signal 24(3):734–741.

Togawa S, Ishii J, Ishikura A, Tanaka T, Ogino C, Kondo A. 2010. Importance of asparagine residues at positions 13 and 26 on the amino-terminal domain of human somatostatin receptor subtype-5 in signaling. J Biochem 147(6):867–873.

Wright JW, Yamamoto BJ, Harding JW. 2008. Angiotensin receptor subtype mediated physiologies and behaviors: new discoveries and clinical targets. Prog Neurobiol 84(2):157–181.

Part II

Microbial yeast biosensors to monitor heterodimer formation for human G-protein-coupled receptors

Chapter 1: Rapid, facile detection of heterodimer partners for target human G-protein-coupled receptors using a modified split-ubiquitin membrane yeast two-hybrid system

Introduction

The potentially large functional and physiological diversity of dimerization among G-protein-coupled receptors (GPCRs) has generated a great deal of excitement due to the opportunity for novel drug discovery (George et al., 2002; Panetta and Greenwood, 2008). The findings of physiologically relevant GPCR dimers raise the prospect of developing new drugs against a wide range of diseases by focusing on the machinery of targeted dimers because ligand-induced conformational changes in GPCR dimers could affect ligand affinity and signaling function (Ayoub et al., 2004; Percherancier et al., 2005). Since the human genome encodes more than 800 GPCR genes (Fredriksson et al., 2003), the possible combinations of physiologically significant GPCR heterodimers would be immeasurable. However, due to the existence of numerous combinations, the sets of GPCR dimers are almost entirely unknown and thus their dominant roles are still poorly understood.

Techniques to observe the dimerization of GPCRs include atomic force microscopy, electrophoresis, co-immunoprecipitation, cross-linkage, and fluorescence and bioluminescence resonance energy transfer (FRET and BRET) (Ayoub et al., 2004; Percherancier et al., 2005; Pfleger and Eidne, 2005). The FRET and BRET approaches are especially helpful for in vivo analysis and therefore are widely used for the studies of dimerized GPCRs. However, although the FRET and BRET techniques permit the

direct monitoring of GPCR dimerization, it might be difficult to use these techniques to achieve rapid and facile identification of dimerizable candidates among numerous GPCR combinations.

To overcome this limitation, here we established a specialized method to screen candidate heterodimer partners for target GPCRs based on the split-ubiquitin membrane yeast two-hybrid method. In addition, since our system is independent from the activation of mitogen-activated protein kinase (MAPK) signal, it permits not only the identification of heterodimer partners, but also the monitoring of ligand-induced conformational changes.

Materials and Methods

Media. Synthetic dextrose (SD) media contained 6.7 g/l yeast nitrogen base without amino acids (YNB) (BD Diagnostic Systems, Sparks, MD, USA) and 20 g/l glucose. YPDA media contained 10 g/l yeast extract, 20 g/l peptone, 20 g/l glucose and 55 mg/l adenine. Amino acids and nucleotides (60 mg/l leucine, 40 mg/l tryptophan, 40 mg/l adenine, 20 mg/l histidine or 20 mg/l uracil) were supplemented into SD media to provide the relevant auxotrophic components. For solid plates, 2% agar was added to the media.

Yeast strains. All yeast strains were generated from NMY51 (Dualsystems Biotech AG, Schlieren, Switzerland) as a parental backbone strain and are listed in **Table 1**. Transformation with linear DNA fragments was performed by using the lithium acetate method (Gietz et al., 1992). To eliminate the *URA3* selectable marker in each transformation step, we basically followed previous procedures (Iguchi et al., 2010;

Togawa et al., 2010) with the marker recycling method (Akada et al., 2006). All oligonucleotides used for the strain constructions are listed in **Table 2**. To disrupt the target genes (*STE20*, *STE11* and *STE2*), the first half of DNA fragments containing upstream regions of target genes and *URA3* selectable marker were PCR-amplified from pGK406 (Ishii et al., 2009) by using gene-specific oligonucleotides. The last half of DNA fragments containing downstream regions of target genes and homologous sequences to eliminate *URA3* marker were PCR-amplified from NMY51 genomic DNA by using gene-specific oligonucleotides. These amplified fragments were then used as the templates for overlap PCR. The combined linear fragments were introduced into appropriate parental yeast strains, and the transformants were selected on SD solid media lacking uracil. After confirming integration of the fragments at the correct positions, the cells were maintained on SC media containing 1 mg/ml 5-fluoroorotic acid (5-FOA, Fluorochem, Derbyshire, UK) to eliminate *URA3* marker.

Plasmids. All plasmids used for the assays are listed in **Table 3**. The transformation procedure followed the lithium acetate method (Gietz et al., 1992).

All oligonucleotides are listed in **Table 2**. The bait proteins (X) were fused with a C-terminal ubiquitin moiety linked to an artificial transcription factor (X-Cub) in pBT3-C (Dualsystems Biotech AG, Schlieren, Switzerland). The prey proteins (Y) were fused with an N-terminal moiety of split-ubiquitin with I13G mutation (Y-Nub*G*) in pPR3-C (Dualsystems Biotech AG).

Bait vectors: For bait vectors, several promoters exhibiting distinctive expression strength were substituted for the original weak *CYC1* promoter of pBT3-C as follows.

PHO5 promoter (stronger than *CYC1* promoter) was PCR-amplified with

oligonucleotides o1 and o2. The *Sac*II-*Xba*I *PHO5* promoter was inserted at the *Sac*II-*Xba*I site on pBT3-C, resulting in the plasmid pBPH3-C.

TPI1 promoter (stronger than *PHO5* promoter) was PCR-amplified with oligonucleotides o3 and o4. The *Sac*II-*Xba*I *TPI1* promoter was inserted at the *Sac*II-*Xba*I site on pBT3-C, resulting in the plasmid pBTP3-C.

TDH3 promoter (stronger than *TPI1* promoter) was PCR-amplified with oligonucleotides o5 and o6. The *Sac*II-*Xba*I *TDH3* promoter was inserted at the *Sac*II-*Xba*I site on pBT3-C, resulting in the plasmid pBTD3-C.

GPCR expression plasmids: The bait and prey plasmids used for the expression of GPCRs were constructed as follows. Full length *STE2* genes encoding yeast pheromone receptor were PCR-amplified with oligonucleotide pairs: o7 and o8; o9 and o10. The *Xba*I-*Hind*III *STE2* gene fragments were inserted at the *Xba*I-*Hind*III site on pBT3-C, pBPH3-C, pBTP3-C and pBTD3-C, resulting in the plasmids pBT3-STE2, pBPH3-STE2, pBTP3-STE2 and pBTD3-STE2, respectively. The *Spe*I-*Eco*RI *STE2* gene fragment was inserted at the *Spe*I-*Eco*RI site on pPR3-C, resulting in the plasmid pPR3-STE2.

Truncated *STE2* genes that lack the C-terminal domain (Ste2ΔC) were PCR-amplified with oligonucleotide pairs: o7 and o11; o9 and o12. The *Xba*I-*Hind*III *STE2ΔC* gene fragments were inserted at the *Xba*I-*Hind*III site on pBT3-C and pBTP3-C, resulting in the plasmid pBT3-STE2ΔC and pBTP3-STE2ΔC, respectively. The *Spe*I-*Eco*RI *STE2ΔC* gene fragment was inserted at the *Spe*I-*Eco*RI site on pPR3-C, resulting in the plasmid pPR3-STE2ΔC.

Deletional *STE2* genes that lack the domains from TM6 until C-terminal tail (TM1-5) were PCR-amplified with oligonucleotide pairs: o7 and o13; o9 and o14. The

*Xba*I-*Hind*III *TM1-5* gene fragment was inserted at the *Xba*I-*Hind*III site on pBT3-C, resulting in the plasmid pBT3-STE2TM1-5. The *Spe*I-*Eco*RI *TM1-5* gene fragment was inserted at the *Spe*I-*Eco*RI site on pPR3-C, resulting in the plasmid pPR3-STE2TM1-5.

Deletional *STE2* genes that lack the domains from the N-terminal tail to TM5 and C-terminal domain (TM6-7) were PCR-amplified with oligonucleotide pairs: o15 and o11; o16 and o12. The *Xba*I-*Hind*III *TM6-7* gene fragment was inserted at the *Xba*I-*Hind*III site on pBT3-C, resulting in the plasmid pBT3-STE2TM6-7. The *Spe*I-*Eco*RI *TM6-7* gene fragment was inserted at the *Spe*I-*Eco*RI site on pPR3-C, resulting in the plasmid pPR3-STE2TM6-7.

The *HXT1* gene encoding glucose transporter was PCR-amplified with oligonucleotides o17 and o18. The *Spe*I-*Eco*RI *HXT1* gene fragment was inserted at the *Spe*I-*Eco*RI site on pPR3-C, resulting in the plasmid pPR3-HXT1.

GABBR1a genes encoding $GABA_{B1a}$ receptor were PCR-amplified with oligonucleotide pairs: o19 and o20; o21 and o22. The *Xba*I-*Hind*III *GABBR1a* gene fragment was inserted at the *Xba*I-*Hind*III site on pBTP3-C, resulting in the plasmid pBTP3-GABBR1a. The *Spe*I-*Eco*RI *GABBR1a* gene fragment was inserted at the *Spe*I-*Eco*RI site on pPR3-C, resulting in the plasmid pPR3-GABBR1a.

GABBR2 genes encoding $GABA_{B2}$ receptor were PCR-amplified with oligonucleotide pairs: o23 and o24; o25 and o26. The *Xba*I-*Hind*III *GABBR2* gene fragments were inserted at the *Xba*I-*Hind*III site on pBTP3-C and pBTD3-C, resulting in the plasmid pBTP3-GABBR2 and pBTD3-GABBR2, respectively. The *Spe*I-*Eco*RI *GABBR2* gene fragment was inserted at the *Spe*I-*Eco*RI site on pPR3-C, resulting in the plasmid pPR3-GABBR2.

AGTR1 genes encoding AT_1 (angiotensin type 1) receptor were PCR-amplified with

oligonucleotide pairs: o27 and o28; o29 and o30. The *Xba*I-*Hind*III *AGTR1* gene fragments were inserted at the *Xba*I-*Hind*III site on pBT3-C and pBTP3-C, resulting in the plasmid pBT3-AGTR1 and pBTP3-AGTR1, respectively. The *Spe*I-*Eco*RI *AGTR1* gene fragment was inserted at the *Spe*I-*Eco*RI site on pPR3-C, resulting in the plasmid pPR3-AGTR1.

AGTR2 gene encoding AT_2 (angiotensin type 2) receptor was PCR-amplified with oligonucleotides o31 and o32. The *Spe*I-*Eco*RI *AGTR2* gene fragment was inserted at the *Spe*I-*Eco*RI site on pPR3-C, resulting in the plasmid pPR3-AGTR2.

MTNR1A genes encoding MT_1 (melatonin 1A) receptor were PCR-amplified with oligonucleotide pairs: o33 and o34; o35 and o36. The *Xba*I-*Hind*III *MTNR1A* gene fragments were inserted at the *Xba*I-*Hind*III site on pBT3-C, resulting in the plasmid pBT3-MTNR1A and pBPH3-MTNR1A, respectively. The *Spe*I-*Eco*RI *MTNR1A* gene fragment was inserted at the *Spe*I-*Eco*RI site on pPR3-C, resulting in the plasmid pPR3-MTNR1A.

MTNR1B gene encoding MT_2 (melatonin 1B) receptor was PCR-amplified with oligonucleotides o37 and o38. The *Spe*I-*Eco*RI *MTNR1B* gene fragment was inserted at the *Spe*I-*Eco*RI site on pPR3-C, resulting in the plasmid pPR3-MTNR1B.

SSTR2 genes encoding somatostatin receptor 2 were PCR-amplified with oligonucleotide pairs: o39 and o40; o41 and o42. The *Xba*I-*Hind*III *SSTR2* gene fragments were inserted at the *Xba*I-*Hind*III site on pBT3-C, pBPH3-C, pBTP3-C and pBTD3-C, resulting in the plasmid pBT3-SSTR2, pBPH3-SSTR2, pBTP3-SSTR2 and pBTD3-SSTR2, respectively. The *Spe*I-*Eco*RI *SSTR2* gene fragment was inserted at the *Spe*I-*Eco*RI site on pPR3-C, resulting in the plasmid pPR3-SSTR2.

SSTR5 genes encoding somatostatin receptor 5 were PCR-amplified with

oligonucleotide pairs: o43 and o44; o45 and o46. The *Xba*I-*Hind*III *SSTR5* gene fragment was inserted at the *Xba*I-*Hind*III site on pBTD3-C, resulting in the plasmid pBTD3-SSTR5. The *Spe*I-*Eco*RI *SSTR5* gene fragment was inserted at the *Spe*I-*Eco*RI site on pPR3-C, resulting in the plasmid pPR3-SSTR5.

ADRB2 genes encoding β_2-adrenergic receptor were PCR-amplified with oligonucleotide pairs: o47 and o48; o49 and o50. The *Xba*I-*Hind*III *ADRB2* gene fragments were inserted at the *Xba*I-*Hind*III site on pBT3-C, pBTP3-C and pBTD3-C, resulting in the plasmid pBT3-ADRB2, pBTP3-ADRB2 and pBTD3-ADRB2, respectively. The *Spe*I-*Eco*RI *ADRB2* gene fragment was inserted at the *Spe*I-*Eco*RI site on pPR3-C, resulting in the plasmid pPR3-ADRB2.

HTR1A genes encoding 5-hydroxytryptamine (serotonin) receptor 1A were PCR-amplified with oligonucleotide pairs: o51 and o52; o53 and o54. The *Xba*I-*Hind*III *HTR1A* gene fragments were inserted at the *Xba*I-*Hind*III site on pBPH3-C and pBTP3-C, resulting in the plasmid pBPH3-HTR1A and pBTP3-HTR1A, respectively. The *Spe*I-*Eco*RI *HTR1A* gene fragment was inserted at the *Spe*I-*Eco*RI site on pPR3-C, resulting in the plasmid pPR3-HTR1A.

EDNRB gene encoding endothelin receptor type B was PCR-amplified with oligonucleotides o55 and o56. The *Spe*I-*Cla*I *EDNRB* gene fragment was inserted at the *Spe*I-*Cla*I site on pPR3-C, resulting in the plasmid pPR3-EDNRB.

NTSR1 gene encoding neurotensin receptor 1 was PCR-amplified with oligonucleotides o57 and o58. The *Spe*I-*Eco*RI *NTSR1* gene fragment was inserted at the *Spe*I-*Eco*RI site on pPR3-C, resulting in the plasmid pPR3-NTSR1.

NTSR2 gene encoding neurotensin receptor 2 was PCR-amplified with oligonucleotides o59 and o60. The *Spe*I-*Eco*RI *NTSR2* gene fragment was inserted at the *Spe*I-*Eco*RI site

on pPR3-C, resulting in the plasmid pPR3-NTSR2.

Table 1. Yeast strains used in this study

Strain	Genotype	Source
NMY51	*MAT**a** his3Δ200 trp1-901 leu2-3, 112 ade2 LYS2::(lexAop)$_4$-HIS3 ura3::(lexAop)$_8$-lacZ ade2::(lexAop)$_8$-ADE2 GAL4*	Dualsystems Biotech AG
NMY61	NMY51 *ste20*Δ	This study
NMY62	NMY51 *ste11*Δ	This study
NMY63	NMY51 *ste11*Δ *ste2*Δ	This study

Table 2. List of oligonucleotides.

Yeast strain construction		
	Name	**Sequence**
	dSTE20up-URA3_fw	5'-GCAAGCAACCCAAACTTCTTCCCTTCACTGCCTCACACCCCATCCTAAATATC CCACAAGATCCTCGACTAATACAAGAATTTTTTGTTCTTTTTTTTGA
	dSTE20up-URA3_rv	5'-CTTGTGGGATATTTAGGATGGGGTAATAACTGATATAATT
	dSTE20dn_fw	5'-AATTATATCAGTTATTACCCCATCCTAAATATCCCACAAGATCCTCGACTAATAC AAGAAACGTAGCAAGCAGGGTACAC
	dSTE20dn_rv	5'-CTCCTTCGTTACATAGAACGCAGACAGATG
	dSTE11up-URA3_fw	5'-TATTCATATTTACACACATGCATAAAGAGAGACCACTTAATAAAGCTAGTATGAT AAGATCACCGGTAGACGAAATATACTTTTTTGTTCTTTTTTTTGA
	dSTE11up-URA3_rv	5'-ATCTTATCATACTAGCTTTAGGGTAATAACTGATATAATT
	dSTE11dn_fw	5'-AATTATATCAGTTATTACCCTAAAGCTAGTATGATAAGATCACCGGTAGACGAAA TATACAAAAGGGCTACTTATTAATT
	dSTE11dn_rv	5'-TCACCTCGCAAAGAAAGGCCTGTTTCTTCG
	dSTE2up-URA3_fw	5'-TTTCTTTTCACCTGCTCTGGCTATAATTATAATTGGTTACTTAAAAATGCACCGT TAAGAACCATATCCAAGAATCAAAATTTTTTGTTCTTTTTTTTGA
	dSTE2up-URA3_rv	5'-TCTTAACGGTGCATTTTTAAGGGTAATAACTGATATAATT
	dSTE2dn_fw	5'-AATTATATCAGTTATTACCCTTAAAAATGCACCGTTAAGAACCATATCCAAGAAT CAAAATCAAAATTTACGGCTTTGAAAAAGTAATTTCGTGACCTTC
	dSTE2dn_rv	5'-AAGATTAACTGTATATATTGCCTGAGAGTTCTAGATCATG
Plasmid construction		
	Name	**Sequence**
o1	SacII_PHO5p_fw	5'-AAAACCGCGGTTTTCTTTGTCTGCACAAAG
o2	XbaI_PHO5p_rv	5'-AAAATCTAGATGGTAATCTCGAATTTGCTT
o3	SacII_TPI1p_fw	5'-AAAACCGCGGCTACTTATTCCCTTCGAGAT
o4	XbaI_TPI1p_rv	5'-AAAATCTAGATTTTAGTTTATGTATGTGTT
o5	SacII_TDH3p_fw	5'-GGGGCCGCGGGAATAAAAAACACGCTTTTT
o6	XbaI_TDH3p_rv	5'-CCCCTCTAGATTTGTTTGTTTATGTGTGTT
o7	XbaI_STE2_fw	5'-AAAATCTAGAATGTCTGATGCGGCTCCTTC
o8	HindIII_lin_STE2_rv	5'-GGGGAAGCTTGAACCTCCGCCACCTGATAAATTATTATTATCTTCAG
o9	SpeI_STE2_fw	5'-GGGGACTAGTATGTCTGATGCGGCTCCTTC
o10	EcoRI_lin_STE2_rv	5'-GGGGGAATTCGGAACCTCCGCCACCTGATAAATTATTATTATCTTCAG
o11	HindIII_lin_STE2-304_rv	5'-GGGGAAGCTTGAACCTCCGCCACCTGATTTGGATGCATTATTAGCAG
o12	EcoRI_lin_STE2-304_rv	5'-GGGGGAATTCGGAACCTCCGCCACCTGATTTGGATGCATTATTAGCAG

o13	HindIII_lin_STE2-236_rv	5'-GGGGAAGCTTGAACCTCCGCCACCTGAAAGGAATCTTCTTGATCTAA
o14	EcoRI_lin_STE2-236_rv	5'-GGGGGAATTCGGAACCTCCGCCACCTGAAAGGAATCTTCTTGATCTAA
o15	XbaI_STE2-237_fw	5'-GGGGTCTAGAATGGGTCTCAAGCAGTTCGA
o16	SpeI_STE2-237_fw	5'-GGGGACTAGTATGGGTCTCAAGCAGTTCGA
o17	SpeI_HXT1sm_fw	5'-GGGGACTAGTATGAACTCAACTCCCGATCTAATATCTCCT
o18	EcoRI_lin_HXT1_rv	5'-GGGGGAATTCGGAACCTCCGCCACCTGATTTCCTGCTAAACAAACTCTTG
o19	XbaI_GABBR1a_fw	5'-AAAATCTAGAATGTTGCTGCTGCTGCTACT
o20	HindIII_lin_GABBR1a_rv	5'-GGGGAAGCTTGAACCTCCGCCACCTGACTTATAAAGCAAATGCACTC
o21	SpeI_GABBR1a_fw	5'-AAAAACTAGTATGTTGCTGCTGCTGCTACT
o22	EcoRI_lin_GABBR1a_rv	5'-GGGGGAATTCGGAACCTCCGCCACCTGACTTATAAAGCAAATGCACTC
o23	XbaI_GABBR2_fw	5'-AAAATCTAGAATGGCTTCCCCGCGGAGCTC
o24	HindIII_lin_GABBR2_rv	5'-TTTTAAGCTTGAACCTCCGCCACCTGACAGGCCCGAGACCATGACTC
o25	SpeI_GABBR2_fw	5'-AAAAACTAGTATGGCTTCCCCGCGGAGCTC
o26	EcoRI_lin_GABBR2_rv	5'-TTTTGAATTCGGAACCTCCGCCACCTGACAGGCCCGAGACCATGACTC
o27	XbaI_AGTR1_fw	5'-AAAATCTAGAATGATTCTCAACTCTTCTAC
o28	HindIII_lin_AGTR1_rv	5'-GGGGAAGCTTGAACCTCCGCCACCTGACTCAACCTCAAAACATGGTG
o29	SpeI_AGTR1_fw	5'-GGGGACTAGTATGATTCTCAACTCTTCTAC
o30	EcoRI_lin_AGTR1_rv	5'-GGGGGAATTCGGAACCTCCGCCACCTGACTCAACCTCAAAACATGGTG
o31	SpeI_AGTR2_fw	5'-TTTTACTAGTATGAAGGGCAACTCCACCCT
o32	EcoRI_lin_AGTR2_rv	5'-TTTTGAATTCGGAACCTCCGCCACCTGAAGACACAAAGGTCTCCATTT
o33	XbaI_MTNR1A_fw	5'-TTTTTCTAGAATGCAGGGCAACGGCAGCGC
o34	HindIII_lin_MTNR1A_rv	5'-GGGGAAGCTTGAACCTCCGCCACCTGAAACGGAGTCCACCTTTACTA
o35	SpeI_MTNR1A_fw	5'-TTTTACTAGTATGCAGGGCAACGGCAGCGC
o36	EcoRI_lin_MTNR1A_rv	5'-GGGGGAATTCGGAACCTCCGCCACCTGAAACGGAGTCCACCTTTACTA
o37	SpeI_MTNR1B_fw	5'-GGGGACTAGTATGTCAGAGAACGGCTCCTT
o38	EcoRI_lin_MTNR1B_rv	5'-AAAAGAATTCGGAACCTCCGCCACCTGAGAGAGCATCTGCCTGGTGCT
o39	XbaI_SSTR2_fw	5'-AAAATCTAGAATGGACATGGCGGATGAGCC
o40	HindIII_lin_SSTR2_rv	5'-AAAAAAGCTTGAACCTCCGCCACCTGAGATACTGGTTTGGAGGTCTC
o41	SpeI_SSTR2_fw	5'-CCCCACTAGTATGGACATGGCGGATGAGCC
o42	EcoRI_lin_SSTR2_rv	5'-AAAAGAATTCGGAACCTCCGCCACCTGAGATACTGGTTTGGAGGTCTC
o43	XbaI_SSTR5_fw	5'-AAAATCTAGAATGGAGCCCCTGTTCCCAGC
o44	HindIII_lin_SSTR5_rv	5'-TTTTAAGCTTGAACCTCCGCCACCTGACAGCTTGCTGGTCTGCATAA
o45	SpeI_SSTR5_fw	5'-AAAAACTAGTATGGAGCCCCTGTTCCCAGC
o46	EcoRI_lin_SSTR5_rv	5'-AAAAGAATTCGGAACCTCCGCCACCTGACAGCTTGCTGGTCTGCATAA
o47	XbaI_ADRB2_fw	5'-TTTTTCTAGAATGGGGCAACCCGGGAACGG
o48	HindIII_lin_ADRB2_rv	5'-TTTTAAGCTTGAACCTCCGCCACCTGACAGCAGTGAGTCATTTGTAC

o49	SpeI_ADRB2_fw	5'-AAAAACTAGTATGGGGCAACCCGGGAACGG
o50	EcoRI_lin_ADRB2_rv	5'-AAAAGAATTCGGAACCTCCGCCACCTGACAGCAGTGAGTCATTTGTAC
o51	XbaI_HTR1A_fw	5'-AAAATCTAGAATGGATGTGCTCAGCCCTGG
o52	HindIII_lin_HTR1A_rv	5'-TTTTAAGCTTGAACCTCCGCCACCTGACTGGCGGCAGAACTTACACT
o53	SpeI_HTR1A_fw	5'-GGGGACTAGTATGGATGTGCTCAGCCCTGG
o54	EcoRI_lin_HTR1A_rv	5'-GGGGGAATTCGGAACCTCCGCCACCTGACTGGCGGCAGAACTTACACT
o55	SpeI_EDNRB_fw	5'-GGGGACTAGTATGCAGCCGCCTCCAAGTCT
o56	ClaI_lin_EDNRB_rv	5'-GGGGATCGATGGAACCTCCGCCACCTGAAGATGAGCTGTATTTATTAC
o57	SpeI_NTSR1_fw	5'-GGGGACTAGTATGCGCCTCAACAGCTCCGC
o58	EcoRI_lin_NTSR1_rv	5'-AAAAGAATTCGGAACCTCCGCCACCTGAGTACAGCGTCTCGCGGGTGG
o59	SpeI_NTSR2_fw	5'-TTTTACTAGTATGGAAACCAGCAGCCCGCG
o60	EcoRI_lin_NTSR2_rv	5'-AAAAGAATTCGGAACCTCCGCCACCTGAGGTCCGGGTTTCTGGGGGAT

Table 3. List of plasmids

Plasmid name	Expressed protein[a,b]	Vector backbone	Promoter	Source
Bait				
pCCW-Alg5	Alg5-Cub	–	CYC1	Dualsystems Biotech AG
pBT3-C	Cub	–	CYC1	Dualsystems Biotech AG
pBPH3-C	Cub	pBT3-C	PHO5	This study
pBTP3-C	Cub	pBT3-C	TPI1	This study
pBTD3-C	Cub	pBT3-C	TDH3	This study
pBT3-STE2	Ste2(full length)-Cub	pBT3-C	CYC1	This study
pBPH3-STE2	Ste2(full length)-Cub	pBPH3-C	PHO5	This study
pBTP3-STE2	Ste2(full length)-Cub	pBTP3-C	TPI1	This study
pBTD3-STE2	Ste2(full length)-Cub	pBTD3-C	TDH3	This study
pBT3-STE2ΔC	Ste2(aa 1-304)-Cub	pBT3-C	CYC1	This study
pBTP3-STE2ΔC	Ste2(aa 1-304)-Cub	pBTP3-C	TPI1	This study
pBT3-STE2TM1-5	Ste2(aa 1-236)-Cub	pBT3-C	CYC1	This study
pBT3-STE2TM6-7	Ste2(aa 237-304)-Cub	pBT3-C	CYC1	This study
pBTP3-GABBR1a	GABBR1a-Cub	pBTP3-C	TPI1	This study
pBTP3-GABBR2	GABBR2-Cub	pBTP3-C	TPI1	This study
pBTD3-GABBR2	GABBR2-Cub	pBTD3-C	TDH3	This study
pBT3-AGTR1	AGTR1-Cub	pBT3-C	CYC1	This study
pBTP3-AGTR1	AGTR1-Cub	pBTP3-C	TPI1	This study
pBT3-MTNR1A	MTNR1A-Cub	pBT3-C	CYC1	This study
pBPH3-MTNR1A	MTNR1A-Cub	pBPH3-C	PHO5	This study
pBT3-SSTR2	SSTR2-Cub	pBT3-C	CYC1	This study
pBPH3-SSTR2	SSTR2-Cub	pBPH3-C	PHO5	This study
pBTP3-SSTR2	SSTR2-Cub	pBTP3-C	TPI1	This study
pBTD3-SSTR2	SSTR2-Cub	pBTD3-C	TDH3	This study
pBTD3-SSTR5	SSTR5-Cub	pBTD3-C	TDH3	This study
pBT3-ADRB2	ADRB2-Cub	pBT3-C	CYC1	This study
pBTP3-ADRB2	ADRB2-Cub	pBTP3-C	TPI1	This study
pBTD3-ADRB2	ADRB2-Cub	pBTD3-C	TDH3	This study
pBPH3-HTR1A	HTR1A-Cub	pBPH3-C	PHO5	This study
pBTP3-HTR1A	HTR1A-Cub	pBTP3-C	TPI1	This study
Prey				
pAI-Alg5	Alg5-Nub*I*	–	ADH1	Dualsystems Biotech AG

pPR3-C	Nub*G*	–	ADH1	Dualsystems Biotech AG
pPR3-STE2	Ste2(full length)-Nub*G*	pPR3-C	ADH1	This study
pPR3-STE2ΔC	Ste2(aa 1-304)-Nub*G*	pPR3-C	ADH1	This study
pPR3-STE2TM1-5	Ste2(aa 1-236)-Nub*G*	pPR3-C	ADH1	This study
pPR3-STE2TM6-7	Ste2(aa 237-304)-Nub*G*	pPR3-C	ADH1	This study
pPR3-HXT1	Hxt1(full length)-Nub*G*	pPR3-C	ADH1	This study
pPR3-GABBR1a	GABBR1a-Nub*G*	pPR3-C	ADH1	This study
pPR3-GABBR2	GABBR2-Nub*G*	pPR3-C	ADH1	This study
pPR3-AGTR1	AGTR1-Nub*G*	pPR3-C	ADH1	This study
pPR3-AGTR2	AGTR2-Nub*G*	pPR3-C	ADH1	This study
pPR3-MTNR1A	MTNR1A-Nub*G*	pPR3-C	ADH1	This study
pPR3-MTNR1B	MTNR1B-Nub*G*	pPR3-C	ADH1	This study
pPR3-SSTR2	SSTR2-Nub*G*	pPR3-C	ADH1	This study
pPR3-SSTR5	SSTR5-Nub*G*	pPR3-C	ADH1	This study
pPR3-ADRB2	ADRB2-Nub*G*	pPR3-C	ADH1	This study
pPR3-HTR1A	HTR1A-Nub*G*	pPR3-C	ADH1	This study
pPR3-EDNRB	EDNRB-Nub*G*	pPR3-C	ADH1	This study
pPR3-NTSR1	NTSR1-Nub*G*	pPR3-C	ADH1	This study
pPR3-NTSR2	NTSR2-Nub*G*	pPR3-C	ADH1	This study

a) Cub indicates the Cub-LexA-VP16 fusion protein

b) Nub*G* indicates Nub with I13G mutation

Agar diffusion bioassay. An agar diffusion bioassay (halo assay) was performed to measure growth inhibition in response to signal-induced cell-cycle arrest (Ishii et al., 2006). Cells were grown in YPDA media overnight at 30°C. Sterilized paper filter disks (6 mm in diameter) were placed on a square Petri dish, and various amounts of α-factor pheromone (Zymo Research, Orange, CA, USA) were spotted onto the disks. YPDA medium containing 20 g/l agar (maintained at 50°C) was inoculated with the grown cells to give an initial optical density of 5×10^{-4} at 600 nm ($OD_{600} = 5 \times 10^{-4}$), and the suspension was immediately poured into the dish. The plates were incubated at 30°C for 1 to 2 days.

Evaluation of receptor dimerization. Cub and Nub*G* fusion constructs (**Table 3**) were co-transformed into yeast strains. Cells were grown in SD media lacking leucine and tryptophan overnight at 30°C on a rotatory shaker set at 150 rpm and then harvested to evaluate receptor dimerization by growth assay and β-galactosidase assay.

Growth assay. Harvested cells were washed with distilled water, and cell suspensions were prepared to give an OD_{600} of 10. Seven microliters of serial dilutions of cell suspensions (1:10) were spotted on SD agar plates lacking leucine, tryptophan, adenine and histidine. The plates were incubated at 30°C.

β-D-galactosidase activity assay. β-D-galactosidase activity was determined by using chlorophenol red β-D-galactopyranoside (CPRG) (Roche Applied Science, Indianapolis, IN, USA) as the chromogenic substrate. The procedure basically followed the method described in the Yeast Protocols Handbook (Clontech Laboratories, Inc./Takara Bio

Company). Harvested cells were washed once with buffer 1 [100 mM 4-(2-hydroxyethyl)-1-piperazineethanesulfonic acid (HEPES), 150 mM NaCl, 4 mM L-aspartic acid hemimagnesium salt hydrate, 10 g/l bovine serum albumin (BSA) and 0.05% polyoxyethylene sorbitan monolaurate (Tween 20); pH 7.25-7.30] and resuspended in buffer 1 to give an OD_{600} of 10. Four microliters of chloroform and 7 μl of 0.1% SDS were added to 100 μl of cell suspension, the mixtures were agitated with a vortex, and then buffer 1 (700 μl) containing 2.23 mM CPRG was added to the mixtures. After incubation for 10 min at room temperature, 500 μl of 3 mM $ZnCl_2$ was added to stop the enzyme reaction. After centrifugation, the OD_{578} of supernatants were measured with a spectrophotometer. β-Gal units were calculated as 1,000 × OD_{578} / (10 min × 0.1 ml × OD_{600}).

Ligand assay. Harvested cells were inoculated into 5 mL of fresh SD media containing ligand to give an initial OD_{600} of 0.03. They were incubated at 30ºC with shaking at 150 rpm for up to 18 h. Afterwards, the β-D-galactosidase activity was performed.

Model screening. A small-sized prey GPCR library (**Table 4**) was transformed into yeast strain NMY63 harboring pBT3-AGTR1 by using the lithium acetate method (Gietz et al., 1992). Transformants were selected on SD medium lacking leucine, tryptophan, adenine and histidine for bait-prey interaction. Prey plasmids were isolated from 30 positive clones, amplified in *Escherichia coli*, and analyzed by sequencing analysis.

Table 4. List of prey GPCR library.

Prey plasmid name
pPR3-AGTR1
pPR3-ADRB2
pPR3-HTR1A
pPR3-SSTR2
pPR3-SSTR5
pPR3-EDNRB
pPR3-NTSR1
pPR3-NTSR2
pPR3-C(Control)

Results and Discussion

While the original split-ubiquitin system enables comprehensive screening of protein-protein interactions (Stagljar et al., 1998), it is intrinsically possible that the addition of ligand triggers activation of pheromone signaling via endogenous yeast heterotrimeric G-protein (Ishii et al., 2010). The activation of pheromone signaling in yeast induces cell cycle arrest in G1 phase and triggers global changes in transcription of mating-related genes (Elion et al., 1993). The ligand-induced G1 arrest that is exposed as robust growth inhibition in yeast cells (Ishii et al., 2008) might lead to an inadequate assessment of reporter gene activity. Therefore, we constructed a yeast deletion mutant lacking the *STE20* or *STE11* gene involved in the activation of the MAPK cascade by using NMY51 as the parental strain with an aim to enable screening of GPCR dimers with and without ligand (**Figure 1** and **Table 1**). Halo bioassays responding to α-factor pheromone showed the formations of a thin halo and no halos with 100 μg of α-factor in NMY61 (*ste20*Δ) and NMY62 (*ste11*Δ) yeast strains, respectively, revealing that *ste11*Δ allele provides more strict avoidance of signal-promoted growth arrest in the presence of ligand (**Figure 2A**). For checking the expressions of reporter genes, the growth assays in the presence of ligand were carried out (**Figure 2B**). While the strains harboring mock vectors pBT3-C and pPR3-C were used as negative controls, those harboring pCCW-Alg5 and pAI-Alg5 to express Alg5-Nub*I* and Alg5-Cub-LexA-VP16 were used as positive controls. Alg5-Nub*I* is a yeast membrane protein fused with a WT Nub tag. The Nub*I* tag interacts spontaneously with any Cub tag-containing constructs (Iyer et al., 2005; Kittanakom et al., 2009). The deletion mutants (*ste20*Δ and *ste11*Δ) avoided the robust growth inhibition and therefore could allow the growth assays with *ADE2* and *HIS3* reporter genes even in the presence

of ligand (**Figure 2B**). We used the MAPK-defective NMY62 yeast strain for the following experiments.

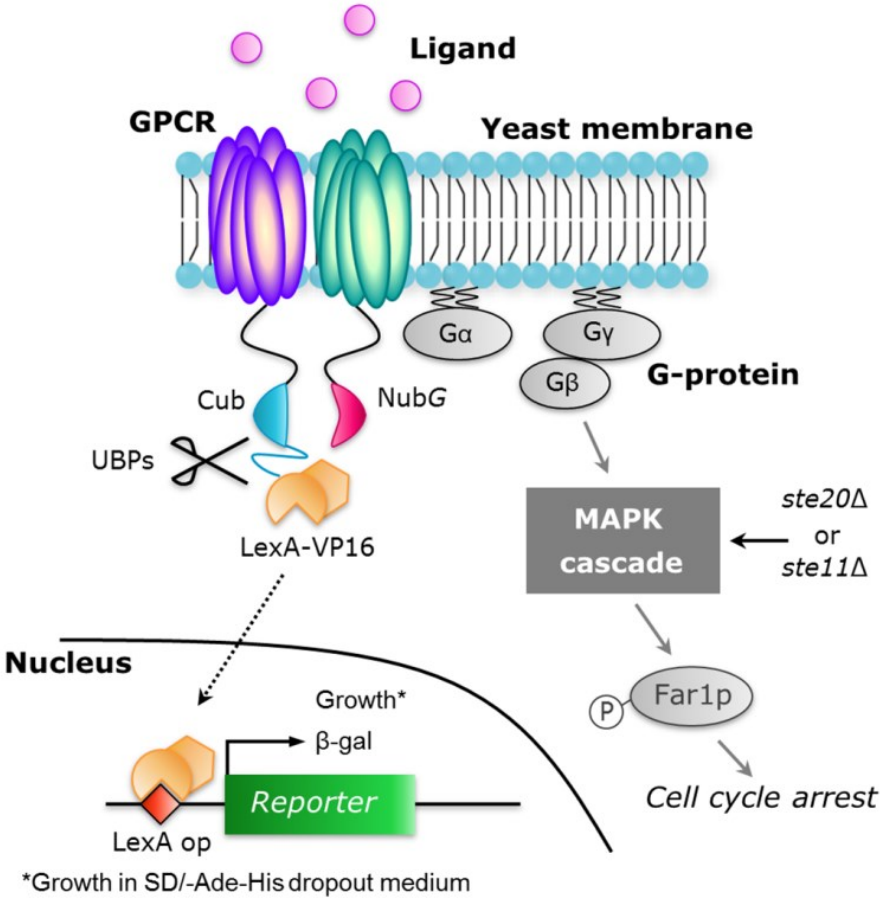

Fig. 1. Schematic illustration of yeast pheromone signaling pathway and principle for GPCR dimerization assay based on split-ubiquitin system in yeast. Agonistic ligand binding to the GPCR leads to the activation of heterotrimeric G-proteins, the mitogen-activated protein kinase (MAPK) cascade and a cyclin-dependent kinase inhibitor Far1p. Phosphorylated Far1p induces G1 cell-cycle arrest. The *STE20* or *STE11* gene located upstream of the MAPK cascade was disrupted in the NMY51 strain. In the split-ubiquitin yeast two-hybrid system, Nub*G* will only efficiently interact with Cub when the proteins to which the two split tags are attached interact with each other, resulting in the formation of a Nub*G*/Cub complex. This complex is recognized by ubiquitin-specific proteases (UBPs), which release the artificial transcription factor (LexA-VP16) from the Cub-containing construct. LexA-VP16 then enters the nucleus via diffusion and binds to the LexA-binding sites upstream of the reporter genes. In this study, the GPCRs are fused to the split-ubiquitin and are expressed in MAPK-defective mutant yeast strain of NMY51 to allow the monitoring of GPCR dimerizations and conformational changes responding to binding of ligand.

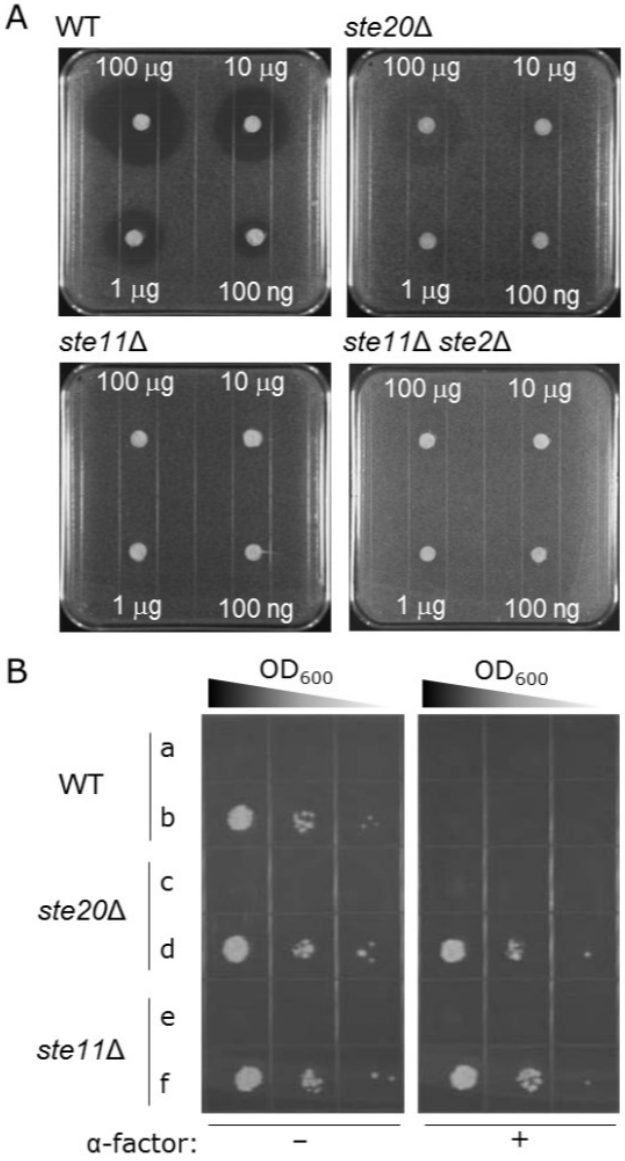
A
WT
100 μg
10 μg
1 μg
100 ng
ste20Δ
100 μg
10 μg
1 μg
100 ng
ste11Δ
100 μg
10 μg
1 μg
100 ng
ste11Δ ste2Δ
100 μg
10 μg
1 μg
100 ng
B
OD600
OD600
WT
a
b
ste20Δ
c
d
ste11Δ
e
f
α-factor:
–
+

Fig. 2. *ste11*Δ allele allowed more strict avoidance of signal-promoted growth arrest in the presence of ligand. (A) Halo-bioassay (agonist-induced growth arrest assay) for *STE20*-, *STE11*- and *STE2*-gene-disrupted strains: NMY51 (WT); NMY61 (*ste20*Δ); NMY62 (*ste11*Δ); and NMY63 (*ste11*Δ *ste2*Δ). Each paper filter disk was spotted with the indicated amount of α-factor. (B) Growth assay of NMY51 (WT; **a,b**), NMY61 (*ste20*Δ; **c,d**) and NMY62 (*ste11*Δ; **e,f**) strains on SD –Leu, Trp, Ade and His dropout plates. Yeast strains harboring pBT3-C/pPR3-C or pCCW-Alg5/pAI-Alg5 respectively expressed Cub/Nub*G* (negative control; **a,c,e**) or Alg5-Cub/Alg5-Nub*I* (positive control; **b,d,f**). Each cell was spotted in serial 10-fold dilutions on selective agar plates with or without 5 μM of α-factor. Nub*I* is a WT Nub tag and interacts spontaneously with Cub.

To test the viability of split-ubiquitin–based reporter gene assays for detecting GPCR dimers, we first analyzed the homodimerization of endogenous yeast pheromone receptor (Ste2p) in the NMY62 yeast strain. The N-terminal moiety of split-ubiquitin with an I13G mutation (Nub*G*) and the C-terminal ubiquitin moiety linked to an artificial transcription factor (Cub-LexA-VP16) (Stagljar et al., 1998) were respectively designed to genetically fuse to the C-termini of Ste2p receptors by using original pPR3-C (prey) and pBT3-C (bait) split-ubiquitin vectors (**Table 3**). Upon *in vivo* protein-protein interaction, the reconstituted ubiquitin leads to cleavage and release of LexA-VP16 by ubiquitin-specific proteases (UBPs) (Stagljar et al., 1998); therefore, the dimerization of Ste2p should be detected via the transcription activation of the reporter genes (*ADE2*, *HIS3*, and *lacZ*) (**Figure 1** and **Table 1**). However, the cells coexpressing Ste2p-Nub*G* and Ste2p-Cub-LexA-VP16 never grew on the adenine/histidine-deficient selectable media (**Figure 3A**). Therefore, we replaced the weak *CYC1* promoter of the original pBT3-C bait vector by comparatively strong *PHO5*, *TPI1* and *TDH3* promoters ($P_{CYC1} < P_{PHO5} < P_{TPI1} < P_{TDH3}$). As a result, the expression of Ste2p-Cub-LexA-VP16 by the *TPI1* and *TDH3* promoters prompted cell growth on the selection media when combined with the expression of Ste2p-Nub*G* (**Figure 3B** and **C**). Even though previous report expressed the Ste2p in relatively low expression manner (Gehret et al., 2006), our result did not show evidence of dimerization for the Ste2p expressed under the control of the *CYC1* promoter in the split-ubiquitin system. This is assumed that attached transcription factor might be not present at levels adequate to activate the response.

Then, we replaced the full-length Ste2p receptors with a truncated version that lacks the C-terminal tails (Ste2ΔC; amino acids 1–304) to adjust the distance between

the C-termini of the receptors (Gehret et al., 2006), providing an increased signal-to-noise (S/N) ratio (under the control of the *TPI1* promoter; **Figure 4A** and **B**). Furthermore, we replaced the *TPI1* promoter with the *CYC1* promoter of the bait vector again, which resulted in much lower background cell growth and a drastically improved S/N ratio (**Figure 5A** and **B**). Since the truncation of the C-termini of Ste2p receptors had been reported to increase in the number of receptor sites (Konopka et al., 1988), the greatly enriched receptors at the plasma membrane might have provided the drastic improvement of S/N ratio. These results indicate that the bait receptor is predominant for successful detection of the dimerized receptors. Thus, the consideration of the receptor's expression manner is important to screen the GPCR dimer partners, because the leaky background cell growth often brings unanticipated candidates.

In the optimized system, Hxt1p never presented background cell growth in the dimerization assay with the Ste2ΔC receptor (**Figure 5A**). Previously, Overton et al. had used the Hxt1p as the negative control for FRET analysis of Ste2p dimerization and confirmed the subcellular localization of it at the plasma membrane (Overton and Blumer, 2000). The β-galactosidase assay that reflects *lacZ* reporter enzyme activity also displayed similar trends (**Figure 5B**). The addition of ligand had no effect on the dimerization events of Ste2ΔC, since the MAPK-defective NMY62 yeast strain displayed unchanged growth in the presence of α-factor (**Figure 5A**). We additionally constructed two types of deletion mutants in which the TM6–7 domains and the TM1–5 domains were removed, respectively (TM1–5 (amino acids 1–236) and TM6–7 (amino acids 237–304)) (**Figure 6A**). Overton et al. also indicated that self-association of TM6–7 had not been detected, and plasma membrane localization of the YFP-tagged TM1–5 and TM6–7 was observed (Overton and Blumer, 2002). As previously indicated

(Overton and Blumer, 2002), only TM1–5 formed the homodimer (**Figure 6B** and **C**), showing that our system is applicable to examine critical domains involved in the dimerization of 7TM receptors.

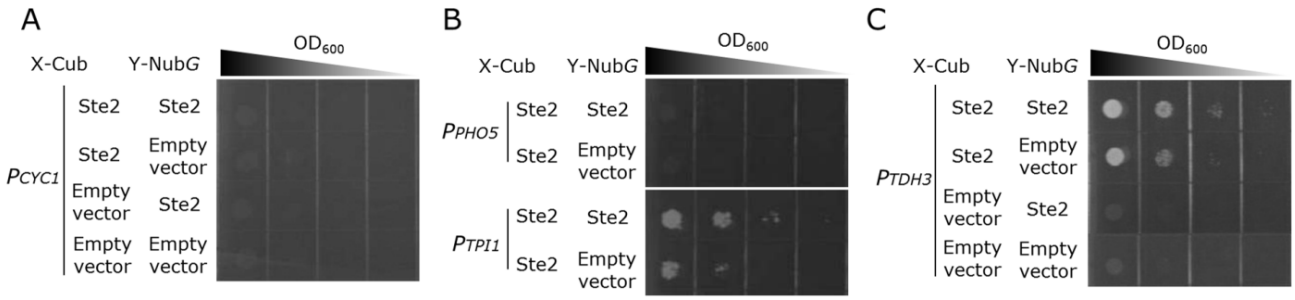

Fig. 3. Effect of promoter on detection of dimerization of yeast Ste2p receptor in NMY62 strain. NMY62 yeast strain was transformed with the plasmids expressing indicated protein pairs and grown on SD –Leu, Trp, Ade and His dropout plate at 30ºC. (A) *CYC1* promoter. (B) *PHO5* promoter and *TPI1* promoter. (C) *TDH3* promoter.

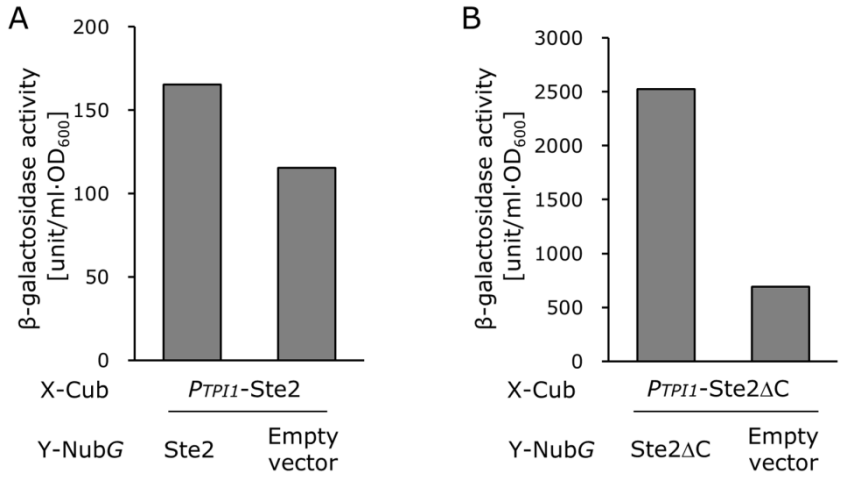

Fig. 4. Effect of removal of C-terminal tail on detection of dimerization of yeast Ste2p receptor in NMY62 strain. NMY62 yeast strain was transformed with plasmids expressing indicated protein pairs. Quantitative β-galactosidase assays for full-length Ste2p receptor under the control of *TPI1* promoter (A) and Ste2p receptor that lacks the C-terminal tail (Ste2ΔC) under the control of *TPI1* promoter (B).

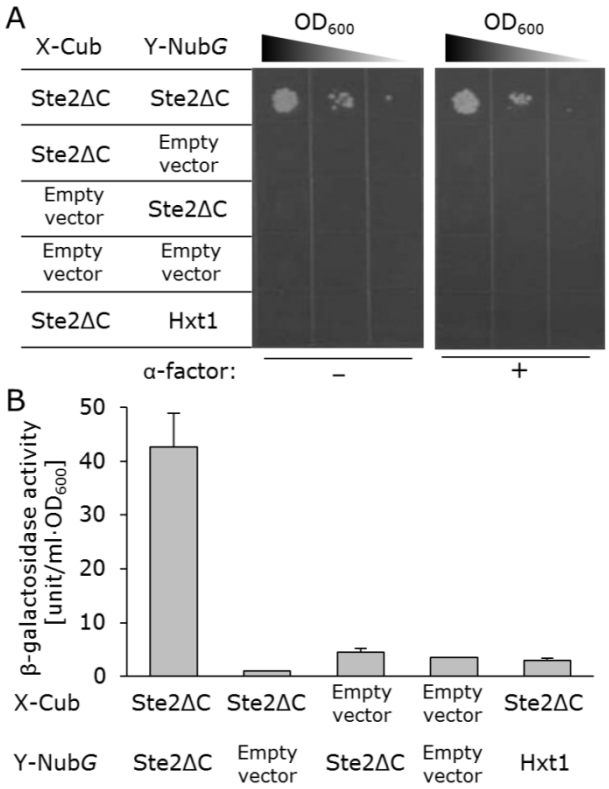

Fig. 5. Detection for dimerization of yeast truncated Ste2p lacking the carboxy-terminal tail (Ste2ΔC) receptor in NMY62 strain. Growth and quantitative β-galactosidase activity of yeast cells expressing various combinations of Cub and Nub*G* fusions. The control bait plasmid was pBT3-C mock vector (empty vector). The control prey plasmids were pPR3-C mock vector (empty vector) and pPR3-HXT1. (A) Growth assay without α-factor (*left panels*) and with 5 μM α-factor (*right panels*). Each cell was spotted in serial 10-fold dilutions on SD –Leu, Trp, Ade and His dropout plate. (B) Quantitative β-galactosidase assay. Error bars represent the standard deviations (n = 3).

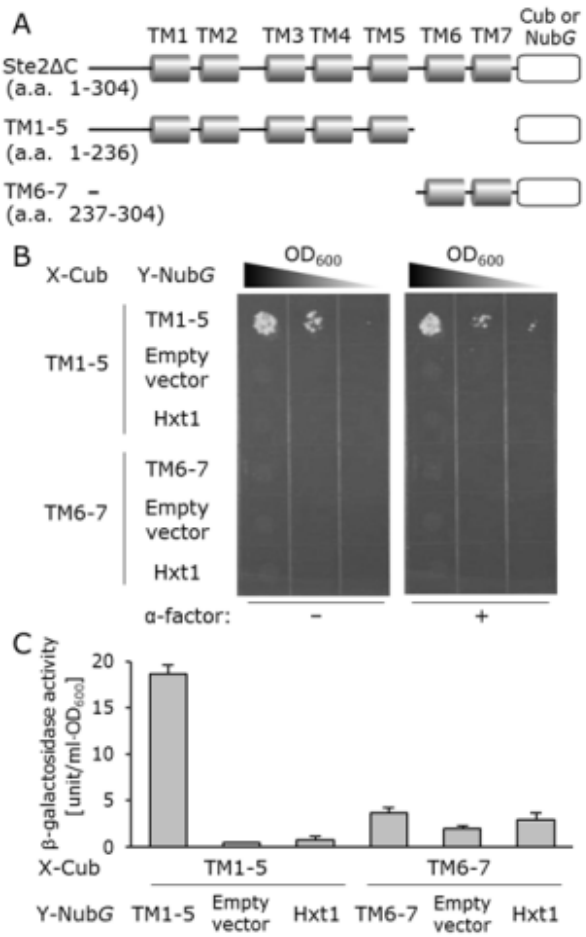

Fig. 6. Detection for dimerization of yeast Ste2p deletion mutants (TM1–5 and TM6–7) in NMY62 strain. (A) Schematic of Ste2ΔC and the deletion mutants. Transmembrane (TM) domains are indicated with pillar-type boxes, and the Cub (Cub-LexA-VP16) or Nub*G* (Nub with I13G mutation) is depicted as a rounded rectangle. (B) Growth assay without α-factor (*left panels*) and with 5 μM α-factor (*right panels*). Each cell was spotted in serial 10-fold dilutions on SD –Leu, Trp, Ade and His dropout plate. (C) Quantitative β-galactosidase activity in yeast cells containing various combinations of plasmids. Error bars represent the standard deviations (n = 3). The control prey plasmids were pPR3-C mock vector (empty vector) and pPR3-HXT1.

Subsequently, we validated the capability of our system to detect human GPCR heterodimer pairs. To avoid competitive dimerization with the endogenous yeast Ste2p receptor, we constructed an NMY63 mutant strain in which the *STE2* gene was additionally deleted (**Table 1** and **Figure 7**). Since clear evidence for the functional role of GPCR homodimer and heterodimer pairs was first obtained for class C receptors, such as $GABA_B$ receptors (Kaupmann et al., 1998), we tested the dimerization of $GABA_{B2}$ receptor (GABBR2) with $GABA_{B1a}$ receptor (GABBR1a). The β-galactosidase assay clearly showed the specific activities both for $GABA_{B2}$/$GABA_{B2}$ and $GABA_{B2}$/$GABA_{B1a}$ couples (**Figure 8A** and **9A**). This result was coincident with the fact that $GABA_{B2}$ receptor could form not only heterodimer with $GABA_{B1a}$ receptor but also homodimer (Maurel et al., 2004, 2008), indicating that the split-ubiquitin-based approach could detect the homodimerization and heterodimerization of $GABA_{B2}$ receptors. Additionally, the β-galactosidase assay for dimerization of $GABA_{B1a}$ receptor also showed similar results (**Figure 10**).

In contrast to the widely accepted concept of class C GPCR dimerization, the significance of *in vivo* dimerization of class A GPCRs remains controversial (Prezeau et al., 2010). Since a growing amount of evidence indicates that class A GPCRs are able to form dimers or higher-ordered oligomers *in vivo* (Albizu et al., 2010; Rivero-Müller et al., 2010), we next evaluated class A GPCR heterodimer pairs. As class A GPCRs, AT_1 and AT_2 angiotensin receptors (AGTR1 and AGTR2) were selected. Consistent with previous reports (Lyngsø et al., 2009; Porrello et al., 2011), the β-galactosidase assay also illustrated the formation of heterodimers between AGTR1 and AGTR2 (**Figure 8B** and **9B**).

Next, we aimed to apply our system to screen new candidate heterodimer partners

of AGTR1 receptor within the class A GPCRs, except for AGTR2. The *CYC1* promoter was selected for expressing AGTR1 as a bait protein (**Figure 9B**). As a model candidate library, we constructed the prey vectors to express AGTR1 (as a positive control), β_2-adrenergic receptor (ADRB2), 5-hydroxytryptamine (serotonin) receptor 1A (HTR1A), somatostatin receptor 2 (SSTR2), somatostatin receptor 5 (SSTR5), endothelin receptor type B (EDNRB), neurotensin receptor 1 (NTSR1) and neurotensin receptor 2 (NTSR2) (**Table 3** and **4**) and then mixed equal amounts of these 9 prey vectors (containing pPR3-C mock vector). After introduction of the constructed library into the NMY63 yeast strains harboring AGTR1 bait vector, the selection with *ADE2*/*HIS3* growth reporter genes was performed (**Figure 11A**). A total of 30 colonies was generated on the adenine/histidine-deficient selection media (**Figure 11A**). Following isolation of prey plasmids from each colony, the obtained GPCR clones were determined by sequencing analysis. Ten clones of AGTR1 were dominantly identified as the homodimer (33.3%), whereas 5 clones of SSTR2 (16.7%), 3 clones of ADRB2 (10.0%) and 3 clones of HTR1A (10.0%) were successfully screened as the candidate heterodimer partners for AGTR1.

To validate the success or failure of the screening, we measured the β-galactosidase activities of the yeast cells separately co-transformed with the AGTR1 bait vector and 9 other prey vectors including the previously reported AGTR1/ADRB2 heterodimer pairs (Barki-Harrington et al., 2003), yeast Ste2p control receptor and mock control. The results likely reflected the occupancies of identified clones, indicating that our system succeeded in screening heterodimer candidates (**Figure 11B**). Additionally, β-galactosidase activities measured with other GPCRs as bait proteins were fairly consistent with the results of the screening and also revealed new candidates

for heterodimer pairs including SSTR2/HTR1A, SSTR2/ADRB2, and HTR1A/EDNRB (**Figure 12A–C** and **9C–E**). Our experiments indicated that Ste2p could not co-oligomerize with the human GPCRs (**Figure 11B** and **12A–C**).

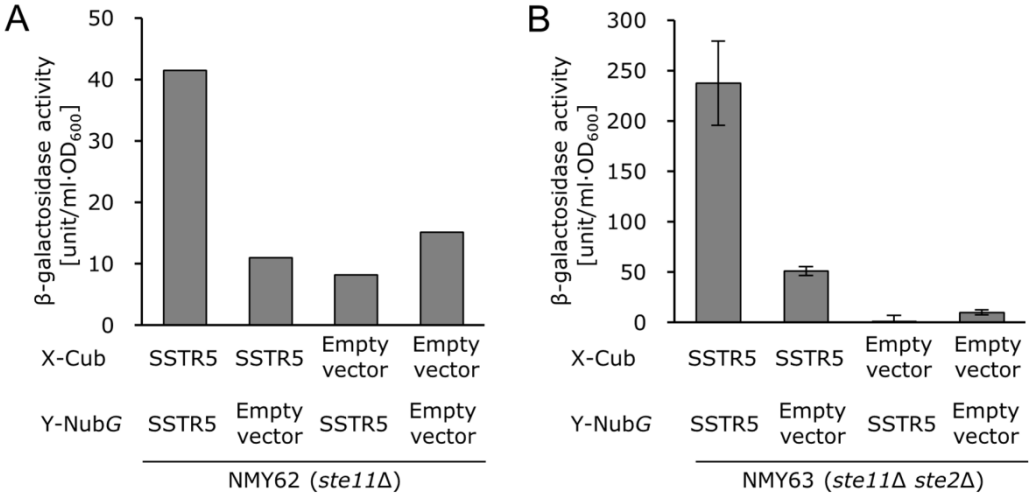

Fig. 7. Detection of homodimerization of human SSTR5 receptor in NMY62 or NMY63 strains. NMY63 yeast strain was transformed with plasmids expressing indicated protein pairs. Quantitative β-galactosidase assays for the NMY62 strain (A) and NMY63 strain (B).

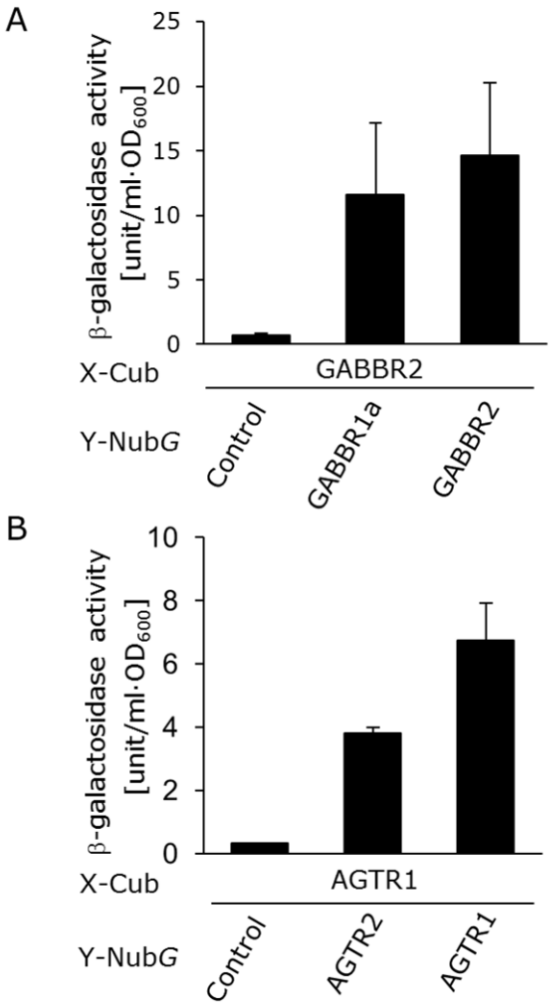

Fig. 8. Dimerization assays of human GPCRs. Quantitative β-galactosidase assay. (A) Detection of $GABA_{B1a}$/$GABA_{B2}$ (GABBR1a/GABBR2) heterodimers. (B) Detection of AT_1/AT_2 (AGTR1/AGTR2) heterodimers. Error bars represent the standard deviations (n = 3). The control prey plasmid was pPR3-C mock vector.

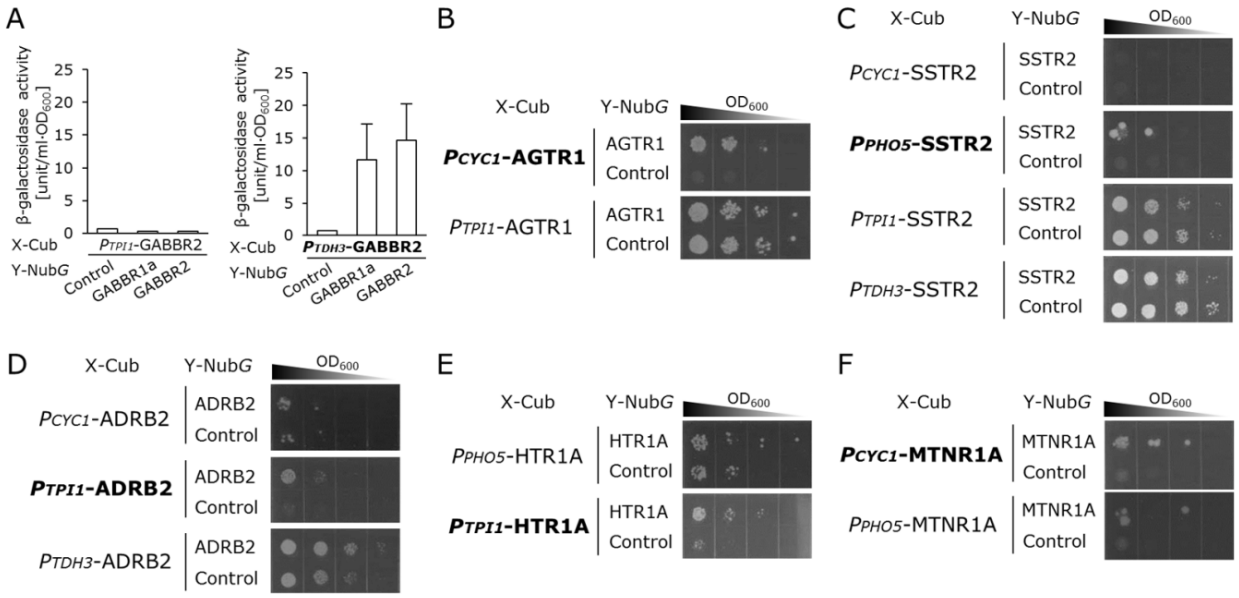

Fig. 9. Optimization of promoter to detect homodimerization of human GPCRs in NMY63 strain. NMY63 yeast strain was transformed with plasmids expressing the indicated protein pairs. (A) Quantitative β-galactosidase assays. (B–F) Growth assays on SD –Leu, Trp, Ade and His dropout plate at 30ºC. (A) $GABA_{B2}$ receptor (GABBR2) (B) AT_1 angiotensin receptor (AGTR1) (C) MT_1 melatonin receptor (MTNR1A) (D) somatostatin receptor 2 (SSTR2) (E) β_2-adrenergic receptor (ADRB2) (F) 5-hydroxytryptamine (serotonin) receptor 1A (HTR1A). The control prey plasmid was pPR3-C mock vector.

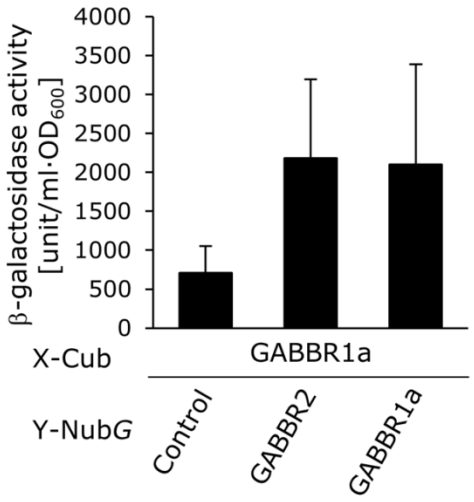

Fig. 10. Detection of homo- and hetero-dimerization of human $GABA_{B1a}$ receptor with $GABA_{B2}$ receptor in NMY63 strain. Quantitative β-galactosidase assay. NMY63 yeast strain was transformed with plasmids expressing indicated protein pairs. Error bars represent the standard deviations (n = 3). The control prey plasmid was pPR3-C mock vector.

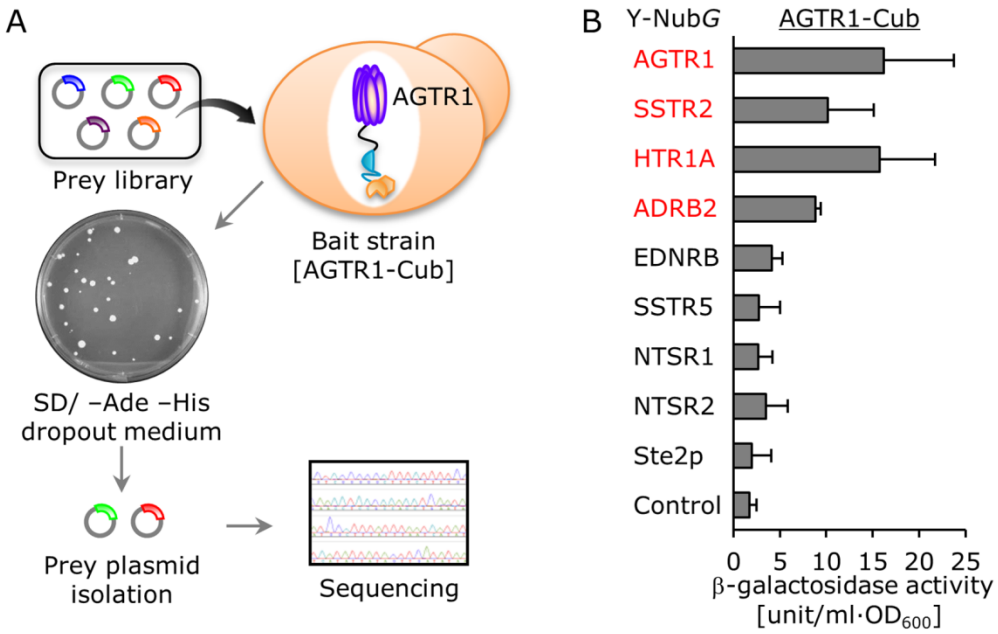

Fig. 11. Screening of candidate heterodimer partners of AT_1 angiotensin receptor (AGTR1). (A) Workflow of a yeast two-hybrid screen. Prey library was transformed into the NMY63 yeast strains harboring AGTR1 bait vector, and the selection with growth reporter genes was performed. Following isolation of prey plasmids from each colony, the obtained GPCR clones were determined by sequencing analysis. (B) Quantitative β-galactosidase assays for homo- and hetero-dimerization of AGTR1 in NMY63 strain. NMY63 yeast strain was transformed with GPCR-Nub*G* indicated at the left and AGTR1-Cub-LexA-VP16. The control prey plasmid was pPR3-C mock vector. Error bars represent the standard deviations (n = 3).

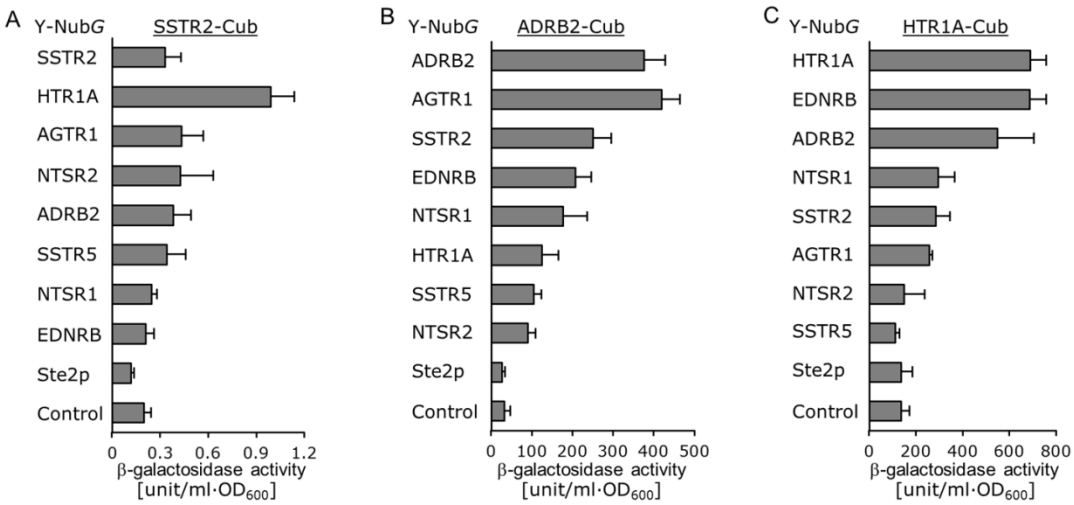

Fig. 12. Quantitative β-galactosidase assays for homo- and hetero-dimerization between human-GPCRs in NMY63 strain. NMY63 yeast strain was transformed with GPCR-Nub*G* indicated at the left and SSTR2-Cub-LexA-VP16 (A), ADRB2-Cub-LexA-VP16 (B), or HTR1A-Cub-LexA-VP16 (C). The control prey plasmid was pPR3-C mock vector. Error bars represent the standard deviations (n = 3).

Additionally, we measured the β-galactosidase activities of the yeast cells separately co-transformed with the AGTR1 bait vector and GABBR1a, GABBR2, MT_1 and MT_2 melatonin receptor (MTNR1A and MTNR1B) prey vectors. The results indicated new candidates for heterodimer pairs including AGTR1/GABBR1a and AGTR1/MTNR1B (**Figure 13A**). Thus, the obtained results from all heterodimerization assays with the split-ubiquitin system might have implicated a general statement about the ability of various human GPCRs to heterooligomerize with each other.

Finally, we performed detection of not only the dimer formation of target human GPCRs but also the ligand-mediated conformational changes in living yeast cells. In the case of AGTR1 the addition of 10 μM of native ligand, angiotensin II, did not affect the states of the homodimerized and heterodimerized receptors with AGTR2 (**Figure 13B**). MT_1 and MT_2 melatonin receptors (MTNR1A and MTNR1B) not only form heterodimers, but also induce a conformational change within the heterodimers (Ayoub et al., 2004). In addition, it has been reported that expressions of MTNR1A and MTNR1B in yeast activated the pheromone signaling pathway via the endogenous yeast G-proteins in response to the native ligand melatonin (Brown et al., 2000; Kokkola et al., 1998). β-galactosidase assays based on the split-ubiquitin technique in the MAPK-defective NMY63 yeast strain allowed successful detection of the conformational change of MTNR1A/MTNR1B heterodimers in the presence of melatonin (**Figure 13C** and **9F**), suggesting that our system can detect ligand-mediated conformational changes as well as the heterodimer formations. Moreover, we also tested the detection of the conformational change of $GABA_{B2}$/$GABA_{B1a}$ heterodimers in the presence of GABA (**Figure 13D**). While the addition of 100 μM of GABA did not affect the states of the $GABA_{B2}$ homodimers, the β-galactosidase assay exposed the

conformational change of $GABA_{B2}$/$GABA_{B1a}$ heterodimers in consistency with previous reports (Matsushita et al., 2010) (**Figure 13D**).

Because a positive result in the assay potentially could come about through indirect association of receptors via a third protein or close co-localization, it is important to re-evaluate the irrefragability with other methods or in human cells. Additionally, there is no guarantee that association is actually physiologically relevant. However, it is also true that this system could narrow down the new candidates of GPCR heterodimers with a bit of effort. If one accepts these uncertainties, the assay provides a nice way of monitoring changes that does not depend on effective downstream signaling through the GPCR pathway.

In summary, we have developed a specialized method to screen candidate heterodimer partners for target GPCRs based on the split-ubiquitin membrane yeast two-hybrid method. This modified system permitted the rapid and facile detection of not only the heterodimer formation of target human GPCRs, but also the ligand-mediated conformational changes in living yeast cells. Since budding yeast *Saccharomyces cerevisiae* can functionally express human GPCRs (Ishii et al., 2012; Li et al., 2007), construction of a large prey library would be beneficial for the identification of heterodimer candidates as the partners of target human GPCRs. Our system will be a useful tool to assist in the intermolecular mapping of interactions among GPCRs and uncover potential targets for the development of new therapeutic agents.

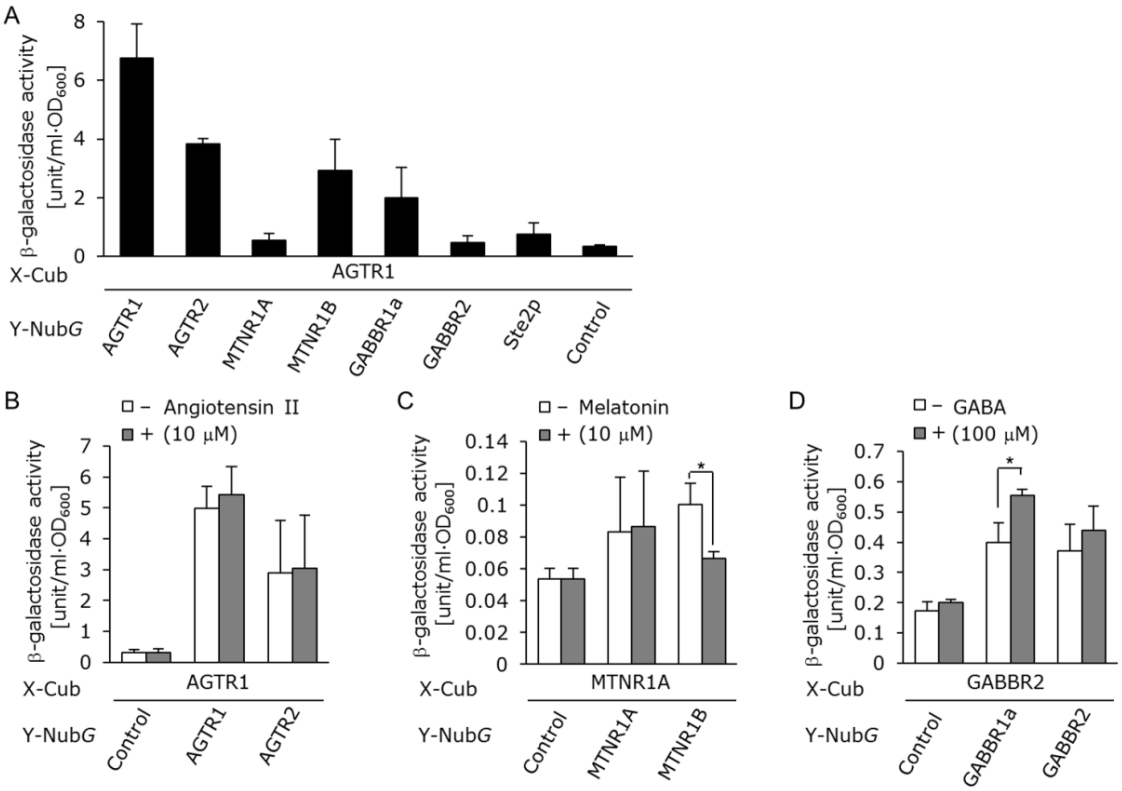

Fig. 13. Detection for dimerization and ligand-induced conformational changes of human GPCRs. (A) Quantitative β-galactosidase assays for heterodimerization of AGTR1 in NMY63 strain. NMY63 yeast strain was transformed with GPCR-Nub*G* indicated at the bottom and AGTR1-Cub-LexA-VP16. (B–D) Ligand assays for detection of conformational changes in GPCR dimerizations. (B) AT_1/AT_2 (AGTR1/AGTR2) heterodimers. Incubation time, 18 h. Angiotensin II conc., 0 or 10 μM. (C) MT_1/MT_2 (MTNR1A/MTNR1B) heterodimers. Incubation time, 18 h. Melatonin conc., 0 or 10 μM. (D) $GABA_{B1a}/GABA_{B2}$ (GABBR1a/GABBR2) heterodimers. Incubation time, 18 h. GABA conc., 0 or 100 μM. The control prey plasmid was pPR3-C mock vector. Error bars represent the standard deviations ($n = 3$). (*$P < 0.05$).

References

Akada R, Kitagawa T, Kaneko S, Toyonaga D, Ito S, et al. (2006) PCR-mediated seamless gene deletion and marker recycling in Saccharomyces cerevisiae. Yeast 23: 399–405.

Albizu L, Cottet M, Kralikova M, Stoev S, Seyer R, et al. (2010) Time-resolved FRET between GPCR ligands reveals oligomers in native tissues. Nat Chem Biol 6: 587–594.

Ayoub MA, Levoye A, Delagrange P, Jockers R (2004) Preferential formation of MT1/MT2 melatonin receptor heterodimers with distinct ligand interaction properties compared with MT2 homodimers. Mol Pharmacol 66: 312–321.

Barki-Harrington L, Luttrell LM, Rockman HA (2003) Dual inhibition of beta-adrenergic and angiotensin II receptors by a single antagonist: a functional role for receptor-receptor interaction in vivo. Circulation 108: 1611–1608.

Brown AJ, Dyos SL, Whiteway MS, White JH, Watson MA, et al. (2000) Functional coupling of mammalian receptors to the yeast mating pathway using novel yeast/mammalian G protein α-subunit chimeras. Yeast 16: 11–22.

Elion EA, Satterberg B, Kranz JE (1993) FUS3 phosphorylates multiple components of the mating signal transduction cascade: evidence for STE12 and FAR1. Mol Biol Cell 4: 495–510.

Fredriksson R, Lagerström MC, Lundin LG, Schiöth HB (2003) The G-protein-coupled receptors in the human genome form five main families. Phylogenetic analysis, paralogon groups, and fingerprints. Mol Pharmacol 63: 1256–1272.

Gehret AU, Bajaj A, Naider F, Dumont ME (2006) Oligomerization of the yeast alpha-factor receptor: implications for dominant negative effects of mutant

receptors. J Biol Chem 281: 20698–20714.

George SR, O'Dowd BF, Lee SP (2002) G-protein-coupled receptor oligomerization and its potential for drug discovery. Nat Rev Drug Discov 1: 808–820.

Gietz D, St Jean A, Woods RA, Schiestl RH (1992) Improved method for high efficiency transformation of intact yeast cells. Nucleic Acids Res 20: 1425.

Iguchi Y, Ishii J, Nakayama H, Ishikura A, Izawa K, et al. (2010) Control of signalling properties of human somatostatin receptor subtype-5 by additional signal sequences on its amino-terminus in yeast. J Biochem 147: 875–884.

Ishii J, Matsumura S, Kimura S, Tatematsu K, Kuroda S, et al. (2006) Quantitative and dynamic analyses of G protein-coupled receptor signaling in yeast using Fus1, enhanced green fluorescence protein (EGFP), and His3 fusion protein. Biotechnol Prog 22: 954–960.

Ishii J, Tanaka T, Matsumura S, Tatematsu K, Kuroda S, et al. (2008) Yeast-based fluorescence reporter assay of G protein-coupled receptor signalling for flow cytometric screening: FAR1-disruption recovers loss of episomal plasmid caused by signalling in yeast. J Biochem 143: 667–674.

Ishii J, Izawa K, Matsumura S, Wakamura K, Tanino T, et al. (2009) A simple and immediate method for simultaneously evaluating expression level and plasmid maintenance in yeast. J Biochem 145: 701–708.

Ishii J, Fukuda N, Tanaka T, Ogino C, Kondo A (2010) Protein–protein interactions and selection: yeast-based approaches that exploit guanine nucleotide-binding protein signaling. FEBS J 277: 1982–1995.

Ishii J, Yoshimoto N, Tatematsu K, Kuroda S, Ogino C, et al. (2012) Cell wall trapping of autocrine peptides for human G-protein-coupled receptors on the yeast cell

surface. PLoS One 7: e37136.

Iyer K, Bürkle L, Auerbach D, Thaminy S, Dinkel M, et al. (2005) Utilizing the split-ubiquitin membrane yeast two-hybrid system to identify protein-protein interactions of integral membrane proteins. Sci STKE 2005: pl3.

Kaupmann K, Malitschek B, Schuler V, Heid J, Froestl W, et al. (1998) GABA(B)–receptor subtypes assemble into functional heteromeric complexes. Nature 396: 683–687.

Kittanakom S, Chuk M, Wong V, Snyder J, Edmonds D, et al. (2009) Analysis of membrane protein complexes using the split-ubiquitin membrane yeast two-hybrid (MYTH) system. Methods Mol Biol 548: 247–271.

Kokkola T, Watson MA, White J, Dowell S, Foord SM, et al. (1998) Mutagenesis of human Mel1a melatonin receptor expressed in yeast reveals domains important for receptor function. Biochem Biophys Res Commun 249: 531–536.

Konopka JB, Jenness DD, Hartwell LH (1988) The C-terminus of the S. cerevisiae alpha-pheromone receptor mediates an adaptive response to pheromone. Cell 54: 609–620.

Li B, Scarselli M, Knudsen CD, Kim SK, Jacobson KA, et al. (2007) Rapid identification of functionally critical amino acids in a G protein-coupled receptor. Nat Methods 4: 169–174.

Lyngsø C, Erikstrup N, Hansen JN (2009) Functional interactions between 7TM receptors in the renin-angiotensin system--dimerization or crosstalk? Mol Cell Endocrinol 302: 203–212.

Matsushita S, Nakata H, Kubo Y, Tateyama M (2010) Ligand-induced rearrangements of the GABA(B) receptor revealed by fluorescence resonance energy transfer. J

Biol Chem 285: 10291–10299.

Maurel D, Kniazeff J, Mathis G, Trinquet E, Pin JP, et al. (2004) Cell surface detection of membrane protein interaction with homogeneous time-resolved fluorescence resonance energy transfer technology. Anal Biochem 329: 253–262.

Maurel D, Comps-Agrar L, Brock C, Rives ML, Bourrier E, et al. (2008) Cell-surface protein-protein interaction analysis with time-resolved FRET and snap-tag technologies: application to GPCR oligomerization. Nat Methods 5: 561–567.

Overton MC, Blumer KJ (2000) G-protein-coupled receptors function as oligomers in vivo. Curr Biol 10: 341–344.

Overton MC, Blumer KJ (2002) The extracellular N-terminal domain and transmembrane domains 1 and 2 mediate oligomerization of a yeast G protein–coupled receptor. J Biol Chem 277: 41463–41472.

Panetta R, Greenwood MT (2008) Physiological relevance of GPCR oligomerization and its impact on drug discovery. Drug Discov Today 13: 1059–1066.

Percherancier Y, Berchiche YA, Slight I, Volkmer-Engert R, Tamamura H, et al. (2005) Bioluminescence resonance energy transfer reveals ligand-induced conformational changes in CXCR4 homo- and heterodimers. J Biol Chem 280: 9895–9903.

Pfleger KD, Eidne KA (2005) Monitoring the formation of dynamic G-protein-coupled receptor-protein complexes in living cells. Biochem J 385: 625–637.

Porrello ER, Pfleger KD, Seeber RM, Qian H, Oro C, et al. (2011) Heteromerization of angiotensin receptors changes trafficking and arrestin recruitment profiles. Cell Signal 23: 1767–1776.

Prezeau L, Rives ML, Comps–Agrar L, Maurel D, Kniazeff J, et al. (2010) Functional crosstalk between GPCRs: with or without oligomerization. Curr Opin Pharmacol

10: 6–13.

Rivero-Müller A, Chou YY, Ji I, Lajic S, Hanyaloglu AC, et al. (2010) Rescue of defective G protein-coupled receptor function in vivo by intermolecular cooperation. Proc Natl Acad Sci USA 107: 2319–2324.

Stagljar I, Korostensky C, Johnsson N, te Heesen S (1998) A genetic system based on split-ubiquitin for the analysis of interactions between membrane proteins in vivo. Proc Natl Acad Sci USA 95: 5187–5192.

Togawa S, Ishii J, Ishikura A, Tanaka T, Ogino C, et al. (2010) Importance of asparagine residues at positions 13 and 26 on the amino-terminal domain of human somatostatin receptor subtype-5 in signalling. J Biochem 147: 867–873.

Chapter 2: Simultaneous method for analyzing dimerization and signaling of G-protein-coupled receptor in yeast by dual-color reporter system

Introduction

Seven-transmembrane G-protein-coupled receptors (GPCRs) represent the largest and the most ubiquitous of protein families, regulating a number of signaling events within the membrane receptors (Fredriksson et al., 2003; Rasmussen et al., 2007). In response to a remarkable range of stimuli, such as neurotransmitters, hormones, ions, and sensory substances, these receptors regulate the metabolism, secretory properties, electrical activity, shape, and motility of virtually all mammalian cells (Lefkowitz and Shenoy, 2005). Their key roles in cell signaling have made GPCRs frequent pharmaceutical and therapeutic targets for drug discovery (Gudermann et al., 1995).

It is now clear that GPCRs interact with a range of proteins, including other GPCRs (Bockaert et al., 2010; Ferré and Franco, 2010; Ritter and Hall, 2009). Identifying and elucidating the function of such interactions will significantly enhance our understanding of cellular function, with the promise of new and improved pharmaceuticals. Evidence suggests that oligomerization (dimerization, including homo-dimerization and hetero-dimerization) of GPCRs is important for their trafficking to and from the plasma membrane (Benkirane et al., 1997; Grosse et al., 1997; Jordan et al., 2001; Margeta-Mitrovic et al., 2000), for agonist binding activity (Jordan and Devi, 1999; Mijares et al., 2000; Potter et al., 1991), for signal transduction (AbdAlla et al., 2000; Hebert et al., 1996), and for down-regulation of receptor expression (Cvejic and Devi, 1997; Yesilaltay and Jenness, 2000).

Currently, the ascendancy of GPCRs as molecular targets has gradually decreased among newly developed Food and Drug Administration (FDA)-approved drugs (Drews, 2000; Overington et al., 2006), in part because conventional screening trials have been exhausted. Therefore, new screening trials, such as heterodimer-targeted ligand screening, are required for further drug discovery. Notably, dimerization can increase the diversity of the regulation and modulation of GPCR signaling, and thus the specific evaluation of signaling properties among variously dimerized receptors will have important implications not only for the development of new drugs but also for the understanding of signaling networks (Jordan and Devi, 1999).

The budding yeast *Saccharomyces cerevisiae* is an attractive host cell system for the study of GPCR signaling, because this fungus can simplify analyses of complicated mammalian GPCR signaling systems. Haploid yeast cells encode a single endogenous GPCR (Ste2p) and harbor a monopolistic G-protein (pheromone) signaling pathway; thus, the use of yeast as a host precludes the signaling cross-talk and unexpected activation of intrinsic GPCRs or G-proteins that is observed when using mammalian host cells (Dowell and Brown, 2002; Fukutani et al., 2012; Iguchi et al., 2010; Stewart et al., 2009; Togawa et al., 2010). Therefore, heterologous expression in yeast often has been used for analysis of ligand-mediated signaling properties, mutational analysis of critical amino acid residues, and identification of agonistic ligands for human and other mammalian GPCRs (Ishii et al., 2010). In previous work, we reported the use of a split-ubiquitin yeast two-hybrid method (a genetic screening approach that detects protein-protein interactions) to identify hetero-dimerization by human GPCRs (Nakamura et al., 2013).

In the present work, we describe a unique system to simultaneously detect

dimerization and signaling of GPCRs, using a combination of the split-ubiquitin yeast two-hybrid assay and a G-protein signaling assay. To enable this strategy, we established a dual-color fluorescent reporter detection method using flow cytometry. As we report here, we used the yeast endogenous GPCR (Ste2p) and its natural ligand (α-factor) to demonstrate our concept. In addition, by using mutant Ste2p receptors and the human SSTR5 somatostatin receptor, we validated the applicability of our system for the simultaneous detection of dimerization and signaling by these receptors.

Materials and Methods

Media

Synthetic dextrose (SD) medium was formulated as 6.7 g/L yeast nitrogen base without amino acids (YNB) (BD-Diagnostic Systems, Sparks, MD, USA) and 20 g/L glucose. To generate SDM71 medium, SD medium was adjusted to pH 7.1 with 200 mM MOPSO buffer (Nacalai Tesque, Kyoto, Japan). YPD medium was formulated as 10 g/L yeast extract (Nacalai Tesque), 20 g/L peptone (BD-Diagnostic Systems), and 20 g/L glucose. As appropriate, SD medium was supplemented with amino acids or nucleotides (20 mg/L histidine, 60 mg/L leucine, 20 mg/L methionine, 20 mg/L uracil, or 40 mg/L tryptophan). For solid medium, agar was added at 20 g/L.

Construction of plasmids

All plasmids used in this study are summarized in **Table 1**. All oligonucleotides used for the plasmid constructions are listed in **Table 2**.

The plasmid used for expression of the far-red variant of tetrameric fluorescent protein DsRed-Express2 (E2-Crimson) was constructed as follows. A DNA fragment

encoding the *E2-Crimson* gene was PCR-amplified from pE2-Crimson (Takara Bio, Shiga, Japan) using the oligonucleotides o1 and o2, digested with *Nhe*I+*Eco*RI, and inserted into the same sites between the *PGK1* promoter (P_{PGK1}) and the *PGK1* terminator (T_{PGK1}) on pGK426 (Ishii et al., 2009), yielding the plasmid pGK426-E2-Crimson.

To integrate the artificial transcription factor (LexA-VP16)-responsive *E2-Crimson* reporter gene at the yeast *TRP1* chromosomal locus, a plasmid containing the following cassette was constructed. The cassette fused a chimeric *GAL1* promoter (including eight LexA operators) with the *E2-Crimson* gene, all flanked by *TRP1* homologous sequences. Upon transformation of yeast cells, the resulting cassette was expected to disrupt the *TRP1* gene. The resulting *trp1* auxotroph then could be used as a recipient for transformation (via selection for *TRP1* prototrophy) with the split-ubiquitin prey plasmids, which contained the *TRP1* selectable marker. A DNA fragment containing the fusion of eight LexA operators (390 bp) and the partial *GAL1* promoter was PCR-amplified from NMY51 (Dualsystems Biotech AG, Schlieren, Switzerland) genomic DNA using oligonucleotides o3 and o4. A fragment harboring the *E2-Crimson* gene was PCR-amplified from pE2-Crimson with oligonucleotides o5 and o6. The amplified fragments were digested with *Bam*HI+*Eco*RI and *Eco*RI+*Cla*I (respectively) and ligated together into *Bam*HI, *Cla*I-cleaved pBlueScript II KS(+) vector (Agilent Technologies, Santa Clara, CA, USA). The resultant plasmid was named pBlue-$(lexAop)_8$-E2-Crimson. A DNA fragment containing a sequence (300 bp) internal to the *TRP1* locus was PCR-amplified from BY4741 genomic DNA using oligonucleotides o7 and o8. A DNA fragment containing the *URA3* selectable marker (along with 40 nucleotides of the internal portion of *TRP1* at the downstream end) was

PCR-amplified from pRS426 (American Type Culture Collection, Manassas, VA) using oligonucleotides o9 and o10. The amplified fragments were digested with *Sac*II+*Xba*I and *Xba*I+*Bam*HI (respectively) and ligated together into *Sac*II, *Bam*HI-cleaved pBlue-(lexAop)$_8$-E2-Crimson. The resultant plasmid was named pBlue-URA3-(lexAop)$_8$-E2-Crimson. A DNA fragment containing the homologous sequence at the *TRP1* promoter (upstream of *TRP1* gene; 250 bp) was PCR-amplified from BY4741 genomic DNA using oligonucleotides o11 and o12. The amplified fragment was digested with *Cla*I+*Xho*I and ligated into pBlue-URA3-(lexAop)$_8$-E2-Crimson digested with the same enzymes. The resultant plasmid was named pBlue-URA3-(lexAop)$_8$-E2-Crimson-TRP1.

For expressing Ste2p and mutant proteins, the constructs were designed to encode protein lacking the C-terminal cytoplasmic tail, which contributes to receptor internalization and desensitization but is dispensable for agonist binding and signaling (Reneke et al., 1988). The plasmids for expressing Ste2p proteins were constructed as follows. To introduce point mutations for bait plasmids, gene fragments encoding the upstream (amino acids 1–62) and downstream (amino acids 53–304) ends of mutated Ste2p were PCR-amplified from pBT3-STE2ΔC (Nakamura et al., 2013) using oligonucleotides o13 + o14 and o15 + o16 for G56A; o13 + o17 and o18 + o16 for G60A; o13 + o19 and o20 + o16 for G56A/G60A; o13 + o21 and o22 + o16 for G56L; o13 + o23 and o24 + o16 for G60L; o13 + o25 and o26 + o16 for G56L/G60L. These amplified fragments then were used as the templates for overlap PCR with oligonucleotides o13 and o16. For prey plasmids, an equivalent PCR process was performed, except that oligonucleotides o13 and o16 were replaced with oligonucleotides o27 and o28, respectively. For bait plasmids, the resulting linear *STE2*

(or *ste2*) fragments were digested with *Xba*I+*Hind*III and ligated into similarly digested pBT3-C (Dualsystems Biotech AG, Schlieren, Switzerland), resulting in plasmids designated pBT3-STE2ΔC-G56A, -G60A, -G56AG60A, -G56L, -G60L, or -G56LG60L, respectively. For prey plasmids, the resulting linear *STE2* (or *ste2*) fragments were digested with *Spe*I+*Eco*RI and ligated into similarly digested pPR3-C (Dualsystems Biotech AG, Schlieren, Switzerland), resulting in plasmids designated pPR3-STE2ΔC-G56A, -G60A, -G56AG60A, -G56L, -G60L, or -G56LG60L, respectively.

Construction of yeast strains

Yeast strains used in this study are listed in **Table 1**. Transformation with linear DNA fragments was performed using the lithium acetate method (Gietz et al., 1992). To eliminate the *URA3* selectable marker at each transformation step, we followed previous procedures (Iguchi et al., 2010; Togawa et al., 2010) modified to incorporate the marker recycling method (Akada et al., 2006). All oligonucleotides used for the strain constructions are listed in **Table 2**.

The strain expressing enhanced green fluorescent protein (EGFP) was generated as follows. First, using previously described methods (Iguchi et al., 2010), a *sst2*Δ allele was inserted into a *ste2*Δ single mutant strain derived from BY4741 (Brachmann et al., 1998) (obtained from the *Saccharomyces* Genome Deletion Project (Winzeler et al., 1995)). The resulting *sst2*Δ *ste2*Δ double mutant was designated MI-50. Next, the pheromone-responsive *FIG1* gene of MI-50 was replaced with a reporter gene (*EGFP*) encoding EGFP. Gene replacement was performed as follows. A DNA fragment containing the *FIG1* promoter, *EGFP* gene, 40 nucleotides (of *FIG1* terminator), *URA3*

Table 1. Yeast strains and plasmids used in this study.

Strain or plasmid	Description	Reference or source
Strain		
NMY51	*MAT**a** his3Δ200 trp1-901 leu2-3, 112 ade2 LYS2::(lexAop)$_4$-HIS3 ura3::(lexAop)$_8$-lacZ ade2::(lexAop)$_8$-ADE2 GAL4*	Dualsystems Biotech AG
BY4741	*MAT**a** his3Δ1 leu2Δ0 met15Δ0 ura3Δ0*	Brachmann et al. (1998)
MI-10	BY4741 *ste2*Δ::*kanMX4*	Winzeler et al. (1999) purchased from Invitrogen, Carlsbad, CA, USA
MI-50	MI-10 *sst2*Δ	This study
MIF-50	MI-50 *fig1*Δ::*EGFP*	This study
MIFLE-50	MIF-50 *trp1*Δ::*(lexAop)$_8$-E2-Crimson*	This study
IMFD-50	BY4741 *sst2*Δ::*AUR1-C ste2*Δ::*LEU2 fig1*Δ::*EGFP his3*Δ::P_{FIG1}-*EGFP*	Togawa et al. (2010)
IMFD-250	BY4741 *sst2*Δ::*AUR1-C **ste2Δ** fig1*Δ::*EGFP his3*Δ::P_{FIG1}-*EGFP*	This study
IMFDLE-250	IMFD-250 *trp1*Δ::*(lexAop)$_8$-E2-Crimson*	This study
Plasmid		
pGK426	Yeast expression vector containing *PGK1* promoter, 2μ origin, and *URA3* marker	Ishii et al. (2009)
pGK426-E2-Crimson	*E2-Crimson* in pGK426	This study
pGK425	Yeast expression vector containing *PGK1* promoter, 2μ origin, and *LEU2* marker	Ishii et al. (2009)
pGK425-EGFP	*EGFP* in pGK425	Ishii et al. (2009)
pBlueScript II KS(+)	Cloning vector	Agilent Technologies
pBlue-(lexAop)$_8$-E2-Crimson	*(lexAop)$_8$-E2-Crimson* in pBlueScript II KS(+)	This study
pBlue-URA3-(lexAop)$_8$-E2-Crimson	*TRP1(300 bp)-URA3-(lexAop)$_8$-E2-Crimson* in pBlue-(lexAop)$_8$-E2-Crimson	This study
pBlue-URA3-(lexAop)$_8$-E2-Crimson-TRP1	*TRP1(300 bp)-URA3-(lexAop)$_8$-E2-Crimson-P_{TRP1}(250 bp)* in pBlue-URA3-(lexAop)$_8$-E2-Crimson	This study
pBT3-C	Cub-LexA-VP16 expression vector containing *CYC1* promoter, *CEN/ARS* origin, and *LEU2* marker	Dualsystems Biotech AG
pPR3-C	NubG expression vector containing *ADH1* promoter, 2μ origin, and *TRP1* marker	Dualsystems Biotech AG
pCCW-Alg5	Alg5-Cub-LexA-VP16 expression, *CYC1* promoter, *CEN/ARS* origin, and *LEU2* marker	Dualsystems Biotech AG
pAI-Alg5	Alg5-NubI expression, *ADH1* promoter, 2μ origin, and *TRP1* marker	Dualsystems Biotech AG
pBT3-STE2ΔC	*STE2ΔC* in pBT3-C	Nakamura et al. (2013)

pPR3-STE2ΔC	*STE2ΔC* in pPR3-C	Nakamura et al. (2013)
pBT3-STE2ΔC-G56A	*STE2ΔC (G56A)* mutant in pBT3-C	This study
pBT3-STE2ΔC-G60A	*STE2ΔC (G60A)* mutant in pBT3-C	This study
pBT3-STE2ΔC-G56AG60A	*STE2ΔC (G56A/G60A)* mutant in pBT3-C	This study
pBT3-STE2ΔC-G56L	*STE2ΔC (G56L)* mutant in pBT3-C	This study
pBT3-STE2ΔC-G60L	*STE2ΔC (G60L)* mutant in pBT3-C	This study
pBT3-STE2ΔC-G56LG60L	*STE2ΔC (G56L/G60L)* mutant in pBT3-C	This study
pPR3-STE2ΔC-G56A	*STE2ΔC (G56A)* mutant in pPR3-C	This study
pPR3-STE2ΔC-G60A	*STE2ΔC (G60A)* mutant in pPR3-C	This study
pPR3-STE2ΔC-G56AG60A	*STE2ΔC (G56A/G60A)* mutant in pPR3-C	This study
pPR3-STE2ΔC-G56L	*STE2ΔC (G56L)* mutant in pPR3-C	This study
pPR3-STE2ΔC-G60L	*STE2ΔC (G60L)* mutant in pPR3-C	This study
pPR3-STE2ΔC-G56LG60L	*STE2ΔC (G56L/G60L)* mutant in pPR3-C	This study
pBTD3-SSTR5	SSTR5-Cub-LexA-VP16 expression, *TDH3* promoter, *CEN/ARS* origin, and *LEU2* marker	Nakamura et al. (2013)
pPR3-SSTR5	*SSTR5* in pPR3-C	Nakamura et al. (2013)
pPR3-SSTR2	*SSTR2* in pPR3-C	Nakamura et al. (2013)
pPR3-ADRB2	*ADRB2* in pPR3-C	Nakamura et al. (2013)
pPR3-STE2	*STE2* in pPR3-C	Nakamura et al. (2013)

Table 2. List of oligonucleotides.

	Name	Sequence
o1	NheI_E2-Crimson_fw	5'-TTTTGCTAGCATGGATAGCACTGAGAACGT
o2	EcoRI_E2-Crimson_rv	5'-AAAAGAATTCCTACTGGAACAGGTGGTGGC
o3	BamHI_lexAop_fw	5'-CCCCGGATCCTCGACTGCTGTATATAAAAC
o4	EcoRI_PGAL1_rv	5'-GGGGGAATTCTATAGTTTTTTCTCCTTGAC
o5	EcoRI_E2-Crimson_fw	5'-CCCCGAATTCATGGATAGCACTGAGAACGT
o6	ClaI_E2-Crimson_rv	5'-TTTTATCGATCTACTGGAACAGGTGGTGGC
o7	SacII_dTRP1_fw	5'-TTTTCCGCGGAAGCTGCACTGAGTAGTATG
o8	XbaI_dTRP1_rv	5'-CCCCTCTAGAACTTGCTGGGTATTATATGT
o9	XbaI_URA3_fw	5'-CCCCTCTAGATTTTTTGTTCTTTTTTTTGA
o10	BamHI_hr40-URA3_rv	5'-CCCCGGATCCACTTGCTGGGTATTATATGTGTGCCCAATAGAAAGAGA ACGGGTAATAACTGATATAATT
o11	ClaI_dTRP1up_fw	5'-GGGGATCGATTTCTTAATCGGCAAAAAAAG
o12	XhoI_dTRP1up_rv	5'-TTTTCTCGAGAAACGTGCACCCGCCCGTCT
o13	XbaI_STE2_fw	5'-AAAATCTAGAATGTCTGATGCGGCTCCTTC
o14	STE2-G56A_rv	5'-CAGCTGCACCACATCTGACA**G**CAAACATAA
o15	STE2-G56A_fw	5'-TTATGTTTG**C**TGTCAGATGTGGTGCAGCTG
o16	HindIII_lin_STE2-304_rv	5'-GGGGAAGCTTGAACCTCCGCCACCTGATTTGGATGCATTATTAGCAG
o17	STE2-G60A_rv	5'-CAGCTGCA**G**CACATCTGACACCAAACATAA
o18	STE2-G60A_fw	5'-TTATGTTTGGTGTCAGATGTG**C**TGCAGCTG
o19	STE2-G56AG60A_rv	5'-CAGCTGCA**G**CACATCTGACA**G**CAAACATAA
o20	STE2-G56AG60A_fw	5'-TTATGTTTG**C**TGTCAGATGTG**C**TGCAGCTG
o21	STE2-G56L_rv	5'-CAGCTGCACCACATCTGACA**AG**AAACATAA
o22	STE2-G56L_fw	5'-TTATGTTT**CT**TGTCAGATGTGGTGCAGCTG
o23	STE2-G60L_rv	5'-CAGCTGCA**AG**ACATCTGACACCAAACATAA
o24	STE2-G60L_fw	5'-TTATGTTTGGTGTCAGATGT**CT**TGCAGCTG
o25	STE2-G56LG60L_rv	5'-CAGCTGCA**AG**ACATCTGACA**AG**AAACATAA
o26	STE2-G56LG60L_fw	5'-TTATGTTT**CT**TGTCAGATGT**CT**TGCAGCTG
o27	SpeI_STE2_fw	5'-GGGGACTAGTATGTCTGATGCGGCTCCTTC
o28	EcoRI_lin_STE2-304_rv	5'-GGGGGAATTCGGAACCTCCGCCACCTGATTTGGATGCATTATTAGCAG
o29	FIG1N_200bp_fw	5'-TAAGATTATGATGGTTTCATGTATGTGTCA
o30	FIG1C_200bp_rv	5'-TTAGTCGCTCATCAAGGTGACAGTAAATAA
o31	dSTE2up-URA3_fw	5'-TTTCTTTTCACCTGCTCTGGCTATAATTATAATTGGTTACTTAAAAATGC ACCGTTAAGAACCATATCCAAGAATCAAAATTTTTTGTTCTTTTTTTTGA

o32	dSTE2up-URA3_rv	5'-TCTTAACGGTGCATTTTTAAGGGTAATAACTGATATAATT
o33	dSTE2dn_fw	5'-AATTATATCAGTTATTACCCTTAAAAATGCACCGTTAAGAACCATATCCA AGAATCAAAATCAAAATTTACGGCTTTGAAAAAGTAATTTCGTGACCTTC
o34	dSTE2dn_rv	5'-AAGATTAACTGTATATATTGCCTGAGAGTTCTAGATCATG

selectable marker, and *FIG1* terminator was PCR-amplified from pMR-FIG1GF (Togawa et al., 2010) with oligonucleotides o29 and o30, and the amplified fragment was introduced into MI-50. After confirming the correct integration, the *URA3* marker was "popped-out" by homologous recombination using counter-selection with 5-fluoroorotic acid (5-FOA, Fluorochem, Derbyshire, UK). The resultant strain was designated MIF-50.

To provide leucine auxotrophy, the *LEU2* marker located at the *ste2*Δ locus of the IMFD-50 strain (Togawa et al., 2010) was eliminated using marker recycling. The first half of a DNA fragment, consisting of the upstream region of the *STE2* gene and the *URA3* selectable marker, was PCR-amplified from pGK406 (Ishii et al., 2009) using oligonucleotides o31 and o32. The second half of the fragment, consisting of the downstream region of *STE2* and the sequences upstream of the *STE2* chromosomal locus (to facilitate excision of the *URA3* marker) was PCR-amplified from BY4741 genomic DNA using oligonucleotides o33 and o34. These two amplified fragments were combined using overlap PCR, and the resulting linear construct was transformed into IMFD-50. After confirming integration of the fragments at the correct positions, the *URA3* marker was "popped-out" by counter-selection with 5-FOA, resulting in strain IMFD-250.

To construct the recombinant yeast strain in which the genomic *TRP1* gene was replaced by the *E2-Crimson* reporter gene, the DNA fragment obtained by digesting pBlue-URA3-$(lexAop)_8$-E2-Crimson-TRP1 with *Sac*II and *Xho*I was transformed into MIF-50 and IMFD-250. After confirming correct integration, the *URA3* marker was "popped-out" by counter-selection with 5-FOA. The constructed strains were designated MIFLE-50 and IMFDLE-250, respectively.

Fluorescence microscopy imaging

Yeast transformants were grown in SD medium (supplemented as needed) at 30 °C overnight, and the cells then were inoculated into 5 mL of the respective fresh SD medium to give an initial optical density of 0.03 at 600 nm (OD_{600} = 0.03). The cells were incubated at 30 °C on a rotary shaker at 150 rpm for up to 18 h and then harvested, washed, and resuspended in distilled water. The cell suspensions were observed using a BZ-9000 fluorescence microscope (Keyence, Osaka, Japan). Green fluorescence images were acquired with a 470/40 band-pass filter for excitation and a 535/50 band-pass filter for emission. Red fluorescence images were acquired with a 620/60 band-pass filter for excitation and a 700/75 band-pass filter for emission. Exposure times were 0.2 and 1 s for green and red, respectively.

Flow cytometric analysis

EGFP and E2-Crimson were detected using a BD FACSCanto II flow cytometer equipped with both a 488-nm blue laser and a 633-nm red laser, respectively (Becton, Dickinson and Company, Franklin Lakes, NJ, USA); the data were analyzed using BD FACSDiva software (v5.0; Becton, Dickinson and Company). The EGFP fluorescence signal was collected through a 530/30 nm band-pass filter, and the GFP-A mean of 10,000 cells was defined as ‘green fluorescent intensity’. The E2-Crimson fluorescence signal was collected through a 660/20 nm band-pass filter, and the APC-A mean of 10,000 cells was defined as ‘far-red fluorescent intensity’.

Ste2p assays

Yeast strains transformed with the wild-type or mutated Ste2p expression plasmids

were grown in SD medium (supplemented as needed) at 30 °C overnight, and the cells then were inoculated into 5 mL of the respective fresh SD medium to give an initial OD_{600} = 0.03. The cells were incubated at 30 °C on a rotary shaker at 150 rpm for up to 18 h and harvested, washed, and resuspended in water to give an OD_{600} = 10. The resulting yeast cell suspensions were added (at 10 µL /well; to give an OD_{600} = 1) to the wells of 96-well cluster dishes containing fresh SD medium (80 µL/well) supplemented (10 µL/well) with 10 µM α-factor (Zymo Research, Orange, CA, USA) or distilled water (no α-factor control). The plates were incubated at 30 °C with shaking (150 rpm) for 4 h. After incubation, the samples containing the yeast cells were diluted with 1 mL per well of sheath fluid, and fluorescence was analyzed by flow cytometry.

hSSTR5 assay

Cultivation conditions for the hSSTR5 assay were modified from a previous report (Ishii et al., 2012a). Briefly, yeast strains transformed with the hSSTR5 expression plasmids were grown in SD medium (supplemented as needed) at 30 °C overnight, and were inoculated into 5 mL of the respective fresh SD medium to give an initial OD_{600} = 0.03. The cells then were grown at 30 °C on a rotary shaker at 150 rpm for up to 18 h and harvested, washed, and resuspended in water to yield an OD_{600} = 10. The resulting yeast cell suspensions were added (at 10 µL /well; to give an OD_{600} = 1) to the wells of 96-well cluster dishes containing fresh SDM71 medium (80 µL/well) supplemented (10 µL/well) with 10 µM somatostatin (SST) (Calbiochem, Darmstadt, Germany) or distilled water (no SST control). The plates were incubated at 30 °C with shaking (150 rpm) for 4 h. After incubation, the samples containing the yeast cells were diluted with 1 mL of sheath fluid, and fluorescence was analyzed by flow cytometry.

Halo bioassay to test growth arrest response to G-protein signal

An agar diffusion bioassay (halo assay), performed as described previously (Ishii et al., 2006), was used to measure the response to and recovery from pheromone-induced cell-cycle arrest. Briefly, yeast transformants were grown in SD medium at 30 °C overnight. Sterilized paper filter disks (6 mm in diameter) were placed on square size Petri dishes and various amounts of α-factor pheromone were spotted onto the disks. Fifty milliliters of SD medium containing 20 g/L agar (and maintained at 50 °C) was inoculated with the yeast cells to an initial OD_{600} of 5×10^{-4}, and the suspension was used to overlay the paper disk-containing plate. The plates were incubated at 30 °C for 4 days.

Results and Discussion

General strategy

The aim of this study was to establish a method, using recombinant yeast strains, that permitted simultaneous analyses of dimerization and of signaling by GPCRs. Such a technique is expected to provide various advantages for GPCR studies. To achieve this goal, we designed a dual-color fluorescent reporter detection system based on the combination of a previously reported split-ubiquitin two-hybrid system (Stagljar et al., 1998) with a G-protein signaling assay system (Iguchi et al., 2010; Togawa et al., 2010). As detection readouts, we selected red and green fluorescent reporter genes for monitoring dimerization and signaling events of GPCRs, respectively. An outline of our strategy is shown in **Figure 1**.

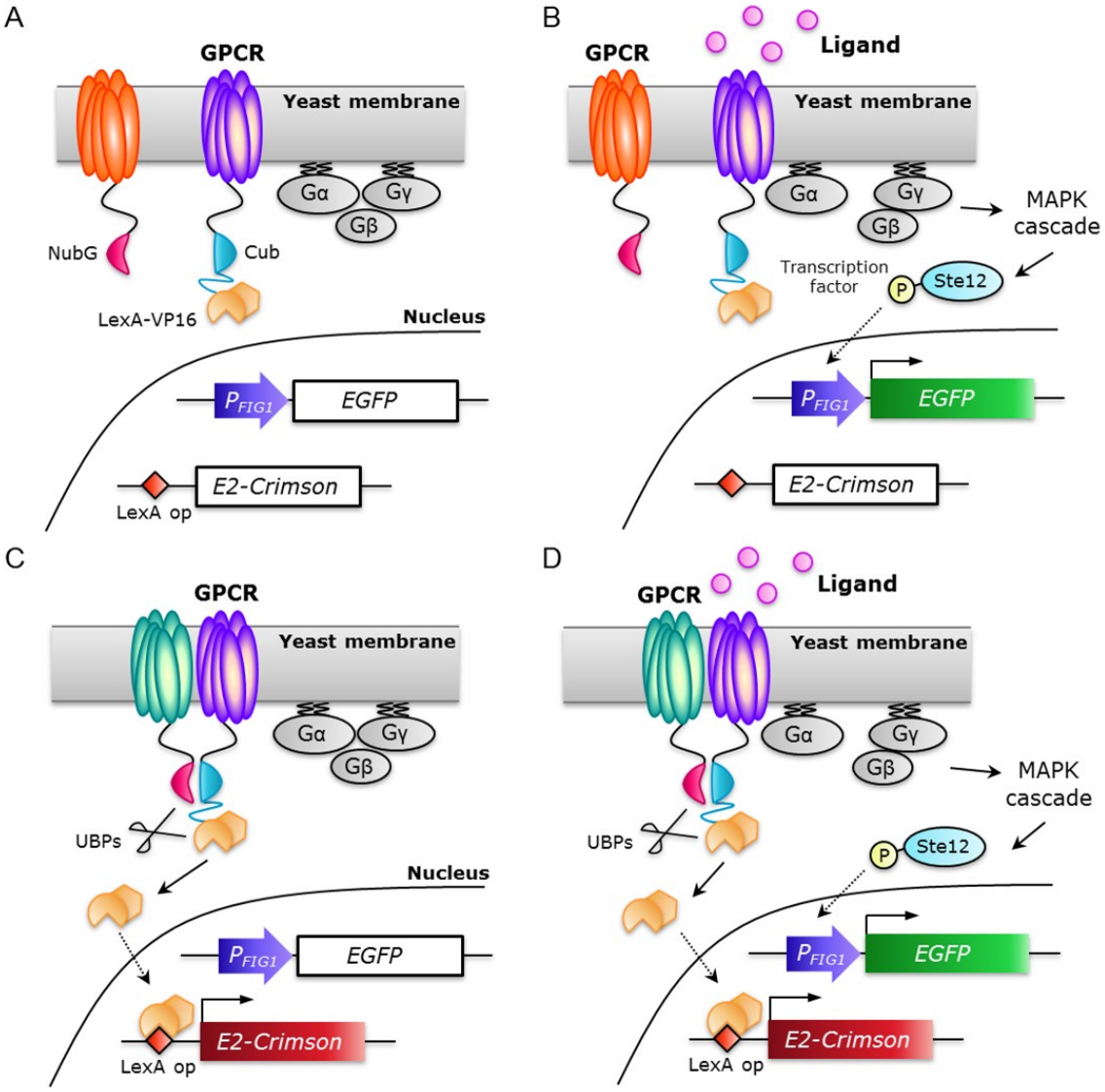
A
GPCR
Yeast membrane
Gα
Gγ
Gβ
NubG
Cub
LexA-VP16
Nucleus
P_{FIG1}
EGFP
E2-Crimson
LexA op
B
GPCR
Ligand
Yeast membrane
Gα
Gγ
Gβ
MAPK cascade
Transcription factor
P
Ste12
P_{FIG1}
EGFP
E2-Crimson
C
GPCR
Yeast membrane
Gα
Gγ
Gβ
UBPs
Nucleus
P_{FIG1}
EGFP
E2-Crimson
LexA op
D
GPCR
Ligand
Yeast membrane
Gα
Gγ
Gβ
MAPK cascade
UBPs
P
Ste12
P_{FIG1}
EGFP
E2-Crimson
LexA op

Fig. 1. Schematic illustration of the strategy for simultaneous analysis of dimerization and signaling by GPCRs. (A,B) No-dimerization pairs. (C,D) Dimerization pairs. (A,C) Without agonistic ligand. (B,D) With agonistic ligand. The yeast pheromone signaling pathway is shown, along with the regulatory changes of fluorescence reporter genes in response to ligand. This pathway is extensively used for the GPCR assay. Agonistic ligand binding to the GPCR leads to activation of heterotrimeric G-proteins. The activated G-proteins subsequently induce activation of the mitogen-activated protein kinase (MAPK) cascade, resulting in expression of the *EGFP* reporter gene. In the split-ubiquitin yeast two-hybrid system, NubG efficiently interacts with Cub only when the proteins to which the two split tags are attached interact with each other, resulting in the formation of a NubG/Cub complex. This complex is recognized by ubiquitin-specific proteases (UBPs), which release the artificial transcription factor (TF; LexA-VP16) from the Cub-containing construct. The TF then enters the nucleus via diffusion and binds to the *lexA*-binding sites upstream of the *E2-Crimson* reporter gene.

The yeast split-ubiquitin two-hybrid system has been applied most recently to the detection of homo- and hetero-dimerizations of human GPCRs (Nakamura et al., 2013). The developed system successfully identified candidate heterodimer partners for target human GPCRs. Briefly, separate constructs were used to encode proteins that fused either the N- or C-terminal moiety of a split-ubiquitin to the C-terminus of a GPCR (**Figure 1**). Notably, the N-terminal moiety of the split-ubiquitin included an I13G mutation (NubG), while the C-terminal moiety of the split-ubiquitin included an artificial transcription factor domain (Cub-LexA-VP16). Upon *in vivo* protein-protein interaction, the reconstituted ubiquitin served as a substrate for the action of ubiquitin-specific proteases (UBPs), resulting in the release of the LexA-VP16 transcription factor. The transcription factor then entered the nucleus and induced the transcriptional activation of growth and colorimetric reporter genes (*ADE2*, *HIS3*, and *lacZ*). Therefore, the system permitted monitoring of dimerization by GPCRs. In the present study, the assay was modified to incorporate the red fluorescent reporter gene as the assay read-out.

The yeast-based GPCR signaling assay is a previously developed approach to monitoring the pheromone signaling machinery (Ishii et al., 2010). Specifically, heterologous GPCRs were expressed on yeast cell surface membranes; binding of agonistic ligands to the receptors triggered the activation of the mitogen-activated protein kinase (MAPK) cascade via yeast endogenous or chimeric G-proteins (Minic et al., 2005) (**Figure 1**). The signal led to the phosphorylation of transcription factor Ste12p, inducing the expression of reporter genes in a pheromone-responsive manner. Several laboratories have reported the use of an *EGFP* gene (placed under the control of the pheromone-responsive *FIG1* or *FUS1* promoter) to detect G-protein signaling

(Fukuda et al., 2011; Hara et al., 2012; Ishii et al., 2012a; Ishii et al., 2012b). This detection approach permitted a variety of applications, including ligand screening and mutational analysis (Ishii et al., 2012b; Ladds et al., 2005; Minic et al., 2005).

Based on these techniques, we designed a red and green dual-color detection method combined with flow cytometry, which permitted high-throughput cell sorting, facilitating simultaneous analyses of GPCR dimerization and signaling.

Determination of two fluorescent proteins for dual-color fluorescent reporter system

To allow dual-color flow cytometric analyses, we explored the combined use of two fluorescent proteins harboring chromophores with sufficiently distinct emission peaks. One of these, enhanced green fluorescent protein (EGFP) (excitation maximum, 490 nm; >90% efficiency at 488 nm; emission maximum, 510 nm) (Lybarger et al., 1998), has been widely used as a reporter gene for flow cytometry. As the partner for dual-color detection, we employed a recently described far-red variant of DsRed-Express2 (E2-Crimson) (excitation maximum, 611 nm; ≈42% efficiency at 633 nm; emission maximum, 646 nm) (Strack et al., 2009).

To test whether E2-Crimson and EGFP are suitable for the flow cytometric dual-color detection, we first generated the autonomous replicating plasmids pGK426-E2-Crimson and pGK425-EGFP to express constitutively each fluorescent protein under the control of the *PGK1* promoter. Yeast BY4741 wild-type strains harboring these plasmids or mock vectors were generated, and their far-red and green fluorescence was evaluated.

Using fluorescence microscopy, the two fluorescence signals were cleanly

resolvable and never interfered with each other's emission spectra (**Figure 2**). Subsequently, we measured the fluorescence level of each yeast cell under the condition of simultaneous 2-laser excitation (488 and 633 nm line) with the flow cytometer (**Figure 3**). As expected, fluorescence signals from these two proteins could be completely distinguished by the flow cytometry with standard optical systems. In addition, the average fluorescence of cells co-expressing E2-Crimson and EGFP was equivalent to that of cells expressing either reporter alone. Thus, we concluded that combination of far-red and green fluorescent proteins (E2-Crimson and EGFP) are optimally fitted to dual-color fluorescent detection.

Evaluation of LexA-VP16-responsive *E2-Crimson* reporter gene expression

To permit the far-red fluorescence-based split-ubiquitin yeast two-hybrid assay, we constructed the yeast strains MIFLE-50 and IMFDLE-250, in which the *E2-Crimson* reporter gene was expressed in response to the release of LexA-VP16 transcription factor (**Table 1**). Because the MIFLE-50 or IMFDLE-250 strains originally harbored *EGFP* (as single- or double-copy reporters), these strains were expected to permit dual-color fluorescent detection of dimerization and signaling by GPCRs.

To check the expression of the *E2-Crimson* reporter gene, we determined the mean intensity of fluorescence per yeast cell by flow cytometry. The yeast strains harboring mock vectors pBT3-C and pPR3-C were used as negative controls, and those harboring pCCW-Alg5 and pAI-Alg5 (which express Alg5-NubI and Alg5-Cub-LexA-VP16, respectively) were used as positive controls (**Table 1**). Alg5-NubI is a yeast membrane protein modified with a wild-type Nub tag. The NubI tag usually interacts spontaneously with any Cub tag-containing construct (Iyer et al., 2005; Kittanakom et

al., 2009). As shown in **Figure 4**, the E2-Crimson fluorescence of positive controls was much higher than that of negative controls, indicating that the *E2-Crimson* reporter gene was expressed. These data demonstrated that reconstitution of the split-ubiquitin and release of the LexA-VP16 transcription factor led to expression of the *E2-Crimson* reporter gene.

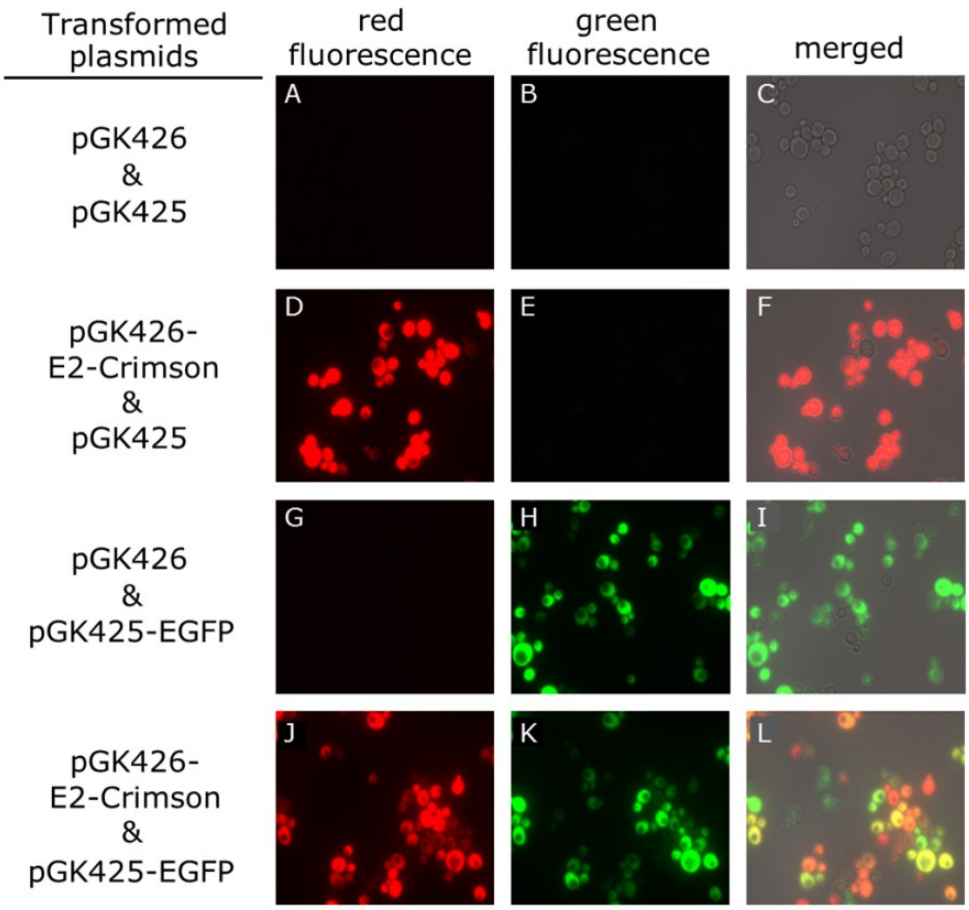

Fig. 2. Fluorescence microscope images of yeast strain BY4741 harboring pGK426-E2-Crimson and/or pGK425-EGFP. All transformants were grown in SD selective medium for 18 h. (**A-C**) pGK426/pGK425-containing cells are shown as viewed under red (A) or green filters (B) or presented as a merged image (C). (**D-F**) pGK426-E2-Crimson/pGK425-containing cells are shown as viewed under red (D) or green (E) filters or presented as a merged image (F). (**G-I**) pGK426/pGK425-EGFP-containing cells are shown as viewed under red (G) or green (H) filters or presented as a merged image (I). (**J-L**) pGK426-E2-Crimson/pGK425-EGFP-containing cells are shown as viewed under red (J) or green (K) filters or presented as a merged image (L).

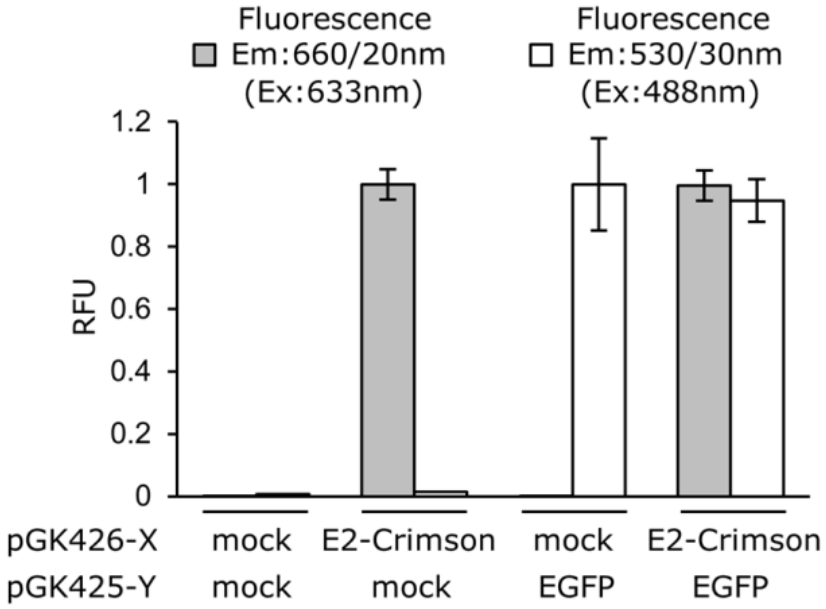

Fig. 3. Dual-color flow cytometric analysis of yeast strain BY4741 harboring pGK426-E2-Crimson and/or pGK425-EGFP. All transformants were grown in SD selective medium for 18 h. Solid bars: Cells were excited at 633 nm and emission detected at 660/20 nm (E2-Crimson). Open bars: Cells were excited at 488 nm and emission detected at 530/30 nm (EGFP). The relative E2-Crimson fluorescence units (red-RFU) were normalized by dividing the red fluorescent intensities of each yeast strain by those of a yeast strain harboring pGK426-E2-Crimson/pGK425. The relative EGFP fluorescence units (green-RFU) were normalized by dividing the green fluorescent intensities of each yeast strain by those of a yeast strain harboring pGK426/pGK425-EGFP. Data are presented as the mean ± standard deviation of separate runs (n = 3 each).

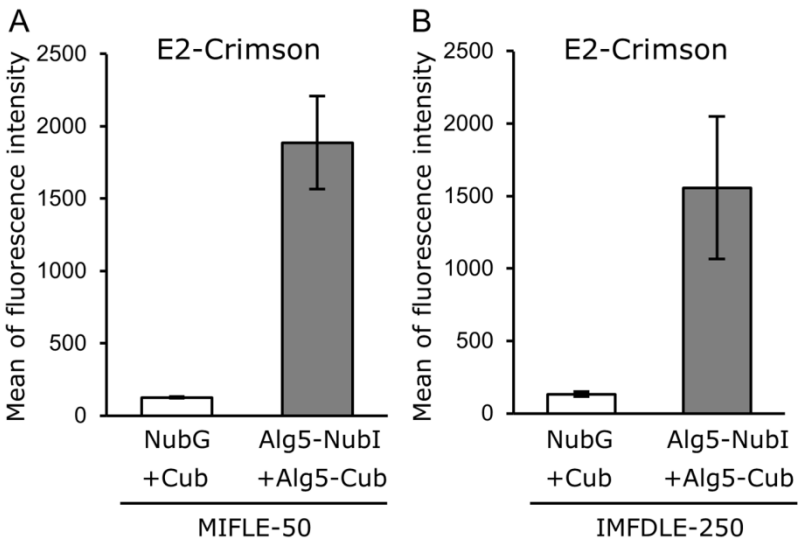

Fig. 4. Induction of *E2-Crimson* reporter gene by LexA-VP16. To check induction of the *E2-Crimson* reporter gene by LexA-VP16 from split-ubiquitin, yeast strains expressing Cub/NubG (negative control) or Alg5-Cub/Alg5-NubI (positive control) were constructed. All transformants were grown in SD selective medium for 18 h. Values represent the mean far-red E2-Crimson fluorescence signal for 10,000 cells, as measured by flow cytometry. Data are presented as the mean ± standard deviation of separate runs (n = 3 each). (A) MIFLE-50, (B) IMFDLE-250.

Simultaneous detection for dimerization and signaling by Ste2p

To validate the application of our method for simultaneous analyses of both dimerization and signaling by GPCRs, we first analyzed homo-dimerization and signaling by the yeast endogenous GPCR (Ste2p). Previous studies of dimerization reported the use of a truncated Ste2p receptor (lacking the C-terminal tail; Ste2ΔC) to reduce the distance between the C-termini of the receptor pair (Gehret et al., 2006; Nakamura et al., 2013). Therefore, we transformed our IMFDLE-250 yeast strain with pPR3-STE2ΔC and pBT3-STE2ΔC to provide co-expression of the proteins encoded by Ste2ΔC-NubG and Ste2ΔC-Cub-LexA-VP16. As a control, pPR3-C split-ubiquitin mock vector was used in place of pPR3-STE2ΔC (**Table 1**). The resulting transformants were cultivated in the presence and absence of 10 μM α-factor (a Ste2p agonist), and the fluorescence level of each strain was measured by flow cytometry (**Figure 5**).

In the dimerization assay with the Ste2ΔC-encoding constructs, the cells co-expressing Ste2ΔC-NubG and Ste2ΔC-Cub-LexA-VP16 displayed an increase in E2-Crimson fluorescence (**Figure 5A**); an equivalent elevation of far-red fluorescence was not seen in cells harboring the mock prey plasmid, suggesting that expression of the *E2-Crimson* reporter gene reflected dimerization of Ste2ΔC. Concurrently, we also verified that our system permitted the detection of Ste2p signaling. As expected, addition of 10 μM α-factor increased the EGFP fluorescence intensity in both cells (**Figure 5B**). Thus, we confirmed the validity of this platform for simultaneously analyzing dimerization and signaling by the yeast Ste2p receptor.

Similarly, we conducted an equivalent experiment using MIFLE-50, a strain that harbors a single-copy *EGFP* reporter gene. Compared with the IMFDLE-250 strain, the MIFLE-50 strain exhibited almost the same mean E2-Crimson intensity and a lower

EGFP intensity (**Figure 6**).

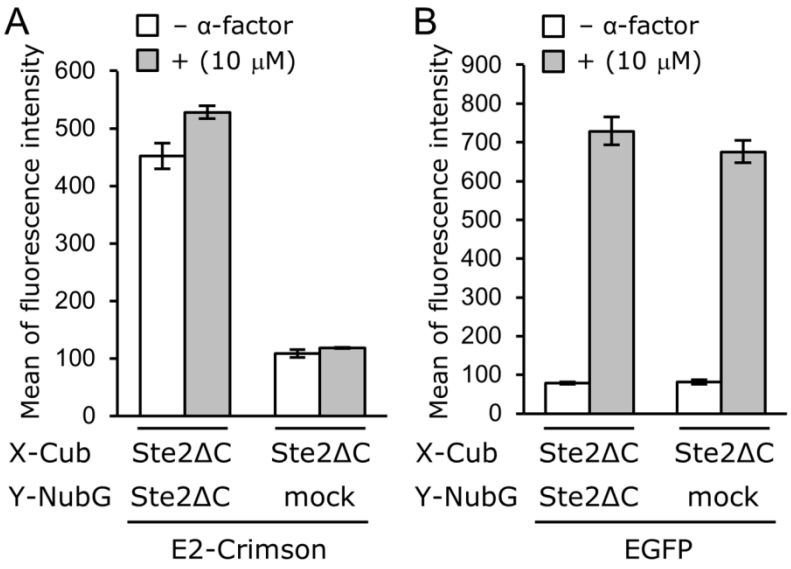

Fig. 5. Simultaneous detection of dimerization and signaling by truncated yeast Ste2p receptor (lacking the carboxy-terminal tail; Ste2ΔC) in IMFDLE-250 strain. The IMFDLE-250 yeast strain was transformed with plasmids encoding the indicated protein pairs. All transformants were grown in SD selective medium for 18 h. The cells then were incubated for another 4 h in SD selective medium with or without 10 μM α-factor. The mean E2-Crimson (A) and EGFP (B) fluorescence of 10,000 cells was measured by flow cytometry. Data are presented as the mean ± standard deviation of separate runs (n = 3 each).

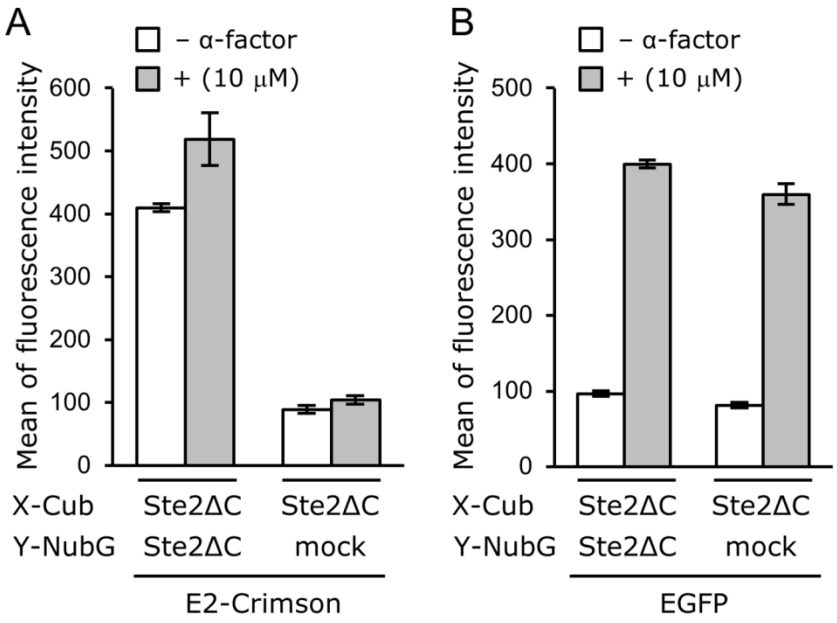

Fig. 6. Simultaneous detection of dimerization and signaling by truncated yeast Ste2p receptor (lacking the carboxy-terminal tail; Ste2ΔC) in MIFLE-50 strain. The MIFLE-50 yeast strain was transformed with plasmids encoding the indicated protein pairs. All transformants were grown in SD selective medium for 18 h. The cells then were incubated for another 4 h in SD selective medium with or without 10 μM α-factor. The mean E2-Crimson (A) and EGFP (B) fluorescence of 10,000 cells was measured by flow cytometry. Data are presented as the mean ± standard deviation of separate runs (n = 3 each).

Simultaneous detection of dimerization and signaling using Ste2p mutants

Subsequently, mutated Ste2p receptors with dimerization-defective and/or signaling-defective point mutations were analyzed to confirm the validity of the method. Reports suggested that the first transmembrane domain (TM1) forms a component of the interface between the two receptors in the Ste2p dimer (Overton and Blumer, 2002; Overton et al., 2003; Wang and Konopka, 2009). Additionally, the replacement of either or both glycine residues (Gly56 and Gly60) in TM1 by alanine or leucine (G56A(L) and/or G60A(L)) was shown to convert the Ste2p receptor into a dimerization-defective protein (Overton et al., 2003). The substitution of the glycine residues with bulky hydrophobic leucine residues resulted in stronger dimerization defects than those seen with Gly-to-Ala substitutions, presumably because of steric clashing (Overton et al., 2003). Moreover, the Gly-to-Leu mutants (G56L and/or G60L) showed signaling-defective characteristics, whereas the Gly-to-Ala mutants (G56A and/or G60A) still retained some ability to transduce the α-factor signal response (Overton et al., 2003). Therefore, these mutants were used to verify the utility of the method developed in the present paper.

To check the signaling properties of strains harboring each of the 6 constructed mutated genes, we performed halo bioassays (agonist-induced growth arrest) and checked for zones of growth inhibition. The yeast strain IMFDLE-250 expressing the G60A mutant exhibited normal signaling properties (**Figure 7**). The cells expressing the G56A single mutant or the G56A/G60A double mutant were able to transduce the signal, albeit with reduced efficacy (**Figure 7**). In contrast, cells expressing any of the leucine substitution mutants (G56L, G60L, or G56L/G60L) exhibited strong signaling defects (**Figure 7**). These results confirmed that our detection method yielded results consistent

with those reported previously with known *ste2* mutants (Overton et al., 2003).

Next, we assessed these mutants in the dual-color detection system to validate the feasibility of simultaneous analyses of dimerization and signaling by the Ste2p mutant proteins. The fluorescence of the E2-Crimson and EGFP reporters in IMFDLE-250 strains expressing these Ste2p mutants was quantitatively evaluated by flow cytometry. As shown in **Figure 8**, the Ste2p receptors with G56A and/or G60A mutations displayed significantly reduced E2-Crimson fluorescence while exhibiting essentially intact EGFP fluorescence (**Figure 8A** and **8B**). These results indicated that these mutant proteins were impaired in homo-dimerization but retained meaningful signaling function. On the other hand, the Ste2p receptors with G56L and/or G60L mutations exhibited decreases in both E2-Crimson and EGFP fluorescence, showing that these Leu-substituted mutants were impaired for both dimerization and signaling. These assays were consistent with the results of the halo assays and those of the previous report (Overton et al., 2003). Thus, our simultaneous detection system was validated for the evaluation of GPCR mutants.

Simultaneous detection of dimerization and signaling by human SSTR5

Somatostatin (SST) is a cyclic neuropeptide known as a growth hormone release-inhibiting factor; SST receptors are therapeutic targets for treatment of acromegaly, Cushing's disease, and Alzheimer's disease (Ben-Shlomo and Melmed, 2008; Lamberts et al., 1994; Saito et al., 2005). Heterologous expression of the human SST receptor subtype-5 (hSSTR5) in yeast has been shown to activate pheromone signaling via endogenous yeast G-protein in response to the native ligand SST (Togawa et al., 2010).

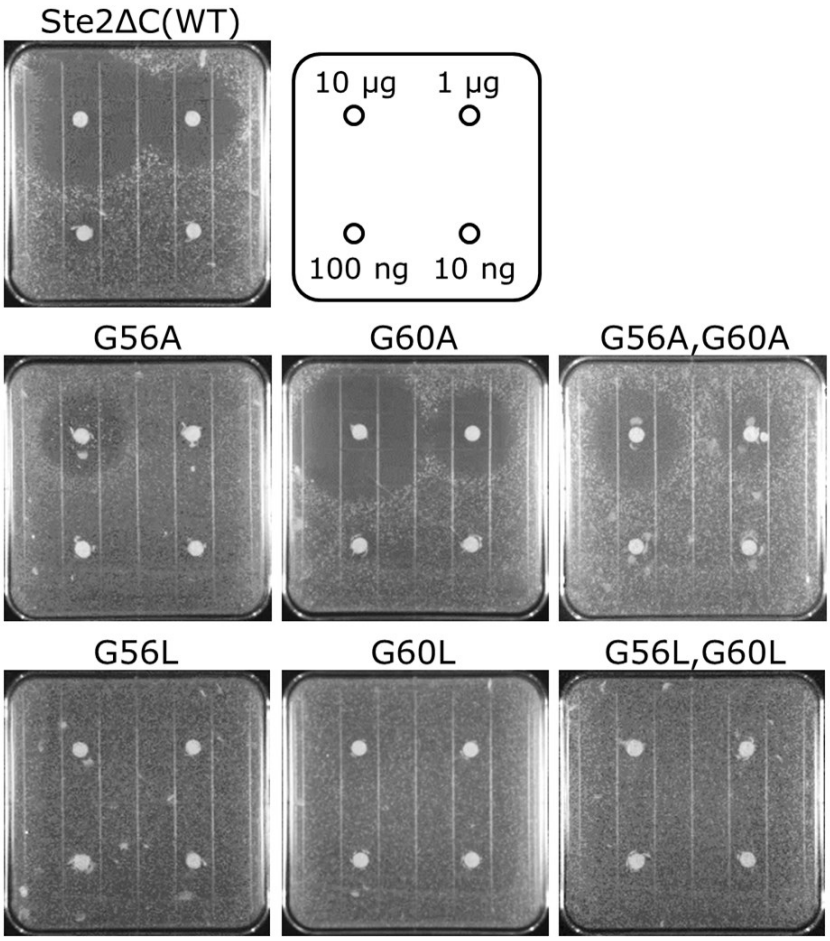

Fig. 7. Effects of substitutions at either or both glycine residues (Gly56 and Gly60) in TM1 on Ste2p receptor signal transduction. The IMFDLE-250 yeast strain was transformed with the plasmids encoding the indicated wild-type or mutant receptors. Halo bioassay (agonist-induced growth arrest) was performed with synthetic α-factor pheromone spotted onto filter disks at the amounts indicated in the schematic diagram.

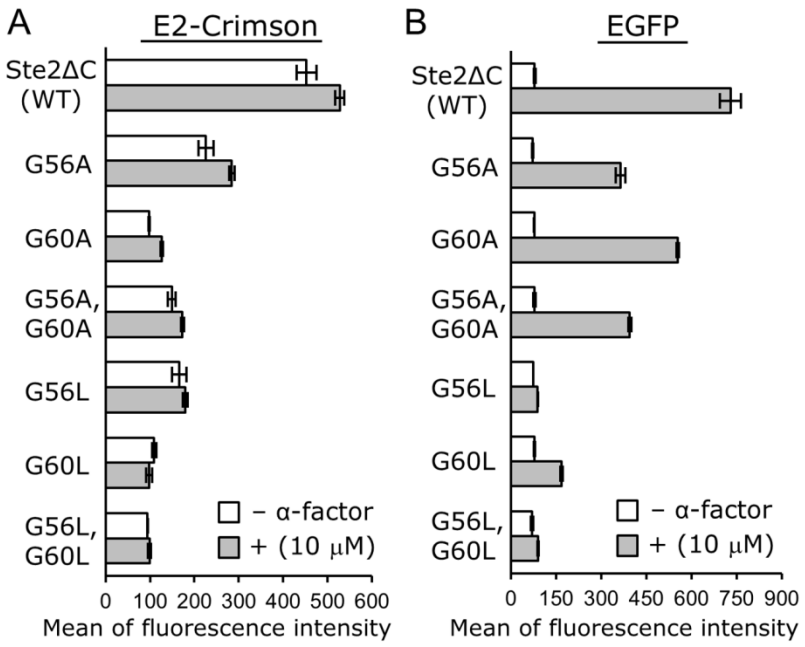

Fig. 8. Simultaneous analysis of dimerization and signaling by Ste2p mutant receptors in IMFDLE-250 strain. The IMFDLE-250 yeast strain was transformed with plasmids encoding the indicated Ste2p mutant receptors. All transformants were grown in SD selective medium for 18 h. The cells then were incubated for another 4 h in SD selective medium with or without 10 μM α-factor. The mean E2-Crimson (A) and EGFP (B) fluorescence of 10,000 cells was measured by flow cytometry. Data are presented as the mean ± standard deviation of separate runs (n = 3 each).

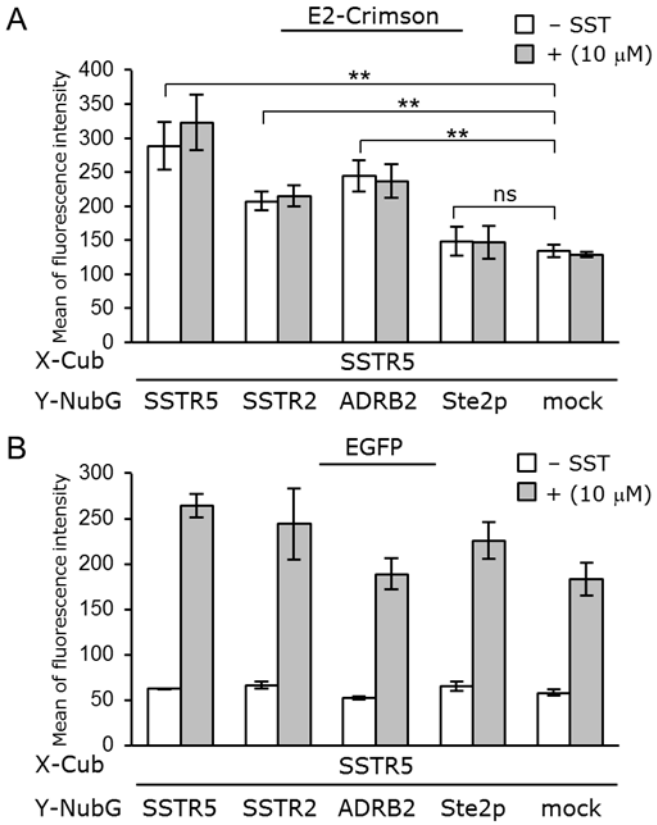

Fig. 9. Simultaneous detection of homo- and hetero-dimerization and signaling by human somatostatin receptor subtype-5 (SSTR5) in IMFDLE-250 strain. The IMFDLE-250 yeast strain was transformed with plasmids encoding various GPCR-NubG constructs (indicated below each graph; "Y-NubG") and SSTR5-Cub-LexA-VP16 ("X-Cub"). All transformants were grown in SD selective medium for 18 h. The cells then were incubated for another 4 h in SDM71 selective medium with or without 10 μM SST. The mean E2-Crimson (A) and EGFP (B) fluorescence of 10,000 cells was measured by flow cytometry. Data are presented as the mean ± standard deviation of separate runs (n = 3 each). Statistical significance was assessed by the t-test (ns, not significant, $^{**}P < 0.01$).

Yeast strain IMFDLE-250, which had been engineered to express hSSTR5, was cultivated in the presence and absence of 10 μM SST, and the fluorescence of each strain was measured by flow cytometry (**Figure 9**). In the dimerization assay, cells co-expressing hSSTR5-NubG and hSSTR5-Cub-LexA-VP16 (**Table 1**) displayed increased E2-Crimson fluorescence compared with mock control cells (co-expressing hSSTR5-Cub-LexA-VP16 and NubG) (**Figure 9A**, $P < 0.01$, *t*-test), consistent with the detection of hSSTR5 homo-dimerization. In cells co-expressing hSSTR5-NubG and hSSTR5-Cub-LexA-VP16, as in control cells, growth in the presence of 10 μM SST increased EGFP fluorescence (**Figure 9B**), confirming the detection of SST-induced G-protein signaling. However, cells co-expressing hSSTR5-NubG and hSSTR5-Cub-LexA-VP16 exhibited increased EGFP fluorescence compared with mock control cells (**Figure 9B**). This elevation in green fluorescence suggests that signaling levels are enhanced in cells co-expressing hSSTR5-NubG and hSSTR5-Cub-LexA-VP16 because of the greatly enriched expression level of hSSTR5 receptor derived from hSSTR5-NubG expressing prey vector (harboring multi-copy origin and robust *ADH1* promoter).

Finally, we engineered IMFDLE-250 yeast cells co-harboring human SST receptor subtype-2 (hSSTR2), human β_2-adrenergic receptor (hADRB2), or Ste2p expression prey plasmid (fusion forms with NubG) with the hSSTR5-Cub-LexA-VP16 expression bait plasmid. These combinations have included the previously reported hSSTR2/hSSTR5 and hADRB2/hSSTR5 heterodimer pairs (Grant et al., 2008; Somvanshi et al., 2011). After cultivation in the presence and absence of 10 μM SST, the fluorescence of each strain was measured by flow cytometry (**Figure 9**). Cells co-expressing hSSTR5-Cub-LexA-VP16 and hSSTR2-NubG or hADRB2-NubG (**Table**

1) exhibited E2-Crimson fluorescence ($P < 0.01$, *t*-test), while the cells co-expressing hSSTR5-Cub-LexA-VP16 and Ste2p-NubG and the mock control cells did not exhibit fluorescence (**Figure 9A**). Our experiments clearly showed that hSSTR5 could not co-oligomerize with Ste2p. In contrast, hSSTR5 could interact with hSSTR2 and hADRB2. In the signaling assays, all cells displayed SST-induced EGFP fluorescence, even though the hADRB2-NubG expression plasmid did not enhance the fluorescence levels upon SST exposure (as in the case with the mock control strain; **Figure 9B**). Taken together, these results indicated that hSSTR5 could form heterodimers both by congeneric interactions (between hSSTR5 and hSSTR2 moieties) and by heterogeneic interactions (between hSSTR5 and hADRB2 moieties). Both classes of hetero-dimerization are consistent with the previous reports (including our earlier results) (Grant et al., 2008; Nakamura et al., 2013; Somvanshi et al., 2011). Our results also suggest that the hetero-dimerization between hSSTR5 and hADRB2 did not change the signaling properties induced by SST stimulation. In addition, the strain harboring hSSTR5-Cub-LexA-VP16/Ste2p-NubG could give a slightly increased green fluorescent signal when treated with SST (compared with the mock control strain; **Figure 9B**). This suggested that co-expression of Ste2p-NubG with hSSTR5-Cub-LexA-VP16 increased the transactivation of *EGFP* by Ste12p upon the addition of non-relevant SST ligand. These events might be due to the enrichment of the expression level or the localization level to the membrane within the hSSTR5 receptor, although Ste2p would not be probably concerned in its mechanism directly on the ground of the evidence for non-interacting ability with hSSTR5.

Thus, our simultaneous detection system was validated for the heterologous expression and evaluation of human GPCRs. This system would be useful for

identifying an agonist bound to the heterodimer by screening (within a compound library or a plasmid-based peptide library) for ligand candidates that specifically activate the cells co-expressing components of the heterodimer pair.

Conclusion

In this study, we designed a dual-color fluorescent detection method for flow cytometry using EGFP and E2-Crimson. This technique combined a yeast split-ubiquitin two-hybrid system with a yeast G-protein signaling assay to provide a platform for simultaneous analysis of both dimerization and signaling by GPCRs. Using the yeast Ste2p, in both native and mutated forms, as a model for GPCR dimerization, we demonstrated that our technique provides a simple mechanism for simultaneously detecting both dimerization and signaling. In addition, we validated our experimental system by simultaneously monitoring homo- and hetero-dimerization and SST-induced signaling based on heterologously expressed human SSTR5 somatostatin receptor. Since budding yeast *S. cerevisiae* can functionally express human GPCRs (Minic et al., 2005), our system is expected to serve as a powerful tool for defining the mechanisms and functions of GPCR dimerization for uncovering new GPCR heterodimers that participate in regulating physiological functions, and for identifying potential targets for the development of new therapeutic agents.

References

AbdAlla S, Lother H, Quitterer U. 2000. AT1-receptor heterodimers show enhanced G-protein activation and altered receptor sequestration. Nature 407(6800):94–98.

Akada R, Kitagawa T, Kaneko S, Toyonaga D, Ito S, Kakihara Y, Hoshida H, Morimura S, Kondo A, Kida K. 2006. PCR-mediated seamless gene deletion and marker recycling in *Saccharomyces cerevisiae*. Yeast 23(5):399–405.

Benkirane M, Jin DY, Chun RF, Koup RA, Jeang KT. 1997. Mechanism of transdominant inhibition of CCR5-mediated HIV-1 infection by ccr5delta32. J Biol Chem 272(49):30603–30606.

Ben-Shlomo A, Melmed S. 2008. Somatostatin agonists for treatment of acromegaly. Mol Cell Endocrinol 286(1–2):192–198.

Bockaert J, Perroy J, Bécamel C, Marin P, Fagni L. 2010. GPCR interacting proteins (GIPs) in the nervous system: Roles in physiology and pathologies. Annu Rev Pharmacol Toxicol 50:89–109.

Brachmann CB, Davies A, Cost GJ, Caputo E, Li J, Hieter P, Boeke JD. 1998. Designer deletion strains derived from *Saccharomyces cerevisiae* S288C: a useful set of strains and plasmids for PCR-mediated gene disruption and other applications. Yeast 14(2):115–132.

Cvejic S, Devi LA. 1997. Dimerization of the delta opioid receptor: Implication for a role in receptor internalization. J Biol Chem 272(43):26959–26964.

Dowell SJ, Brown AJ. 2002. Yeast assays for G-protein-coupled receptors. Receptors Channels 8(5–6):343–352.

Drews J. 2000. Drug discovery: a historical perspective. Science 287(5460):1960–1964.

Elion EA. 2000. Pheromone response, mating and cell biology. Curr Opin Microbiol 3

(6):573–581.

Ferré S, Franco R. 2010. Oligomerization of G-protein-coupled receptors: A reality. Curr Opin Pharmacol 10(1):1–5.

Fredriksson R, Lagerström MC, Lundin LG, Schiöth HB. 2003. The G-protein-coupled receptors in the human genome form five main families. Phylogenetic analysis, paralogon groups, and fingerprints. Mol Pharmacol 63:1256–1272.

Fukuda N, Ishii J, Kaishima M, Kondo A. 2011. Amplification of agonist stimulation of human G-protein-coupled receptor signaling in yeast. Anal Biochem 417(2): 182–187.

Fukutani Y, Nakamura T, Yorozu M, Ishii J, Kondo A, Yohda M. 2012. The N-terminal replacement of an olfactory receptor for the development of a yeast-based biomimetic odor sensor. Biotechnol Bioeng 109(1):205–212.

Gehret AU, Bajaj A, Naider F, Dumont ME. 2006. Oligomerization of the yeast alpha-factor receptor: Implications for dominant negative effects of mutant receptors. J Biol Chem 281(30):20698–20714.

Gietz D, St Jean A, Woods RA, Schiestl RH. 1992. Improved method for high efficiency transformation of intact yeast cells. Nucleic Acids Res 20(6):1425.

Grant M, Alturaihi H, Jaquet P, Collier B, Kumar U. 2008. Cell growth inhibition and functioning of human somatostatin receptor type 2 are modulated by receptor heterodimerization. Mol Endocrinol 22(10):2278–2292.

Grosse R, Schöneberg T, Schultz G, Gudermann T. 1997. Inhibition of gonadotropin-releasing hormone receptor signaling by expression of a splice variant of the human receptor. Mol Endocrinol 11(9):1305–1318.

Gudermann T, Nürnberg B, Schultz G. 1995. Receptors and G proteins as primary

components of transmembrane signal transduction. Part 1. G-protein-coupled receptors: structure and function. J Mol Med 73(2):51–63.

Hara K, Ono T, Kuroda K, Ueda M. 2012. Membrane-displayed peptide ligand activates the pheromone response pathway in Saccharomyces cerevisiae. J Biochem 151(5): 551–557.

Hebert TE, Moffett S, Morello JP, Loisel TP, Bichet DG, Barret C, Bouvier M. 1996. A peptide derived from a beta2-adrenergic receptor transmembrane domain inhibits both receptor dimerization and activation. J Biol Chem 271(27):16384–16392.

Iguchi Y, Ishii J, Nakayama H, Ishikura A, Izawa K, Tanaka T, Ogino C, Kondo A. 2010. Control of signalling properties of human somatostatin receptor subtype-5 by additional signal sequences on its amino-terminus in yeast. J Biochem 147(6): 875–884.

Ishii J, Matsumura S, Kimura S, Tatematsu K, Kuroda S, Fukuda H, Kondo A. 2006. Quantitative and dynamic analyses of G protein-coupled receptor signaling in yeast using Fus1, enhanced green fluorescence protein (EGFP), and His3 fusion protein. Biotechnol Prog 22(4):954–960.

Ishii J, Tanaka T, Matsumura S, Tatematsu K, Kuroda S, Ogino C, Fukuda H, Kondo A. 2008. Yeast-based fluorescence reporter assay of G protein-coupled receptor signalling for flow cytometric screening: FAR1-disruption recovers loss of episomal plasmid caused by signalling in yeast. J Biochem 143(5):667–674.

Ishii J, Izawa K, Matsumura S, Wakamura K, Tanino T, Tanaka T, Ogino C, Fukuda H, Kondo A. 2009. A simple and immediate method for simultaneously evaluating expression level and plasmid maintenance in yeast. J Biochem 145(6):701–708.

Ishii J, Fukuda N, Tanaka T, Ogino C, Kondo A. 2010. Protein–protein interactions and

selection: yeast-based approaches that exploit guanine nucleotide-binding protein signaling. FEBS J 277(9):1982–1995.

Ishii J, Moriguchi M, Hara KY, Shibasaki S, Fukuda H, Kondo A. 2012a. Improved identification of agonist-mediated Gα(i)-specific human G-protein-coupled receptor signaling in yeast cells by flow cytometry. Anal Biochem 426(2):129–133.

Ishii J, Yoshimoto N, Tatematsu K, Kuroda S, Ogino C, Fukuda H, Kondo A. 2012b. Cell wall trapping of autocrine peptides for human G-protein-coupled receptors on the yeast cell surface. PLoS One 7(5):e37136.

Iyer K, Bürkle L, Auerbach D, Thaminy S, Dinkel M, Engels K, Stagljar I. 2005. Utilizing the split-ubiquitin membrane yeast two-hybrid system to identify protein-protein interactions of integral membrane proteins. Sci STKE 2005(275): pl3.

Jordan BA, Devi LA. 1999. G-protein-coupled receptor heterodimerization modulates receptor function. Nature 399(6737):697–700.

Jordan BA, Trapaidze N, Gomes I, Nivarthi R, Devi LA. 2001. Oligomerization of opioid receptors with beta 2-adrenergic receptors: A role in trafficking and mitogen-activated protein kinase activation. Proc Natl Acad Sci USA 98(1): 343–348.

Kittanakom S, Chuk M, Wong V, Snyder J, Edmonds D, Lydakis A, Zhang Z, Auerbach D, Stagljar I. 2009. Analysis of membrane protein complexes using the split-ubiquitin membrane yeast two-hybrid (MYTH) system. Methods Mol Biol 548:247–271.

Ladds G, Goddard A, Davey J. 2005. Functional analysis of heterologous GPCR signalling pathways in yeast. Trends Biotechnol 23(7):367–373.

Lamberts SW, de Herder WW, Krenning EP, Reubi JC. 1994. A role of (labeled) somatostatin analogs in the differential diagnosis and treatment of Cushing's syndrome. J Clin Endocrinol Metab 78(1):17–19.

Lefkowitz RJ, Shenoy SK. 2005. Transduction of receptor signals by beta-arrestins. Science 308(5721):512–517.

Lybarger L, Dempsey D, Patterson GH, Piston DW, Kain SR, Chervenak R. 1998. Dual-color flow cytometric detection of fluorescent proteins using single-laser (488-nm) excitation. Cytometry 31(3):147–152.

Margeta-Mitrovic M, Jan YN, Jan LY. 2000. A trafficking checkpoint controls GABA(B) receptor heterodimerization. Neuron 27(1):97–106.

Mijares A, Lebesque D, Wallukat G, Hoebeke J. 2000. From agonist to antagonist: Fab fragments of an agonist-like monoclonal anti-beta(2)-adrenoceptor antibody behave as antagonists. Mol Pharmacol 58(2):373–379.

Milligan G. 2008. A day in the life of a G protein-coupled receptor: the contribution to function of G protein-coupled receptor dimerization. Br J Pharmacol 153(Suppl 1): S216–229.

Minic J, Sautel M, Salesse R, Pajot-Augy E. 2005. Yeast system as a screening tool for pharmacological assessment of G protein coupled receptors. Curr Med Chem 12(8):961–969.

Nakamura Y, Ishii J, Kondo A. 2013. Rapid, facile detection of heterodimer partners for target human G-protein-coupled receptors using a modified split-ubiquitin membrane yeast two-hybrid system. PLoS One 8(6):e66793.

Overington JP, Al-Lazikani B, Hopkins AL. 2006. How many drug targets are there? Nat Rev Drug Discov 5(12):993–996.

Overton MC, Blumer KJ. 2002. The extracellular N-terminal domain and transmembrane domains 1 and 2 mediate oligomerization of a yeast G protein-coupled receptor. J Biol Chem 277(44):41463–41472.

Overton MC, Chinault SL, Blumer KJ. 2003. Oligomerization, biogenesis, and signaling is promoted by a glycophorin A-like dimerization motif in transmembrane domain 1 of a yeast G protein-coupled receptor. J Biol Chem 278(49): 49369–49377.

Potter LT, Ballesteros LA, Bichajian LH, Ferrendelli CA, Fisher A, Hanchett HE, Zhang R. 1991. Evidence of paired M2 muscarinic receptors. Mol Pharmacol 39(2): 211–221.

Rasmussen SG, Choi HJ, Rosenbaum DM, Kobilka TS, Thian FS, Edwards PC, Burghammer M, Ratnala VR, Sanishvili R, Fischetti RF, Schertler GF, Weis WI, Kobilka BK. 2007. Crystal structure of the human beta2 adrenergic G-protein-coupled receptor. Nature 450(7168):383–387.

Reneke JE, Blumer KJ, Courchesne WE, Thorner J. 1988. The carboxy-terminal segment of the yeast alpha-factor receptor is a regulatory domain. Cell 55(2): 221–234.

Ritter SL, Hall RA. 2009. Fine-tuning of GPCR activity by receptor-interacting proteins. Nat Rev Mol Cell Biol 10(12):819–830.

Rocheville M, Lange DC, Kumar U, Sasi R, Patel RC, Patel YC. 2000. Subtypes of the somatostatin receptor assemble as functional homo- and heterodimers. J Biol Chem 275(11):7862–7869.

Saito T, Iwata N, Tsubuki S, Takaki Y, Takano J, Huang SM, Suemoto T, Higuchi M, Saido TC. 2005. Somatostatin regulates brain amyloid beta peptide Abeta42

through modulation of proteolytic degradation. Nat Med 11(4):434–439.

Somvanshi RK, Chaudhari N, Qiu X, Kumar U. 2011. Heterodimerization of beta2 adrenergic receptor and somatostatin receptor 5: Implications in modulation of signaling pathway. J Mol Signal 6:9.

Stagljar I, Korostensky C, Johnsson N, te Heesen S. 1998. A genetic system based on split-ubiquitin for the analysis of interactions between membrane proteins *in vivo*. Proc Natl Acad Sci USA 95(9):5187–5192.

Stewart GD, Valant C, Dowell SJ, Mijaljica D, Devenish RJ, Scammells PJ, Sexton PM, Christopoulos A. 2009. Determination of adenosine A1 receptor agonist and antagonist pharmacology using *Saccharomyces cerevisiae*: Implications for ligand screening and functional selectivity. J Pharmacol Exp Ther 331(1):277–286.

Strack RL, Hein B, Bhattacharyya D, Hell SW, Keenan RJ, Glick BS. 2009. A rapidly maturing far-red derivative of DsRed-Express2 for whole-cell labeling. Biochemistry 48(35):8279–8281.

Togawa S, Ishii J, Ishikura A, Tanaka T, Ogino C, Kondo A. 2010. Importance of asparagine residues at positions 13 and 26 on the amino-terminal domain of human somatostatin receptor subtype-5 in signaling. J Biochem 147(6):867–873.

Wang HX, Konopka JB. 2009. Identification of amino acids at two dimer interface regions of the alpha-factor receptor (Ste2). Biochemistry 48(30):7132–7139.

Winzeler EA, Shoemaker DD, Astromoff A, Liang H, Anderson K, Andre B, Bangham R, Benito R, Boeke JD, Bussey H, Chu AM, Connelly C, Davis K, Dietrich F, Dow SW, El Bakkoury M, Foury F, Friend SH, Gentalen E, Giaever G, Hegemann JH, Jones T, Laub M, Liao H, Liebundguth N, Lockhart DJ, Lucau-Danila A, Lussier M, M'Rabet N, Menard P, Mittmann M, Pai C, Rebischung C, Revuelta JL, Riles L,

Roberts CJ, Ross-MacDonald P, Scherens B, Snyder M, Sookhai-Mahadeo S, Storms RK, Véronneau S, Voet M, Volckaert G, Ward TR, Wysocki R, Yen GS, Yu K, Zimmermann K, Philippsen P, Johnston M, Davis RW. 1999. Functional characterization of the *S. cerevisiae* genome by gene deletion and parallel analysis. Science 285(5429): 901–906.

Yesilaltay A, Jenness DD. 2000. Homo-oligomeric complexes of the yeast alpha-factor pheromone receptor are functional units of endocytosis. Mol Biol Cell 11(9): 2873–2884.

GENERAL CONCLUSION

This thesis was carried out with the aim to develop the yeast-based approaches for monitoring signal transmission and heterodimer formation for human GPCRs. Because these biosensors allowed facile detection of not only dimeric receptors but also agonistic ligands, it is applicable to the identification of obscured heterodimer partners and the screening of new peptidic agonists for target human GPCRs. Additionally, we integrated these two systems into a single yeast strain to permit the simultaneous detections of dimerization and signaling of human GPCRs. The constructed yeast biosensors will promote the elucidation of mechanisms and roles in the machinery of GPCR dimerizations, and the discovery of GPCR heterodimer pairs and peptidic sequences as potential therapeutic targets.

In part I, in order to extend the ranges of applicable GPCRs, we constructed an improved fluorescence-based microbial yeast biosensor that can monitor the activation of human GPCR signaling responding to its agonist using tetrameric *Zoanthus* sp. green fluorescent protein (ZsGreen) as a reporter. Since our system is applicable to not only hSSTR5 but also hSSTR2 and hNTSR1, this system can likely be extended to other human GPCRs, which comprise one of the most important types of drug targets being pursued today. In addition, we established a highly sensitive ligand detection system using yeast cell surface display technology that is applicable to peptide screening, and demonstrate that the display of various peptide analogs of neurotensin can activate signaling through the neurotensin receptor in yeast cells. Application of this method will allow the identification of lead peptides from combinatorial peptide libraries to provide

starting points for drug screening.

Moreover, using the refined fluorescence biosensor, we successfully applied to antagonist characterization and site-directed mutagenesis analyses of human HTR1A receptor. To examine the sensing abilities of yeast-based fluorescence reporter system for HTR1A antagonist characterization, we measured antagonist inhibition of the agonist-induced activating HTR1A. In addition, we adopted the yeast-based biosensor to site-directed mutagenesis. Through this work, these results clearly show the importance of the DRY motif for HTR1A function. This yeast-based system using a fluorescent reporter gene will be available for other human GPCRs and be beneficial for simplifying experimental procedures in a GPCR signaling study.

Furthermore we introduced a single mutation at the position of Asn295 on human AGTR1 and used yeast-human chimeric Gα to exert the functional activation of AGTR1 in the recombinant yeast cells that allow the signaling assay with fluorescence reporter. The engineered yeast cells successfully displayed the functional activation of the AGTR1-mediated signaling in response to its agonists, permitting easy monitoring of it with fluorescence reporter assay. In addition, we demonstrated that the autocrined Ang II peptide and its analogs that were produced in the engineered yeast cells by themselves also could activate the AGTR1-mediated signaling. This means that the construction of genetic library and its screening would be viable strategy for the human AGTR1 assay in yeast, and thus the constructed yeast biosensor integrating Asn295-mutated AGTR1 receptor will be applicable to the screens of angiotensin agonists and drug designs.

This study showed that our strategy could apply to various human GPCRs by improving the sensitivity of detection system and modifying the human GPCRs.

In part II, we have developed a specialized method to screen candidate heterodimer partners for target GPCRs based on the split-ubiquitin membrane yeast two-hybrid method. This modified system permitted the rapid and facile detection of not only the heterodimer formation of target human GPCRs, but also the ligand-mediated conformational changes in living yeast cells. Since budding yeast *S. cerevisiae* can functionally express human GPCRs, construction of a large prey library would be beneficial for the identification of heterodimer candidates as the partners of target human GPCRs. Our system will be a useful tool to assist in the intermolecular mapping of interactions among GPCRs and uncover potential targets for the development of new therapeutic agents.

Finally, we designed a dual-color fluorescent detection method for flow cytometry using EGFP and E2-Crimson. This technique combined a yeast split-ubiquitin two-hybrid system with a yeast G-protein signaling assay to provide a platform for simultaneous analysis of both dimerization and signaling by GPCRs. Using the yeast Ste2p, in both native and mutated forms, as a model for GPCR dimerization, we demonstrated that our technique provides a simple mechanism for simultaneously detecting both dimerization and signaling. In addition, we validated our experimental system by simultaneously monitoring homo- and hetero-dimerization and SST-induced signaling based on heterologously expressed human SSTR5 somatostatin receptor. Our system is expected to serve as a powerful tool for defining the mechanisms and functions of GPCR dimerization for uncovering new GPCR heterodimers that participate in regulating physiological functions, and for identifying potential targets for the development of new therapeutic agents.

In conclusion, we established the yeast-based approaches for elucidating the relationship between functions and structures of human GPCRs. For evaluating GPCR functions, we improved the system to monitor signal transmission for human GPCRs. For examining GPCR structures, we developed the system to monitor heterodimer formation among different types of human GPCRs. Finally, we combined these two systems to simultaneously monitor the dimerization and the signaling. The findings of physiologically relevant GPCR dimers raise the prospect of developing new drugs against a wide range of diseases by focusing on the machinery of targeted dimers. This study is expected to provide a helpful tool for the elucidating of molecular biological functions of GPCR dimers and for the screening of GPCR dimer-specific agonistic ligands.

ACKNOWLEDGMENTS

This is a thesis submitted by the author to Kobe University for the degree of Doctor of Engineering. The studies reported here were carried out between 2008 and 2014 under the direction of Professor Akihiko Kondo in the Laboratory of Biochemical Engineering, Department of Chemical Science and Engineering, Graduate School of Engineering, Kobe University.

First of all, the author would like to express his sincerest gratitude to his research advisor, **Professor Akihiko Kondo**, for continuous guidance and invaluable suggestions during the course of his studies. Next, the author would like to express his hearty gratitude to **Professor Hideki Fukuda** for invaluable discussion throughout this research. The author would also like to express his gratitude to **Associate Professor Jun Ishii** for invaluable discussion, kind support and heartfelt encouragement during the conduct of this research. Without his warm support, this thesis would not exist. The author is also deeply grateful to **Associate Professor Chiaki Ogino**, **Tsutomu Tanaka**, **Tomohisa Hasunuma**, **Kiyotaka Hara** and **Fumio Matsuda** (Osaka University) for valuable advice and hearty encouragement throughout this research.

The author wishes to express his gratitude to the official reviewer, **Professor Takashi Nishino** and **Hideki Yamaji**, who had time to take interest in the manuscript and to give constructive criticism at the final stage of preparation.

The author also wishes to acknowledge the contribution of **Dr. Seiji Sato** and **Dr. Atsushi Okamoto** (Asubio Pharma Co., Ltd.) for valuable discussion, technical advice

and providing cDNA of GPCRs. The helpful discussions and advice of, **Dr. Nobuo Fukuda** (National Institute of Advanced Industrial Science and Technology), **Mr. Yusuke Iguchi** (Keyence Co., Ltd.) and **Mr. Shota Togawa** (Otsuka Pharmaceutical Factory, Inc.) are gratefully acknowledged.

The technical assistance and hearty encouragement of **Ms. Norika Takemoto** are also sincerely acknowledged. The author also thank to **Ms. Shizuka Tateno-Matsumura**, **Ms. Satoko Kin**, **Ms. Misa Ishigami**, **Dr. Yuya Nishimura**, **Mr. Shintaro Ryo** (Kao Co., Ltd.), **Ms. Asami Oda** (Oji Paper Co., Ltd.), **Ms. Misato Kaishima**, **Mr. Takamichi Hashimoto**, **Dr. Shuhei Noda** (RIKEN), **Dr. Takuya Matsumoto**, and all the members of Professor Kondo's laboratory.

This work was supported by Grants-in-aid for a Research Fellowship for Young Scientists from the Japanese Society for the Promotion of Science, the Naito Foundation, and Special Coordination Funds for Promoting Science and Technology, Creation of Innovation Centers for Advanced Interdisciplinary Research Areas (Innovative Bioproduction Kobe; iBioK) from the Ministry of Education, Culture, Sports, Science and Technology (MEXT) of Japan.

Last but not least, the author expresses his deep appreciation to his parents, **Kou** and **Yumiko Nakamura**, for continuous moral and financial support, and to his sisters for invaluable support and encouragement. Without family's support, the author would not have been able to devote himself to research and complete his thesis.

Yasuyuki Nakamura

Department of Chemical Science and Engineering

Graduate School of Engineering

Kobe University

PUBLICATION LISTS

PART I.

Chapter 1

Nakamura Y., Ishii J., Kondo A. (2013) Bright fluorescence monitoring system utilizing *Zoanthus* sp. green fluorescent protein (*ZsGreen*) for human G-protein-coupled receptor signaling in microbial yeast cells. PLoS One. 8(12): e82237.

Chapter 2

Nakamura Y., Ishii J., Kondo A. Applications of microbial signaling sensor using *Zoanthus* sp. green fluorescent protein for antagonist characterization and site-directed mutagenesis of human serotonin 1A receptor. *Under preparation.*

Chapter 3

Nakamura Y., Ishii J., Kondo A. Construction of a yeast-based signaling biosensor for human angiotensin II type 1 receptor via functional coupling between Asn295-mutated receptor and Gpa1/G_{i3} chimeric Gα. Biotechnol. Bioeng. *Under revision*.

PART II.

Chapter 1

Nakamura Y., Ishii J., Kondo A. (2013) Rapid, facile detection of heterodimer partners for target human G-protein-coupled receptors using a modified split-ubiquitin membrane yeast two-hybrid system. PLoS One. 8(6): e66793.

Chapter 2

Nakamura Y., Takemoto N., Ishii J., Kondo A. (2014) Simultaneous method for analyzing dimerization and signaling of G-protein-coupled receptor in yeast by dual-color reporter system. Biotechnol. Bioeng. 111(3): 586−596.